Methods in Molecular Biology 1699

Springer Protocols

Wei Wu *Editor*

MicroRNA and Cancer

Methods and Protocols

Second Edition

Humana Press

METHODS IN MOLECULAR BIOLOGY

Series Editor
John M. Walker
School of Life and Medical Sciences
University of Hertfordshire
Hatfield, Hertfordshire, AL10 9AB, UK

For further volumes:
http://www.springer.com/series/7651

MicroRNA and Cancer

Methods and Protocols

Second Edition

Edited by

Wei Wu

Department of Medicine, Helen Diller Family Comprehensive Cancer Center, University of California in San Francisco, San Francisco, CA, USA

Humana Press

Editor
Wei Wu
Department of Medicine, Helen Diller Family Comprehensive Cancer Center
University of California in San Francisco
San Francisco, CA, USA

ISSN 1064-3745 ISSN 1940-6029 (electronic)
Methods in Molecular Biology
ISBN 978-1-4939-7433-7 ISBN 978-1-4939-7435-1 (eBook)
DOI 10.1007/978-1-4939-7435-1

Library of Congress Control Number: 2017955683

Printed on acid-free paper

This Humana Press imprint is published by Springer Nature
The registered company is Springer Science+Business Media, LLC
The registered company address is: 233 Spring Street, New York, NY 10013, U.S.A.

Preface

The discovery of microRNAs (miRNAs or miRs) heralded an exciting era in biology and started a new chapter in regulation of human genes. The miRNAs are a class of small endogenous noncoding RNAs (~22 nt) that fine-tune gene expression at the posttranscriptional level, mainly through binding 3′-UTR of mRNAs. They are involved in stem cell self-renewal, cellular development, differentiation, proliferation, and apoptosis.

Small miRNAs have big impacts in cancer development. Among the many miRNAs, a subset was identified as regulators of neoplastic transformation and tumor progression, invasion and metastasis as well as tumor-initiating cells (cancer stem cells). The widespread deregulation of miRNomes has been unveiled in diverse cancers compared to normal tissues. The oncomirs (oncogenic miRNAs), TSmiRs (tumor-suppressive miRNAs), and Metasta-miRs (cancer metastasis associated miRNAs) comprise an important part of the cancer genome and, hence, they have pivotal diagnostic and prognostic significance. Moreover, cancer-associated miRNAs are proving worthwhile as effective cancer biomarkers for individualized medicine and potential therapeutic targets.

Six years after publication of the first edition of our book about "microRNA and cancer," it has become a very popular reference in colleges, universities, and research institutes and I was encouraged to publish a second edition. This second edition provides the latest information at the forefront of miRNAs biology as it is being applied worldwide to cancer research. It is organized in the same style as the first edition with a review section and a protocol section. The review section is focused on current cancer research topics related to microRNA functions, including the roles of microRNAs in DNA damage, cancer-immune system interaction, cancer cell resistance, APOBEC gene expression, and gene expression noise. The protocol section is focused on experimental applications of microRNAs in various types of cancer and the scope of research covers detection of circulating microRNA, discovery of microRNA signatures using miRseq technology, evaluation of microRNA delivery systems, microRNA-based therapeutics, and finally, microRNA sequencing analysis.

MicroRNA research is a fast growing field and microRNAs are pivotal elements in cancer biology. An individual miRNA interferes with a broad range of mRNAs and, conversely, a single mRNA could be targeted by a variety of miRNAs. The complexity of miRNA::mRNA interactions is far-reaching in our understanding to date. This book provides the basic principles of experimental and computational methods for the study of microRNAs in cancer research and, therefore, provides a firm grounding for those who wish to develop further applications.

I am especially indebted to Drs. Shu Zheng, Suzanne D. Conzen, and Trever Bivona for giving me the opportunity to gain substantial experience in cancer research and I thank Dr. Fred G. Biddle for all kinds of support. Heartfelt gratitude goes to my family, who continue to patiently support me as I put forward my efforts related to the publication. Without their confidence and continuous support, many things would not have been possible. Also, I thank Professor John Walker for his encouragement and all staff from Springer for their hard work to produce the book. Finally, I am grateful to all the contributing authors for providing their high quality manuscripts.

San Francisco, CA, USA *Wei Wu M.D., Ph.D.*

Contents

Preface . . . . . *v*
Contributors . . . . . *ix*

PART I REVIEW

1 Noncoding RNAs in DNA Damage Response: Opportunities for Cancer Therapeutics 3
Wani Arjumand, Asia Asiaf, and Shiekh Tanveer Ahmad

2 MicroRNAs in Breast Cancer: Diagnostic and Therapeutic Potential 23
Asia Asiaf, Shiekh Tanveer Ahmad, Wani Arjumand, and Mohammad Afzal Zargar

3 Involvement of miRNAs and Pseudogenes in Cancer 45
Lütfi Tutar, Aykut Özgür, and Yusuf Tutar

4 MicroRNAs Reprogram Tumor Immune Response 67
Wei Cao, Wenfang Cheng, and Wei Wu

5 Apolipoprotein B mRNA Editing Enzyme, Catalytic Polypeptide-Like Gene Expression, RNA Editing, and MicroRNAs Regulation 75
Wei Cao and Wei Wu

6 MicroRNAs Change the Landscape of Cancer Resistance 83
Jun Zhu, Wei Zhu, and Wei Wu

7 MicroRNA, Noise, and Gene Expression Regulation 91
Wei Wu

PART II PROTOCOL SECTION

8 Deep Sequencing Reveals a MicroRNA Expression Signature in Triple-Negative Breast Cancer 99
Yao-Yin Chang, Liang-Chuan Lai, Mong-Hsun Tsai, and Eric Y. Chuang

9 Detection of Plasma MicroRNA Signature in Osteosarcoma Patients 113
Wendy Allen-Rhoades and Jason T. Yustein

10 Identification of E6/E7-Dependent MicroRNAs in HPV-Positive Cancer Cells 119
Anja Honegger, Daniela Schilling, Holger Sültmann, Karin Hoppe-Seyler, and Felix Hoppe-Seyler

11 Combination of Anti-miRNAs Oligonucleotides with Low Amounts of Chemotherapeutic Agents for Pancreatic Cancer Therapy 135
Marta Passadouro and Henrique Faneca

12 Evaluation of MicroRNA Delivery In Vivo 155
Rikki A.M. Brown, Kirsty L. Richardson, Felicity C. Kalinowski, Michael R. Epis, Jessica L. Horsham, Tasnuva D. Kabir, Marisa H. De Pinho, Dianne J. Beveridge, Lisa M. Stuart, Larissa C. Wintle, and Peter J. Leedman

13 Angiogenesis Analysis by In Vitro Coculture Assays in Transwell Chambers in Ovarian Cancer 179
Ali Flores-Pérez, Dolores Gallardo Rincón, Erika Ruiz-García, Raquel Echavarria, Laurence A. Marchat, Elizbeth Álvarez-Sánchez, and César López-Camarillo

14 Application of Individual qPCR Performance Parameters for Quality Control of Circulating MicroRNA Data 187
Anna Brunet-Vega, María Elisa Quílez, María José Ramírez-Lázaro, and Sergio Lario

15 Construction of Multi-Potent MicroRNA Sponge and Its Functional Evaluation 201
Suhwan Chang

16 MicroRNA Sequencing Data Analysis Toolkits 211
Wei Wu

Index *217*

Contributors

Shiekh Tanveer Ahmad • *Clarke H. Smith Brain Tumour Centre, Arnie Charbonneau Cancer Institute, Cumming School of Medicine, 2A25 HRIC, University of Calgary, Calgary, AB, Canada*

Elizbeth Alvarez-Sánchez • *Posgrado en Ciencias Genómicas, Universidad Autónoma de la Ciudad de México, Benito Juarze, CDMX, Mexico*

Wendy Allen-Rhoades • *Department of Pediatrics, Baylor College of Medicine, Houston, TX, USA*

Wani Arjumand • *Robson DNA Science Centre, Arnie Charbonneau Cancer Institute, Cumming School of Medicine, 2A32 HRIC, University of Calgary, Calgary, AB, Canada*

Asia Asiaf • *Department of Biochemistry, Faculty of Science, University of Kashmir, Hazratbal Srinagar, J&K, India*

Dianne J. Beveridge • *Laboratory for Cancer Medicine, Harry Perkins Institute of Medical Research, University of Western Australia Centre for Medical Research, Nedlands, WA, Australia*

Rikki A.M. Brown • *Laboratory for Cancer Medicine, Harry Perkins Institute of Medical Research, University of Western Australia Centre for Medical Research, Nedlands, WA, Australia*

Anna Brunet-Vega • *Oncology Service, Hospital de Sabadell, Corporació Sanitària Parc Taulí, Institut Universitari Parc Taulí-UAB, Sabadell, Spain; Fundació Parc Taulí, Corporació Sanitària Parc Taulí, Institut Universitari Parc Taulí-UAB, Sabadell, Spain*

Wei Cao • *Translational Medical Center, Zhengzhou Central Hospital, Affiliated to Zhengzhou University, Zhengzhou, People's Republic of China*

Suhwan Chang • *Department of Biomedical Sciences, University of Ulsan College of Medicine, Asan Medical Center, Seoul, South Korea*

Yao-Yin Chang • *Department of Electrical Engineering, Graduate Institute of Biomedical Electronics and Bioinformatics, National Taiwan University, Taipei, Taiwan; Bioinformatics and Biostatistics Core, NTU Center of Genomic Medicine, Taipei, Taiwan*

Wenfang Cheng • *Department of Gastroenterology, The First Affiliated Hospital of Nanjing Medical University, Nanjing, Jiangsu Province, China*

Eric Y. Chuang • *Department of Electrical Engineering, Graduate Institute of Biomedical Electronics and Bioinformatics, National Taiwan University, Taipei, Taiwan; Bioinformatics and Biostatistics Core, NTU Center of Genomic Medicine, Taipei, Taiwan*

Marisa H. De Pinho • *Laboratory for Cancer Medicine, Harry Perkins Institute of Medical Research, University of Western Australia Centre for Medical Research, Nedlands, WA, Australia*

Raquel Echavarria • *Posgrado en Ciencias Genómicas, Universidad Autónoma de la Ciudad de México, Benito Juarze, CDMX, Mexico*

Michael R. Epis • *Laboratory for Cancer Medicine, Harry Perkins Institute of Medical Research, University of Western Australia Centre for Medical Research, Nedlands, WA, Australia*

Henrique Faneca • *Center for Neuroscience and Cell Biology, University of Coimbra, Coimbra, Portugal; Department of Life Sciences, Faculty of Science and Technology, University of Coimbra, Coimbra, Portugal*

Ali Flores-Pérez • *Posgrado en Ciencias Genómicas, Universidad Autónoma de la Ciudad de México, Benito Juarze, CDMX, Mexico*
Anja Honegger • *Molecular Therapy of Virus-Associated Cancers (F065), German Cancer Research Center (DKFZ), Heidelberg, Germany*
Felix Hoppe-Seyler • *Molecular Therapy of Virus-Associated Cancers (F065), German Cancer Research Center (DKFZ), Heidelberg, Germany*
Karin Hoppe-Seyler • *Molecular Therapy of Virus-Associated Cancers (F065), German Cancer Research Center (DKFZ), Heidelberg, Germany*
Jessica L. Horsham • *Laboratory for Cancer Medicine, Harry Perkins Institute of Medical Research, University of Western Australia Centre for Medical Research, Nedlands, WA, Australia*
Tasnuva D. Kabir • *Laboratory for Cancer Medicine, Harry Perkins Institute of Medical Research, University of Western Australia Centre for Medical Research, Nedlands, WA, Australia*
Felicity C. Kalinowski • *Laboratory for Cancer Medicine, Harry Perkins Institute of Medical Research, University of Western Australia Centre for Medical Research, Nedlands, WA, Australia*
César López-Camarillo • *Posgrado en Ciencias Genómicas, Universidad Autónoma de la Ciudad de México, Benito Juarze, CDMX, Mexico*
Liang-Chuan Lai • *Department of Physiology, College of Medicine, National Taiwan University, Taipei, Taiwan*
Sergio Lario • *Digestive Diseases Service, Hospital de Sabadell, Corporació Sanitària Parc Taulí, Institut Universitari Parc Taulí-UAB, Sabadell, Spain; Fundació Parc Taulí, Corporació Sanitària Parc Taulí, Institut Universitari Parc Taulí-UAB, Sabadell, Spain; Centro de Investigación Biomédica en Red de Enfermedades Hepáticas y Digestivas (CIBERehd), Instituto de Salud Carlos III, Madrid, Spain*
Peter J. Leedman • *Laboratory for Cancer Medicine, Harry Perkins Institute of Medical Research, University of Western Australia Centre for Medical Research, Nedlands, WA, Australia; School of Medicine and Pharmacology, The University of Western Australia, Nedlands, WA, Australia*
Laurence A. Marchat • *Programa en Biomedicina Molecular y Red de Biotecnología, Escuela Nacional de Medicina y Homeopatía, Instituto Politécnico Nacional, Ciudad de México, CDMX, Mexico*
Aykut Özgür • *Division of Biochemistry, Department of Basic Sciences, Faculty of Pharmacy, Cumhuriyet University, Sivas, Turkey*
Marta Passadouro • *Center for Neuroscience and Cell Biology, University of Coimbra, Coimbra, Portugal; Department of Life Sciences, Faculty of Science and Technology, University of Coimbra, Coimbra, Portugal*
María Elisa Quílez • *Oncology Service, Hospital de Sabadell, Corporació Sanitària Parc Taulí, Institut Universitari Parc Taulí-UAB, Sabadell, Spain; Digestive Diseases Service, Hospital de Sabadell, Corporació Sanitària Parc Taulí, Institut Universitari Parc Taulí-UAB, Sabadell, Spain; Fundació Parc Taulí, Corporació Sanitària Parc Taulí, Institut Universitari Parc Taulí-UAB, Sabadell, Spain*
María José Ramírez-Lázaro • *Digestive Diseases Service, Hospital de Sabadell, Corporació Sanitària Parc Taulí, Institut Universitari Parc Taulí-UAB, Sabadell, Spain; Centro de Investigación Biomédica en Red de Enfermedades Hepáticas y Digestivas (CIBERehd), Instituto de Salud Carlos III, Madrid, Spain*

Kirsty L. Richardson • *Laboratory for Cancer Medicine, Harry Perkins Institute of Medical Research, University of Western Australia Centre for Medical Research, Nedlands, WA, Australia*
Dolores Gallardo Rincón • *Laboratorio de Medicina Translacional, Instituto Nacional de Cancerología, Tlalpan, CDMX, Mexico*
Erika Ruiz-García • *Laboratorio de Medicina Translacional, Instituto Nacional de Cancerología, Tlalpan, CDMX, Mexico*
Holger Sültmann • *Cancer Genome Research (B063), German Cancer Research Center (DKFZ) and German Cancer Consortium (DKTK), Heidelberg, Germany*
Daniela Schilling • *Cancer Genome Research (B063), German Cancer Research Center (DKFZ) and German Cancer Consortium (DKTK), Heidelberg, Germany*
Lisa M. Stuart • *Laboratory for Cancer Medicine, Harry Perkins Institute of Medical Research, University of Western Australia Centre for Medical Research, Nedlands, WA, Australia*
Mong-Hsun Tsai • *Institute of Biotechnology, College of Bio-resources and Agriculture, National Taiwan University, Taipei, Taiwan*
Lütfi Tutar • *Department of Molecular Biology and Genetics, Faculty of Arts and Sciences, Ahi Evran University, Kırşehir, Turkey*
Yusuf Tutar • *Division of Biochemistry, Department of Basic Sciences, Faculty of Pharmacy, Cumhuriyet University, Sivas, Turkey; Department of Nutrition and Dietetics, Health Sciences Faculty, University of Health Sciences, Üsküdar, Istanbul, Turkey*
Larissa C. Wintle • *Laboratory for Cancer Medicine, Harry Perkins Institute of Medical Research, University of Western Australia Centre for Medical Research, Nedlands, WA, Australia*
Wei Wu • *Department of Medicine, Helen Diller Family Comprehensive Cancer Center, University of California in San Francisco, San Francisco, CA, USA*
Jason T. Yustein • *Department of Pediatrics, Baylor College of Medicine, Houston, TX, USA*
Mohammad Afzal Zargar • *Department of Biochemistry, Faculty of Science, University of Kashmir, Hazratbal Srinagar, J&K, India*
Jun Zhu • *Jiangsu Cancer Hospital, Nanjing, Jiangsu, China*
Wei Zhu • *Department of Oncology, First Affiliated Hospital of Nanjing Medical University, Nanjing, PR China*

Part I

Review

Chapter 1

Noncoding RNAs in DNA Damage Response: Opportunities for Cancer Therapeutics

Wani Arjumand, Asia Asiaf, and Shiekh Tanveer Ahmad

Abstract

DNA repair machinery preserves genomic integrity, which is frequently challenged through endogenous and exogenous toxic insults, and any sort of repair machinery malfunctioning ultimately manifests in the form of several types of terrible human diseases such as cancers (Hoeijmakers, Nature 411(6835): 366–374, 2001). Noncoding RNAs (ncRNAs) are crucial players of DNA repair machinery in a cell and play a vital role in maintaining genomic stability, which is essential for its survival and normal functioning thus preventing tumorigenesis. To preserve the integrity of the genome, cells initiate a specific cellular response, recognized as DNA damage response (DDR), which includes several distinct DNA repair pathways. These repair pathways permit normal cells to repair DNA damage or induce apoptosis and cell cycle arrest in case the damage is irreparable. Disruption of these pathways in cancer leads to an increase in genomic instability and mutagenesis. Recently, emerging evidence suggests that ncRNAs play a critical role in the regulation of DDR. There is an extensive crosstalk between ncRNAs and the canonical DDR signaling pathway. DDR-induced expression of ncRNAs can provide a regulatory mechanism to accurately control the expression of DNA damage responsive genes in a spatio-temporal manner. DNA damage alters expression of a variety of ncRNAs at multiple levels including transcriptional regulation, post-transcriptional regulation, and RNA degradation and vice versa, wherein ncRNAs can directly regulate cellular processes involved in DDR by altering expression of their targeting genes, with a particular emphasis on microRNAs (miRNAs) and long noncoding RNAs (lncRNAs). Relationship between the defects in the DDR and deregulation of related ncRNAs in human cancers is one of the established, which is growing stronger with the advent of high-throughput sequencing techniques such as next-generation sequencing. Understanding of the mechanisms that explain the association between ncRNAs and DDR/DNA repair pathways will definitely increase our understanding on human tumor biology and on different responses to diverse drugs. Different ncRNAs interact with distinct DDR components and are promising targets for improving the effects to overcome the resistance to conventional chemotherapeutic agents. In this chapter, we will focus the role of ncRNAs in the DNA damage, repair, and cancer.

Key words MicroRNAs, DNA damage response, Cancer, Genomic instable

1 Introduction

The cell cycle is tightly regulated in all the cells during normal developmental processes. Loss of control of the cell cycle is found in many cancers. Checkpoints are the most important cell cycle

Wei Wu (ed.), *MicroRNA and Cancer: Methods and Protocols*, Methods in Molecular Biology, vol. 1699,
DOI 10.1007/978-1-4939-7435-1_1,

regulatory machinery, which act as a brake when there is an abnormal processing of DNA replication. Human DNA is exposed to a variety of exogenous and endogenous genotoxic insults such as ultraviolet (UV) radiation, ionizing radiation (IR), numerous genotoxic chemicals, and the byproducts of cellular metabolism such as reactive oxidative species on a daily basis, which can result in DNA damage. Tens of thousands of DNA damage events occur every day in our cells, and many different mechanisms have evolved to deal with them [1, 2]. The DDR is a collective term used for the plethora of different intra- and inter-cellular signaling events and enzyme activities that result from the induction and detection of DNA damage. Such events may ultimately result in cell-cycle arrest, regulation of DNA replication, and the repair or bypass of DNA damage. Should DNA repair not be possible or suboptimal repair lead to an unsupportable level of genomic instability, DDR can also impact downstream cell fate decisions, such as cell death or senescence that can either be dependent or independent of the immune system [3, 4]. If the DNA errors can be repaired successfully, checkpoint signals will be attenuated and the cell cycle will be restarted. If the DNA damage is beyond the repair capacity of the DDR machinery, cell fate may be permanent senescence or apoptosis, or cells will continue to divide with aberrant DNA. Therefore, the complete checkpoint system is a vital cellular component guarding the integrity of genetic information. Given the fundamental role of DDR in maintaining genome integrity, this complex signalling network requires accurate regulatory mechanisms to respond to different types of DNA lesions in different stages of the cell cycle. Dysregulation DDR is associated with a predisposition to cancer and affects responses to DNA-damaging anticancer therapy. Dysfunction of one DNA repair pathway may be compensated for by the function of another compensatory DDR pathway, which may be increased and contribute to the resistance to DNA-damaging chemotherapy and radiotherapy. Recently, there has been accumulating experimental evidence that witnesses noncoding RNAs—including microRNAs (miRNAs), long noncoding RNAs (lncRNAs), DNA damage response RNAs (DDRNAs), DSB-induced RNAs (diRNAs), small interfering RNA (siRNAs), and piwi-interacting RNAs (piRNAs)—are emerging new players in DDR. In this chapter, we will discuss first the relation between the DNA damage events and cancer that are beyond doubt grown from strength to strength. After that we highlight the role of ncRNAs in DNA damage response pathways and their potential to serve as diagnostic markers and at the same time as therapeutic targets in cancer management.

2 DNA Damage and Carcinogenesis

As already mentioned the DNA in a cell on a regular basis is exposed to a variety of exogenous and endogenous genotoxic insults that have potential to cause serious damage to genetic information coded and may interfere with faithful replication and also transcription of the said information. To tackle these threats every cell is guarded with DNA damage response machinery. Most of the oncogenic alterations in humans that include but are not limited to mutations, translocations, amplifications, deletions, and epigenetic modifications are manifestation of the inefficient repair of damaged DNA. There are multiple mechanisms of DNA repair. The DDR pathways opted by a cell to fix the damage to DNA depends upon the type of damage induced and the cell cycle status. Defect in one DDR may be compensated for by the increased activity of other elements or pathways so as not to let the cell compromise with DNA damage repair capacity. This feature of DDR presents both challenges and opportunities for cancer treatment. DNA-damaging therapy gets its biggest challenge due to upregulation of DNA repair pathways that cause resistance to DNA-damaging chemotherapy and radiotherapy and so inhibitors of these pathways have the potential to sensitize cells to these therapies. This is the rationale behind the development and use of DDR inhibitors in combination with DNA-damaging agents to target the DDR pathways so as to render the cell inefficient to repair the lesions caused by DNA damage. In other words, the pathways that are lost represent vulnerabilities in the DNA repair capacity of the cancer cell that can be exploited by selecting the appropriate chemotherapy to induce unrepairable—and hence more cytotoxic—DNA damage. These include base modification (repaired by direct repair and base excision repair (BER)), base mismatch (repaired by mismatch repair), intrastrand crosslinks (ICL), and DNA–protein crosslinks (repaired by ICL repair and nucleotide excision repair (NER)), stalled replication forks (repaired by homologous recombination (HR), NER, and the Fanconi Anemia (FA) pathway), single-strand breaks (SSB; repaired by BER and HR), and double-strand breaks (DSB) (repaired by HR and non-homologous end-joining (NHEJ)). These different DNA lesions and their corresponding repair mechanisms have been demonstrated in Fig. 1 [5]. The use of specific inhibitors of DDR pathways as a strategy to tackle the chemo- and radio-resistance is exhibited by cancer cells. Here under, one by one we will discuss the DDR options and the kind of damage those fix, and how they are being exploited to develop to induce irreparable DNA damage in cancer cells.

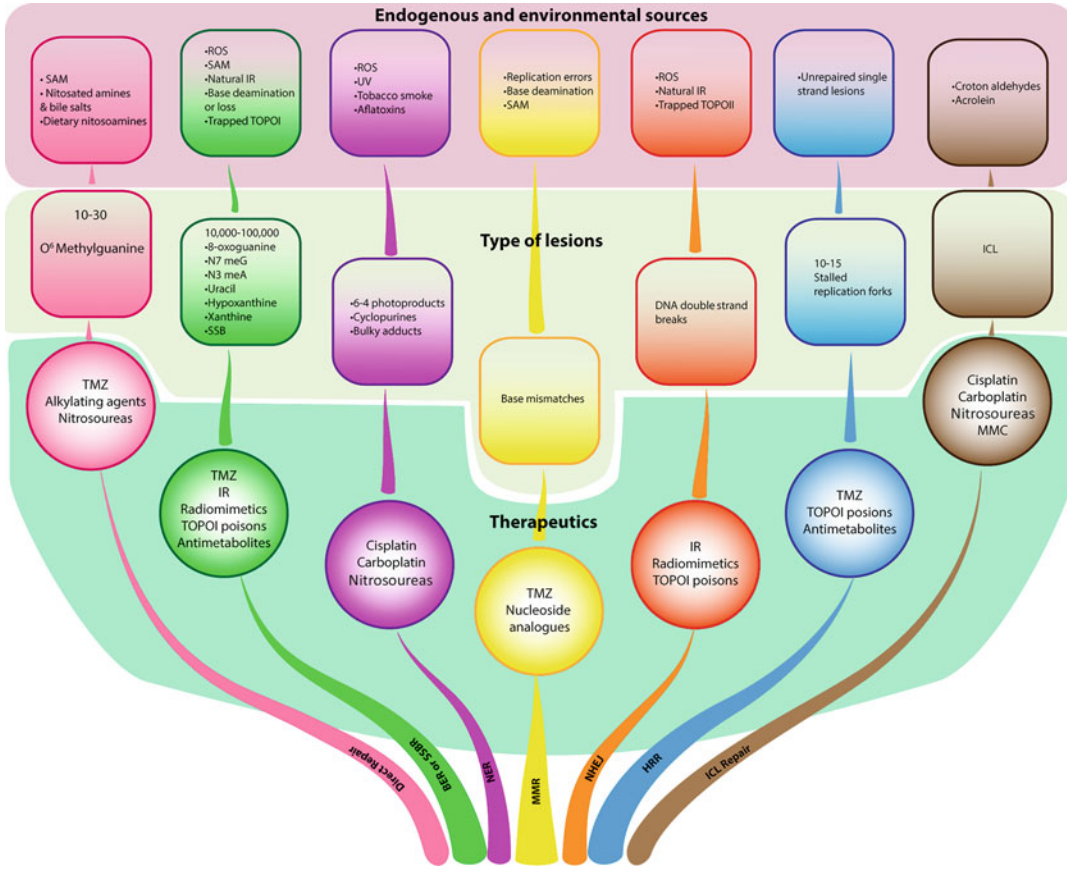

Fig. 1 Endogenous and environmental sources of DNA damage are presented in the boxes in topmost area of figure with *light pink background*. Types of lesions caused are presented in boxes in the middle with *beige color background* (the numbers at the top of each boxes represent the type of lesions occurring per cell per day). The DNA-damaging therapeutic agents that are responsible for the corresponding DNA lesion are shown in the boxes in the bottom area with *light green background*. The corresponding type of DDR pathways that are activated in response to the DNA damage induced by the therapeutic DNA-damaging agents and environmental events are shown in shapes with similar colors along same branch. Abbreviations: *BER* base excision repair, *HRR* homologous recombination repair, *ICL* interstrand crosslink, *IR* ionizing radiation, *MMC* mitomycin C, *NER* nucleotide excision repair, *NHEJ* non-homologous end joining, *ROS* reactive oxygen species, *SAM* S-adenosyl methionine, *SSB* single-strand break, *SSBR* SSB repair, *TMZ* temozolomide, *TOPO* topoisomerase, *UV* ultraviolet. *(Figure modified from Nicola J. Curtin. Nature Reviews Cancer 12, 801–817)*

2.1 Direct Repair

This is the simplest form of DNA repair that is done by the direct reversal of the lesion. O^6-methylguanine DNA methyltransferase (MGMT) demethylates O^6-methylguanine lesions, which are formed as a result of erroneous methylation by S-adenosylmethionine (SAM) and other alkylations at the O^6-position of guanine that are induced by dietary nitrosamines or chemotherapy agents—for example, temozolomide (TMZ), dacarbazine (DTIC), and nitrosoureas (also known as carmustine) [6] (Fig. 1). If this lesion is left unrepaired, O^6-methylguanine is mutagenic as it

distorts pairing with cytosine or thymidine, and thus leads G:C to A:T transitions on DNA replication. Although this enzyme is ubiquitously expressed but levels of expression may vary across different tissues. The tumor cells express highest levels of MGMT and are associated with resistance to BCNU and TMZ [7]. The comparatively higher levels of MGMT expression that are frequently found in cancer cells than normal cells suggest that its depletion with pseudo-substrates might provide a viable strategy to sensitize cancer cells to O^6 alkylating agents such as TMZ. One such pseudo-substrate, O^6-benzylguanine, was successful in depleting MGMT and significantly increased nitrosourea and TMZ cytotoxicity preclinically, especially the bone marrow cells [8]. Later, it was also used in clinical trials in treating gliomas where it proved safe, effective, and most importantly able to cross blood brain barrier [9], However, O^6-benzylguanine enhanced TMZ- and BCNU-induced myelosuppression [8] limited its potential to pass further clinical trials. Several other pseudo-substrates have been developed; however, none so far proved successful in clinic. A more practical approach would be the exploitation of low MGMT levels caused by epigenetic silencing in some specific cancers. A more promising approach may be the exploitation of reduced MGMT activity owing to epigenetic silencing in some cancers [10]. Astrocytomas patients with MGMT promoter methylation responded better to BCNU. Likewise, the glioma patients with epigenetic silencing of MGMT were very sensitive to TMZ plus radiotherapy (the current standard-of-care) [11]. Therefore, MGMT promoter methylation status could be very helpful for stratifying patients for treatment with TMZ, with or without radiotherapy. This is a very good example of targeting the DNA repair machinery for the effective DNA-damaging drugs to treat cancers.

2.2 Nucleotide Excision Repair

NER repairs the helix-distorting adducts on DNA (for example, those caused by ultraviolet (UV) radiation and tobacco smoke) and also contributes to the repair of intrastrand and interstrand cross-links (ICLs). The xeroderma pigmentosum (XP) proteins and ERCC1 are important proteins involved in both the NER and ICL repair pathways [12] (Fig. 1). Hereditary defects in NER pathway genes cause UV sensitivity and skin cancer development [13]. Patients with defects in NER exhibit sensitivity to platinum agent therapy; due to poor capacity to repair ICLs [14] and the measurement of levels of crucial NER enzymes could thus be used for patient stratification. However, there are currently no small-molecule inhibitors of NER.

2.3 Base Excision Repair

DSBs are one of the most common endogenous lesions. They are caused directly from DNA sugar damage or induced by ROS. Indirectly they may arise from BER-mediated enzymatic excision of damaged bases following their spontaneous deamination,

oxidation, or alkylation [15] (Fig. 1). The most common ROS-induced base oxidations are 8-oxoguanine, which mispairs with adenine, and 5-hydroxycytosine that mispairs with thymine. As oxidative damage is generally high in tumors due to high metabolism, oncogenic signaling, and mitochondrial dysfunction, there is almost 100-fold more 8-oxoguanine in cancer tissues in comparison to normal tissues [16].

SSB repair and BER are used synonymously as they involve the same components and differ only in the initial recognition step. Typically, a damaged base is removed first by BER glycosylases to form abasic sites and then BER endonucleases generate a "nick" (generating SSB), which, along with directly induced SSBs, act as substrates for SSB repair. The BER pathway has two types depending upon the length of the patch replaced; short patch BER (includes a single nucleotide replacement), which is the predominant pathway and long patch BER (2–13 nucleotides are replaced) [17]. The main enzymes of this pathway include glycosylases, endonucleases, DNA polymerases, and DNA ligases, with poly (ADP-ribose) polymerase 1(PARP1) and PARP2 facilitating the process (Fig. 2). Although PARP1 plays an important role in BER, but it is also important in DNA double-strand break (DSB) repair. The binding of PARP1 to DNA breaks activates it, and this is necessary for the recruitment of XRCC1 and other BER proteins in the pathway [18]. BER repairs DNA damage that is therapeutically induced by ionizing radiation (IR), DNA methylating agents,

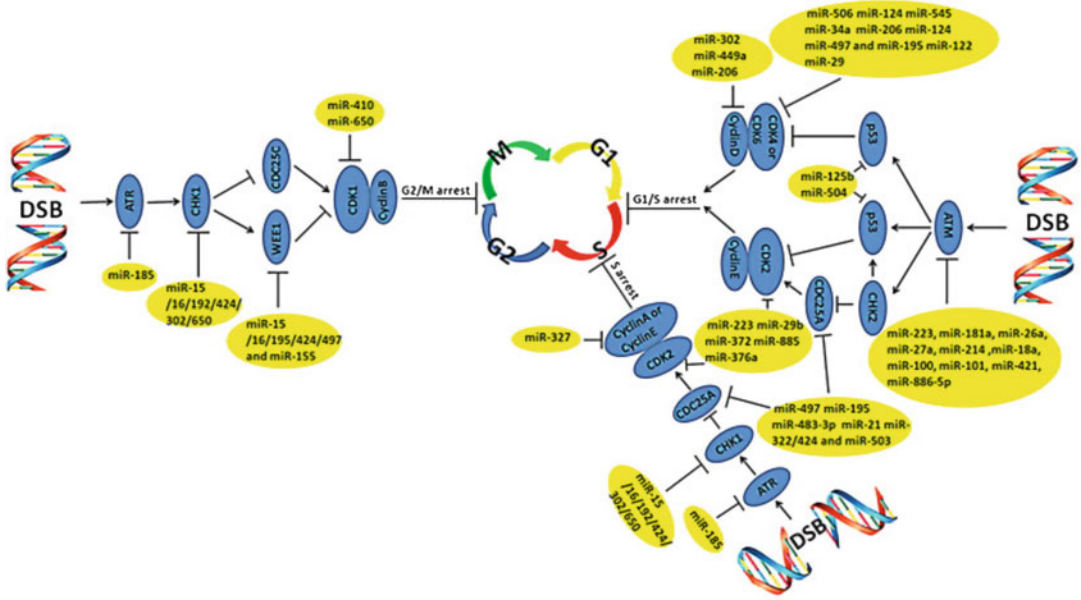

Fig. 2 This figure depicts how miRNAs modulate cell cycle regulatory proteins after DNA damage is induced by targeting key genes involved in cell cycle control. For details, refer to text (*Figure adapted from C. Zhang & G. Peng. Mutation Research/Reviews in Mutation Research, 763, 202–211*)

topoisomerase I poisons, etc. Genetic variation in BER genes has been found to be associated with cancer [19]. The BER pathway is an attractive target for the modulation of chemosensitivity and radiosensitivity. Various studies have shown how inhibitors of DNA polymerase-β (Pol β), flap endonuclease 1 (FEN1), ligase 1, and ligase 3 enhance sensitivity to IR, TMZ, and the alkylating agent methyl methanesulphonate (MMS), respectively [5]. Plethora of preclinical evidence is indicating how radiosensitization is bestowed by PARP inhibition along with TMZ treatment, and this regimen will potentially avoid toxicities observed with the chemotherapy combinations. Clinical trials with combination of cytotoxic DNA-damaging agents along with PARP inhibitors are underway and interim results look promising in brain metastatic patients [20].

2.4 Mismatch Repair

This type of DNA damage repair rectifies the errors that arise out of replication where a wrong nucleotide is inserted or bade is deleted or inserted. Dysfunction of this DDR pathway increases mutation rates up to 1000-fold, results in microsatellite instability (MSI), and has been found to be associated with cancer development [21]. MSI-high cancer has shown high frequency of mutation in DDR genes with microsatellite regions, like ATM, MRE11 etc., potentially conferring sensitivity to some DNA-damaging agents [22]. The dark side of the defects in MMR is the tolerance to TMZ, platinum agents, and some nucleoside analogues, which leads to drug resistance. Instead of inhibiting the MMR pathway, efforts are made to reactivate epigenetically silenced MLH1 (an MMR gene). However, clinical trials have shown adverse reactions with this kind of strategy.

2.5 Non-homologous End Joining

There are on an average about 10–50 DSBs per cell per day that arise endogenously, majority is ROS-induced DNA damage, which is increased in tumor cells [23]. DSBs are among the most difficult lesions to repair and, if left unrepaired, lead to cell death. DSBs are ligated by NHEJ with minimal end processing. Although it is not error free, it is active in all the phases of the cell cycle predominantly in the G0 phase and the G1 phase, and is responsible for the rapid repair of up to 85% of IR-induced DSBs [24]. DSBs result directly from therapeutic exposure to IR and to topoisomerase II poisons, and indirectly from the stalling of replication forks due to single-stranded lesions. The NHEJ pathway involves proteins such as KU70 (or XRCC6), KU80 (or XRCC5), DNA-dependent protein kinase catalytic subunit (DNA-PKcs). KU70–KU80–DNA-PKcs form a complex known as DNA-PK—artemis, XRCC4–XLF, and ligase 4 (Fig. 3). ATM and the MRN complex (which comprises MRE11, RAD50, and Nijmegen breakage syndrome protein 1 (NBS1)) recognizes the DSB as an initial event which later is joined by the NHEJ repair machinery. Dysfunction of the NHEJ pathway has been identified as being associated with cancer. The most

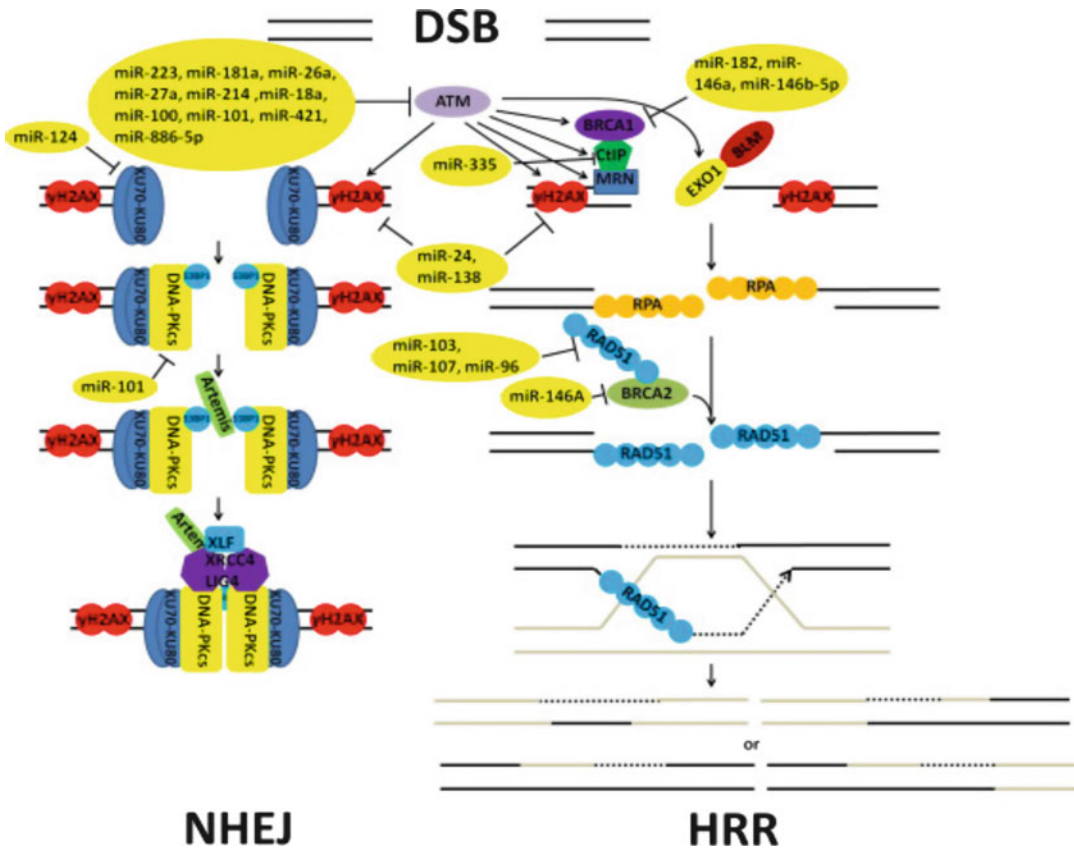

Fig. 3 This figure reveals the components of two major DDR pathways, i.e., NHEJ and HRR protein components as targets of miRNAs to modulate their efficacy in repairing the DNA damage. For details, refer to text (*Figure adapted from C. Zhang & G. Peng. Mutation Research/Reviews in Mutation Research, 763, 202–211*)

important member of this machinery, DNA-PKcs, is a member of the PI3K-related protein kinase (PIKK) family of enzymes that also includes ATM, ataxia-telangiectasia, and Rad3-related (ATR) and mTOR. DNA-PKcs levels and activity were higher in patient-derived B cell chronic lymphocytic leukaemia (B-CLL) cells that were stratified as having poor prognosis than in good prognosis B-CLL cells. Many agents that acted as DSB repair pathway inhibitor have progressed to clinical trials, except a dual mTOR and DNA-PKcs inhibitor, CC-115, that is undergoing early clinical evaluation [5]. Combinations of DNA-PKcs inhibitors with radiotherapy seem to be a plausible approach toward the treatment of cancer patients on the basis of the profound radiosensitization seen in a number of preclinical models and the reduced likelihood of toxicities that might be predicted from a combination with systemic chemotherapy.

2.6 Homologous Recombination Repair

The HRR pathway of DSB repair is a highly complex process that involves myriad of proteins and mainly is active during the S and G2 phases of the cell cycle [25]. The broken DNA ends of a DSB are resected to allow invasion of the single strands into the sister chromatid, which functions as a template for the accurate resynthesis of the damaged DNA. The sister chromatids are attached at this point of time that allows the use of sister chromatid as the template strand. Although this pathway repairs only a minor proportion of DSBs, it may be the most crucial as it is high fidelity to ensure error-free repair of the DSBs. It also resolves the stalled and collapsed replication forks, as well as single-ended DSBs, and also (in cooperation with the NER and Fanconi anaemia pathways) the processing of ICLs [26]. HRR is crucial for the maintenance of genomic stability, and the function of the entire pathway can be compromised by the loss of any member. This pathway includes many important tumor suppressors such as BRCA1, BRCA2, and ATM (Fig. 3). Tumors with HRR defects are highly sensitive to cross-linking agents (such as cisplatin, carboplatin, and nitrosoureas) and DSBs that are induced by radiation. HRR-defective cells are hypersensitive to certain antimetabolites that induce base lesions and/or replication fork stalling for instance, gemcitabine [27]. Cancer cells usually have high frequency of defects in HRR which may underlie the efficacy of cytotoxic therapy and provide a rationale for the use of inhibitors of HRR to sensitize tumors cells with functional HRR to conventional chemotherapy. Moreover, HRR-defective cells are selectively killed by PARPis. Mirin is an inhibitor of MRE11 endonuclease activity but as MRE11 lies upstream of both HRR and NHEJ, so it is difficult to determine whether inhibition of HRR or inhibition of NHEJ by mirin contributes most to sensitization. Activating phosphorylation of RAD51 and RAD51 focus formation are dependent on the proto-oncogene ABL1; and the BCR-ABL1 inhibitor imatinib sensitized cells to DNA crosslinking agents and IR [28]. Other prototype RAD51 inhibitors have been identified but the most common way to target HRR is by inhibition of the ATM–CHK2 or ATR–CHK1 pathways.

2.7 Cell Cycle Checkpoints

Checkpoints are one of the most important cell cycle regulatory machinery, which act as a guard against any abnormal processing of DNA replication. Whenever there is genotoxic stress inside a cell, it stops cycling by activating checkpoint machinery, which then allows DNA repair systems to correct replication errors. The cell then decides whether to proceed again for division or stop to allow cell death, depending upon the status of DNA damage repair. If DNA can be repaired successfully, checkpoint signals will be attenuated and the cell cycle will be restarted. If the DNA damage cannot be properly repaired, cell fate may be permanent senescence or apoptosis, or cells will continue to divide with aberrant DNA (leads to transformation). Therefore, one can say that the checkpoint system

is a vital and central cellular component, guarding the integrity of genetic information [29]. The DNA damage checkpoint network contains three types of components namely sensors, transducers, and effectors: the MRN complex and RPA for example are typically considered sensors, Ataxia telangiectasia-mutated (ATM), ataxia telangiectasia and Rad3-related(ATR), and DNA-PK are referred to as transducers or mediators, and their main downstream transducers are Chk1, Chk2, and p53, which regulate several substrate effectors and propagate the checkpoint signal [30]. For instance, the Cdc25A is a major effector, whose degradation results in the inactivation of Cdk1 and Cdk2, leading to intra-S or G2 phase arrest. As mentioned already earlier in this chapter, ATM and DNA-PK respond mainly to DSBs, whereas ATR is activated by single-strand DNA and stalled DNA replication forks [31]. The ATM-Chk2 and the ATR-Chk1 pathways are the major types of checkpoint pathways to be activated in response to DNA damage. Phosphorylation of Ser1981 or Thr68 residues are the markers of activation of human ATM or Chk2 protein, respectively. The cell cycle checkpoint proteins are usually found altered in cancers cells compared to normal cells. There is a constitutive activation of the ATM-Chk2 pathway found in urinary bladder cancer, early breast, and colon cancers [32]. ATMpS1981, Chk2pT68, and γ-H2AX have been also found to be overexpressed in prostate intraepithelial neoplasias (PINs) compared to normal prostate gland and carcinoma [33]. The DDR and oncogene-induced senescence (OIS) are usually found activated in precancerous lesions, but rarely observed in advanced stages which may suggest that the malignant cells find ways to overcome checkpoints and OIS [34]. Evidence suggests that both apoptosis and senescence are suppressed in cancer development. When progressing from pre-neoplastic lesions to a malignant form, cells have to override the DNA damage checkpoint barrier, either by inhibition or attenuation. Inactivation or mutation of p53 is a frequent way of escaping DDR-induced senescence [34]. However, mechanisms by which DDR signaling is attenuated are not well understood.

The Wee1 tyrosine kinase functions in the G2/M checkpoint by negatively regulating the Cdk1/cyclin B protein complex by catalyzing inhibitory phosphorylation of Cdk1, leading to G2/M checkpoint activation in response to DNA damage. It has been reported to be overexpressed in colon cancer, seminoma, breast cancer, osteosarcoma, and glioblastoma, vulvar squamous cell carcinoma, and poor disease-free survival in melanoma patients [35]. Paradoxically, studies have shown reduced Wee1 expression in in colon cancer, prostate cancer, and non-small cell lung cancer [36]. Thus, it is still a matter of debate whether it acts as a tumor suppressor or oncogene.

Polo-like kinase 1 (Plk1) is a key regulator of the G2/M checkpoint, and its activity is important for mitotic progression

after recovery from the DNA damage checkpoint. Plk1 regulates cyclin B1 by phosphorylating its cytoplasmic retention signal and on the other hand, promotes both the phosphatase activity and translocation of CDC25 to the nucleus by phosphorylating it [37]. Moreover, Plk1 triggers degradation of the mitotic regulator Wee1 and Claspin, thus facilitates G2/M checkpoint recovery [38]. Overexpression of Plk1 protein has been observed in multiple human cancer tissues, such as head and neck cancer, non-small-cell lung cancer, esophageal cancer, gastric cancer, pancreatic cancer, colorectal cancer, and breast cancer [35]. Plk1 has also been shown to be a prognosis marker for many of the cancers studied. Studies indicate that Plk1 could be an oncogene [39]. Other very important checkpoint regulators are FoxM1, Wip1, PP2A, Claspin, etc., which have been found closely associated with cancer development or progression.

3 miRNAa and DNA Damage Response

Up to now in this chapter we discussed the fundamental principles of DNA damage repair and its dysfunction across different cancers. After a genotoxic insult, the first and foremost response generated by DDR machinery involves transcriptional upregulation of its gene components and their optimal translation into respective active protein products. The mRNAs involved in DDR pathways are regulated via miRNAs. miRNAs are required for almost every aspect of cellular responses to DNA damage, including sensing DNA damage, transducing damage signals, repairing damaged DNA, activating cell cycle checkpoints, and inducing apoptosis.

3.1 MicroRNAs Holding the Switch of DNA Damage Response

miRNAs are small noncoding RNAs of approximately 20–22 nucleotides in length in their mature form. The process by which a precursor miRNA becomes a mature miRNA involves different biological steps. The biogenesis of miRNAs starts in the nucleus where transcription of the primary miRNA (pri-miRNA) undergoes many steps of maturation. The maturation process begins with a nuclear RNase III Drosha together with the cofactor DGCR8 that cut the stem–loop to release a pre-miRNA [40]. pre-miRNA is exported to cytoplasm through the complex EXP5–Ran·GTP, where maturation is completed [41]. Here, pre-miRNA is cleaved by Dicer, a RNase III family protein, generating a small RNA duplex ~22 nucleotides in length. The pre-miRNA is subsequently loaded on Ago protein to form a complex called pre-RNA-induced silencing complex (pre-RISC), which removes the passenger strand to generate a mature RISC [42]. Once the mature complex is formed, next binds to its target mRNA, leading to the silencing of the mRNA through mRNA cleavage or translational repression or deadenylation, depending on miRNA affinity to the mRNA

target. A single miRNA could have a large spectrum of target mRNAs, suggesting that miRNAs have a key regulatory role in a vast number of biological roles.

Expression profile of miRNAs is altered by DNA damage when cells are exposed to different types of genotoxic agents: UV radiation, IR, oxidative stress, and chemical mutagens [43]. During DNA damage there is differential expression of miRNAs, a subset of miRNAs are upregulated and another subset of miRNAs are downregulated. miRNA expression can return to the basal level 24 h after DNA damage. DNA damage induces alterations in miRNA expression at multiple levels including transcriptional regulation, post-transcriptional regulation, and degradation (Fig. 1). In turn miRNAs are required for almost every aspect of cellular responses to DNA damage, including sensing DNA damage, transducing damage signals, repairing damaged DNA, activating cell cycle checkpoints, and inducing apoptosis.

3.2 DNA Damage Regulates miRNAs both Transcriptionally and Post-transcriptionally

DNA damage activates transcription factors, such as p53, c-myc, and c-jun, which play a classic role in regulating miRNA expression. miRNA expression profiling of p53 wild-type cells and p53-deficient cells has suggested how intricate is transcriptional regulation of miRNAs and DNA damage through the mediation of p53 (Fig. 2) [44]. Differential expression of miRNAs was first to pick miR-34 family as transcriptional target of p53. Later various studies showed that DNA damage induces the miR-34 family in a p53-dependent manner [45]. p53 has important miRNA targets among which it transcriptionally activates miR-15a/16, miR-29, miR-107, miR-145, miR-192, miR-194, miR-215, and miR-605 and transcriptionally represses miR-17-92 (Fig. 2) [43]. By regulating their target genes, p53-induced miRNAs can modulate DDR and cell cycle progression after damage is induced. Notably, p53-induced miRNAs can in turn activate and stabilize p53, and this process forms a regulatory loop between these miRNAs and p53. Similar to p53, many other DDR transcription factors such as nuclear factor-kappa B (NF-kB), E2F1, c-jun, and Myc are involved in modulating miRNA expression. In the future, characterization of promoter regions of miRNA genes will help us comprehensively understand the interplay between DNA damage-induced transcriptional factor and miRNA expression.

Once the miRNAs are transcribed they need to be processed into their mature active forms. DNA damage can affect miRNA expression by regulating these essential steps of miRNA processing and maturation. DNA damage induces phosphoinositide 3-kinase (PI3K)-like protein kinases ATM, ATR, and DNA-PKcs, which later phosphorylate signaling cascade of DDR [46] and also play a central role in regulating miRNA expression after DNA damage. Studies have shown that DNA damage-induced miRNAs biogenesis can occur in an ATM-dependent manner. ATM activation can

phosphorylate KH-type splicing regulatory protein (KSRP), interacts with Drosha and Dicer. KSRP recognizes and binds to terminal loop of premature miRNAs and regulates their maturation in response to DNA damage. This ultimately leads to alterations in the expression of multiple miRNAs. BRCA1 is too activated by ATM after DNA damage and can directly interact with Drosha, DEAD box RNA helicase p68 (DDX5), and pri-miRNAs and facilitates their maturation [47]. Recently, ATM-activated AKT kinase was shown to phosphorylate Nup153, a key component of the nucleopore, that leads to its enhanced interaction with Exportin-5 (XPO5). Through this there is an increase in levels of export of precursor miRNAs (pre-miRNAs). Overall these studies demonstrate that DNA damage response can affect miRNA expression by regulating pre-miRNA maturation. The other two PI3K-like protein kinases, ATR and DNA-PKcs, have also been found to regulate miRNA expression after DNA damage. Drosha is known to interact with DGCR8 to form a microprocessor complex, which plays a key role in regulating the turnover of miRNA biogenesis. Additionally, IR activates the epidermal growth factor receptor/ERBB family of receptor tyrosine kinases, yielding enhanced activity of MAPK/Erk or PI3K/Akt pathway. Down the cascade both Akt and EGFR signaling modulates stability of Ago2 and Dicer-TRBP complex to affect miRNA maturation [48]. Yet another study reported that UV damage can trigger a cell cycle-dependent relocalization of Ago2 into stress granules and thus change miRNA levels.

Another form of miRNA regulation is by their degradation after DNA damage. Single-stranded miRNA can be degraded by the 5′–3′ exoribonuclease XRN2 or 3′–5′ exoribonuclease human polynucleotide phosphorylase. miRNAs binding to MCPIP1 can facilitate the process of pre-miRNA degradation [49]. Recently, nucleotidyl transferase PAP-associated domain containing 5 (PAPD5) and the poly(A)-specific ribonuclease PARN have been shown to work together to mediate 3′ adenylation and subsequent degradation of miR-21. However, the mechanism behind the degradation of miRNA by DNA damage is further to be elucidated.

3.3 miRNAs Regulated DDR Machinery Components

Reciprocally, miRNAs sense the DNA damage and respond with the modulation of DDR genes. For instance, H2AX is a well-established sensor protein that can detect and mark damaged DNA by its phosphorylated form (γ-H2AX), which provides a molecular platform to attract DDR machinery and repair the damage. Recent studies have shown that miR-24 and miR-138 directly target H2AX to modulate DDR [50]. miR-138 negatively regulates H2AX expression, thereby increases chromosomal instability after DNA damage. Studies have found out, overexpression of miR-138 inhibits HR-mediated DNA repair of DSBs and enhances cellular sensitivity to DNA-damaging agents, such as cisplatin, camptothecin, and IR. This effect was rescued with overexpression

of γ-H2AX [51]. These results suggest that miRNAs can regulate upstream DDR signaling.

miRNAs have potential to function as signal transducers by directly targeting kinases involved in DDR. For example, ATM has been shown to be a gene target of a variety of miRNAs, including miR-223, miR-181a, miR-26a, miR-27a, miR-214, and miR-18a [43]. These miRNAs enhance sensitivity to IR and etoposide by regulating the ATM-mediated signaling pathway. There are reports of miR-101 directly targeting DNA-PKcs, thereby sensitizing the non-small cell lung cancer cells to IR. miR-185 enhances radiosensitivity by regulating ATR. Collectively, these studies showed that miRNAs regulate DNA damage response by acting as signal transducers.

miRNAs have been shown to modulate DDR by targeting the effectors of DDR. They regulate cell cycle progression after DNA damage by targeting CHK1, retinoblastoma 1 serine phosphates from human chromosome 3 (RBSP3), cyclin D, CDC25a, p21, CDK2, WEE1, PLK1, etc. [43]. RBSP3 protein is a target of miR-100, cyclin D is a target of miR-34c, CHK1 is a target of miR-424, CDK4 and CDK6 are a target of miR-506, cyclin D1 and CDK4 are a target of miR-545, and all of these target proteins are crucial for progression through different cell cycle checkpoints. Thus, by regulating their expression, miRNAs play a vital role during the transformation of normal cells after DNA damage insults, potentially mastering the decision whether the cell proceeds with cell cycles despite genomic instability or opts for death through apoptosis or senescence [43] miRNAs are not only involved in regulating cell cycle proteins but also target multiple proteins involved in both DSB repair pathways, NHEJ and HRR (Fig. 3). For instance NHEJ component Ku70 is a target of miR-124. On similar lines HR repair key protein BRCA1 is targeted by miR-9, later sensitizes cells to cisplatin-induced DNA damage in ovarian cancer. Additional miRNAs such as miR-182, miR-146a, and miR-146b-5p have also been found to target BRCA1 (Fig. 3) [52].

4 Clinical Relevance of MicroRNAs in Cancer

MicroRNAs are ideal biomarkers owing to high stability under storage and handling conditions and their presence in blood, urine, and other body fluids. Specifically, detection of levels of microRNAs in blood plasma and serum has the potential for an earlier cancer diagnosis and to predict prognosis and response to therapy as their expression could reflect the information distributed on millions of target genes [53]. After the discovery of the association of miRNAs in development of human cancers, cell-free miRNAs (cfmiRNAs) have been shown to exist with remarkable stability in various types of body fluids, including blood [54] and

the advantages of using cfmiRNAs in cancer diagnosis include the low cost and comfort of the assays used for cfmiRNAs analysis, as well as the quick results using PCR-based methods from the first day of diagnosis and before any therapeutic intervention. Methods of detection, such as microarray analysis and deep-sequencing, enable a comprehensive profiling of cell-free miRNAs, even from low amounts of RNA samples. To enhance the sensitivity and specificity of biomarker panel's combinational use of multiple miRNAs are available. High and low expression levels of miRNA are linked with chemoresistance, suggesting that cfmiRNAs that originate from primary tumors or cells within the tumor microenvironment could be promising biomarkers to predict chemotherapeutic response. The valuation of multiple miRNA expression levels, also referred to as miRNA signatures, can accurately predict prognosis in various types of cancers [55].

Studies have shown that serum cfmiRNAs remain stable even after being subject to severe conditions that would generally degrade most miRNAs. Regardless of the presence of RNase activity in plasma, incubation of plasma at room temperature for up to 24 h or subjection to up to eight freeze-thaw cycles had minimal effect on cfmiRNA levels, In contrast, synthetic miRNAs added directly to plasma degrade rapidly [55]. In addition to this, identification of extracellular AGO2–miRNA complexes in plasma raises the possibility that cells release a functional miRNA-induced silencing complex into the blood [56]. Presently, a number of miRNA detection methods, including northern blotting, in situ hybridization, RT-PCR, microarray, and deep sequencing, are commonly used. Detection of cfmiRNAs is essentially the same as that of cellular miRNA, apart from the extremely low initial amount of starting material. Still, there are some sample-specific considerations.

Underneath, we summarize the advantages and limitations of the three major techniques for detecting cfmiRNAs and that include: qRT-PCR, microarray, and deep sequencing [57]. The advantages of RT-PCR are that it is highly sensitive and specific, it has high dynamic range, is suitable for quantification and there is no need for special equipment and also it is user and lab friendly; however, the limitations include low/medium throughput and it can detect only annotated miRNAs. While advantage of using microarray is that it is high-throughput and relatively low cost with the limitations of being not suitable for accurate quantification and can detect only annotated miRNAs and has low dynamic range. On the other hand, deep sequencing is used for the detection of novel miRNA and splicing variants (isomiRs) and it has the ability to distinguish similar sequences, with the limitations of being highly cost effective and requires special equipment and bioinformatician, with relatively high amount of starting material.

5 Clinical Relevance of miRNAs as Diagnostic and Prognostic Markers

Recently, small molecules or protein drugs, such as monoclonal antibodies, designed against molecules with deregulated activity, have been generated and used with conventional therapies [58, 59]. Due to their role microRNAs are considered target molecules and effective therapeutic options for cancer. MicroRNAs involved in the regulation of DNA damage/repair mechanisms can be considered markers to predict the response to therapy and can be employed in future to define personalized treatments [60]. In this respect, expression levels of miRNAs could be evaluated in serum and tumor specimens to make the treatment more effective. Several studies have documented the clinical relevance of cfmiRNAs as diagnostic and prognostic markers for a variety of cancers, using blood plasma or serum for their analyses [54]. To better understand, below are several studies discussing the utility of cfmiRNAs in gynecological cancers.

In patients with ovarian cancer, high serum levels of miR-34a were related to lymph node disease and distant metastases [61]. Additionally, upregulated serum levels of miR-221 and miR-21 were independent unfavorable prognostic factors significantly associated with the International Federation of Gynecology and Obstetrics (FIGO) stage and tumor grade [62]. Cervical squamous cell carcinoma patients have deregulated miRNAs levels that are related with lymph-node metastasis, acting as an important risk factor of disease progression and has been associated with tumor invasion. Decreased serum levels of miR-218 have been correlated with later stages cervical adenocarcinoma and lymph-node metastasis [63]. In another study, serum levels of miR-20a and miR-203 were analyzed in patients with stage I-IIA of cervical cancer. Of this panel, serum miR-20a alone could even discriminate between lymph node-positive and lymph node-negative tumors, with an AUC of 0.734, sensitivity of 75%, and specificity of 72% [64].

6 Conclusion

miRNAs play an essential role in several biological and pathological processes leading to cancer initiation, progression, and metastasis formation and are therefore key players in cell fate decisions and maintenance and hereby counteract the plasticity and de-differentiation processes underlying oncogenesis. The investigation of microRNA-modulated gene regulation in the DDR and its association in cancer pathogenesis and progression will help to better understand and describe the impact of these small molecules in DNA damage/repair mechanisms. The identification of miRNA-modulated genes and the effects of miRNAs deregulated functions

will make it promising to acquire information about the prognosis, the chemoresistance, and ultimately the response to therapeutic treatments in cancer. In conclusion, well-designed description of the network including proteins able to suppress or induce miRNAs as well as miRNAs and targets will deliver substantial information about prognosis and therapy of cancer. Although we still have a way to go in identifying key miRNAs of clinical significance in various cancers, the rapid progress in the field will help many preclinical projects to humans in the near future.

References

1. Ciccia A, Elledge SJ (2010) The DNA damage response: making it safe to play with knives. Mol Cell 40(2):179–204
2. Jackson SP, Bartek J (2009) The DNA-damage response in human biology and disease. Nature 461(7267):1071–1078
3. d'Adda di Fagagna F et al (2003) A DNA damage checkpoint response in telomere-initiated senescence. Nature 426 (6963):194–198
4. Freund A et al (2010) Inflammatory networks during cellular senescence: causes and consequences. Trends Mol Med 16(5):238–246
5. Curtin NJ (2012) DNA repair dysregulation from cancer driver to therapeutic target. Nat Rev Cancer 12(12):801–817
6. Tubbs JL, Pegg AE, Tainer JA (2007) DNA binding, nucleotide flipping, and the helix-turn-helix motif in base repair by O 6-alkylguanine-DNA alkyltransferase and its implications for cancer chemotherapy. DNA Repair 6 (8):1100–1115
7. Dolan ME, Moschel RC, Pegg AE (1990) Depletion of mammalian O6-alkylguanine-DNA alkyltransferase activity by O6-benzylguanine provides a means to evaluate the role of this protein in protection against carcinogenic and therapeutic alkylating agents. Proc Natl Acad Sci 87(14):5368–5372
8. Rabik CA, Njoku MC, Dolan ME (2006) Inactivation of O 6-alkylguanine DNA alkyltransferase as a means to enhance chemotherapy. Cancer Treat Rev 32(4):261–276
9. Friedman HS et al (1998) Phase I trial of O6-benzylguanine for patients undergoing surgery for malignant glioma. J Clin Oncol 16 (11):3570–3575
10. Esteller M et al (1999) Inactivation of the DNA repair gene O6-methylguanine-DNA methyltransferase by promoter hypermethylation is a common event in primary human neoplasia. Cancer Res 59(4):793–797
11. Hegi ME et al (2005) MGMT gene silencing and benefit from temozolomide in glioblastoma. N Engl J Med 352(10):997–1003
12. Naegeli H, Sugasawa K (2011) The xeroderma pigmentosum pathway: decision tree analysis of DNA quality. DNA Repair 10(7):673–683
13. Andressoo J-O, Hoeijmakers JH, de Waard H (2005) Nucleotide excision repair and its connection with cancer and ageing. Adv Exp Med Biol 570:45–83
14. Usanova S et al (2010) Cisplatin sensitivity of testis tumour cells is due to deficiency in interstrand-crosslink repair and low ERCC1-XPF expression. Mol Cancer 9(1):1
15. Lindahl T (1993) Instability and decay of the primary structure of DNA. Nature 362 (6422):709–715
16. Wiseman H, Halliwell B (1996) Damage to DNA by reactive oxygen and nitrogen species: role in inflammatory disease and progression to cancer. Biochem J 313(Pt 1):17
17. De Vos M, Schreiber V, Dantzer F (2012) The diverse roles and clinical relevance of PARPs in DNA damage repair: current state of the art. Biochem Pharmacol 84(2):137–146
18. El-Khamisy SF et al (2003) A requirement for PARP-1 for the assembly or stability of XRCC1 nuclear foci at sites of oxidative DNA damage. Nucleic Acids Res 31(19):5526–5533
19. Larsen E et al (2007) Organ and cell specificity of base excision repair mutants in mice. Mutat Res 614(1):56–68
20. Shaw EG et al (2012) Randomized trial of radiation therapy plus procarbazine, lomustine, and vincristine chemotherapy for supratentorial adult low-grade glioma: initial results of RTOG 9802. J Clin Oncol 30(25):3065–3070
21. Umar A et al (2004) Revised Bethesda Guidelines for hereditary nonpolyposis colorectal cancer (Lynch syndrome) and microsatellite instability. J Natl Cancer Inst 96(4):261–268

22. Ham MF et al (2006) Impairment of double-strand breaks repair and aberrant splicing of ATM and MRE11 in leukemia–lymphoma cell lines with microsatellite instability. Cancer Sci 97(3):226–234
23. Vilenchik MM, Knudson AG (2003) Endogenous DNA double-strand breaks: production, fidelity of repair, and induction of cancer. Proc Natl Acad Sci 100(22):12871–12876
24. Mahaney BL, Meek K, Lees-Miller SP (2009) Repair of ionizing radiation-induced DNA double-strand breaks by non-homologous end-joining. Biochem J 417(3):639–650
25. Shrivastav M, De Haro LP, Nickoloff JA (2008) Regulation of DNA double-strand break repair pathway choice. Cell Res 18 (1):134–147
26. Deans AJ, West SC (2011) DNA interstrand crosslink repair and cancer. Nat Rev Cancer 11 (7):467–480
27. Evers B, Helleday T, Jonkers J (2010) Targeting homologous recombination repair defects in cancer. Trends Pharmacol Sci 31 (8):372–380
28. Choudhury A et al (2009) Targeting homologous recombination using imatinib results in enhanced tumor cell chemosensitivity and radiosensitivity. Mol Cancer Ther 8 (1):203–213
29. Shiloh Y (2003) ATM and related protein kinases: safeguarding genome integrity. Nat Rev Cancer 3(3):155–168
30. Bartek J, Lukas J (2007) DNA damage checkpoints: from initiation to recovery or adaptation. Curr Opin Cell Biol 19(2):238–245
31. Falck J, Coates J, Jackson SP (2005) Conserved modes of recruitment of ATM, ATR and DNA-PKcs to sites of DNA damage. Nature 434(7033):605–611
32. Bartkova J et al (2005) DNA damage response as a candidate anti-cancer barrier in early human tumorigenesis. Nature 434 (7035):864–870
33. Fan C et al (2006) ATM activation is accompanied with earlier stages of prostate tumorigenesis. Biochim Biophys Acta 1763 (10):1090–1097
34. Larsson L-G (2011) Oncogene-and tumor suppressor gene-mediated suppression of cellular senescence. Semin Cancer Biol 21 (6):367–376
35. Wang H et al (2015) DNA damage checkpoint recovery and cancer development. Exp Cell Res 334(2):350–358
36. Vriend LE et al (2013) WEE1 inhibition and genomic instability in cancer. Biochim Biophys Acta 1836(2):227–235
37. Strebhardt K, Ullrich A (2006) Targeting polo-like kinase 1 for cancer therapy. Nat Rev Cancer 6(4):321–330
38. Van Vugt MA, Brás A, Medema RH (2004) Polo-like kinase-1 controls recovery from a G2 DNA damage-induced arrest in mammalian cells. Mol Cell 15(5):799–811
39. Smith MR et al (1997) Malignant transformation of mammalian cells initiated by constitutive expression of the polo-like kinase1. Biochem Biophys Res Commun 234 (2):397–405
40. Lee Y et al (2003) The nuclear RNase III Drosha initiates microRNA processing. Nature 425(6956):415–419
41. Lund E et al (2004) Nuclear export of microRNA precursors. Science 303(5654):95–98
42. Chang H et al (2014) TAIL-seq: genome-wide determination of poly (A) tail length and 3′ end modifications. Mol Cell 53(6):1044–1052
43. Zhang C, Peng G (2015) Non-coding RNAs: an emerging player in DNA damage response. Mutat Res Rev Mutat Res 763:202–211
44. He L et al (2007) A microRNA component of the p53 tumour suppressor network. Nature 447(7148):1130–1134
45. Cheng C-Y et al (2014) miR-34 cooperates with p53 in suppression of prostate cancer by joint regulation of stem cell compartment. Cell Rep 6(6):1000–1007
46. Ashley AK et al (2014) DNA-PK phosphorylation of RPA32 Ser4/Ser8 regulates replication stress checkpoint activation, fork restart, homologous recombination and mitotic catastrophe. DNA Repair 21:131–139
47. Kawai S, Amano A (2012) BRCA1 regulates microRNA biogenesis via the DROSHA microprocessor complex. J Cell Biol 197 (2):201–208
48. Zeng Y et al (2008) Phosphorylation of Argonaute 2 at serine-387 facilitates its localization to processing bodies. Biochem J 413 (3):429–436
49. Lin CL et al (2012) Crystal structure of human polynucleotide phosphorylase: insights into its domain function in RNA binding and degradation. Nucleic Acids Res 40(9):4146–4157
50. Srivastava N et al (2011) miR-24-2 controls H2AFX expression regardless of gene copy number alteration and induces apoptosis by targeting antiapoptotic gene BCL-2: a potential for therapeutic intervention. Breast Cancer Res 13(2):R39
51. Wang Y et al (2011) MicroRNA-138 modulates DNA damage response by repressing histone H2AX expression. Mol Cancer Res 9 (8):1100–1111

52. Chang S, Sharan SK (2012) BRCA1 and microRNAs: emerging networks and potential therapeutic targets. Mol Cells 34(5):425–432
53. Pritchard CC, Cheng HH, Tewari M (2012) MicroRNA profiling: approaches and considerations. Nat Rev Genet 13(5):358–369
54. Cortez MA et al (2011) MicroRNAs in body fluids—the mix of hormones and biomarkers. Nat Rev Clin Oncol 8(8):467–477
55. Dvinge H et al (2013) The shaping and functional consequences of the microRNA landscape in breast cancer. Nature 497 (7449):378–382
56. Arroyo JD et al (2011) Argonaute2 complexes carry a population of circulating microRNAs independent of vesicles in human plasma. Proc Natl Acad Sci 108(12):5003–5008
57. Schwarzenbach H et al (2014) Clinical relevance of circulating cell-free microRNAs in cancer. Nat Rev Clin Oncol 11(3):145–156
58. Jonker DJ et al (2007) Cetuximab for the treatment of colorectal cancer. N Engl J Med 357 (20):2040–2048
59. Ferrara N, Hillan KJ, Novotny W (2005) Bevacizumab (Avastin), a humanized anti-VEGF monoclonal antibody for cancer therapy. Biochem Biophys Res Commun 333(2):328–335
60. Zhao L et al (2012) Regulatory mechanisms and clinical perspectives of miRNA in tumor radiosensitivity. Carcinogenesis 33 (11):2220–2227
61. Schwarzenbach H, Hoon DS, Pantel K (2011) Cell-free nucleic acids as biomarkers in cancer patients. Nat Rev Cancer 11(6):426–437
62. Hong F et al (2013) Prognostic significance of serum microRNA-221 expression in human epithelial ovarian cancer. J Int Med Res 41 (1):64–71
63. Yu J et al (2012) Circulating microRNA-218 was reduced in cervical cancer and correlated with tumor invasion. J Cancer Res Clin Oncol 138(4):671–674
64. Zhao S et al (2013) Circulating miRNA-20a and miRNA-203 for screening lymph node metastasis in early stage cervical cancer. Genet Test Mol Biomarkers 17(8):631–636

Chapter 2

MicroRNAs in Breast Cancer: Diagnostic and Therapeutic Potential

Asia Asiaf, Shiekh Tanveer Ahmad, Wani Arjumand, and Mohammad Afzal Zargar

Abstract

MicroRNAs (miRNAs) are a large family of small, approximately 20–22 nucleotide, noncoding RNAs that regulate the expression of target genes, at the post-transcriptional level. miRNAs are involved in virtually diverse biological processes and play crucial roles in cellular processes, such as cell differentiation, proliferation, and apoptosis. Accumulating lines of evidence have indicated that miRNAs play important roles in the maintenance of biological homeostasis and that aberrant expression levels of miRNAs are associated with the onset of many diseases, including cancer. It is possible that the diverse roles that miRNAs play, have potential to provide valuable information in a clinical setting, demonstrating the potential to act as both screening tools for the stratification of high-risk patients, while informing the treatment decision-making process. Increasing evidence suggests that some miRNAs may even provide assistance in the diagnosis of patients with breast cancer. In addition, miRNAs may themselves be considered therapeutic targets, with inhibition or reintroduction of a particular miRNA capable of inducing a response in-vivo. This chapter discusses the role of miRNAs as oncogenes and tumor suppressors in breast cancer development and metastasis. It focuses on miRNAs that have prognostic, diagnostic, or predictive potential in breast cancer as well as the possible challenges in the translation of such observations to the clinic.

Key words MicroRNA, Breast cancer, Oncogenic miRNA, Tumor suppressor miRNA

1 Introduction

MicroRNAs (miRNAs) are short noncoding RNAs 20–24 nucleotides in length that play important role in virtually all biological pathways in mammals and other multicellular organisms [1]. These miRNAs account for 1–2% of the human genome and are highly conserved in nearly all organisms [2]. Under normal conditions, miRNAs are fundamental regulators of cellular processes that have physiological significance, including cell proliferation, differentiation, and apoptosis [3, 4]. Deregulation of a single or small subset of miRNAs has been reported to have a profound effect on the expression pattern of several hundred mRNAs [5, 6] which can lead

Wei Wu (ed.), *MicroRNA and Cancer: Methods and Protocols*, Methods in Molecular Biology, vol. 1699,
DOI 10.1007/978-1-4939-7435-1_2,

the cells toward transformation [7, 8]. Their role of miRNAs in human cancer is further supported by the fact that more than 50% of human miRNAs are localized in fragile chromosomal regions associated with amplifications, deletions, or translocations that occur during tumor development. The first definitive demonstration of involvement of miRNAs in human cancer came from molecular studies characterizing the 13q14 deletion in human chronic lymphocytic leukemia (CLL), which revealed that this smallest region of deletion contained two clustered miRNAs, miR-15a and miR-16-1. Subsequently, the expression of these miRNAs was found to be downregulated or lost in 50–60% of human CLL [9]. Following this initial finding, the altered miRNA expression levels have subsequently been detected by different groups in many types of human tumors, e.g., miR-21 is upregulated in glioblastoma [10]. This gene was found to be expressed at a 5–100-fold higher rate in gliomas than in normal tissue. miRNA-155 is upregulated 100-fold in Hodgkin lymphoma, in pediatric Burkitt lymphoma, and in primary mediastinal and diffuse large-B-cell lymphomas. miR-155 has also been reported to be upregulated in breast carcinomas, which indicates that there are additional roles for this gene outside of the hematopoietic system [11]. Taken together, these data demonstrate that miRNAs play a double role in cancer, behaving both as tumor suppressors (as is the case for *miR-15*a and *miR-16-1*) or oncogenes (as is the case for *miR-155* or members of the *miR-17–92* cluster). In breast cancer, a number of miRNAs have been identified as tumor suppressors or oncogenes and have been characterized as critical regulators of tumor initiation, metastasis, and chemoresistance.

2 Biosynthesis of miRNA

The biogenesis of miRNA is schematically presented in Fig. 1. Generally, miRNAs genes are transcribed as pri-miRNA precursor by RNA polymerase II, either as separate transcriptional units or located within the introns of protein coding genes. The pri-miRNAs are processed in the nucleus by the endonuclease, Drosha, and the double-stranded RNA-binding protein, Pasha (also known as DGCR8), into ~70-nucleotide pre-miRNAs, which fold into imperfect stem-loop structures [12, 13]. The pre-miRNAs are then exported into the cytoplasm by the RAN GTP-dependent transporter exportin 5 [14–16], where a cytoplasmic RNAse III enzyme, Dicer, cleaves them into a double-stranded RNA of ~22 nucleotides in length, referred to as the miRNA:miRNA* duplex [17–19]. Subsequently, the miRNA:miRNA* duplex is incorporated into the multiprotein RNA-induced silencing complex (miRISC), holding key proteins such as AGO2 and GW182. The mature miRNA strand is preferentially retained in the

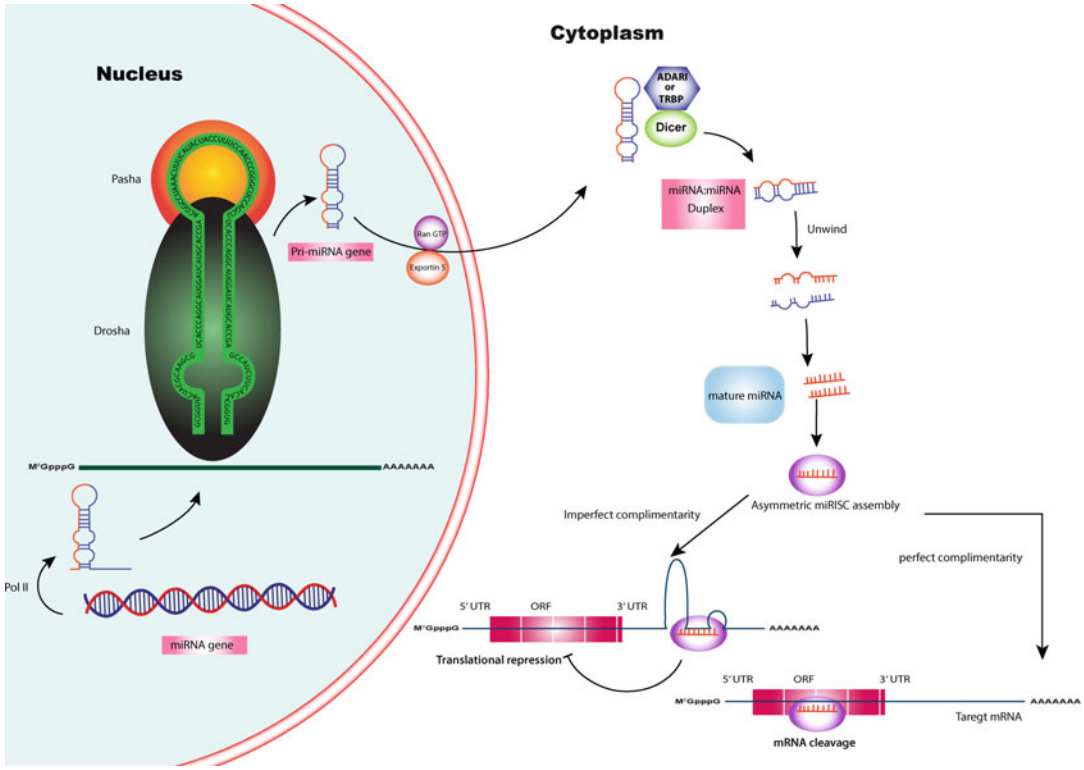

Fig. 1 The first step toward the generation of MicroRNA (miRNA) genes generally involves the transcription by RNA Polymerase II (Pol II) within the nucleus to form large pri-miRNA transcripts, which are then capped (^{7}MGpppG) and polyadenylated (AAAAA). Later these pri-miRNA transcripts are processed by the RNase III enzyme Drosha-DGCR8 and its co-factor, Pasha, to about 70-nucleotide pre-miRNA precursor. RAN–GTP and exportin 5 transport the pre-miRNA into the cytoplasm. Inside the cytoplasm RNase III enzyme, Dicer and RNA-binding protein (TRBP) or adenosine deaminase acting on RNA 1 (ADAR1) process the pre-miRNA to generate a transient 22-nucleotide miRNA:miRNA duplex. This duplex is then loaded into the miRNA-associated multi-protein RNA-induced silencing complex (miRISC) (*light purple*). One of the two miRNA strands in the duplex is selected as a guide strand, whereas the complementary strand (miRNA) is usually degraded. The mature miRNA within the miRISC then binds to complementary sites in the mRNA target to negatively regulate gene expression in one of two ways that depend on the degree of complementarity between the miRNA and its target. miRNAs that bind to mRNA targets with imperfect complementarity block target gene expression at posttranslational level. Complementary sites for miRNAs using this mechanism are generally found in the 3′ untranslated regions (3′ UTRs) of target mRNAs. miRNAs that bind to their mRNA targets with nearly perfect complementarity induce target-mRNA cleavage, e miRNAs using this mechanism bind to miRNA complementary sites that are generally found in the coding sequence or open reading frame (ORF) of the mRNA target

functional miRISC complex and negatively regulates its target genes. The mature miRNA recognizes its complementary sequences in the 3′ untranslated region (UTR) of their target mRNAs via seed region, typically positions 2–7 in the miRNA. However, the recent studies have suggested that miRNAs can bind to 5′ UTR or open reading frame (ORF) of the target mRNA [20, 21]. In mammals, miRNAs are predicted to regulate

more than 50% of all protein-coding genes. They regulate gene expression through a posttranscriptional mechanism either by translational repression or by degradation of the target mRNA. In most cases, miRNAs bind only in part to their complementary target mRNA sequence [22]. While the incomplete complementary binding leads to repression of translation or deadenylation of the target mRNA, a complete complementary binding leads to direct mRNA cleavage and degradation of the target. Growing body of evidence indicates that miRNAs can also serve as activators of gene expression by targeting gene regulatory sequences. Target sites for these miRNAs have been found in gene promoters, and these complementary sequences are as common as those within the 3′ UTR of mRNAs [23]. For example, a putative target site for miR-373 has been identified in the promoter of E-cadherin, and transfection of miR-373 and its precursor hairpin RNA into cells of the prostate carcinoma cell line PC-3 induced E-cadherin expression [24].

3 Deregulation of MicroRNAs in Breast Cancer

According to the International Agency for Research on Cancer (IARC) (http://www.iarc.fr/) statistics, in 2012, 1.7 million women (11.9%) were diagnosed with breast cancer and 6.3 million women were alive who had been diagnosed with breast cancer in the past 5 years. Breast cancer is still the most common cause of cancer death among women, accounting for 522,000 deaths in 2012 [25]. Technological advancements in the last decade have helped the researches to understand this complex disease more thoroughly. Based on gene expression profile and the phenotype, the breast cancer can be divided into six major. The six major subtypes are luminal A, luminal B, tumor enriched with human epidermal growth factor receptor 2 (Her2), basal-like, normal-like, and claudin-low subtype [26, 27]. Histologically, breast cancer can be divided into in situ and invasive carcinoma, both of which can be further subdivided into ductal and lobular subtypes. Regardless of vast improvement in the overall prognosis and survival rate of patients with noninvasive breast cancer, advanced metastatic breast carcinoma remains a life-threatening disease. To develop more effective treatments, it is essential to understand the molecular mechanisms underlying breast tumor development and the acquisition of malignancy. Scientists have been trying to elucidate the molecular mechanisms that cause cancer development and cancer prevention. Various studies suggest that miRNAs play a critical role in breast cancer [28–32]. An early study of miR expression profiling in 86 breast tumors and normal tissues identified numerous miRs dysregulated in breast cancer, and generated a signature capable of discriminating between normal and malignant breast tissues [11].

Subsequently Blenkiron and colleagues profiled 309 miRNAs in 93 breast tumors, derived signatures that distinguish between molecular subtypes, and validated their classification power in an external data set [33], and also demonstrated significant associations between the expression of several miRs and clinicopathological features of disease. Other smaller studies have generated signatures that accurately predict hormone receptor status [34, 35]. These results suggest that there is a potential role for miRNAs not only to facilitate in the diagnosis, prognosis, and predictions in treatment responses, but also to function as novel therapeutic targets and replacement therapies. Although a plethora of miRNAs have been reported to be implicated in breast cancer initiation, progression, and/or metastasis, it is beyond the scope of this chapter to attempt a detailed discussion of all miRs that are implicated in breast cancer. In this chapter, we attempt to provide an overview of our current knowledge about the miRNAs, their functions as tumor suppressors or oncogenes in human breast cancer and briefly discuss their applications to clinical approaches, especially their potential to be diagnostic markers and therapeutic targets.

4 Oncogenic miRNAs

Oncogenic miRNAs are frequently overexpressed in cancer and they exert their oncogenic potential by repressing the expression of tumor suppressor gene/s mainly involved in apoptosis, cell proliferation, cell invasion or metastasis, and stimulating oncogenic transcription factors [36]. Following are the few important miRNAs and miRNA families that have been extensively studied and established as oncomirs in breast cancer.

4.1 miR-10 Family

miRNA-10 family consists of miR-10a and miR-10b, is situated within the homeobox (Hox) clusters of genes. Since they are co-regulated with Hox genes and target Hox transcripts, it is likely that this miRNA family may play pivotal roles during the development process [37]. miR-10 family has been reported to be upregulated in numerous cancers including glioblastoma [38], liver, colon cancer [39], acute myeloid leukemia [40], melanoma [41], pancreatic cancer [42], and hepatocellular carcinoma [43].

In case of breast cancer, miR-10 family is reported to be involved in both the development and metastasis through miR-10a and miR-10b, respectively [41]. miR-10b is highly overexpressed in metastatic breast cancer cells and induces cell migration and invasion in murine xenograft model of breast cancer via targeting HOXD10 gene [44]. The mechanisms of tumor metastasis and invasive functions of miR-10b appear to be dependent on cell type and pattern of expression of its targets in a given cell type. Overexpression of miR-10b leading to cancer metastasis has been

associated with the metastasis-promoting transcription factor Twist that induces epithelial-to-mesenchymal transition (EMT) [44]. E-cadherin, another important determinant of EMT, has also been proposed to be a target of miR-10b [45]. Thus, it appears that miR-10b influences metastasis through a complex regulation of multiple factors that determine EMT. Chang et al., reported a trend toward increased expression of miR-10a in breast tumors compared to matched tumor associated normal tissues. This study implicated both miR-10a/b expression to be associated with adverse outcomes for breast cancer patients [46]. A study by Pogribny et al. also showed higher expression of miR-10a in breast cancer MCF-7 cell lines with an inbuilt resistance to cisplatin. This analysis also identified a potential role for miR-10a in the regulation of cellular proteins, including homeobox family HOXD10, tumor suppressor p27, and ER-alpha (ERα) [47]. Similarly, another recent study identified role of miR10b in resistance to tamoxifen through down-regulation of HDAC4 [48]. The other reported downstream targets for miR-10b include T-lymphoma invasion and metastasis-1 factor [49], stress-induced cell surface molecule MICB [50], tat-interacting protein 30 [51], etc.

However, the role of miR-10a as an oncomir in the context of breast cancer is controversial as its expression has recently been shown to display tumor suppressor roles. Elevated miR-10a expression in estrogen receptor (ER)-positive tumors was associated with a longer relapse-free time following Tamoxifen treatment [52]. Reduced expression of miR-10a has been reported in breast cancer [53, 54].

One further feature of miR-10 activity is particularly surprising; miR-10a induces, rather than inhibits, protein expression through binding to cellular transcripts via their 5′ UTRs [20]. This shows that miR-10a binding to the 5′ UTR results in mechanistic effects deviating from 3′ UTR binding. 5′ UTRs of several Terminal OligoPyrimidine tract (TOP) mRNAs, which encode ribosomal protein and translation initiation factors, have been reported to have noncanonical binding sites for miR-10a. These studies suggest that miR-10a may positively control global protein synthesis via the stimulation of ribosomal protein mRNA translation and ribosome biogenesis and hereby affect the ability of cells to undergo transformation.

4.2 miR21

miR-21 was one of the first oncogenic miRs to be characterized, being frequently overexpressed in numerous tumors, a finding initially made in glioblastoma [10] and soon afterward in breast cancer [11], lung cancer [55], and chronic lymphocytic leukemia [56]. Previous studies have demonstrated that miR-21 played a key role in tumor progression and metastasis [57–59]. Overall (i.e., tumor lysate-derived) miR-21 expression is a marker of poor prognosis in breast tumors and correlates with advanced stage, and

metastasis, and with poor survival independently of grade and stage, and with recurrence of breast cancer [60–62]. Functional studies showed that knockdown of miR-21 inhibits MCF7-derived tumor growth in xenograft models via reduced proliferation and increased apoptosis, and Bcl-2 is implicated as a possible miR-21 target [59]. Additional analysis of metastatic MDA-MB-231 breast cancer cells demonstrated that knockdown of miR21 results in decreased invasion and lung metastasis [63]. This investigation identified two more targets of miR-21, which are programmed cell death-4 (PDCD4) and maspin [63]. PDCD4 and maspin both negatively enhance invasion and metastasis and thereby provide more targets for miR-21 in human breast cancers. The other targets of miR21 include tropomyosin 1 (TPM1), which suppresses anchorage-independent growth in vitro [64], tumor suppressor gene phosphatase and tensin homolog (PTEN) [60], and Sprouty2 (SPRY2) [65]. Further studies should explore miR-21 targets in order to appreciate the benefit of targeted therapy for breast cancer.

4.3 miR-17-92

The *miR-17-92* cluster produces a single polycistronic transcript that yields six individual mature miRNAs, including miR-17, 18a, 19a, 20, 19b, and 92 and is located at chromosome 13q31. Based on the sequence homology and seed conservation, the six *mir-17-92* components belong to four distinct miRNA families, *miR-17* (including *miR-17* and *20*), *miR-18*, *miR-19* (including *miR-19a* and *19b*), and *miR-92* family. *miR-17-92* is an oncogene with pleiotropic functions in regulating multiple cellular processes that contribute to tumor development. Its upregulation in tumor cells evades apoptotic response, enhances cell proliferation, triggers angiogenesis, blocks differentiation, and promotes metastasis. *miR-17-92* is also highly enriched in a variety of hematopoietic malignancies [66], as well as multiple solid tumor types including breast cancer [39, 66]. miR-17-5p was shown to be highly expressed in invasive MDA-MB-231 breast cancer cells but not in noninvasive MCF-7 breast cancer cells. Ectopic expression of this miRNA in MCF-7 cells induced invasive and migratory abilities by targeting HBP1/β-catenin pathway. Similarly, downregulation of endogenous miR-17-5p suppresses the migration and invasion of MDA-MB-231 cells in vitro [67]. Deep sequencing of triple negative breast cancer (TNBC) samples also revealed a threefold increase of miR-17/92 levels [68]. This cluster is also found to be relatively upregulated in basal tumors [33]. Interestingly, these tumors are frequently deficient in the tumor-suppressing PI3-kinase signaling regulator PTEN [69], and PTEN has been shown to be targeted by miR-19 in multiple cell types [70]. So possibly miR-19 is oncogenic, especially in ER-negative tumors.

It was surprising to find that the miR-17-92 cluster could act as a tumor suppressor in some circumstances. Loss of heterozygosity at 13q12-q13 is associated with multiple tumor progression and

weak prognosis, including breast cancer, retinoblastoma, squamous cell carcinoma of the larynx, nasopharyngeal carcinoma, and hepatocellular carcinoma [71]. The likelihood of such is further supported by the occurrence of heterozygous deletion of *miR-17-92* in the tissues of ovarian cancer, breast cancer, and melanomas [41]. The evidence for roles of mir 17-92 as an oncogene in cancer is overwhelming, so this paradoxical tumor suppressive role of *miR-17-92* remains to be determined. Furthermore, enforced *miR-17* expression also reduced proliferation in breast cancer cells, at least in part, due to repression of the AIB1 gene [72]. Yu et al. demonstrated that Cyclin D1, which has been demonstrated as an oncogenic protein in breast cancer cell, is negatively regulated by *miR-17-5p* and *miR-20a* [73], which itself induces the expression of the cluster, forming a novel regulatory feedback loop. These unexpected findings revealed the biological context-specific flexibility of *miR-17-92* functions, which is likely dictated by the target specificity and the extent of posttranscriptional repression.

4.4 miR-155

The miR-155 is overexpressed in multiple human carcinomas, including breast cancer [39]. It is an effective suppressor of the execution phase of apoptosis, due to its action on caspase 3 [74]. Recent studies have investigated the targets of miR-155. The tumor-suppressor gene suppressor of cytokine signaling 1 (*SOCS1*) has been demonstrated to be the target of miR-155 in breast cancer cell lines [75, 76]. The expression of *SOCS1* was found to be inversely correlated to miR-155 expression in human breast cancer cells. Ectopic expression of miR-155 also significantly promoted proliferation of breast cancer cells and the development of tumors in vivo. Furthermore, inhibition of SOCS1 inversely correlated to pro-tumorigenesis function of miR-155, which indicates that miR-155 negatively regulates *SOCS1*. Another study in normal mouse mammary gland epithelial cells (NMuMG cells) also showed that miR-155 is upregulated by the TGF-β pathway and mediates TGF-β-induced epithelial-to-mesenchymal transition (EMT) and cell invasion [77]. Researchers have found that the ectopic expression of miR-155 in NMuMG cells induces tight junction dissolution and promotes cell migration and invasion. Furthermore, the ectopic expression of miR-155 inhibits the expression of *RhoA*, a prometastatic gene regulating EMT in a multiphasic manner. These results indicate that miR-155 is regulated by the TGF-β/smad pathway and also downregulates the RhoA protein expression to enhance the acquisition of EMT phenotype. Also, by demonstrating that miR-155 is highly expressed in invasive tumors but not in noninvasive cancer samples, it was shown that miR-155 is linked to cancer invasiveness in human breast cancers [78]. Therefore, the miR-155 appears to play an essential role in breast cancer metastasis due to its implications in the acquisition of EMT and increased potential for invasion and metastasis.

Another role of miR-155 in the regulation of cell survival is seen through the downregulation of its direct target FOXO3a in breast cancer. Ectopic expression of miR-155 induced cell survival and chemoresistance to several agents, while the knockdown of miR-155 led to apoptosis and increased chemosensitivity [79]. In this investigation, it was found that overexpression of miR-155 led to repression of FOXO3a protein without changing mRNA levels, and the knockdown of miR-155 resulted in increased FOXO3a expression. This study revealed that there is an inverse correlation between miR-155 and FOXO3a, suggesting that miR-155 inhibition could present a promising therapeutic potential for breast cancer.

5 Tumor Suppressor MicroRNAs

Tumor-suppressor miRNAs are underexpressed in cancer cells and suppress oncogene expression, thereby controlling cellular differentiation, proliferation, etc. [36]. In regard to the global downregulation of miRNAs in cancer, it is worth mentioning that the majority of miRNAs have a tumor-suppressive function, some of which exhibit anti-metastatic properties as well.

5.1 Let-7 Family

Let-7 was discovered in *Caenorhabditis elegans* as an essential factor for cell type determination during embryogenesis and is conserved throughout the animal phyla [80]. Let-7 miRNAs comprise one of the largest and most highly expressed families of miRNAs, possessing potentially anti-carcinogenic properties in a variety of tissues [81]. The let-7 family consists of 10 members identified in humans, including let-7a, let-7b, let-7c, let-7d, let-7e, let-7f, let-7g, let-7i, miR-98, and miR-202. Let-7 exerts its anti-carcinogenic activity through transcriptional repression of many onco-fetal mRNAs and other pro-proliferative and/or pro-metastatic targets, such as NR6A1, IGF2BP1, IGF2BP2, and HMGA2 [82–84]. In normal physiology, let-7 is involved in muscle formation, cell adhesion, and regulation of gene expression and development. Let-7 miRNA family biogenesis is tightly regulated by cellular factors that regulate processing by DGCR8/DROSHA in the nucleus and by DICER1 cleavage in the cytoplasm. Most notable are LIN28A and LIN28B, which negatively regulate let-7 family miRNAs via their RNA-binding domains (RBDs) [85, 86]. LIN28A works in concert with TRIM25 and TUT4 to mediate oligo-uridylation at the 3′ terminal of pre-let-7 and its subsequent degradation [87, 88]. LIN28B is believed to sequester pri-let-7 miRNAs within the nucleolus and blocks its processing by DGCR8 and DROSHA [87]. Let-7 family expression is downregulated in many tumors, including lung cancer [89], gastric cancer [90], colon cancer [91], and Burkitt lymphoma [92]. In breast cancer it is lost at an early

stage of disease progression [93]. Yu et al. investigated the role of let-7 in distinguishing breast tumor-initiating cells (BT-IC) from other differentiated progeny. Let-7 family miRNAs were found to be markedly reduced in BT-IC and increased with differentiation. Restoration of let-7 in BT-IC resulted in reduced proliferation, mammosphere formation, and the proportion of undifferentiated cells in vitro and reduced metastasis in vivo by silencing its target genes H-Ras (transforming protein p21) and HMGA2 (high-mobility group AT-hook 2). On the other hand, when let-7 was antagonized, non-BT-IC experienced higher self-renewal ability. This research suggests that let-7 affects self-renewal ability of cancer cells, so cancer therapy by targeting let-7 in breast cancer patients could be beneficial and could serve as a novel treatment option [94].

Another proposed role for let-7 is its involvement in signaling through estrogen receptor. Previous research revealed that estradiol (E2) stimulates expression of eight members of the let-7 family [95]. Recent analysis reported that there is an inverse association between the expression of ER-alpha and various members of the let-7 family [96]. The let-7 family miRNAs were found to be downregulated in human breast cancer cells at stages of ductal carcinoma in situ (DCIS) and invasive ductal carcinoma (IDC) in comparison to the benign stage. Overexpression of let-7 family members in ER-positive cells resulted in downregulated ER-alpha activity, reduced cell proliferation, and induced apoptosis.

5.2 miR-200 Family

miR-200 family comprises five members that include miR-200a, miR-200b, miR-200c, miR-141, and miR-429. miR-200 family members are potent inhibitors of EMT, which is in part mediated through the regulation of E-cadherin, transcriptional repressors ZEB1 (also known as deltaEF1) and ZEB2 (also known as SIP1) [97–99]. miR-200 family was found to be lost in invasive breast cancer cell lines with mesenchymal phenotypes and also in regions of metaplastic breast cancer specimens lacking E-cadherin. Enforced constitutive expression of miR-200 in mesenchymal cells significantly increased E-cadherin expression and altered cell morphology to an epithelial phenotype [98, 99]. miR-200c represses breast cancer cell migration, stress fiber formation, migration, invasion and elongation and thus, metastasis by targeting actin-regulatory proteins FHOD1 and PPM1F [100]. Several reports have linked low miR-200 levels with aggressiveness and increased chemotherapy resistance in breast cancer [101]. However, the role of miR-200 family in breast cancer metastasis still remains controversial. Although mounting evidence suggests that miR-200 family regulates the E-cadherin expression and EMT transition, this does not necessarily predict the invasiveness and metastatic potential. miR-200 family has been shown to regulate BMI1, PLCG1, FAP-1, TGF-β2, and Suz12, hence acting as

tumors suppressor [102]. On the other hand, miR-200 that promotes a mesenchymal to epithelial cell transition (MET) by inhibiting ZEB2 expression, overexpression of this miRNA in mouse breast cancer cell lines unexpectedly promotes distant metastasis [103]. Korpal et al. also strengthen this concept in clinical and experimental models of breast cancer metastasis. Ectopic expression of miR-200 family in weakly metastatic 4TO7 cells enhances metastasis in part through downregulation of Sec23a [104]. This suggests a dual role for miR-200 family members in breast cancer progression. Evidently more robust investigations are needed to define its role in metastasis. However, cellular content may play a mechanistic role in these differences.

A recent study on miR-200 revealed that miR-200 members can have pronounced therapeutic effects on decreasing angiogenesis and metastasis formation in ovarian, lung, renal, and basal-like breast cancer models through IL-8 and CXCL1 regulation [105]. These findings thereby suggest that it has important translational implications on the path to clinical development of miRNA-based therapies.

5.3 miR-205

miR-205 is markedly downregulated in cells that had undergone TGF-β induced EMT and in the triple-negative primary breast cancers [105, 106]. This suggests that miR-205 activity is very similar to that of the miR-200 family, which is also associated with negative regulation of EMT. The miR-205 expression is significantly underexpressed in breast tumor samples compared to the matched normal breast tissue [107]. Furthermore, its expression is restricted to basal epithelium of normal mammary ducts and lobules and is reduced or completely eliminated in matching tumor specimen, which indicates that it is associated with a good prognosis [93]. In addition, ectopic expression of miR-205 in breast cancer cells resulted in the inhibition of cell proliferation, anchorage independent growth, and cell invasion. This miR-205-mediated suppression is through direct targeting of ErbB3 and VEGF-A [107]. Another study by a different group explored miR-205 target genes in breast cancer patients. It revealed that miR-205 directly targets Her3 and interferes with the PI3K/Akt survival pathway in addition to improving responsiveness to tyrosine kinase inhibitor drugs like gefitinib and lapatinib [108]. In breast cancer, overexpression of HER2 is characteristic of an aggressive subset of tumors. Due to its negative regulation of the HER3 receptor, mir205 could improve the responsiveness to specific anticancer therapies. Re-expression of miRNA 205 strongly reduces cell proliferation, cell cycle progression, and clonogenic potential in vitro and inhibits tumor growth in vivo. This oncosuppressive activity is in part exerted experimentally through targeting E2F1 and LAMC1 which are regulators of cell cycle progression and cell adhesion, proliferation, and migration, respectively [109].

Recently, miR-205 was identified as a critical regulator of mammary stem cell maintenance that acts by direct targeting of ZEB1 and NOTCH2 [99, 110]; therefore, chemical modification of miR-205 to stabilize miRNA activity might be beneficial to breast cancer treatment.

5.4 miR-145

Several reports have revealed that miR-145 is significantly downregulated in breast cancer specimen compared with healthy normal breast tissue, as demonstrated by microarray and northern blot analyses [11, 111]. miR-145 exerts its potent tumor suppressive function by silencing different target genes in stage-specific events. Spizzo et al. have shown that miR-145 has pro-apoptotic effect in breast cancer cell lines which is dependent on upregulation of TP53 indicating that miR-145 activates the TP53 pathway. Furthermore, miR-145 directly represses estrogen receptor-α (ER-α) protein expression and induces apoptosis in both ER-α positive and wild type TP53-expressing breast cancer cells [112]. These results suggest that miR-145 re-expression therapy could be beneficial in a specific group of patients with ER-alpha-positive and/or TP53 wild-type tumors. In addition, TP53 activation can, in turn, stimulate miR-145 expression, thus establishing a positive regulatory death loop, partially by impairing the murine double minute 2 (MDM2)-p53 feedback loop, [112, 113]. This could in part explain why miR-145 is frequently downregulated in p53-mutated cancers. Another study showed that miR-145 can directly target and silence a well-known oncogene c-Myc, which regulates cell growth and proliferation leading to inhibition of tumor cell growth both in vitro and in vivo [114]. miR-145 also plays a role in suppression of metastasis in breast cancer. For example, miR145 inhibits EMT by blocking the expression of Oct4, and downstream transcriptional factors, Snail, ZEB1 and ZEB2. Another study revealed that MiR-145 suppresses cell invasion and lung metastasis of breast cancer in vitro and in vivo, partly due to the silencing of mucin 1 (MUC1). This silencing of MUC1 further causes a reduction of β-catenin as well as the cadherin 11, which has oncogenic potential [115]. Gotte et al. described cell-cell adhesion proteins, JAM-A and fascin as novel targets of miR-145; suppression of which drastically decreases breast cancer cell motility [116]. Kim et al. evaluated the therapeutic potency of miR-145 against breast cancer and found that adenoviral construct of miR-145 (Ad-miR-145) resulted in significant suppression of tumor growth in both the in vitro and in vivo models. Furthermore, a treatment of Ad-miR-145 in combination with 5-FU produced enhanced retardation of tumor growth, as compared with 5-FU alone [117]. miR145 also play a role in inhibition of tumor angiogenesis in addition to tumor growth and invasion by targeting N-RAS, ARF6, and VEGF-A that were previously implicated in these phenotypes [118, 119].

6 MicroRNAs as Diagnostic Biomarkers for Breast Cancer

Early detection of breast cancer is of utmost importance to improve prognosis. Therefore, the identification of new diagnostic biomarkers remains a persisting quest. Breast cancer samples show a distinct and unique miRNA expression profile compared to normal adjacent tissues. For example, in breast cancer, the first miRNA profiling study identified a 13-miRNA signature that could correctly differentiate breast cancer from normal breast tissues with 100% accuracy [11]. Blenkiron et al. also identified 133 miRNAs that displayed abnormal expression levels in breast tumor tissues compared with normal breast tissues [33].

In the last few years, there has been growing interest in circulating miRNAs as cancer biomarkers due to their surprising stability, and the noninvasiveness of their detection. The first study that described specific circulating miRNAs associated with cancer was by Lawrie et al., who in 2008 found high levels of miR-155, miR-210, and miR-21 in patients with diffuse large B-cell lymphoma and demonstrated a significant association of high levels of miR-21 with relapse-free survival [120]. Since then, several studies have reported the clinical relevance of circulating miRNAs as diagnostic and prognostic markers for a variety of cancer entities, which used mainly blood plasma or serum for their analyses [121].

Zhu et al. [122] were the first to investigate the miRNA profiles in the sera of cancer patients and healthy subjects; this group revealed that the serum levels of miR-155 were differentially expressed between hormone-sensitive and hormone-insensitive breast cancer patients. Furthermore, a meta-analysis concerning miR-155 showed highly sensitive and specific diagnostic accuracy [123]. In a recent study, Kodahl et al. identified a signature of nine circulating miRNAs from the serum that was capable of discriminating between ER-positive early-stage breast cancer and healthy controls [124]. Chan and colleagues [125], by comparing miRNA profiles between serum samples from breast cancer patients and healthy volunteers, identified four miRNAs as significant diagnostic markers. In addition, miR-34a appears to have a role in tumor progression, as patients with breast cancer with advanced-stage disease had higher serum miR-34a levels than in patients at early tumor stages, and changes in serum levels of miR-34a, miR-10b, and miR-155 correlated with the presence of metastases [126]. Cuk and colleagues [127] described another four upregulated miRNAs in plasma of patients with stage I or II breast cancer, making them attractive biomarkers for early breast cancer detection. Subsequently, another study reported three upregulated miRNAs and one downregulated miRNA in patients with breast cancer compared with normal controls [128]. A prospective study

described three significantly overexpressed serum miRNAs in women who finally developed breast cancer (cases) compared with breast cancer-free controls [129]. This study introduces a new understanding of miRNA function by describing their potential to predict increased risk of developing breast cancer. These reports suggest that circulating miRNAs may be promising candidate biomarkers for the early detection of breast cancers; however, more work is warranted to improve the sensitivities and specificities of detection systems for circulating miRNAs.

7 miRs as Targets for Therapeutic Intervention

The revealing role of miRNAs functioning as potential oncogenes and tumor suppressors in tumorigenesis has generated great interest in using them as a new treatment paradigm for cancer. Currently, many researchers are attempting to restore the function of putative tumor suppressor miRNAs using miRNA mimics or expression vectors, or block the function of putative oncogenic miRNAs using antisense oligonucleotides or expression vectors containing complementary sequences [130].

Antagomirs were the first antisense miRNA inhibitors demonstrated to work in mammals, containing 2′-O-methyl-modified ribose sugars and terminal phosphorothioates along with a 3′-end conjugated cholesterol group [131], which enables them to be successfully delivered to the plasma membrane through association with high- and low-density lipoproteins that bind cell surface membrane receptors [132]. Importantly, antagomirs displayed high bioavailability as well as improved stability and target specific affinity [131]. In one of the pioneering studies demonstrating the utility of miRNA inhibitors in a cancer setting, Weinberg and colleagues identified miR-10b as upregulated in metastatic breast cancer and showed that upregulation of miR-10b alone can confer metastatic potency to otherwise non-metastatic breast cancer cell lines [44]. The same research group extended their work on xenograft metastatic breast cancer mouse models and demonstrated that therapeutic treatment (intravenous injections) with cholesterol-conjugated 2′-O-methyl-derived inhibitors of miR-10b resulted in a robust inhibition of metastasis to the lung while leaving tumor growth at the primary site of infusion unaffected. However, regardless of success toward metastasis inhibition following intravenous delivery of anti-miR-10 cholesterol-conjugated antagomir in a breast cancer mouse model, antagomir composition altered liver and spleen sizes, serum proteins, and metabolite concentration, indicating that nontoxic systemic in vivo delivery of these molecules remains the key challenge [133]. Furthermore, the successful clinical application of antagomirs has been hampered by the high doses needed [132].

Nowadays, chemically modified miRNA have been formulated that have better chances of in-vivo stability and functionality, but still they face the challenge of penetration into a cell. Due to size and negative charge of nucleic acids, miRNA modulators are prevented from crossing hydrophobic lipid layer membranes, finally they get cleared by renal filtration. Due to the mentioned limitations, the modified and unmodified miRNA modulators has been engineered using viral and non-viral carriers for efficient delivery, aiming at achieving tumor-specific systems, and simultaneously biocompatible, biodegradable and capable of immune evasion.

As discussed earlier in this chapter that the tumor suppressor let-7 miRNA family is downregulated in many human cancers and has been shown to target prominent oncogenes, such as KRAS, MYC, and HMGA2 [92, 134, 135]. Therefore, restoring let-7 levels in tumors is an attractive therapeutic option that if successfully delivered to tumor cells could potentially abrogate the oncogenesis. One study using this approach found out that both lipid-formulated let-7b and lentiviral expression of let-7a resulted in reduced tumor burden in a KRas-driven model of lung cancer [136]. Similarly in breast cancer murine model, tumor growth and metastasis inhibition was achieved by using a lentiviral vector encoding a specific miRNA sponge targeting miR-494 [137]. Preclinical viral delivery approaches although successful to some extent, nevertheless, are associated with several practical limitations. The requirement of these delivery tools for nuclear localization, potential immunogenicity and, when integrative, potential activation of oncogenes and inactivation of tumor suppressor genes, the chances of making it to clinical practice are low and thus struggle continues for the development of safer delivery vehicles.

Yet another approach is using liposomes, which are vesicles, composed of an aqueous inner compartment enclosed in a lipid bilayer carrying payloads in the core, including nucleic acids, for transportation. The hydrophilicity and negative charge of nucleic acids in the core are counterbalanced by cationic charge of lipids, resulting in complexes with a net positive charge that facilitates cellular uptake through endocytosis by interaction with anionic molecules at the cell surface. The cistronic miR-143/145 cluster is lost across many different cancers and their re-expression is considered a promising mode of therapy [138]. The systemic administration of a liposome-formulated miR-143/145 expression vector has been found to result in reduced outgrowth of pancreatic cancer xenografts [139]. Hence, miRNA is emerging as an important family of molecules with promising perspectives for therapy in cancer. However, as for other drug classes, the efficacy and safety of miRNA-derived drugs must be carefully assessed and will most likely depend on cellular context and pre-existing genetic and epigenetic lesions.

8 Conclusion

In this chapter, we have summarized the roles of miRNAs in cancer biology, with a particular emphasis on breast cancer. Plethora of studies has revealed that difference in expression levels of miRNAs in both tumor tissues and body fluids are associated with the patient condition and tumor stage. However, a comprehensive understanding of how miRNA networks work together to regulate genes and cellular pathways would certainly have large impact on our understanding of breast cancer pathogenesis, and thus will open newer vistas for improving the therapeutic outcome of breast cancer patients. A beneficial next step would be to identify the genome-wide targets of associated miRNAs. Furthermore, it would be interesting to translate our miRNA knowledge into a clinical setting to explore their practical applications, which relies on successful identification of miRNA signatures as cancer biomarkers and development of miRNA-based targeted therapeutics.

References

1. Garzon R, Calin GA, Croce CM (2009) MicroRNAs in cancer. Annu Rev Med 60:167–179
2. Kim VN (2005) MicroRNA biogenesis: coordinated cropping and dicing. Nat Rev Mol Cell Biol 6(5):376–385
3. Bruce JP et al (2015) Identification of a microRNA signature associated with risk of distant metastasis in nasopharyngeal carcinoma. Oncotarget 6(6):4537
4. Esquela-Kerscher A, Slack FJ (2006) Oncomirs - microRNAs with a role in cancer. Nat Rev Cancer 6(4):259–269
5. Jeansonne D et al (2015) Anti-tumoral effects of miR-3189-3p in glioblastoma. J Biol Chem 290(13):8067–8080
6. Pinatel EM et al (2014) miR-223 is a coordinator of breast cancer progression as revealed by bioinformatics predictions. PLoS One 9 (1):e84859
7. Ben-Hamo R, Efroni S (2015) MicroRNA regulation of molecular pathways as a generic mechanism and as a core disease phenotype. Oncotarget 6(3):1594
8. Sotiropoulou G et al (2009) Emerging roles of microRNAs as molecular switches in the integrated circuit of the cancer cell. RNA 15 (8):1443–1461
9. Calin GA et al (2002) Frequent deletions and down-regulation of micro-RNA genes miR15 and miR16 at 13q14 in chronic lymphocytic leukemia. Proc Natl Acad Sci 99 (24):15524–15529
10. Chan JA, Krichevsky AM, Kosik KS (2005) MicroRNA-21 is an antiapoptotic factor in human glioblastoma cells. Cancer Res 65 (14):6029–6033
11. Iorio MV et al (2005) MicroRNA gene expression deregulation in human breast cancer. Cancer Res 65(16):7065–7070
12. Denli AM et al (2004) Processing of primary microRNAs by the microprocessor complex. Nature 432(7014):231–235
13. Lee Y et al (2003) The nuclear RNase III Drosha initiates microRNA processing. Nature 425(6956):415–419
14. Lund E et al (2004) Nuclear export of microRNA precursors. Science 303(5654):95–98
15. Yi R et al (2003) Exportin-5 mediates the nuclear export of pre-microRNAs and short hairpin RNAs. Genes Dev 17(24):3011–3016
16. Bohnsack MT, Czaplinski K, Gorlich D (2004) Exportin 5 is a RanGTP-dependent dsRNA-binding protein that mediates nuclear export of pre-miRNAs. RNA 10(2):185–191
17. Bagga S et al (2005) Regulation by let-7 and lin-4 miRNAs results in target mRNA degradation. Cell 122(4):553–563
18. Grishok A et al (2001) Genes and mechanisms related to RNA interference regulate expression of the small temporal RNAs that control C. elegans developmental timing. Cell 106 (1):23–34

19. Hutvagner GR et al (2001) A cellular function for the RNA-interference enzyme Dicer in the maturation of the let-7 small temporal RNA. Science 293(5531):834–838
20. Orom UA, Nielsen FC, Lund AH (2008) MicroRNA-10a binds the 5′ UTR of ribosomal protein mRNAs and enhances their translation. Mol Cell 30(4):460–471
21. Qin W et al (2010) miR-24 regulates apoptosis by targeting the open reading frame (ORF) region of FAF1 in cancer cells. PLoS One 5 (2):e9429
22. Bartel DP (2009) MicroRNAs: target recognition and regulatory functions. Cell 136 (2):215–233
23. Portnoy V et al (2011) Small RNA and transcriptional upregulation. Wiley Interdiscip Rev RNA 2(5):748–760
24. Place RF et al (2008) MicroRNA-373 induces expression of genes with complementary promoter sequences. Proc Natl Acad Sci 105 (5):1608–1613
25. Asiaf A et al (2015) Protein expression and methylation of MGMT, a DNA repair gene and their correlation with clinicopathological parameters in invasive ductal carcinoma of the breast. Tumor Biol 36(8):6485–6496
26. Sorlie T et al (2001) Gene expression patterns of breast carcinomas distinguish tumor subclasses with clinical implications. Proc Natl Acad Sci 98(19):10869–10874
27. Perou CM et al (2000) Molecular portraits of human breast tumours. Nature 406 (6797):747–752
28. Fabian MR, Sonenberg N (2012) The mechanics of miRNA-mediated gene silencing: a look under the hood of miRISC. Nat Struct Mol Biol 19(6):586–593
29. Liu C, Tang DG (2011) MicroRNA regulation of cancer stem cells. Cancer Res 71 (18):5950–5954
30. Iorio MV, Croce CM (2012) MicroRNA dysregulation in cancer: diagnostics, monitoring and therapeutics. A comprehensive review. EMBO Mol Med 4(3):143–159
31. Nair VS, Maeda LS, Ioannidis JPA (2012) Clinical outcome prediction by microRNAs in human cancer: a systematic review. J Natl Cancer Inst 104(7):528–540
32. Lu Y et al (2011) Anti-microRNA-222 (anti-miR-222) and-181B suppress growth of tamoxifen-resistant xenografts in mouse by targeting TIMP3 protein and modulating mitogenic signal. J Biol Chem 286 (49):42292–42302
33. Blenkiron C et al (2007) MicroRNA expression profiling of human breast cancer identifies new markers of tumor subtype. Genome Biol 8(10):R214
34. Mattie MD et al (2006) Optimized high-throughput microRNA expression profiling provides novel biomarker assessment of clinical prostate and breast cancer biopsies. Mol Cancer 5(1):24
35. Lowery AJ et al (2009) MicroRNA signatures predict oestrogen receptor, progesterone receptor and HER2/neu receptor status in breast cancer. Breast Cancer Res 11(3):R27
36. Zhang B et al (2007) microRNAs as oncogenes and tumor suppressors. Dev Biol 302 (1):1–12
37. Lund AH (2010) miR-10 in development and cancer. Cell Death Diff 17(2):209–214
38. Gaur A et al (2007) Characterization of microRNA expression levels and their biological correlates in human cancer cell lines. Cancer Res 67(6):2456–2468
39. Volinia S et al (2006) A microRNA expression signature of human solid tumors defines cancer gene targets. Proc Natl Acad Sci U S A 103 (7):2257–2261
40. Jongen-Lavrencic M et al (2008) MicroRNA expression profiling in relation to the genetic heterogeneity of acute myeloid leukemia. Blood 111(10):5078–5085
41. Zhang L et al (2006) microRNAs exhibit high frequency genomic alterations in human cancer. Proc Natl Acad Sci 103(24):9136–9141
42. Bloomston M et al (2007) MicroRNA expression patterns to differentiate pancreatic adenocarcinoma from normal pancreas and chronic pancreatitis. JAMA 297 (17):1901–1908
43. Varnholt H et al (2008) MicroRNA gene expression profile of hepatitis C virus- associated hepatocellular carcinoma. Hepatology 47(4):1223–1232
44. Ma L, Teruya-Feldstein J, Weinberg RA (2007) Tumour invasion and metastasis initiated by microRNA-10b in breast cancer. Nature 449(7163):682–688
45. Liu Y et al (2012) MicroRNA-10b targets E-cadherin and modulates breast cancer metastasis. Med Sci Monit 18(8):BR299–BR308
46. Chang C-H et al (2014) The prognostic significance of RUNX2 and miR-10a/10b and their inter-relationship in breast cancer. J Transl Med 12(1):257
47. Pogribny IP et al (2010) Alterations of microRNAs and their targets are associated with acquired resistance of MCF-7 breast cancer cells to cisplatin. Int J Cancer 127 (8):1785–1794

48. Ahmad A et al (2015) Functional role of miR-10b in tamoxifen resistance of ER-positive breast cancer cells through down-regulation of HDAC4. BMC Cancer 15(1):540
49. Moriarty CH, Pursell B, Mercurio AM (2010) miR-10b targets Tiam1 implications for Rac activation and carcinoma migration. J Biol Chem 285(27):20541–20546
50. Tsukerman P et al (2012) MiR-10b down-regulates the stress-induced cell surface molecule MICB, a critical ligand for cancer cell recognition by natural killer cells. Cancer Res 72(21):5463–5472
51. Ouyang H et al (2014) microRNA-10b enhances pancreatic cancer cell invasion by suppressing TIP30 expression and promoting EGF and TGF-Î² actions. Oncogene 33 (38):4664–4674
52. Hoppe R et al (2013) Increased expression of miR-126 and miR-10a predict prolonged relapse-free time of primary oestrogen receptor-positive breast cancer following tamoxifen treatment. Eur J Cancer 49 (17):3598–3608
53. Khan S et al (2015) MicroRNA-10a is reduced in breast cancer and regulated in part through retinoic acid. BMC Cancer 15 (1):1
54. Perez-Rivas LG et al (2014) A microRNA signature associated with early recurrence in breast cancer. PLoS One 9(3):e91884
55. Yanaihara N et al (2006) Unique microRNA molecular profiles in lung cancer diagnosis and prognosis. Cancer Cell 9(3):189–198
56. Fulci V et al (2007) Quantitative technologies establish a novel microRNA profile of chronic lymphocytic leukemia. Blood 109 (11):4944–4951
57. Yan LX et al (2012) Knockdown of miR-21 in human breast cancer cell lines inhibits proliferation, in vitro migration and in vivo tumor growth. Breast Cancer Res 13(1):R2
58. Huang T-H et al (2009) Up-regulation of miR-21 by HER2/neu signaling promotes cell invasion. J Biol Chem 284 (27):18515–18524
59. Si ML et al (2007) miR-21-mediated tumor growth. Oncogene 26(19):2799–2803
60. Huang G-L et al (2009) Clinical significance of miR-21 expression in breast cancer: SYBR-green I-based real-time RT-PCR study of invasive ductal carcinoma. Oncol Rep 21 (3):673–679
61. Rask L et al (2014) Differential expression of miR-139, miR-486 and miR-21 in breast cancer patients sub-classified according to lymph node status. Cell Oncol 37(3):215–227
62. Tang Y et al (2014) High expression levels of miR-21 and miR-210 predict unfavorable survival in breast cancer: a systemic review and meta-analysis. Int J Biol Markers 30(4): e347–e358
63. Zhu S et al (2008) MicroRNA-21 targets tumor suppressor genes in invasion and metastasis. Cell Res 18(3):350–359
64. Zhu S et al (2007) MicroRNA-21 targets the tumor suppressor gene tropomyosin 1 (TPM1). J Biol Chem 282 (19):14328–14336
65. Kwak HJ et al (2011) Downregulation of Spry2 by miR-21 triggers malignancy in human gliomas. Oncogene 30 (21):2433–2442
66. Lu J et al (2005) MicroRNA expression profiles classify human cancers. Nature 435 (7043):834–838
67. Li H et al (2011) miR-17-5p promotes human breast cancer cell migration and invasion through suppression of HBP1. Breast Cancer Res Treat 126(3):565–575
68. Farazi TA et al (2011) MicroRNA sequence and expression analysis in breast tumors by deep sequencing. Cancer Res 71 (13):4443–4453
69. Saal LH et al (2008) Recurrent gross mutations of the PTEN tumor suppressor gene in breast cancers with deficient DSB repair. Nat Genet 40(1):102–107
70. Olive V et al (2009) miR-19 is a key oncogenic component of mir-17-92. Genes Dev 23(24):2839–2849
71. Coller HA, Forman JJ, Legesse-Miller A (2007) "Myc'ed messages": myc induces transcription of E2F1 while inhibiting its translation via a microRNA polycistron. PLoS Genet 3(8):e146
72. Hossain A, Kuo MT, Saunders GF (2006) Mir-17-5p regulates breast cancer cell proliferation by inhibiting translation of AIB1 mRNA. Mol Cell Biol 26(21):8191–8201
73. Yu Z et al (2008) A cyclin D1/microRNA 17/20 regulatory feedback loop in control of breast cancer cell proliferation. J Cell Biol 182(3):509–517
74. Ovcharenko D et al (2007) Genome-scale microRNA and small interfering RNA screens identify small RNA modulators of TRAIL-induced apoptosis pathway. Cancer Res 67 (22):10782–10788
75. Jiang S et al (2010) MicroRNA-155 functions as an OncomiR in breast cancer by targeting the suppressor of cytokine signaling 1 gene. Cancer Res 70(8):3119–3127

76. Zhang M et al (2011) MicroRNA-155 may affect allograft survival by regulating the expression of suppressor of cytokine signaling 1. Med Hypotheses 77(4):682–684
77. Kong W et al (2008) MicroRNA-155 is regulated by the transforming growth factor beta/Smad pathway and contributes to epithelial cell plasticity by targeting RhoA. Mol Cell Biol 28(22):6773–6784
78. Corcoran C et al (2011) Intracellular and extracellular microRNAs in breast cancer. Clin Chem 57(1):18–32
79. Kong W et al (2010) MicroRNA-155 regulates cell survival, growth, and chemosensitivity by targeting FOXO3a in breast cancer. J Biol Chem 285(23):17869–17879
80. Reinhart BJ et al (2000) The 21-nucleotide let-7 RNA regulates developmental timing in *Caenorhabditis elegans*. Nature 403 (6772):901–906
81. Bassing I, Slack FJ, GroÃŸhans H (2008) Let-7 microRNAs in development, stem cells and cancer. Trends Mol Med 14(9):400–409
82. Lee YS, Dutta A (2007) The tumor suppressor microRNA let-7 represses the HMGA2 oncogene. Genes Dev 21(9):1025–1030
83. Boyerinas B et al (2008) Identification of let-7- regulated oncofetal genes. Cancer Res 68 (8):2587–2591
84. Gurtan AM et al (2013) Let-7 represses Nr6a1 and a mid-gestation developmental program in adult fibroblasts. Genes Dev 27 (8):941–954
85. Piskounova E et al (2008) Determinants of microRNA processing inhibition by the developmentally regulated RNA-binding protein Lin28. J Biol Chem 283(31):21310–21314
86. Viswanathan SR, Daley GQ, Gregory RI (2008) Selective blockade of microRNA processing by Lin28. Science 320(5872):97–100
87. Piskounova E et al (2011) Lin28A and Lin28B inhibit let-7 microRNA biogenesis by distinct mechanisms. Cell 147 (5):1066–1079
88. Choudhury NR et al (2014) Trim25 is an RNA-specific activator of Lin28a/TuT4-mediated uridylation. Cell Rep 9 (4):1265–1272
89. Takamizawa J et al (2004) Reduced expression of the let-7 microRNAs in human lung cancers in association with shortened postoperative survival. Cancer Res 64 (11):3753–3756
90. Zhang H-H et al (2007) Detection of let-7a microRNA by real-time PCR in gastric carcinoma. World J Gastroenterol: WJG 13 (20):2883–2888
91. Akao Y, Nakagawa Y, Naoe T (2006) Let-7 microRNA functions as a potential growth suppressor in human colon cancer cells. Biol Pharm Bull 29(5):903–906
92. Sampson VB et al (2007) MicroRNA let-7a down-regulates MYC and reverts MYC-induced growth in Burkitt lymphoma cells. Cancer Res 67(20):9762–9770
93. Sempere LF et al (2007) Altered MicroRNA expression confined to specific epithelial cell subpopulations in breast cancer. Cancer Res 67(24):11612–11620
94. Yu F et al (2007) Let-7 regulates self renewal and tumorigenicity of breast cancer cells. Cell 131(6):1109–1123
95. Bhat-Nakshatri P et al (2009) Estradiol-regulated microRNAs control estradiol response in breast cancer cells. Nucleic Acids Res 37(14):4850–4861
96. Zhao Y et al (2011) Let-7 family miRNAs regulate estrogen receptor alpha signaling in estrogen receptor positive breast cancer. Breast Cancer Res Treat 127(1):69–80
97. Park S-M et al (2008) The miR-200 family determines the epithelial phenotype of cancer cells by targeting the E-cadherin repressors ZEB1 and ZEB2. Genes Dev 22(7):894–907
98. Korpal M et al (2008) The miR-200 family inhibits epithelial-mesenchymal transition and cancer cell migration by direct targeting of E-cadherin transcriptional repressors ZEB1 and ZEB2. J Biol Chem 283(22):14910–14914
99. Gregory PA et al (2008) The miR-200 family and miR-205 regulate epithelial to mesenchymal transition by targeting ZEB1 and SIP1. Nat Cell Biol 10(5):593–601
100. Jurmeister S et al (2012) MicroRNA-200c represses migration and invasion of breast cancer cells by targeting actin-regulatory proteins FHOD1 and PPM1F. Mol Cell Biol 32 (3):633–651
101. Chen J et al (2012) Down-regulation of microRNA-200c is associated with drug resistance in human breast cancer. Med Oncol 29 (4):2527–2534
102. Singh R, Mo Y-Y (2013) Role of microRNAs in breast cancer. Cancer Biol Ther 14 (3):201–212
103. Dykxhoorn DM et al (2009) miR-200 enhances mouse breast cancer cell colonization to form distant metastases. PLoS One 4 (9):e7181
104. Korpal M et al (2011) Direct targeting of Sec23a by miR-200s influences cancer cell secretome and promotes metastatic colonization. Nat Med 17(9):1101–1108

105. Pecot CV et al (2013) Tumour angiogenesis regulation by the miR-200 family. Nat Commun 4:2427
106. Radojicic J et al (2011) MicroRNA expression analysis in triple-negative (ER, PR and Her2/neu) breast cancer. Cell Cycle 10(3):507–517
107. Wu H, Zhu S, Mo Y-Y (2009) Suppression of cell growth and invasion by miR-205 in breast cancer. Cell Res 19(4):439–448
108. Iorio MV et al (2009) microRNA-205 regulates HER3 in human breast cancer. Cancer Res 69(6):2195–2200
109. Piovan C et al (2012) Oncosuppressive role of p53-induced miR-205 in triple negative breast cancer. Mol Oncol 6(4):458–472
110. Chao C-H et al (2014) MicroRNA-205 signaling regulates mammary stem cell fate and tumorigenesis. J Clin Invest 124 (7):3093–3106
111. Wang S et al (2009) miR-145 inhibits breast cancer cell growth through RTKN. Int J Oncol 34(5):1461–1466
112. Spizzo R et al (2010) miR-145 participates with TP53 in a death-promoting regulatory loop and targets estrogen receptor- alpha in human breast cancer cells. Cell Death Diff 17 (2):246–254
113. Zhang J et al (2013) Loss of microRNA-143/145 disturbs cellular growth and apoptosis of human epithelial cancers by impairing the MDM2-p53 feedback loop. Oncogene 32 (1):61–69
114. Sachdeva M et al (2009) p53 represses c-Myc through induction of the tumor suppressor miR-145. Proc Natl Acad Sci 106 (9):3207–3212
115. Sachdeva M, Mo Y-Y (2010) MicroRNA-145 suppresses cell invasion and metastasis by directly targeting mucin 1. Cancer Res 70 (1):378–387
116. Gotte M et al (2010) miR-145-dependent targeting of junctional adhesion molecule A and modulation of fascin expression are associated with reduced breast cancer cell motility and invasiveness. Oncogene 29 (50):6569–6580
117. Kim S-J et al (2011) Development of microRNA-145 for therapeutic application in breast cancer. J Control Release 155 (3):427–434
118. Zou C et al (2012) MiR-145 inhibits tumor angiogenesis and growth by N-RAS and VEGF. Cell Cycle 11(11):2137–2145
119. Eades G et al (2015) lincRNA-RoR and miR-145 regulate invasion in triple-negative breast cancer via targeting ARF6. Mol Cancer Res 13(2):330–338
120. Shen J et al (2011) Diagnosis of lung cancer in individuals with solitary pulmonary nodules by plasma microRNA biomarkers. BMC Cancer 11(1):1
121. Cortez MA et al (2011) MicroRNAs in body fluids – the mix of hormones and biomarkers. Nat Rev Clin Oncol 8(8):467–477
122. Zhu W et al (2009) Circulating microRNAs in breast cancer and healthy subjects. BMC Res Notes 2(1):89
123. Wang F et al (2014) Increased circulating microRNA-155 as a potential biomarker for breast cancer screening: a meta-analysis. Molecules 19(5):6282–6293
124. Kodahl AR et al (2014) Novel circulating microRNA signature as a potential non-invasive multi-marker test in ER-positive early-stage breast cancer: a case control study. Mol Oncol 8(5):874–883
125. Chan M et al (2013) Identification of circulating microRNA signatures for breast cancer detection. Clin Cancer Res 19 (16):4477–4487
126. Roth C et al (2010) Circulating microRNAs as blood-based markers for patients with primary and metastatic breast cancer. Breast Cancer Res 12(6):R90
127. Cuk K et al (2013) Circulating microRNAs in plasma as early detection markers for breast cancer. Int J Cancer 132(7):1602–1612
128. Ng EKO et al (2013) Circulating microRNAs as specific biomarkers for breast cancer detection. PLoS One 8(1):e53141
129. Godfrey AC et al (2013) Serum microRNA expression as an early marker for breast cancer risk in prospectively collected samples from the sister study cohort. Breast Cancer Res 15 (3):R42
130. Takeshita F et al (2010) Systemic delivery of synthetic microRNA-16 inhibits the growth of metastatic prostate tumors via downregulation of multiple cell-cycle genes. Mol Ther 18 (1):181–187
131. Krutzfeldt J et al (2005) Silencing of microRNAs in vivo with 'antagomirs'. Nature 438 (7068):685–689
132. Broderick JA, Zamore PD (2011) MicroRNA therapeutics. Gene Ther 18(12):1104–1110
133. Ma L et al (2010) Therapeutic silencing of miR-10b inhibits metastasis in a mouse mammary tumor model. Nat Biotechnol 28 (4):341–347
134. Johnson SM et al (2005) RAS is regulated by the let-7 microRNA family. Cell 120 (5):635–647

135. Park S-M et al (2007) Let-7 prevents early cancer progression by suppressing expression of the embryonic gene HMGA2. Cell Cycle 6 (21):2585–2590
136. Trang P et al (2011) Systemic delivery of tumor suppressor microRNA mimics using a neutral lipid emulsion inhibits lung tumors in mice. Mol Ther 19(6):1116–1122
137. Liu Y et al (2012) MicroRNA-494 is required for the accumulation and functions of tumor-expanded myeloid-derived suppressor cells via targeting of PTEN. J Immunol 188 (11):5500–5510
138. Kitade Y, Akao Y (2010) MicroRNAs and their therapeutic potential for human diseases: microRNAs, miR-143 and-145, function as anti-oncomirs and the application of chemically modified miR-143 as an anti-cancer drug. J Pharmacol Sci 114 (3):276–280
139. Pramanik D et al (2011) Restitution of tumor suppressor microRNAs using a systemic nanovector inhibits pancreatic cancer growth in mice. Mol Cancer Ther 10(8):1470–1480

Chapter 3

Involvement of miRNAs and Pseudogenes in Cancer

Lütfi Tutar, Aykut Özgür, and Yusuf Tutar

Abstract

Our understanding of cancer pathways has been changed by the determination of noncoding transcripts in the human genome in recent years. miRNAs and pseudogenes are key players of the noncoding transcripts from the genome, and alteration of their expression levels provides clues for significant biomarkers in pathogenesis of diseases. Especially, miRNAs and pseudogenes have both oncogenic and tumor-suppressive roles in each step of cancer tumorigenesis. In this current study, association between oncogenes and miRNAs-pseudogenes was reviewed and determined in human cancer by the CellMiner web-tool.

Key words miRNA, Pseudogene, Cancer, Biomarker, CellMiner

1 Introduction

Since their discovery, miRNAs and pseudogenes have been considered diagnostic and prognostic biomarkers and are known to play key roles in all cancer types. miRNAs are a family of small, endogenous, and evolutionarily conserved noncoding ribonucleic acid molecules comprised of about 18–24 nucleotides that have been taken part in the regulation of several essential, functional, and cellular processes [1]. Majority of pseudogenes do not code for functional proteins and considered functionless copies of genes which are originated from functional genes that were widely known as "junk" DNA [1–3].

miRNAs are members of a small noncoding RNA family which are comprised of about 18–24 nucleotides. To date, there are approximately 2000 miRNAs identified in human genome (http://www.mirbase.org). miRNAs are mostly involved in RNA silencing and organization of gene expression. miRNAs are characterized as leading regulators of coding genes in human genome at the post-transcriptional level and they are operated in diagnosis, prognosis, and gene targeting in molecular medicine. miRNAs have been found to have connections with cancer and many other diseases including heart diseases, diabetes, neurodegenerative diseases,

Wei Wu (ed.), *MicroRNA and Cancer: Methods and Protocols*, Methods in Molecular Biology, vol. 1699,
DOI 10.1007/978-1-4939-7435-1_3,

immune-related diseases, infection diseases. High-throughput experimental and computational bioinformatics studies have signified that miRNAs play key roles in each step of the oncogenic cancer pathways. Thus, miRNAs have considerable potential as biomarkers in all cancer types [4–7].

Pseudogenes are abundant and ubiquitous dysfunctional protein-coding gene copies that are originally derived from functional genes. Pseudogenes are familiar with premature stop codons and frame-shift insertions/deletions [8, 9]. Pseudogenes are estimated to be around 20,000 in the human genome, and 6% of pseudogenes are determined by experimental and computational approaches. Pseudogenes function at DNA, RNA, and protein levels independently or in a related trend to their parent genes. Human genome project outcomes and progress in next-generation sequencing (NGS) have indicated the importance of pseudogenes in regulation of genes and they are defined as key gene regulators at the DNA level [9, 10]. Many studies evidenced that expression levels of pseudogenes are linked to pathogenesis. Notably, pseudogenes play significant roles in regulation of tumor suppressors and oncogenes in cancer cells. Understanding the mechanism of pseudogenes and their relation with oncogenes and miRNAs may provide significant clues to clarify oncogenic pathways [11, 12].

Expression patterns of miRNAs and pseudogenes have been extensively studied on human cancer [1]. Microarray-based miRNA and pseudogene profiling experiments were demonstrated that vast majority of miRNAs and pseudogenes related to apoptosis, angiogenesis, metastasis, and cell proliferation in cancer [3, 11, 12]. Growing number of characterized miRNAs and pseudogenes should be analyzed and their functions need to be determined in different cancer types. Therefore, computational bioinformatics tools have attained interest in miRNA and pseudogene connected research in order to determine specific targets. Hence, many web-based tools (CellMiner, TargetScan, miR2Disease, PhenomiR, HMDD, miRGator, and DIANA-TarBase) have been settled for detection of miRNAs and pseudogenes [13]. CellMiner (http://discover.nci.nih.gov/cellminer/) database was created with original microarray data on NCI-60 cancer cell lines panel. CellMiner provides rapid data for interaction between 22,379 genes and 360 miRNAs along with 20,503 chemical compounds including 102 FDA approved drugs in 60 diverse human cancer cell lines [14, 15]. Identified key miRNAs and pseudogenes may provide a starting point for new strategies to design gene-based human cancer remedial drugs. The primary aim of this study is clarifying the connection between miRNAs, pseudogenes, and important oncogenes and related networks in human cancer progression. Further, the differences in expression of miRNAs and pseudogenes between normal tissues and tumor tissues reveal their potential as biomarkers in the diagnosis and treatment of human cancer.

2 miRNA Biogenesis and Function

miRNAs, a family of small RNAs, play key roles in the regulation of several essential, cellular, and functional processes such as tumorigenesis, cell proliferation, differentiation, stem cell maintenance, and apoptosis. In the nucleus, miRNAs are transcribed by RNA polymerase II into pri-miRNAs. Subsequently, pri-miRNAs are cleaved by a microprocessor complex containing the Drosha enzyme and DGCR8 (DiGeorge Syndrome Critical Region 8 Protein) to form stem-loop precursors (pre-miRNAs). Subsequently, premiRNAs are exported from nucleus to the cytoplasm by Exportin-5 and a RanGTP to be one more step further cleaved by Dicer enzyme and the RNA-induced silencing complex (RISC assembly) into 18–24 nucleotides long duplexes containing mature miRNA and the opposite passenger strand called miRNA* which further separated by helicase unwinding. Furthermore, recent works clarified that both miRNA and miRNA*strands of the aforementioned duplex are functionally viable and may take action in target genes [16]. Therefore, −3p and −5p suffixes were respectively endorsed to describe two different sequences of mature miRNAs generated from the 3′ and 5′ ends of the pre-miRNA hairpin (e.g., miR172-3p; miR172-5p). miRNAs increase translational inhibition or degradation of mRNAs. Generally, human miRNAs like all other animal ones are imperfectly pairs with their target genes and give rise to decreased protein level as a result of translation inhibition[1, 5, 17].

miRNAs are involved in all cancer types with two different aspects as oncomirs (oncogenic miRNAs) or tumor-suppressors which are respectively upregulated or downregulated. Expression patterns of miRNAs can be used in classification, prognosis, and diagnosis of various cancer types and they are key factors for cancer related “omics” studies. Currently, many approaches are developed to be used in detection, profiling, and quantification of cancer-linked miRNAs. These approaches may be divided into three major areas as experimental approach, computational bioinformatics approach, and forward genetics. Recent experimental approaches including next-generation sequencing (NGS) and computational approaches as mainly bioinformatics lead to fast, accurate, reproducible, and deeper investigation of miRNAs that were involved in oncogenic pathways with connection to their potential roles as diagnostic and prognostic biomarkers. Experimental approaches have some main tools including northern blotting, direct cloning and sequencing, in situ hybridization, next-generation sequencing, RT-qPCR, and microarray analysis. Since the discovery of miRNAs, computational approaches have been taking part as essential tools to solve miRNA mechanisms.

Generally, results obtained from bioinformatics analysis are confirmed with experimental approaches. Currently, most appropriate plan to study cancer miRNAs combines high-throughput NGS, appropriate bioinformatics tools, and validation with different RT-qPCR analyses. Small-RNA sequencing and RNA-sequencing are two NGS technologies that are notably used to characterize miRNAs, prediction of novel miRNAs, and prediction of potential mRNA targets. Computational bioinformatics tools gave rise to the determination and comparison of miRNAs and their expression levels and fold counts, determination of differentially expressed miRNAs and identification of sequence isoforms between normal and cancer specimens. Subsequently, validation, detection, and quantification of miRNAs were obtained by a Real-Time reverse transcriptase PCR method termed Stem-loop RT-PCR [18, 19].

miRNAs have a considerable potential to be analyzed as biomarkers in diagnostics and prognostics. Generally, miRNA expression patterns are specific to individual tissues and change between normal and cancer tissues [20, 21].

Various work were conducted on tissue-specific deregulation of miRNA expression levels and evidenced potential role of miRNA expression levels as cancer biomarkers with experimental and bioinformatics approaches. miRNA analysis through invasive cancer screening including formalin-fixed tissues and noninvasive diagnostic screening recruiting with circulating cell free miRNAs are feasible and revealing powerful facilities to figure out their potential use as cancer biomarkers [22, 23].

miRNA mimics (miRNA replacement therapy) and miRNA antagonists are the two leading approaches used in miRNA therapeutics. miRNA mimics intention uses the re-introducing tumor suppressive miRNAs into cancer cells. Conversely, when aberrant expression of the target oncomirs is of concern, chemically modified miRNA sequences (antagomiRs or anti-Mirs) play key roles and inhibit oncomirs by binding to one of their mature sequences [24, 25].

3 Biogenesis and Functions of Pseudogenes

Pseudogenes are nonfunctional copies of genes and do not produce full-length proteins. The human genome contains approximately 20,000 pseudogenes that were called “junk DNA” and/or “genomic fossils” in respect to the traditional fashion of pseudogenes. However, recent studies suggest that pseudogenes involved in the regulation of their parent genes, oncogenes, and tumor suppressors. Thus, pseudogenes are related to pathogenesis of many diseases [9, 11]. Generally, pseudogenes are divided in three categories: unprocessed (or duplicated), processed (or retrotransposed), and unitary pseudogenes (Fig. 1) [9]. Unprocessed pseudogenes are

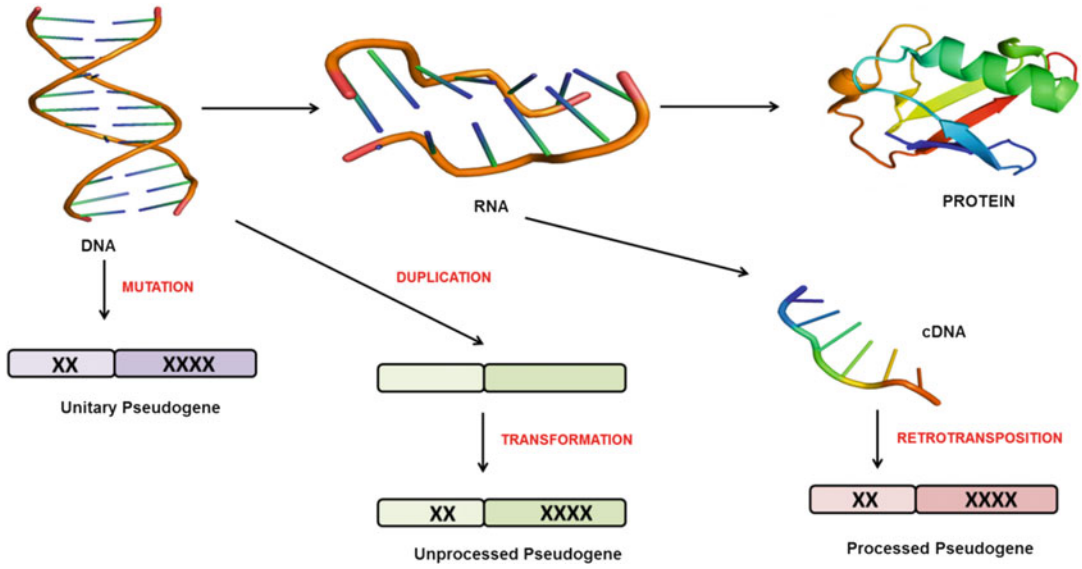

Fig. 1 Pseudogene processing mechanism in the cell (x denotes mutation)

formed through gene duplication events. Unprocessed pseudogenes originate from decay of genes as a result of various modifications, including point mutations, frame shifting events, insertions, and deletions. These modifications account for loss of productivity, RNA expression or protein coding capability of gene, and induce formation of unprocessed pseudogenes. Processed pseudogenes are the most abundant type in the human genome and they are originated via retrotransposition. In the retrotransposition phenomenon, mRNA transcript of a gene is reverse transcribed into a cDNA, and located at another position in the genome. The double-stranded structures of processed pseudogenes are formed from single-stranded RNA by the RNA polymerase III. Therefore, processed pseudogenes lack noncoding intervening sequences (introns and promoters) and have poly-A tail at the 3′ end flanking direct repeats. Contrary to processed and unprocessed pseudogenes, unitary pseudogenes are identified as non-duplicated unprocessed pseudogenes. Spontaneous mutations may disrupt transcription or translation of protein coding genes. Therefore, genes may become nonfunctional during unprocessed pseudogene formation [8–10]. Pseudogenes are involved in tumorigenesis as regulators of tumor suppressors and oncogenes. Majority of pseudogenes are widely expressed in human cancer cells, and individual pseudogenes have been determined by bioinformatics approaches in all types of human cancer. Pseudogenes recruit two different courses to assign specific roles in cancer cells: (i) Pseudogenes perform regulatory activity with parental genes; (ii) Pseudogenes perform independent regulatory activity [11, 12].

4 Key miRNAs and Pseudogenes as Biomarkers for the Treatment and Diagnosis in Cancer

The link between miRNAs and cancer was first described by Calin and colleagues in 2002 [26]. Analyzing a repetitive deletion evidenced that mir-15a and mir-16-1 were coded in the smallest deletion region and were downregulated as tumor suppressors [26]. Outstanding and well-defined tumor suppressor miRNAs are members of the let-7 family. It was reported that let-7 is downregulated in all types of human cancer, causing to upregulation of the proto-oncogenes such as RAS [27], HMGA2 [28], MYC [29], integrin beta 3 [30], the oncofetal gene IMP-1 [31], and the miRNA maturation RNAse Dicer [32, 33]. Briefly, the miRNAs acting as tumor suppressors target oncogenes in order to destroy their mRNAs [34].

Conversely, miRNAs may also function as oncogenes (oncomirs) by their altered expression. Mir-21 is a well-defined and "scandalous" oncomir, which has been found to be upregulated pronouncedly in various cancer types [35]. Many examples of widely expressed miR-21 in both hematopoietic and solid tumors are reported in several cancer-related studies [20, 36–39]. An expression study in the extremely malignant human brain tumor, glioblastoma, evidenced that miR-21 was overexpressed in glioblastomas when compared to brain tissue levels and that knockdown of miR-21 in cultured glioblastoma cells led to augmented apoptotic cell death [40]. Acting as oncomir, miR-21 targets various tumor suppressor genes such as phosphatase and tensin homolog (PTEN) [41], programmed cell death 4 (PDCD4) [42], and tropomyosin 1 (TPM1) [43]. Another extensively analyzed oncogene family is miR-17-92 cluster whose members are extensively expressed in several solid tumors and hematological malignancies [44]. Strikingly, it was evidenced that the miR-17-92 cluster is directly regulated by c-myc which is a frequent oncogene in cancer [45].

Until now, it is reported that numerous miRNAs dramatically deregulated in human cancers. Following the evidence of first connection with cancer-related miRNAs in hematopoietic tumors [26], Michael et al. evidenced deregulation of miRNA expression levels of solid tumors compared to healthy tissues in humans for the first time [34]. Afterward, altered levels of miRNAs have also been discovered in a variety of cancers such as breast cancer [46], Burkitt's lymphoma [47], malignant brain tumors [40], thyroid cancer [48], lung cancer [49, 50], and hepatocellular carcinomas [51].

In various types of cancer, expression of miRNAs also altered and thus regulation of targeted genes switched to affect cancer

growth. In liver cancer, it has been reported that miR-122 is downregulated [52]. MiR-221, miR-222, and miR-21 are explicitly overexpressed in hepatocellular carcinoma (HCC) compared to non-neoplastic livers (NL) [53]. Let-7 is the first miRNA, acting as a tumor suppressor, linked to lung carcinogenesis and is evidenced for inhibition of lung cancer growth in mouse models in addition to human lung cancer cell lines by its upregulation [54, 55]. It has been shown that expression of mir-21 upregulated aberrantly in lung carcinogenesis [56]. Deregulation of miRNAs in breast cancer was first reported by Iorio et al. [46], scientists were reported that mir-125b and mir-145 were downregulated as tumor suppressors; meanwhile, mir-21 and mir-155 were upregulated acting as oncomirs by comparison of normal and cancer tissues. Tumor suppressive role of let-7 family was evidenced by Yu et al. [57] in which expression of miRNAs in mammosphere-derived breast cancer stem cells (CSCs) indicated that let-7 was the tumor suppressor miRNA family. The suppressive role of mir-200c was reported in the inhibition of the clonal expansion of breast cancer cells and suppression of the in vitro growth of embryonic carcinoma cells [58]. An anti-miR-21 transfected cell growth inhibition in breast cancer MCF-7 cells gave rise to both in vivo and in vitro increase of apoptosis and decrease of cell proliferation [59]. miRNA deregulation in CRC tissues was first reported by Michael et al. in 2003 [34]. In this study, tumor suppressors miRNAs, miR-143, and mir-145 were identified to be downregulated in tumor tissue compared to normal colon tissue. Since then, many studies reported tumor suppressor functions of mir-143 and mir-145. Furthermore, researchers showed that the predicted target genes of mir-143 are KRAS, DNMT3A, ERK5 and the predicted target genes of mir-145 are RS-1, c-myc, SOX52 [63–69]. Let-7 was suggested to act as a tumor suppressor in CRC, as well as in other cancers, in many studies [60–62]. Upregulation of oncogenic mir-21 in CRC has also been reported in many studies [42, 63, 64]. In 2002 Calin et al. evidenced downregulation of both mir-15a and mir-16-1 in patients with chronic lymphocytic leukemia (CLL) that brought out the missing contact between miRNA deregulation and hematopoietic cancer [26]. Furthermore, miR-24, miR-125b, miR-21, miR-19, and, miR-155 are other important oncogenic miRNA recruits for leukemia [65–69].

Recent studies demonstrated that pseudogenes have been valuable diagnostic and therapeutic biomarkers in oncology. Shanker and coworkers identified 2082 pseudogene transcripts in cancer cells with bioinformatics techniques. Among them, 248 pseudogenes have specific expression in tumorogenesis [70]. Unprocessed pseudogene, ATP8A2-ψ, was extensively studied in breast cancer.

ATP8A2-ψ is overexpressed in breast cancer cells and in vitro gene knockdown experiments showed an oncogenic role of ATP8A2-ψ [70, 71]. Meanwhile, Han and colleagues developed a computational pipeline and revealed the importance of pseudogenes as prognostic biomarkers in cancer systematically. They detected 9925 pseudogene transcripts in seven main cancer types. Expression profile of these pseudogenes was congruent with expression of miRNA, expression of mRNA, somatic copy number variation, and methylation of DNA in cancer cells [72]. Therefore, pseudogenes have vital and key roles as regulatory members in cancer development and progression pathways.

Yet, in the literature, a relationship between cancer-linked miRNAs and pseudogenes is not well established sufficiently. To shed light on this connection, commonly detected miRNAs were investigated in a microarray data platform; CellMiner. These miRNAs were analyzed with CellMiner web-tool, and their relations with oncogenes and highly correlated top three pseudogenes were reported for human cancer (Table 1).

Recently, a new hypothesis called ceRNA (competing endogenous RNA) was introduced to the literature that expresses that mRNA, pseudogene transcripts, and long noncoding RNAs (lncRNAs) interact with each other and regulate expression of each other by enrollment of MREs (microRNA response elements) to compete for the binding of miRNA [2]. From a ceRNA point of view, pseudogene RNAs may play role as ceRNAs and the connection between miRNAs and pseudogenes may be used in carrying out cancer diagnostic and prognostic approaches.

5 Future Perspectives

In a short while, miRNAs and pseudogenes have become prominent players in all types of human cancer. miRNAs and pseudogenes may provide novel opportunities by recruiting as biological targets in drug design, personalized medicine, cancer therapy, and biomarker development approaches in a near future. Furthermore, ceRNA theory needs to be verified by more deep analysis in various cancer types to reveal networks containing miRNAs and pseudogenes. To have a deep insight into cancer-related miRNAs and pseudogenes as well as ceRNA may open a new opportunity to clarify molecular mechanisms involved in human cancer.

Conflict of Interest: *The authors confirm that this article content has no conflicts of interest.*

Table 1
Correlations between human oncogenes and miRNAs-pseudogenes in human lung, breast, leukemia, prostate, and colorectal cancer

Gene	miRNAs	Correlations	Location	Pseudogenes	Correlations	Location
	Lung cancer					
CADM1	hsa-miR-137	0.409	1p21.3	*HMGB3P18*	0.747	6q22.31
	hsa-miR-106a	0.397	Xq26.2	*RPS26P5*	0.742	21q21.1
	hsa-miR-363	0.386	Xq26.2	*RPL23AP35*	0.692	2q32.1
	hsa-miR-20a	−0.307	13q31.3	*PABPC1P1*	−0.459	4p14
	hsa-miR-135b	−0.312	1q32.2	*PA2G4P3*	−0.42	18q12.1
	hsa-miR-17	−0.328	13q31.3	*PSME2P6*	−0.42	10p12.31
CDH1	hsa-miR-203	0.752	14q32.33	*CDC42BPG*	0.786	11q13.1
	hsa-miR-141	0.718	12p13.31	*ESRP2*	0.742	16q22.1
	hsa-miR-200c	0.715	12p13.31	*DUXAP2*	0.726	8q22.3
	hsa-miR-181a-2	−0.443	9q33.3	*PALM2-AKAP2*	−0.632	9q31.3
	hsa-miR-140-3p	−0.454	16q22.3	*DUSP7*	−0.611	3p21.1
	hsa-miR-140-5p	−0.516	16q22.3	*EEF1A1P29*	−0.583	Xq21.2
CDH13	hsa-miR-138	0.393	3p21.33	*RPS24P4*	0.843	1q42.2
	hsa-miR-137	0.371	1p21.3	*RPL29P19*	0.6	8q11.21
	hsa-miR-100	0.354	11q24.1	*HMGN2P16*	0.522	9p22.3
	hsa-miR-378	−0.336	5q33.1	*OR2B7P*	−0.483	6p22.1
	hsa-miR-30b	−0.383	8q24.22	*PNKP*	−0.431	19q13.32
	hsa-miR-30d	−0.389	8q24.22	*KRTCAP2*	−0.416	1q23.1
FHIT	hsa-miR-663	0.354	20p11.1	*RPL10AP6*	0.747	3p14.2
	hsa-miR-148a	0.35	7p15.2	*RPS27P16*	0.504	7p15.1
	hsa-miR-20a	0.337	13q31.3	*UBE2CBP*	0.488	6q14.1
	hsa-miR-125b	−0.322	11q24.1	*OR52S1P*	−0.408	11p15.4
	hsa-miR-23b	−0.429	9q22.32	*ANXA2P1*	−0.379	4q31.3
	hsa-miR-27b	−0.439	9q22.32	*RNU1-13P*	−0.37	1q21.1
MGMT	hsa-miR-30c	0.419	1p34.2	*SARNP*	0.494	12q13.3
	hsa-miR-484	0.345	16p13.11	*SDHAP3*	0.467	5p15.33
	hsa-miR-200a	0.328	1p36.33	*AKAP5*	0.465	14q23.3
	hsa-miR-125b	−0.359	11q24.1	*GABARAP*	−0.515	17p13.1
	hsa-miR-24-1	−0.367	9q22.32	*GMPPA*	−0.508	2q35
	hsa-miR-100	−0.468	11q24.1	*FKBP14*	−0.497	7p15.1
MLH1	hsa-miR-152	0.386	17q21.33	*EPM2AIP1*	0.568	3p22.2
	hsa-miR-181d	0.287	19p13.12	*RAB3GAP2*	0.449	1q41
	hsa-miR-432	0.265	14q32.31	*DNTTIP2*	0.439	1p22.1
	hsa-miR-10b	−0.316	2q31.1	*FOLR3P1*	−0.572	11q13.4
	hsa-miR-31	−0.368	9p21.3	*LETM1P3*	−0.567	8q22.2
	hsa-miR-31	−0.371	9p21.3	*IPMKP1*	−0.56	13q12.12
RASSF1	hsa-miR-142-3p	0.476	17q23.2	*RPS18P9*	0.586	6q25.1
	hsa-miR-142-5p	0.459	17q23.2	*RBBP8*	0.563	18q11.2
	hsa-miR-106a	0.457	Xq26.2	*HMGN2P7*	0.557	3p24.3
	hsa-miR-151-3p	−0.393	8q24.3	*MRP63P6*	−0.444	5q34
	hsa-miR-151-5p	−0.431	8q24.3	*APOA1BP*	−0.437	1q23.1
	hsa-miR-34a	−0.557	1p36.22	*SYNJ2BP*	−0.436	14q24.2

(continued)

Table 1
(continued)

Gene	miRNAs	Correlations	Location	Pseudogenes	Correlations	Location
ERBB3	hsa-miR-203	0.451	14q32.33	*VN1R37P*	0.842	7q11.21
	hsa-miR-375	0.412	2q35	*RNU7-73P*	0.689	3p22.2
	hsa-miR-30b	0.382	8q24.22	*POU5F1P6*	0.54	3q21.3
	hsa-miR-377	−0.416	14q32.31	*ACTG1P10*	−0.527	Xp11.22
	hsa-miR-376c	−0.417	14q32.31	*OR10AE1P*	−0.515	1q23.3
	hsa-miR-542-5p	−0.423	Xq26.3	*BZW1P1*	−0.504	3q26.2
MET	hsa-miR-151-5p	0.527	8q24.3	*COX5AP2*	0.603	14q22.2
	hsa-miR-151-3p	0.526	8q24.3	*ASAP2*	0.593	2p25.1
	hsa-miR-29a	0.501	7q32.3	*FTH1P10*	0.578	5p15.1
	hsa-miR-18b	−0.501	Xq26.2	*ARHGAP9*	−0.549	12q14.1
	hsa-miR-30e	−0.517	1p34.2	*GUSBP3*	−0.544	5q13.2
	hsa-miR-340	−0.548	5q35.3	*SYNGAP1*	−0.529	6p21.32
NKX2-1	hsa-miR-34c-5p	0.438	11q23.1	*OR7E19P*	0.62	19p13.2
	hsa-miR-517c	0.391	19q13.33	*BTF3P2*	0.6	14q12
	hsa-miR-519a	0.377	19q13.33	*OR7E115P*	0.593	10p13
	hsa-miR-769-5p	−0.263	19q13.2	*RPL24P4*	−0.461	6p21.1
	hsa-miR-330-3p	−0.263	19q13.2	*RBMXP4*	−0.46	4q25
	hsa-miR-652	−0.321	Xq22.3	*RPL24P6*	−0.45	3q29
CEACAM5	hsa-miR-215	0.602	1q41	*GSTM5P1*	0.692	3p25.2
	hsa-miR-194	0.6	1q41	*NARSP1*	0.663	14q12
	hsa-miR-192	0.585	11q13.1	*NDUFB8P3*	0.649	11p13
	hsa-miR-125b	−0.369	11q24.1	*MSNP1*	−0.47	5p14.1
	hsa-miR-140-5p	−0.388	16q22.3	*RPL32P13*	−0.464	4q25
	hsa-miR-455-3p	−0.394	9q33.1	*NUDCP2*	−0.443	2q31.2
AKT1	hsa-miR-324-5p	0.386	17p13.1	*SNX19P3*	0.486	18p11.21
	hsa-miR-107	0.294	10q23.31	*MRPS23P1*	0.477	7p13
	hsa-miR-103	0.293	5q35.1	*OR5M6P*	0.428	11q11
	hsa-miR-31	−0.299	9p21.3	*PABPC1P4*	−0.504	12q14.3
	hsa-miR-31	−0.345	9p21.3	*RPL31P15*	−0.491	2q32.1
				RPS24P18	−0.469	18q12.1
BCL2	hsa-miR-106b	0.375	7q22.1	*RPL21P18*	0.654	12q15
	hsa-miR-93	0.368	7q22.1	*RPL35AP23*	0.618	10q11.23
	hsa-miR-30e	0.345	1p34.2	*GNRHR2P1*	0.61	14q23.1
	hsa-miR-151-3p	−0.399	8q24.3	*ANXA2P2*	−0.576	9p13.3
	hsa-miR-31	−0.403	9p21.3	*ANXA2P1*	−0.512	4q31.3
	hsa-miR-31	−0.428	9p21.3	*NCKAP1*	−0.419	2q32.1
CDH1	hsa-miR-203	0.752	14q32.33	*DUXAP2*	0.726	8q22.3
	hsa-miR-141	0.718	12p13.31	*RPS3AP31*	0.651	8p23.1
	hsa-miR-200c	0.715	12p13.31	*RAB11FIP4*	0.649	17q12
	hsa-miR-181a-2	−0.443	9q33.3	*PALM2-AKAP2*	−0.632	9q31.3
	hsa-miR-140-3p	−0.454	16q22.3	*EEF1A1P29*	−0.583	Xq21.2
	hsa-miR-140-5p	−0.516	16q22.3	*RPL21P87*	−0.549	9q31.3

(continued)

Table 1
(continued)

Gene	miRNAs	Correlations	Location	Pseudogenes	Correlations	Location
EGFR	hsa-miR-30a	0.526	6q13	*ARHGAP29*	0.783	1p21.3
	hsa-miR-30a	0.524	6q13	*COX5AP2*	0.778	14q22.2
	hsa-miR-196b	0.489	7p15.2	*MYL6P3*	0.723	10q21.3
	hsa-miR-18b	−0.527	Xq26.2	*RPS19BP1*	−0.639	22q13.2
	hsa-miR-25	−0.537	7q22.1	*SLC25A5P1*	−0.599	22q13.2
	hsa-miR-652	−0.648	Xq22.3	*RPL7AP34*	−0.584	6q12
VEGFA	hsa-miR-210	0.479	11p15.5	*SAR1AP2*	0.459	10q26.2
	hsa-miR-27b	0.442	9q22.32	*ASNSP1*	0.452	8q11.1
	hsa-miR-27a	0.428	19p13.12	*CDC42EP1*	0.43	22q13.1
	hsa-miR-30e	−0.375	1p34.2	*TGFBRAP1*	−0.531	2q12.2
	hsa-miR-153	−0.391	2q35	*CDK5RAP3*	−0.507	17q21.33
	hsa-miR-766	−0.422	Xq24	*SYNGAP1*	−0.457	6p21.32
APC	hsa-miR-204	0.488	9q21.13	*RASGRP3*	0.542	2p22.3
	hsa-miR-145	0.405	5q33.1	*PNLIPRP3*	0.474	10q25.3
	hsa-miR-99a	0.395	21q21.1	*ZNF300P1*	0.471	5q33.1
	hsa-miR-200b	−0.362	1p36.33	*RPS26P43*	−0.485	11q24.1
	hsa-miR-29c	−0.384	1q32.2	*HMGN2P28*	−0.432	6p25.3: 6p25.2
	hsa-miR-331-3p	−0.526	12q23.1	*RPS29P9*	−0.428	2q33.3
BCL2	hsa-miR-106b	0.375	7q22.1	*RPL21P18*	0.654	12q15
	hsa-miR-93	0.368	7q22.1	*RPL35AP23*	0.618	10q11.23
	hsa-miR-30e	0.345	1p34.2	*GNRHR2P1*	0.61	14q23.1
	hsa-miR-151-3p	−0.399	8q24.3	*ANXA2P2*	−0.576	9p13.3
	hsa-miR-31	−0.403	9p21.3	*ANXA2P1*	−0.512	4q31.3
	hsa-miR-31	−0.428	9p21.3	*MRPS31P2*	−0.381	13q12.11
TP53	hsa-miR-487b	0.364	14q32.31	*RABEP1*	0.493	17p13.2
	hsa-miR-324-3p	0.314	17p13.1	*RPL12P15*	0.434	2q14.3
	hsa-miR-371-5p	0.283	19q13.33	*RPL26P36*	0.424	Xq21.32
	hsa-miR-545	−0.327	Xq13.2	*HERC2P9*	−0.465	15q13.2
	hsa-miR-197	−0.351	1p13.3	*ATF7IP2*	−0.443	16p13.13
	hsa-miR-199b-5p	−0.384	9q34.11	*VENTXP7*	−0.436	3p24.3
KRAS	hsa-miR-200a	0.356	1p36.33	*ARHGAP26*	0.568	5q31.3
	hsa-miR-429	0.348	1p36.33	*RPL39P27*	0.561	12p12.1
	hsa-miR-141	0.339	12p13.31	*SLC9A3P2*	0.559	22q11.22
	hsa-miR-99a	−0.341	21q21.1	*MKRN4P*	−0.486	Xp11.4
	hsa-miR-193a-3p	−0.349	17q12	*RPS26P21*	−0.405	3q13.32
	hsa-miR-455-5p	−0.355	9q33.1	*SLC6A10P*	−0.384	16p11.2
MDM2	hsa-miR-34a	0.637	1p36.22	*TP53INP1*	0.605	8q22.1
	hsa-miR-34a	0.609	1p36.22	*CEACAMP9*	0.508	19q13.2
	hsa-miR-34b	0.497	11q23.1	*RPS10P28*	0.481	19q13.13
	hsa-let-7a	−0.298	9q22.32	*CDC20P1*	−0.341	9q22.1
	hsa-let-7b	−0.306	22q13.31	*PGK1P2*	−0.319	19p13.13
	hsa-miR-130b	−0.318	22q11.23	*EXOSC3P2*	−0.318	19p13.2

(continued)

Table 1
(continued)

Gene	miRNAs	Correlations	Location	Pseudogenes	Correlations	Location
	Breast cancer					
ESR1 (ERα)	hsa-miR-375	0.603	2q35	*RPS17P2*	0.901	5q23.1
	hsa-miR-203	0.552	14q32.33	*GNRHR2P1*	0.838	14q23.1
	hsa-miR-301a	0.498	17q23.2	*RPL36AP46*	0.793	17q23.3
	hsa-miR-29a	−0.414	7q32.3	*LDHBP2*	−0.607	Xq13.3
	hsa-miR-222	−0.467	Xp11.3	*GAPDHP32*	−0.529	1p12
	hsa-miR-221	−0.538	Xp11.3	*PSAT1P1*	−0.476	8q11.22
ESR2 (ERβ)	hsa-miR-211	0.512	15q13.3	*RPL31P44*	0.856	10q21.1
	hsa-miR-514	0.501	Xq27.3	*ITGB1BP3*	0.842	19p13.3
	hsa-miR-509-3p	0.481	Xq27.3	*ARL2BPP7*	0.747	9q31.1
	hsa-miR-221	−0.28	Xp11.3	*RANBP20P*	−0.478	14q11.2
	hsa-miR-505	−0.295	Xq27.1	*NPM1P3*	−0.373	16p13.3
	hsa-miR-7	−0.316	9q21.33	*RPL12P43*	−0.375	Xq24
ERBB2	hsa-miR-151-5p	0.473	8q24.3	*CDC42BPB*	0.586	14q32.33
	hsa-miR-151-3p	0.47	8q24.3	*FOLR3P1*	0.568	11q13.4
	hsa-miR-141	0.438	12p13.31	*LETM1P3*	0.545	8q22.2
	hsa-miR-134	−0.432	14q32.31	*RPL14P4*	−0.547	12q23.1
	hsa-miR-188-5p	−0.441	Xp11.22	*RPL14P1*	−0.52	12q14.2
	hsa-miR-1225-5p	−0.459	16p13.3	*RPL15P11*	−0.479	7q33
EGFR	hsa-miR-30a	0.526	6q13	*ARHGAP29*	0.783	1p21.3
	hsa-miR-196b	0.489	7p15.2	*COX5AP2*	0.778	14q22.2
	hsa-miR-151-3p	0.481	8q24.3	*MYL6P3*	0.723	10q21.3
	hsa-miR-18b	−0.527	Xq26.2	*RPS19BP1*	−0.639	22q13.2
	hsa-miR-25	−0.537	7q22.1	*TERF2IP*	−0.641	16q23.1
	hsa-miR-652	−0.648	Xq22.3	*RPL21P114*	−0.63	15q22.2
MPP2	hsa-miR-125b	0.5	11q24.1	*SRGAP2P1*	0.563	1p11.2: 1p11.1
	hsa-miR-100	0.497	11q24.1	*SEPT7P7*	0.528	9q22.33
	hsa-miR-22*	0.478	17p13.3	*OR10Q2P*	0.493	11q12.1
	hsa-miR-200c	−0.383	12p13.31	*HNRNPF*	−0.581	10q11.21
	hsa-miR-141	−0.391	12p13.31	*RAB11FIP1*	−0.527	8p12
	hsa-miR-32	−0.401	9q31.3	*ARHGAP27*	−0.446	17q21.32
AR	hsa-miR-376c	0.375	14q32.31	*RPL31P42*	0.516	9p22.2
	hsa-miR-377	0.359	14q32.31	*HLF*	0.515	17q22
	hsa-miR-376a	0.359	14q32.31	*RPL39P33*	0.456	17q22
	hsa-miR-202	−0.286	10q26.3	*KRTAP2-1*	−0.425	17q21.31
				GPBP1L1	−0.425	1p34.1
				OR4X2	−0.427	11p11.2
BRCA1	hsa-miR-423-5p	0.369	17q11.2	*RPL19P15*	0.585	9q34.13
	hsa-miR-550*	0.368	7p15.1	*STX17*	0.58	9q31.1
	hsa-miR-106b	0.354	7q22.1	*SMEK2*	0.576	2p16.1
	hsa-miR-521	−0.414	19q13.33	*KRT17P3*	−0.449	17q12
	hsa-miR-522	−0.422	19q13.33	*RBM7*	−0.449	11q23.2
	hsa-miR-517c	−0.474	19q13.33	*HHIPL1*	−0.449	14q32.2

(continued)

Table 1
(continued)

Gene	miRNAs	Correlations	Location	Pseudogenes	Correlations	Location
KRT19	hsa-miR-429	0.764	1p36.33	*KRT19P2*	0.973	12q23.1
	hsa-miR-200a	0.763	1p36.33	*KRT19P1*	0.963	6q13
	hsa-miR-200b	0.753	1p36.33	*ESRP2*	0.778	16q22.1
	hsa-miR-204	−0.431	9q21.13	*DPY19L2P2*	−0.469	7q22.1
	hsa-miR-363	−0.441	Xq26.2	*KLHL21*	−0.47	1p36.31
	hsa-miR-140-5p	−0.481	16q22.3	*HMCN1*	−0.47	1q31.1
PGR	hsa-miR-375	0.535	2q35	*RPS17P2*	0.96	5q23.1
	hsa-miR-301a	0.517	17q23.2	*BNIPL*	0.937	1q21.3
	hsa-miR-148b	0.508	12q13.2	*C1orf168*	0.936	1p32.2
	hsa-miR-29a	−0.412	7q32.3	*GAPDHP63*	−0.56	6q14.1
	hsa-let-7i	−0.481	12q14.2	*GAPDHP45*	−0.561	10p13
	hsa-miR-221	−0.536	Xp11.3	*SLC16A1*	−0.567	1p13.2
RB1	hsa-miR-181a*	0.397	1q32.1	*CCNDBP1*	0.535	15q21.1
	hsa-miR-29c	0.357	1q32.2	*KIAA0564*	0.534	13q14.11
	hsa-miR-181a	0.315	1q32.1	*PCGF5*	0.508	10q23.32
	hsa-miR-24	−0.293	9q22.32	*FABP3P2*	−0.431	13q14.11
	hsa-miR-99a	−0.3	21q21.1	*PLXDC1*	−0.433	17q21.2
	hsa-miR-196a	−0.306	12q13.2	*S1PR5*	−0.433	19p13.2
BCL2	hsa-miR-106b	0.375	7q22.1	*RPL21P18*	0.654	12q15
	hsa-miR-93	0.368	7q22.1	*NPY5R*	0.647	4q32.2
	hsa-miR-30e	0.345	1p34.2	*SNTN*	0.643	3p14.2
	hsa-miR-151-3p	−0.399	8q24.3	*CDC42BPA*	−0.485	1q42.13
	hsa-miR-31*	−0.403	9p21.3	*ANXA1*	−0.488	9q21.13
	hsa-miR-31	−0.428	9p21.3	*SLC12A4*	−0.495	16q22.1
AKT1	hsa-miR-324-5p	0.386	17p13.1	*NMNATP*	0.511	14q31.1
	hsa-miR-107	0.294	10q23.31	*SIVA1*	0.506	14q32.33
	hsa-miR-103	0.293	5q35.1	*VPS45*	0.504	1q21.3
	hsa-miR-31*	−0.299	9p21.3	*RPS24P18*	−0.469	18q12.1
	hsa-miR-31	−0.345	9p21.3	*SEZ6*	−0.471	17q11.2
				SLC6A5	−0.477	11p15.1
TP53	hsa-miR-487b	0.364	14q32.31	*RABEP1*	0.493	17p13.2
	hsa-miR-324-3p	0.314	17p13.1	*SMG6*	0.486	17p13.3
	hsa-miR-371-5p	0.283	19q13.33	*ANKFY1*	0.486	17p13.2
	hsa-miR-545	−0.327	Xq13.2	*VENTXP7*	−0.436	3p24.3
	hsa-miR-197	−0.351	1p13.3	*GOLGA8A*	−0.436	15q14
	hsa-miR-199b-5p	−0.384	9q34.11	*AKIRIN1*	−0.438	1p34.3
VEGFA	hsa-miR-210	0.479	11p15.5	*CDC42EP1*	0.43	22q13.1
	hsa-miR-27b	0.442	9q22.32	*B4GALT1*	0.43	9p13.3
	hsa-miR-27a	0.428	19p13.12	*STAC*	0.429	3p22.3: 3p22.2
	hsa-miR-30e	−0.375	1p34.2	*SYNGAP1*	−0.457	6p21.32
	hsa-miR-153	−0.391	2q35	*ESF1*	−0.458	20p12.1
	hsa-miR-766	−0.422	Xq24	*ADRBK2*	−0.458	22q12.1

(continued)

Table 1
(continued)

Gene	miRNAs	Correlations	Location	Pseudogenes	Correlations	Location
MYC	hsa-miR-378	0.642	5q33.1	*BZRAP1*	0.711	17q23.2
	hsa-miR-106a	0.635	Xq26.2	*PRG2*	0.707	11q12.1
	hsa-miR-142-3p	0.626	17q23.2	*GFI1*	0.706	1p22.1
	hsa-let-7e	−0.568	19q13.32	*CDC42BPB*	−0.606	14q32.33
	hsa-miR-125a-5p	−0.584	19q13.32	*ECE1*	−0.606	1p36.12
	hsa-miR-22	−0.685	17p13.3	*GNA11*	−0.62	19p13.3
PTEN	hsa-miR-148b	0.288	12q13.2	*RPL11P3*	0.597	10q23.31
	hsa-miR-551b	−0.29	3q26.1	*HNRNPH1*	0.566	5q35.3
	hsa-miR-146a	−0.294	5q34	*NACA*	0.563	12q14.1
	hsa-miR-361-3p	−0.313	Xq21.2	*RPS26P57*	−0.383	Xq25
				ODZ1	−0.386	Xq25
				C1orf144	−0.388	1p36.13
RASSF1	hsa-miR-142-3p	0.476	17q23.2	*RPS18P9*	0.586	6q25.1
	hsa-miR-142-5p	0.459	17q23.2	*HMGB2*	0.586	4q34.1
	hsa-miR-106a	0.457	Xq26.2	*KIF15*	0.582	3p21.31
	hsa-miR-151-3p	−0.393	8q24.3	*TGIF1P1*	−0.435	19q13.2
	hsa-miR-151-5p	−0.431	8q24.3	*CPNE3*	−0.436	8q21.3
	hsa-miR-34a	−0.557	1p36.22	*HS1BP3*	−0.436	2p24.1
GSTP1	hsa-miR-221	0.456	Xp11.3	*GSTP1P1*	0.754	12q13.3
	hsa-miR-222	0.451	Xp11.3	*ECHDC1*	0.534	6q22.33
	hsa-miR-361-3p	0.284	Xq21.2	*TFCP2*	0.503	12q13.13
	hsa-miR-331-3p	−0.307	12q23.1	*NUS1P3*	−0.475	13q12.13
	hsa-miR-193b	−0.309	16p13.12	*HPX*	−0.476	11p15.4
	hsa-miR-375	−0.315	2q35	*BLNK*	−0.476	10q23.33: 10q24.1
	Leukemia					
NPM1	hsa-miR-340*	0.457	5q35.3	*SERBP1*	0.605	1p31.3
	hsa-miR-340	0.422	5q35.3	*RPS5*	0.604	19q13.41
	hsa-miR-519a	0.368	19q13.33	*RPS19*	0.598	19q13.12
	hsa-miR-215	−0.315	1q41	*RPL23AP66*	−0.442	12p13.2
	hsa-miR-27b	−0.392	9q22.32	*HNF1A*	−0.442	12q24.31
	hsa-miR-23b	−0.415	9q22.32	*RPS14P7*	−0.443	4q32.2
ABL1	hsa-miR-155	0.45	21q21.3	*SAR1AP2*	0.626	10q26.2
	hsa-miR-181a-2*	0.437	9q33.3	*KLF7*	0.625	2q33.3
	hsa-miR-22*	0.428	17p13.3	*ALPK2*	0.595	18q21.32
	hsa-miR-26b	−0.376	2q35	*APOA1BP*	−0.466	1q23.1
	hsa-miR-141	−0.393	12p13.31	*SRBD1*	−0.466	2p21
	hsa-miR-200c	−0.396	12p13.31	*AKR7A2*	−0.466	1p36.13
BCR	hsa-miR-141	0.536	12p13.31	*PI4KAP2*	0.574	22q11.23
	hsa-miR-200c	0.536	12p13.31	*SLC29A2*	0.567	11q13.1
	hsa-miR-203	0.46	14q32.33	*PARS2*	0.559	1p32.3
	hsa-miR-140-5p	−0.427	16q22.3	*RPL32P1*	−0.476	6p21.32
	hsa-miR-125b	−0.445	11q24.1	*PPAP2A*	−0.477	5q11.2
	hsa-miR-455-3p	−0.479	9q33.1	*FUBP3*	−0.478	9q34.13

(continued)

Table 1
(continued)

Gene	miRNAs	Correlations	Location	Pseudogenes	Correlations	Location
STAT5B	hsa-miR-342-5p	0.532	14q32.31	*RPS15AP23*	0.592	7q33
	hsa-miR-766	0.513	Xq24	*ALDH1A2*	0.591	15q22.2
	hsa-miR-92a-1*	0.49	13q31.3	*EVL*	0.591	14q32.31
	hsa-miR-151-3p	−0.423	8q24.3	*PIGAP1*	−0.466	12q23.2
	hsa-miR-24	−0.451	9q22.32	*NR1D2*	−0.468	3p24.2
	hsa-miR-23a	−0.496	19p13.12	*ULBP3*	−0.469	6q25.1
LMO2	hsa-miR-199b-5p	0.778	9q34.11	*VENTXP7*	0.976	3p24.3
	hsa-miR-129*	0.691	7q32.1	*MS4A3*	0.964	11q12.2
	hsa-miR-191	0.624	3p21.31	*ANKRD55*	0.956	5q11.2
	hsa-miR-151-3p	−0.431	8q24.3	*FTH1P20*	−0.605	2q31.3
	hsa-miR-151-5p	−0.451	8q24.3	*SLC37A3*	−0.609	7q34
	hsa-miR-22	−0.479	17p13.3	*LGMN*	−0.61	14q32.13
PML	hsa-miR-455-5p	0.457	9q33.1	*PARP14*	0.687	3q13.33
	hsa-miR-155	0.429	21q21.3	*PARP12*	0.684	7q34
	hsa-miR-455-3p	0.401	9q33.1	*ZC3HAV1*	0.67	7q34
	hsa-miR-26b	−0.387	2q35	*NIPSNAP1*	−0.393	22q12.2
	hsa-miR-149	−0.413	2q37.3	*CYB5D1*	−0.394	17p13.1
	hsa-miR-148b	−0.416	12q13.2	*DLX6-AS1*	−0.396	7q21.3
RUNX1	hsa-miR-181a*	0.558	1q32.1	*GVINP1*	0.669	11p15.4
	hsa-miR-142-5p	0.517	17q23.2	*PTPRN2*	0.666	7q36.3
	hsa-miR-181b	0.511	1q32.1	*CHI3L2*	0.664	1p13.2
	hsa-miR-24	−0.446	9q22.32	*RPL21P11*	−0.488	14q32.12
	hsa-miR-151-3p	−0.477	8q24.3	*KIAA1598*	−0.489	10q25.3
	hsa-miR-151-5p	−0.508	8q24.3	*GNS*	−0.489	12q14.3
TAL1	hsa-miR-92a-1*	0.653	13q31.3	*PTPRVP*	0.775	1q32.1
	hsa-miR-19b-1*	0.636	13q31.3	*CXorf65*	0.775	Xq13.1
	hsa-miR-146b-5p	0.62	10q24.32	*HIST1H2BO*	0.774	6p22.1
	hsa-miR-27a	−0.595	19p13.12	*S100A11P1*	−0.458	7q22.1
	hsa-miR-23a	−0.638	19p13.12	*HYAL2*	−0.458	3p21.31
	hsa-miR-24	−0.664	9q22.32	*USP13*	−0.458	3q26.32
FOXO3	hsa-let-7b	0.389	22q13.31	*GLYATL1P3*	0.471	11q12.1
	hsa-let-7c	0.325	21q21.1	*TNFRSF18*	0.471	1p36.33
	hsa-let-7a	0.308	9q22.32	*FAM26F*	0.471	6q22.1
	hsa-miR-532-3p	−0.273	Xp11.22	*TRNAK40P*	−0.414	14q24.3
	hsa-miR-32	−0.279	9q31.3	*MDM1*	−0.416	12q15
	hsa-miR-652	−0.365	Xq22.3	*CIAO1*	−0.416	2q11.2
TLX1	hsa-miR-192*	0.459	11q13.1	*CCT7P2*	0.825	5q15
	hsa-miR-142-3p	0.413	17q23.2	*TPPP3*	0.824	16q22.1
	hsa-miR-215	0.405	1q41	*PGC*	0.824	6p21.1
	hsa-miR-130a	−0.356	11q12.1	*MAPK8IP3*	−0.395	16p13.3
	hsa-miR-193a-3p	−0.378	17q12	*NOTCH2*	−0.395	1p12
	hsa-miR-365	−0.403	16p13.12	*SRRM2*	−0.396	16p13.3

(continued)

Table 1
(continued)

Gene	miRNAs	Correlations	Location	Pseudogenes	Correlations	Location
BAALC	hsa-miR-204	0.325	9q21.13	*OR6K4P*	0.844	1q23.2
	hsa-miR-140-3p	0.294	16q22.3	*FREM1*	0.802	9p22.3
	hsa-miR-140-5p	0.287	16q22.3	*FMOD*	0.794	1q32.1
	hsa-miR-200b	−0.282	1p36.33	*HMGN1P37*	−0.381	Xq28
	hsa-miR-29a*	−0.293	7q32.3	*RAB3IP*	−0.384	12q21.1
	hsa-miR-219-5p	−0.341	6p21.32	*SLC37A4*	−0.385	11q23.3
EGFR	hsa-miR-30a	0.526	6q13	*ARHGAP29*	0.783	1p21.3
	hsa-miR-30a*	0.524	6q13	*COX5AP2*	0.778	14q22.2
	hsa-miR-196b	0.489	7p15.2	*SLC35F3*	0.772	1q42.3
	hsa-miR-18b	−0.527	Xq26.2	*SLC25A5P1*	−0.599	22q13.2
	hsa-miR-25	−0.537	7q22.1	*AARS2*	−0.6	6p21.1
	hsa-miR-652	−0.648	Xq22.3	*ZNF589*	−0.601	3p21.31
	Prostate cancer					
AR	hsa-miR-376c	0.375	14q32.31	*RPL31P42*	0.516	9p22.2
	hsa-miR-377	0.359	14q32.31	*HLF*	0.515	17q22
	hsa-miR-376a	0.359	14q32.31	*TIMP4*	0.508	3p25.2
	hsa-miR-202	−0.286	10q26.3	*OR5AQ1P*	−0.41	11q11
				TRIM38	−0.411	6p22.2
				FAM135A	−0.411	6q13
CAV1	hsa-miR-100	0.686	11q24.1	*TRNAK38P*	0.787	19q13.12
	hsa-miR-125b	0.684	11q24.1	*CD44*	0.771	11p13
	hsa-miR-22*	0.616	17p13.3	*MT4*	0.764	16q13
	hsa-miR-92a	−0.563	13q31.3	*RPL34P27*	−0.543	13q12.13
	hsa-miR-17	−0.603	13q31.3	*PARL*	−0.544	3q26.33
	hsa-miR-18b	−0.625	Xq26.2	*ZC3H8*	−0.544	2q13
DLC1	hsa-miR-22*	0.484	17p13.3	*EFEMP2*	0.644	11q13.1
	hsa-miR-455-3p	0.434	9q33.1	*TRAM2*	0.643	6p12.2
	hsa-miR-30a	0.388	6q13	*GPR176*	0.642	15q15.1
	hsa-miR-652	−0.479	Xq22.3	*RPS27P13*	−0.517	4p15.31
	hsa-miR-93	−0.493	7q22.1	*RBBP5*	−0.517	1q32.1
	hsa-miR-25	−0.508	7q22.1	*JTB*	−0.517	1q22
AKT1	hsa-miR-324-5p	0.386	17p13.1	*NMNATP*	0.511	14q31.1
	hsa-miR-107	0.294	10q23.31	*SIVA1*	0.506	14q32.33
	hsa-miR-103	0.293	5q35.1	*VPS45*	0.504	1q21.3
	hsa-miR-31*	−0.299	9p21.3	*RPS24P18*	−0.469	18q12.1
	hsa-miR-31	−0.345	9p21.3	*SEZ6*	−0.471	17q11.2
				SLC6A5	−0.477	11p15.1
EGFR	hsa-miR-30a	0.526	6q13	*ARHGAP29*	0.783	1p21.3
	hsa-miR-30a*	0.524	6q13	*COX5AP2*	0.778	14q22.2
	hsa-miR-196b	0.489	7p15.2	*SLC35F3*	0.772	1q42.3
	hsa-miR-18b	−0.527	Xq26.2	*SLC25A5P1*	−0.599	22q13.2
	hsa-miR-25	−0.537	7q22.1	*AARS2*	−0.6	6p21.1
	hsa-miR-652	−0.648	Xq22.3	*ZNF589*	−0.601	3p21.31

(continued)

Table 1
(continued)

Gene	miRNAs	Correlations	Location	Pseudogenes	Correlations	Location
BCL2	hsa-miR-106b	0.375	7q22.1	*RPL21P18*	0.654	12q15
	hsa-miR-93	0.368	7q22.1	*NPY5R*	0.647	4q32.2
	hsa-miR-30e	0.345	1p34.2	*SNTN*	0.643	3p14.2
	hsa-miR-151-3p	−0.399	8q24.3	*CDC42BPA*	−0.485	1q42.13
	hsa-miR-31*	−0.403	9p21.3	*ANXA1*	−0.488	9q21.13
	hsa-miR-31	−0.428	9p21.3	*SLC12A4*	−0.495	16q22.1
PTEN	hsa-miR-148b	0.288	12q13.2	*RPL11P3*	0.597	10q23.31
	hsa-miR-551b	−0.29	3q26.1	*HNRNPH1*	0.566	5q35.3
	hsa-miR-146a	−0.294	5q34	*NACA*	0.563	12q14.1
	hsa-miR-361-3p	−0.313	Xq21.2	*RPS26P57*	−0.383	Xq25
				ODZ1	−0.386	Xq25
				C1orf144	−0.388	1p36.13
CCND1	hsa-miR-151-5p	0.726	8q24.3	*RPL37P12*	0.457	2q13
	hsa-miR-151-3p	0.685	8q24.3	*NMBR*	0.456	6q24.1
	hsa-miR-22	0.583	17p13.3	*CAPNS1*	0.456	19q12
	hsa-miR-19b-1*	−0.648	13q31.3	*ARHGAP30*	−0.685	1q23.3
	hsa-miR-142-3p	−0.662	17q23.2	*ARHGEF6*	−0.686	Xq26.3
	hsa-miR-142-5p	−0.728	17q23.2	*CEP110*	−0.687	9q33.2
CASP3	hsa-miR-188-5p	0.49	Xp11.22	*CDKN2AIP*	0.544	4q35.1
	hsa-miR-638	0.477	19p13.2	*ERAP1*	0.527	5q15
	hsa-miR-630	0.473	15q24.1	*CD247*	0.524	1q24.2
	hsa-miR-151-5p	−0.443	8q24.3	*ARHGAP39*	−0.399	8q24.3
	hsa-miR-99b	−0.449	19q13.32	*RALGAPA1*	−0.4	14q13.3
	hsa-let-7e	−0.473	19q13.32	*FAM92B*	−0.4	16q24.1
TNFSF10	hsa-miR-196b	0.419	7p15.2	*HMGN2P46*	0.545	15q21.1
	hsa-miR-455-5p	0.298	9q33.1	*LARP1B*	0.542	4q28.1: 4q28.2
	hsa-miR-429	0.294	1p36.33	*HOXA3*	0.54	7p15.2
	hsa-miR-513b	−0.31	Xq27.3	*RWDD1P3*	−0.357	12q21.2
	hsa-miR-660	−0.316	Xp11.22	*RPL13AP7*	−0.358	21q21.3
	hsa-miR-362-3p	−0.324	Xp11.22	*MLX*	−0.358	17q21.31
	Colorectal cancer					
APC	hsa-miR-204	0.488	9q21.13	*RASGRP3*	0.542	2p22.3
	hsa-miR-145	0.405	5q33.1	*PNLIPRP3*	0.474	10q25.3
	hsa-miR-99a	0.395	21q21.1	*ZNF300P1*	0.471	5q33.1
	hsa-miR-200b	−0.362	1p36.33	*RPS26P43*	−0.485	11q24.1
	hsa-miR-29c	−0.384	1q32.2	*HMGN2P28*	−0.432	6p25.3: 6p25.2
	hsa-miR-331-3p	−0.526	12q23.1	*RPS29P9*	−0.428	2q33.3
BAX	hsa-miR-34b*	0.387	11q23.1	*RAB11FIP5*	0.378	2p13.2
	hsa-miR-874	0.338	5q31.2	*ELK3*	0.378	12q23.1
	hsa-miR-29a	0.317	7q32.3	*DPY19L2P1*	0.377	7p14.3
	hsa-miR-301b	−0.345	22q11.23	*ASS1P10*	−0.405	5q32
	hsa-miR-497	−0.351	17p13.1	*CYP1A2*	−0.406	15q24.3
	hsa-miR-15b	−0.428	3q25.33	*TMEM175*	−0.406	4p16.3

(continued)

Table 1
(continued)

Gene	miRNAs	Correlations	Location	Pseudogenes	Correlations	Location
CTNNB1	hsa-miR-211	0.627	15q13.3	*TUBB1P2*	0.688	Yq11.222
	hsa-miR-514	0.505	Xq27.3	*STX7*	0.687	6q23.2
	hsa-miR-146a	0.497	5q34	*SFTPC*	0.687	8p21.3
	hsa-miR-331-3p	−0.368	12q23.1	*BTF3P9*	−0.481	1q42.13
	hsa-miR-96	−0.375	7q32.2	*OR2F2*	−0.481	7q35
	hsa-miR-181d	−0.381	19p13.12	*RPL21P6*	−0.482	14q23.1
KRAS	hsa-miR-200a	0.356	1p36.33	*ARHGAP26*	0.568	5q31.3
	hsa-miR-429	0.348	1p36.33	*RPL39P27*	0.561	12p12.1
	hsa-miR-141	0.339	12p13.31	*SLC9A3P2*	0.559	22q11.22
	hsa-miR-99a	−0.341	21q21.1	*MKRN4P*	−0.486	Xp11.4
	hsa-miR-193a-3p	−0.349	17q12	*RPS26P21*	−0.405	3q13.32
	hsa-miR-455-5p	−0.355	9q33.1	*SLC6A10P*	−0.384	16p11.2
MLH1	hsa-miR-152	0.386	17q21.33	*EPM2AIP1*	0.568	3p22.2
	hsa-miR-181d	0.287	19p13.12	*RAB3GAP2*	0.449	1q41
	hsa-miR-432	0.265	14q32.31	*DNTTIP2*	0.439	1p22.1
	hsa-miR-10b	−0.316	2q31.1	*FOLR3P1*	−0.572	11q13.4
	hsa-miR-31	−0.368	9p21.3	*LETM1P3*	−0.567	8q22.2
	hsa-miR-31	−0.371	9p21.3	*IPMKP1*	−0.56	13q12.12
MMP2	hsa-miR-125b	0.5	11q24.1	*SRGAP2P1*	0.563	1p11.2: 1p11.1
	hsa-miR-100	0.497	11q24.1	*TBX15*	0.561	1p12
	hsa-miR-22*	0.478	17p13.3	*SRPX2*	0.56	Xq22.1
	hsa-miR-200c	−0.383	12p13.31	*DCTPP1*	−0.51	16p11.2
	hsa-miR-141	−0.391	12p13.31	*C3orf46*	−0.513	3q21.2
	hsa-miR-32	−0.401	9q31.3	*PTPN6*	−0.513	12p13.31
MMP7	hsa-miR-10a	0.43	17q21.33	*UGT1A11P*	0.69	2q37.1
	hsa-miR-141	0.365	12p13.31	*PLA2G16*	0.652	11q13.1
	hsa-miR-200a	0.352	1p36.33	*STEAP4*	0.65	7q21.12
	hsa-miR-370	−0.328	14q32.31	*RPSAP10*	−0.46	10p11.23
	hsa-miR-140-3p	−0.368	16q22.3	*CYP20A1*	−0.46	2q33.2
	hsa-miR-140-5p	−0.415	16q22.3	*USP13*	−0.469	3q26.32
MMP9	hsa-miR-129-3p	0.356	11p11.2	*RPS6P12*	0.893	9q21.32
	hsa-miR-877	0.26	6p21.33	*ZP4*	0.886	1q43
	hsa-miR-24-1*	−0.294	9q22.32	*SIGLEC15*	0.884	18q21.1
	hsa-miR-301b	−0.313	22q11.23	*PHKA1P1*	−0.356	1p22.2
	hsa-let-7b	−0.353	22q13.31	*OR6K1P*	−0.365	1q23.2
				MGST2	−0.369	4q31.1
MSH2	hsa-miR-10a*	0.448	17q21.33	*SNRPGP10*	0.516	1q32.2
	hsa-miR-766	0.425	Xq24	*THAP9*	0.516	4q21.22
	hsa-miR-424*	0.425	Xq26.3	*ANAPC1*	0.515	2q13
	hsa-miR-22	−0.36	17p13.3	*ARHGAP20*	−0.499	11q23.1
	hsa-miR-27b	−0.407	9q22.32	*RPS27AP8*	−0.5	3q26.2
	hsa-miR-23b	−0.423	9q22.32	*LRP1*	−0.502	12q14.1

(continued)

Table 1
(continued)

Gene	miRNAs	Correlations	Location	Pseudogenes	Correlations	Location
MSH6	hsa-miR-181b	0.405	1q32.1	*RAB3GAP2*	0.493	1q41
	hsa-miR-296-5p	0.374	20q13.32	*SLC30A6*	0.493	2p22.3
	hsa-miR-766	0.36	Xq24	*NCRNA00116*	0.491	2q13
	hsa-miR-141	−0.304	12p13.31	*RPL34P25*	−0.492	12p12.3
	hsa-miR-200a	−0.313	1p36.33	*GATA6*	−0.494	18q11.2
	hsa-miR-200b	−0.315	1p36.33	*SHISA3*	−0.495	4p13
TP53	hsa-miR-487b	0.364	14q32.31	*RABEP1*	0.493	17p13.2
	hsa-miR-324-3p	0.314	17p13.1	*RPL12P15*	0.434	2q14.3
	hsa-miR-371-5p	0.283	19q13.33	*RPL26P36*	0.424	Xq21.32
	hsa-miR-545	−0.327	Xq13.2	*HERC2P9*	−0.465	15q13.2
	hsa-miR-197	−0.351	1p13.3	*ATF7IP2*	−0.443	16p13.13
	hsa-miR-199b-5p	−0.384	9q34.11	*VENTXP7*	−0.436	3p24.3
TGFBR2	hsa-miR-221	0.46	Xp11.3	*RPL36AP44*	0.449	15q22.2
	hsa-miR-135b	0.439	1q32.2	*TNFRSF21*	0.449	6p12.3
	hsa-miR-222	0.436	Xp11.3	*C1orf175*	0.449	1p32.3
	hsa-miR-195	−0.446	17p13.1	*ATP5EP2*	−0.382	13q12.3
	hsa-miR-497	−0.474	17p13.1	*DHTKD1*	−0.385	10p14
	hsa-miR-296-5p	−0.488	20q13.32	*TCEANC*	−0.387	Xp22.2
SMAD4	hsa-miR-155	0.471	21q21.3	*AGTPBP1*	0.561	9q21.33
	hsa-miR-498	0.397	19q13.33	*C18orf54*	0.555	18q21.2
	hsa-miR-193a-5p	0.365	17q12	*WDR7*	0.549	18q21.31: 18q21.32
	hsa-miR-192	−0.464	11q13.1	*RPL21P75*	−0.54	7p15.3
	hsa-miR-215	−0.47	1q41	*ABHD12B*	−0.54	14q22.1
	hsa-miR-194	−0.481	1q41	*SH3BGRL2*	−0.541	6q14.1

References

1. Tutar L, Tutar E, Tutar Y (2014) MicroRNAs and cancer; an overview. Curr Pharm Biotechnol 15(5):430–437
2. Qu J, Li M, Zhong W, Hu C (2015) Competing endogenous RNA in cancer: a new pattern of gene expression regulation. Int J Clin Exp Med 8(10):17110–17116
3. Poliseno L, Marranci A, Pandolfi PP (2015) Pseudogenes in human cancer. Front Med 2:68
4. Garzon R, Calin GA, Croce CM (2009) MicroRNAs in cancer. Annu Rev Med 60:167–179
5. Schoof CRG, da Silva Botelho EL, Izzotti A, dos Reis Vasques L (2012) MicroRNAs in cancer treatment and prognosis. Am J Cancer Res 2(4):414–433
6. Krol J, Loedige I, Filipowicz W (2010) The widespread regulation of microRNA biogenesis, function and decay. Nat Rev Genet 11 (9):597–610
7. Tutar Y, Özgür A, Tutar E, Tutar L, Pulliero A et al (2016) Regulation of oncogenic genes by MicroRNAs and pseudogenes in human lung cancer. Biomed Pharmacother 83:1182–1190
8. Goodhead I, Darby AC (2015) Taking the pseudo out of pseudogenes. Curr Opin Microbiol 23:102–109
9. Tutar Y (2012) Pseudogenes. Comp Funct Genomics 2012:6–9
10. Korrodi-Gregório L, Abrantes J, Muller T, Melo-Ferreira J, Marcus K et al (2013) Not so pseudo: the evolutionary history of protein phosphatase 1 regulatory subunit 2 and related pseudogenes. BMC Evol Biol 13(1):242
11. Pink RC, Wicks K, Caley DP, Punch EK, Jacobs L et al (2011) Pseudogenes: pseudofunctional or key regulators in health and disease? RNA 17(5):792–798

12. Poliseno L (2012) Pseudogenes: newly discovered players in human cancer. Sci Signal 5 (242):re5
13. Dweep H, Sticht C, Gretz N (2013) In-Silico algorithms for the screening of possible microRNA binding sites and their interactions. Curr Genomics 14(2):127–136
14. Shankavaram UT, Varma S, Kane D, Sunshine M, Chary KK et al (2009) CellMiner: a relational database and query tool for the NCI-60 cancer cell lines. BMC Genomics 10:277
15. Özgür A, Tutar L, Tutar Y (2014) Regulation of heat shock proteins by miRNAs in human breast cancer. Microrna 3(2):118–135
16. Baev V, Milev I, Naydenov M, Vachev T, Apostolova E et al (2014) Insight into small RNA abundance and expression in high- and low-temperature stress response using deep sequencing in Arabidopsis. Plant Physiol Biochem 84:105–114
17. Ribeiro AO, Schoof CRG, Izzotti A, Pereira LV, Vasques LR (2014) MicroRNAs: modulators of cell identity, and their applications in tissue engineering. Microrna 3(1):45–53
18. Poliseno L, Salmena L, Zhang J, Carver B, Haveman WJ et al (2010) A coding-independent function of gene and pseudogene mRNAs regulates tumour biology. Nature 465 (7301):1033–1038
19. Chen C (2005) Real-time quantification of microRNAs by stem-loop RT-PCR. Nucleic Acids Res 33(20):e179
20. Volinia S, Calin GA, Liu C-G, Ambs S, Cimmino A et al (2006) A microRNA expression signature of human solid tumors defines cancer gene targets. Proc Natl Acad Sci U S A 103 (7):2257–2261
21. Lu J, Getz G, Miska EA, Alvarez-Saavedra E, Lamb J et al (2005) MicroRNA expression profiles classify human cancers. Nature 435 (7043):834–838
22. Hui ABY, Shi W, Boutros PC, Miller N, Pintilie M et al (2009) Robust global micro-RNA profiling with formalin-fixed paraffin-embedded breast cancer tissues. Lab Invest 89 (5):597–606
23. Weber JA, Baxter DH, Zhang S, Huang DY, Huang KH et al (2010) The microRNA spectrum in 12 body fluids. Clin Chem 56 (11):1733–1741
24. Gumireddy K, Young DD, Xiong X, Hogenesch JB, Huang Q et al (2008) Small-molecule inhibitors of microRNA miR-21 function. Angew Chem Int Ed Engl 47(39):7482–7484
25. Bader AG, Brown D, Winkler M (2010) The promise of microRNA replacement therapy. Cancer Res 70(18):7027–7030
26. Calin GA, Dumitru CD, Shimizu M, Bichi R, Zupo S et al (2002) Frequent deletions and down-regulation of micro- RNA genes miR15 and miR16 at 13q14 in chronic lymphocytic leukemia. Proc Natl Acad Sci U S A 99 (24):15524–15529
27. Johnson SM, Grosshans H, Shingara J, Byrom M, Jarvis R et al (2005) RAS is regulated by the let-7 microRNA family. Cell 120 (5):635–647
28. Yong SL, Dutta A (2007) The tumor suppressor microRNA let-7 represses the HMGA2 oncogene. Genes Dev 21(9):1025–1030
29. Sampson VB, Rong NH, Han J, Yang Q, Aris V et al (2007) MicroRNA let-7a down-regulates MYC and reverts MYC-induced growth in Burkitt lymphoma cells. Cancer Res 67 (20):9762–9770
30. Muïler D, Bosserhoff A-K (2008) Integrin b 3 expression is regulated by let-7a miRNA in malignant melanoma. Oncogene 27282:6698–6706
31. Boyerinas B, Park SM, Shomron N, Hedegaard MM, Vinther J et al (2008) Identification of let-7-regulated oncofetal genes. Cancer Res 68 (8):2587–2591
32. Forman JJ, Legesse-Miller A, Coller HA (2008) A search for conserved sequences in coding regions reveals that the let-7 microRNA targets dicer within its coding sequence. Proc Natl Acad Sci U S A 105(39):14879–14884
33. Toyota M, Suzuki H, Sasaki Y, Maruyama R, Imai K et al (2008) Epigenetic silencing of microRNA-34b/c and B-cell translocation gene 4 is associated with CpG island methylation in colorectal cancer. Cancer Res 68 (11):4123–4132
34. Michael MZ, O'Connor SM, van Holst Pellekaan NG, Young GP, James RJ (2003) Reduced accumulation of specific microRNAs in colorectal neoplasia. Mol Cancer Res 1 (12):882–891
35. Volinia S, Galasso M, Costinean S, Tagliavini L, Gamberoni G et al (2010) Reprogramming of miRNA networks in cancer and leukemia. Genome Res 20(5):589–599
36. Calin GA, Ferracin M, Cimmino A, Di Leva G, Shimizu M et al (2005) A MicroRNA signature associated with prognosis and progression in chronic lymphocytic leukemia. N Engl J Med 353(17):1793–1801
37. Garzon R, Volinia S, Liu C, Fernandez-cymering C, Palumbo T et al (2008) MicroRNA signatures associated with cytogenetics

and prognosis in acute myeloid leukemia MicroRNA signatures associated with cytogenetics and prognosis in acute myeloid leukemia. Blood 111(6):3183–3189

38. Garzon R, Garofalo M, Martelli MP, Briesewitz R, Wang L et al (2008) Distinctive microRNA signature of acute myeloid leukemia bearing cytoplasmic mutated nucleophosmin. Proc Natl Acad Sci U S A 105 (10):3945–3950
39. Ciafrè SA, Galardi S, Mangiola A, Ferracin M, Liu CG et al (2005) Extensive modulation of a set of microRNAs in primary glioblastoma. Biochem Biophys Res Commun 334 (4):1351–1358
40. Chan JA, Krichevsky AM, Kosik KS (2005) MicroRNA-21 is an antiapoptotic factor in human glioblastoma cells. Cancer Res 65 (14):6029–6033
41. Meng F, Henson R, Wehbe–Janek H, Ghoshal K, Jacob ST et al (2007) MicroRNA-21 regulates expression of the PTEN tumor suppressor gene in human hepatocellular cancer. Gastroenterology 133(2):647–658
42. Frankel LB, Christoffersen NR, Jacobsen A, Lindow M, Krogh A et al (2008) Programmed cell death 4 (PDCD4) is an important functional target of the microRNA miR-21 in breast cancer cells. J Biol Chem 283 (2):1026–1033
43. Zhu S, Si ML, Wu H, Mo YY (2007) MicroRNA-21 targets the tumor suppressor gene tropomyosin 1 (TPM1). J Biol Chem 282(19):14328–14336
44. Mendell JT (2008) miRiad roles for the miR-17-92 cluster in development and disease. Cell 133(2):217–222
45. O'Donnell KA, Wentzel EA, Zeller KI, Dang CV, Mendell JT (2005) c-Myc-regulated microRNAs modulate E2F1 expression. Nature 435(7043):839–843
46. Iorio MV, Ferracin M, Liu CG, Veronese A, Spizzo R et al (2005) MicroRNA gene expression deregulation in human breast cancer. Cancer Res 65(16):7065–7070
47. Metzler M, Wilda M, Busch K, Viehmann S, Borkhardt A (2004) High expression of precursor MicroRNA-155/BIC RNA in children with Burkitt lymphoma. Genes Chromosomes Cancer 39(2):167–169
48. He H, Jazdzewski K, Li W, Liyanarachchi S, Nagy R et al (2005) The role of microRNA genes in papillary thyroid carcinoma. Proc Natl Acad Sci U S A 102(52):19075–19080
49. Takamizawa J, Konishi H, Yanagisawa K, Tomida S, Osada H et al (2004) Reduced expression of the let-7 microRNAs in human lung cancers in association with shortened postoperative survival. Cancer Res 64 (11):3753–3756
50. Hayashita Y, Osada H, Tatematsu Y, Yamada H, Yanagisawa K et al (2005) A polycistronic MicroRNA cluster, miR-17-92, is overexpressed in human lung cancers and enhances cell proliferation. Cancer Res 65 (21):9628–9632
51. Murakami Y, Yasuda T, Saigo K, Urashima T, Toyoda H et al (2006) Comprehensive analysis of microRNA expression patterns in hepatocellular carcinoma and non-tumorous tissues. Oncogene 25:2537–2545
52. Tsai WC, Hsu PWC, Lai TC, Chau GY, Lin CW et al (2009) MicroRNA-122, a tumor suppressor MicroRNA that regulates intrahepatic metastasis of hepatocellular carcinoma. Hepatology 49(5):1571–1582
53. Yoon SO, Chun SM, Han EH, Choi J, Jang SJ et al (2011) Deregulated expression of microRNA-221 with the potential for prognostic biomarkers in surgically resected hepatocellular carcinoma. Hum Pathol 42 (10):1391–1400
54. Esquela-Kerscher A, Trang P, Wiggins JF, Patrawala L, Cheng A et al (2008) The let-7 microRNA reduces tumor growth in mouse models of lung cancer. Cell Cycle 7 (6):759–764
55. Trang P, Medina PP, Wiggins JF, Ruffino L, Kelnar K et al (2010) Regression of murine lung tumors by the let-7 microRNA. Oncogene 29(11):1580–1587
56. Seike M, Goto A, Okano T, Bowman ED, Schetter AJ et al (2009) MiR-21 is an EGFR-regulated anti-apoptotic factor in lung cancer in never-smokers. Proc Natl Acad Sci U S A 106(29):12085–12090
57. Yu F, Yao H, Zhu P, Zhang X, Pan Q et al (2007) Let-7 regulates self renewal and tumorigenicity of breast cancer cells. Cell 131 (6):1109–1123
58. Shimono Y, Zabala M, Cho RW, Lobo N, Dalerba P et al (2009) Downregulation of miRNA-200c links breast cancer stem cells with normal stem cells. Cell 138(3):592–603
59. Si M-L, Zhu S, Wu H, Lu Z, Wu F et al (2007) miR-21-mediated tumor growth. Oncogene 26(19):2799–2803
60. Han HB, Gu J, Zuo HJ, Chen ZG, Zhao W et al (2012) Let-7c functions as a metastasis suppressor by targeting MMP11 and PBX3 in colorectal cancer. J Pathol 226(3):544–555
61. Akao Y, Nakagawa Y, Naoe T (2006) Let-7 MicroRNA functions as a potential growth

suppressor in human colon cancer cells. Biol Pharm Bull 29(5):903–906

62. Wang F, Zhang P, Maa Y, Yang J, Moyer MP et al (2012) NIRF is frequently upregulated in colorectal cancer and its oncogenicity can be suppressed by let-7a microRNA. Cancer Lett 314(2):223–231
63. Chen Y, Ma C, Zhang W, Chen Z, Ma L (2014) Down regulation of miR-143 is related with tumor size, lymph node metastasis and HPV16 infection in cervical squamous cancer. Diagn Pathol 9:88
64. Link A, Balaguer F, Shen Y, Nagasaka T, Lozano JJ et al (2010) Fecal microRNAs as novel biomarkers for colon cancer screening. Cancer Epidemiol Biomarkers Prev 19 (7):1766–1774
65. Medina PP, Nolde M, Slack FJ (2010) OncomiR addiction in an in vivo model of microRNA-21-induced pre-B-cell lymphoma. Nature 467(7311):86–90
66. Mavrakis KJ, Wolfe AL, Oricchio E, Palomero T, de Keersmaecker K et al (2010) Genome-wide RNA-mediated interference screen identifies miR-19 targets in notch-induced T-cell acute lymphoblastic leukaemia. Nat Cell Biol 12(4):372–379
67. Chaudhuri AA, So AY-L, Mehta A, Minisandram A, Sinha N et al (2012) Oncomir miR-125b regulates hematopoiesis by targeting the gene Lin28A. Proc Natl Acad Sci U S A 109(11):4233–4238
68. Han J, Li A, Liu H, Wen X, Zhao M et al (2014) Computational identification of microRNAs in the strawberry (Fragaria x Ananassa) genome sequence and validation of their precise sequences by miR-RACE. Gene 536 (1):151–162
69. Wang M, Tan L, Dijkstra M, van Lom K, Robertus J-L et al (2008) miRNA analysis in B-cell chronic lymphocytic leukaemia: proliferation centres characterized by low miR-150 and high BIC/miR-155 expression. J Pathol 215(1):13–20
70. Kalyana-Sundaram S, Kumar-Sinha C, Shankar S, Robinson DR, Wu YM et al (2012) Expressed pseudogenes in the transcriptional landscape of human cancers. Cell 149(7):1622–1634
71. Welch JD, Baran-Gale J, Perou CM, Sethupathy P, Prins JF (2015) Pseudogenes transcribed in breast invasive carcinoma show subtype-specific expression and ceRNA potential. BMC Genomics 16(1):113
72. Han L, Yuan Y, Zheng S, Yang Y, Li J et al (2014) The pan-cancer analysis of pseudogene expression reveals biologically and clinically relevant tumour subtypes. Nat Commun 5:3963

Chapter 4

MicroRNAs Reprogram Tumor Immune Response

Wei Cao, Wenfang Cheng, and Wei Wu

Abstract

Endogenously produced microRNAs (miRNAs) are predicted to regulate the translation of over two-thirds all human gene transcripts. Certain microRNAs regulate expression of genes that are critically involved in both innate and adaptive immune responses. miRNAs have been demonstrated to function as crucial regulators of immune response under both physiological and pathological conditions. Specifically, different miRNAs have been reported to have a role in controlling the development and the functions of tumor-associated immune cells. Immune cells represent a highly attractive target for microRNA gene therapy approaches, as these cells can be isolated, treated, and then reintroduced into patients. In this chapter, we will discuss how recent discoveries on the roles of microRNAs in immune-regulation will advance the field of cancer immunology and immunotherapy.

Key words MicroRNAs, Immune cells, Tumor microenvironment, Immunotherapy

1 Introduction

Immune system includes innate and adaptive responses. Innate immunity is the first-line defense on foreign invaders such as bacterial, viral infection, or transformed cells. Adaptive immunity is the chronic, second-line defense on pathogenic attack on host, and mainly constitutes of T cells, B cells, and NK cells. In addition, adapted immune cells have memory to react pathogens when encountering them again [1] (Fig. 1). Cancer is transformed, malignant cells in the body, its morphology, genetic makeup, transcriptomic profiling, and proteins presenting on the surface differ from normal cells [2–4]; therefore, immune cells view cancer cells as "foreigners," and try to eliminate them. The cancer immunosurveillance theory describes the dynamic process of cancer cells interacting immune cells: cancer cell elimination, equilibrium, escape via immunoediting [5, 6]. From the point view of cancer cells, the tumor-associated antigens, germline antigen, and mutation-derived neoantigens could produce peptides which result in innate and adaptive immune cell reactions—immunogenicity

Wei Wu (ed.), *MicroRNA and Cancer: Methods and Protocols*, Methods in Molecular Biology, vol. 1699,
DOI 10.1007/978-1-4939-7435-1_4,

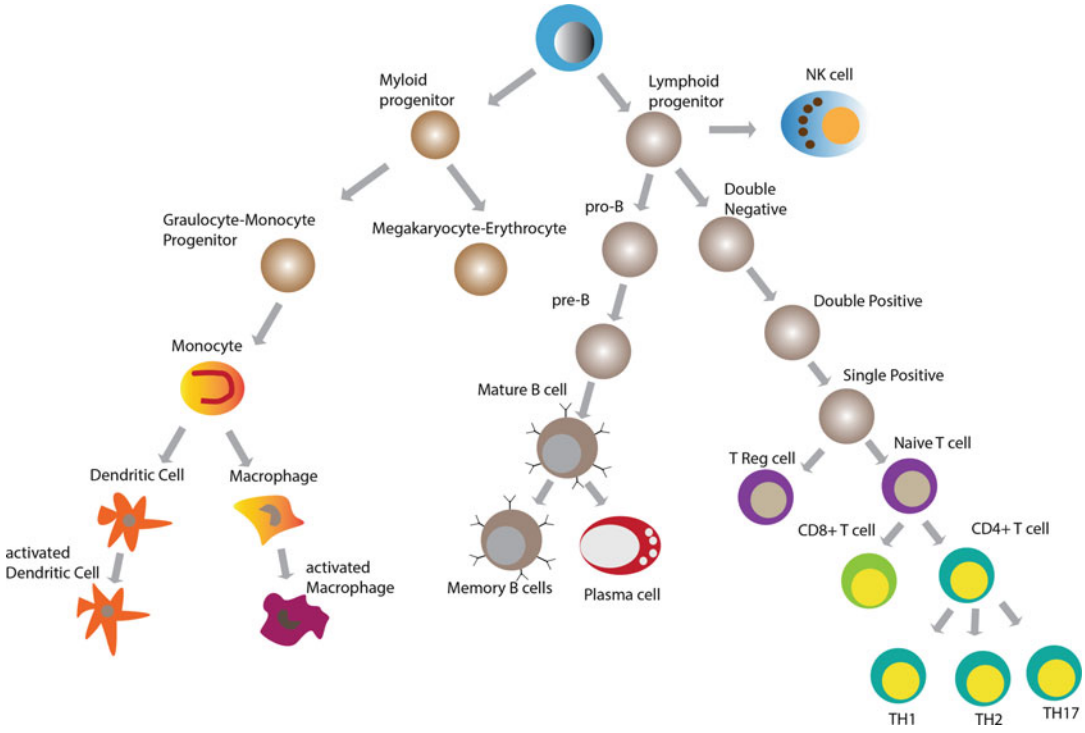

Fig. 1 The diagram illustrates the differentiation of immune cells. The hematopoietic stem cell differentiates into myloid and lymphoid linages under regulatory systems. The Myloid linage follows the trajectory to dendritic cells and macrophages, while the lymphoid linage traces down to B cells, T cells, and NK cells. Each stage may regulate by microRNAs as descripted in the text

[7–11]; cancer cells can turn off these antigen expressions so that differentiated T cells cannot recognize them [12]. On the other hand, cancer cells induce expression of negative molecular such as programed cell death protein 1 ligand (PD-L1) to block cytotoxic T cell activity [13], and therefore, escape the attack from host immune cells. The findings of negative regulatory signaling of T cells are a breakthrough in the cancer immunology and these molecules (PD-1, PD-L1, and CTLA-4) are becoming novel and effective targets for immunotherapy [14–16]. In tumor microenvironment, exosomal vehicles are new communication tools between cancer cells and stromal cells [17, 18]. From the complex biological system, small noncoding RNAs are the key players to execute the functions. In this chapter, we will update our knowledge of microRNA biology and highlight their roles in modulating cancer immune response.

2 MicroRNA Biogenesis

MicroRNAs (miRNAs) are a class of endogenous noncoding small RNA molecules (~22 nucleotides, nt), which play important roles in development, differentiation, proliferation, and apoptosis [19]. Since the miRNAs, lin-4 and let-7, were discovered in the Caenorhabditis elegans [20, 21], thousands of miRNAs have been identified in different species including worms, flies, plants, and humans [22–24]. The most recent release of the miRBase sequence (http://www.mirbase.org/, 14.0 released on September 2009) lists 10,886 different miRNAs identified in all species, among them are 721 human miRNAs. It is predicted that the human genome encodes about 1000 miRNAs [25]. MiRNAs may be transcribed by separate genes or along with the coding genes (located in introns or extrons) [26]. The biogenesis of miRNAs from the primary miRNAs (several hundred nucleotides) to pre-miRNAs and the mature miRNAs is a complicated biochemical process [25]. When the mature miRNAs forming a complex with RISC (RNA-induced silencing complex) bind to the 3′-untranslational region (3′UTR), a cleavage of mRNA transcripts (in case of perfect miRNA:: mRNA complementarity) or translational repression (in case of imperfect complementarity) occurs [27]. The nature of miRNA acting on mRNAs adds an additional layer of fine tuning the gene expression in human genome, offering complexity of gene regulatory network. Deregulation of miRNA:: mRNA interaction contributes to a variety of human diseases including cancer [28].

Mounting evidence shows that miRNAs are aberrantly expressed during cancer development [29, 30], invasion and metastasis [31], angiogenesis [32] and play crucial roles in cancer stem cell regulation [33]. MiRNAs may function as oncogenes (OncomiRs) or tumor suppressors (TSmiRs) in tumors. With the intensive study of miRNomes in almost all types of cancers, the miRNA:: mRNA interactive network is beginning to be pictured for deep understanding of cancer biology. Strikingly, the compelling research on targeting miRNAs as experimental therapy in vitro or in vivo is increasing. The diverse technologies of replacing or inhibiting miRNAs to restore the miRNAs functions have been developed, small molecule modifiers of miRNAs are proposed to regulate the miRNAs activities. The delivery of miRNAs into the mice and nonhuman primates provides the pharmacokinetic base for possible human trial in the nearest future. Of note, some miRANs could reprogram the human cancer cells into pluriopotent ES cell like state (mirPS), which could be further induced into differentiated cell types.

3 MicroRNAs Regulate Immune Cells Development

When the key RNase III enzyme of miR biogenesis, Dicer, is conditionally knock out in immature thymocytes, the expression of T cell receptor-αβ, the mature thymocytes (either CD4+ or CD8 + or both) are dramatically reduced as well as increased apoptosis when cultured in vitro [34]. T regulatory (Treg) cells are the most affected T cell subset by the deletion of Dicer. The rapidly growing body of evidence demonstrate that microRNAs can specifically regulate immune function, for example, miR-181a can modulate B- and T-cell differentiation [35], and Bic/microRNA-155 is required for normal immune function because deficient in miR-155 results in immunodeficient and defect in the function of B cells, T cells, and dendritic cells [36].

Targets have already identified in T cells including microRNAs, miR-17-92 family. In macrophages, miR-125b, miR-146, and miR-155 act as pathogen-associated molecular, miR-34C and miR-214 function as damage-associated molecular [37]. miR-222 and miR-339 serve as targets for cytolytic effectors [35]. These findings support the central role of miRs in T cell differentiation and homeostasis of the adaptive immune system.

4 MicroRNAs Modulate Immune Cells in Microenvironment

The tumor microenvironment is composed of cancer cells and non-cancerous cells so-called stromal cells such as cancer-associated fibroblasts, tumor-associated macrophages, pericytes, endothelial cells, and infiltrating immune cells. Among these cells, macrophages and other immune cells such as T cells and natural killer (NK) cells are the major inflammatory cells infiltrating into the tumor microenvironment [38]. Macrophages within the tumor microenvironment have two different phases: anti-tumorigenic M1 macrophages and protumorigenic M2 macrophages; the process of polarization of macrophage from M1 to M2 is regulated by microRNAs [39].

Myeloid-derived suppressor cells (MDSCs) negatively regulate immune responses by suppressing the antitumor functions of $CD4^+$ and $CD8^+$ T cells or by inhibiting the activities of NK cells. Upregulation of miR-155 and miR-21 in MDSCs induces expansion through the activation of STAT3 signaling, resulting in that promotes tumor aggressiveness via immunosuppression [40]. Upregulation of miR-30d is correlated to increase of T regulatory cells (Treg) recruitment within tumors giving rise to poor clinical outcomes [41]. miR15a/16 could suppress expression of FOXP3 and CTLA4 expression in umbilical cord blood-derived regulatory T

cells [42]. NK cells have been reported regulated by miR150 [43] and miR155 [44].

In nucleophosmin-anaplastic lymphoma kinase (NPM-ALK)-positive anaplastic large cell lymphomas (ALCLs), expression miR-135b conferred IL-17-producing immunophenotype by perturbing mutually antagonistic differentiation programs active during normal lymphocyte differentiation. miR-135b suppression inhibited expression levels of IL-17A, IL-17F, IκBζ, IL-6, and IL-8 in ALCL cells. miR-135b silencing also attenuated the expression of granzyme B and perforin 1, cytotoxic molecules highly expressed in ALCLs, implying that miR-135b exerts a broad range of effects on the ALCL immunophenotype [45].

In tumor microenvironment, CD4 T cells intake tumor-derived extracellular vesicles containing enriched miR-363 from CD40/IL-4-stimulated chronic lymphocytic leukemia tumor B cells and have enhanced migration, immunological synapse signaling, and interaction with tumor cells [46].

More recently, miRs modulate T cells inhibitory signaling pathways, which are effective checkpoint blockades for melanoma, lung cancer. miR-424(322) is inversely correlated with PD-L1, PD-1, CD80, and CTLA-1 expression in ovarian cancer. miR-424 can bind to the 3-UTR region of PD-L1 and CD 80. Overexpression of miR-424 demonstrated a synergistic effect of chemotherapy and immune checkpoint blockade via the activation of CD8 T cells [47].

In addition, recent work has shown that miRNAs of cancer cells modulate the microenvironment via non-cell-autonomous mechanisms, and alterations in the miRNA profiles of neighboring cells that lack genetic abnormalities favor the acquisition of cancer hallmark traits, thereby unexpectedly expanding the roles of miRNAs in tumor microenvironments [48].

5 MicroRNAs as Targets in Immune Therapy

Immunotherapies have emerged as one of the most promising approaches to treat patients with cancer [49]. Recently, there have been many clinical successes using checkpoint receptor blockade, including T cell inhibitory receptors such as CTLA-4 [50], PD-1 [51]. Despite demonstrated successes in a variety of malignancies, responses only typically occur in a subset of patients in multiple cancers. Therefore, determining which patients would derive clinical benefit from immunotherapy is a compelling clinical question. microRNAs, an important aspect of the evolution of tumor microenvironments, is evasion of anti-tumor immune responses. Recent work has suggested that such immune escape of tumors can be broadly classified into two categories, depending on the characteristics of the tumor microenvironment. The “hot” microenvironment is a T-cell-inflamed phenotype with infiltration of T cells and a

broad chemokine profile. Such tumors appear to endure immune attack predominantly by engaging inhibitory effectors of the immune system, such as PD-L1, indoleamine 2,3-dioxygenase (IDO), and regulatory T (Treg) cells. The "cold" microenvironment lacks this T-cell-inflamed phenotype and appears to prevent immunological attack through immune system ignorance and exclusion. In tumors in which the latter mechanism is operative, dense stroma and accumulation of immunosuppressive myeloid or macrophage populations might be observed, instead of T-cell infiltration. miRNA dysregulation in cancer cells appears to contribute to both types of immune escape. Regulation of SDF-1α by miR-126/126* and modulation of tumor stroma reactions by miR-29b may be associated with the latter category of escape [52, 53]. Manipulation of microRNAs regulates PD-1/PD-L1 pathways or CTLA-4 gene expression is an attractive avenue to unleash the suppression of T cells and activation cytotoxic CD8 T cells, this expects to enhance immune checkpoint blockade efficacy. However, the preclinical and clinical trials remain to be investigated.

References

1. Ehrlich P (1909) Über den jetzigen stand der karzinomforschung. Ned Tijdschr Geneeskd 5:273–290
2. Stratton MR, Campbell PJ, Futreal PA (2009) The cancer genome. Nature 458:719–724
3. Hanahan D, Weinberg RA (2011) Hallmarks of cancer: the next generation. Cell 144:646–674
4. Tomasetti C, Vogelstein B (2015) Cancer etiology. Variation in cancer risk among tissues can be explained by the number of stem cell divisions. Science 347:78–81
5. Burnet M (1970) The concept of immunologic surveillance. Prog ExpTumor Res 13:1–27
6. Dunn GP, Old LJ, Schreiber RD (2004) The immunobiology of cancer immunosurveillance and immunoediting. Immunity 21:137–148
7. Gaudin C, Kremer F, Angevin E, Scott V, Triebel F (1999) A hsp70-2 mutation recognized by CTL on a human renal cell carcinoma. J Immunol 162:1730–1738
8. Kawakami Y, Wang X, Shofuda T, Sumimoto H, Tupesis J, Fitzgerald E, Rosenberg S (2001) Isolation of a new melanoma antigen, MART-2, containing a mutated epitope recognized by autologous tumor-infiltrating T lymphocytes. J Immunol 166:2871–2877
9. Linard B, Bezieau S, Benlalam H, Labarriere N, Guilloux Y, Diez E, Jotereau F (2002) A ras-mutated peptide targeted by CTL infiltrating a human melanoma lesion. J Immunol 168:4802–4808
10. Huang J, El-Gamil M, Dudley ME, Li YF, Rosenberg SA, Robbins PF (2004) T cells associated with tumor regression recognize frameshifted products of the CDKN2A tumor suppressor gene locus and a mutated HLA class I gene product. J Immunol 172:6057–6064
11. Lu YC, Robbins PF (2016) Targeting neoantigens for cancer immunotherapy. Int Immunol 28(7):365–370
12. Anagnostou V, Smith KN, Forde PM, Niknafs N, Bhattacharya R, White J, Zhang T, Adleff V, Phallen J, Wali N et al (2016) Evolution of neoantigen landscape during immune checkpoint blockade in non-small cell lung cancer. Cancer Discov 7(3):264–276
13. Freeman GJ, Long AJ, Iwai Y, Bourque K, Chernova T, Nishimura H, Fitz LJ, Malenkovich N, Okazaki T, Byrne MC et al (2000) Engagement of the PD-1 immunoinhibitory receptor by a novel B7 family member leads to negative regulation of lymphocyte activation. J Exp Med 192:1027–1034
14. Hodi FS, O'Day SJ, McDermott DF, Weber RW, Sosman JA, Haanen JB, Gonzalez R, Robert C, Schadendorf D, Hassel JC et al (2010) Improved survival with ipilimumab in patients with metastatic melanoma. N Engl J Med 363:711–723

15. Brahmer JR, Tykodi SS, Chow LQ, Hwu WJ, Topalian SL, Hwu P, Drake CG, Camacho LH, Kauh J, Odunsi K et al (2012) Safety and activity of anti-PD-L1 antibody in patients with advanced cancer. N Engl J Med 366:2455–2465
16. Powles T, Eder JP, Fine GD, Braiteh FS, Loriot Y, Cruz C, Bellmunt J, Burris HA, Petrylak DP, Teng SL et al (2014) MPDL3280A (anti-PD-L1) treatment leads to clinical activity in metastatic bladder cancer. Nature 515:558–562
17. Principe S, Hui AB, Bruce J, Sinha A, Liu FF, Kislinger T (2013) Tumor-derived exosomes and microvesicles in head and neck cancer: implications for tumor biology and biomarker discovery. Proteomics 13:1608–1623
18. Thakur BK, Zhang H, Becker A, Matei I, Huang Y, Costa-Silva B, Zheng Y, Hoshino A, Brazier H, Xiang J et al (2014) Double-stranded DNA in exosomes: a novel biomarker in cancer detection. Cell Res 24:766–769
19. Kato M, Slack FJ (2008) microRNAs: small molecules with big roles—C. elegans to human cancer. Biol Cell 100:71–81
20. Lee RC, Feinbaum RL, Ambros V (1993) The C. elegans heterochronic gene lin-4 encodes small RNAs with antisense complementarity to lin-14. Cell 75:843–854
21. Reinhart BJ, Slack FJ, Basson M, Pasquinelli AE, Bettinger JC, Rougvie AE, Horvitz HR, Ruvkun G (2000) The 21-nucleotide let-7 RNA regulates developmental timing in Caenorhabditis elegans. Nature 403:901–906
22. Lagos-Quintana M, Rauhut R, Lendeckel W, Tuschl T (2001) Identification of novel genes coding for small expressed RNAs. Science 294:853–858
23. Lau NC, Lim LP, Weinstein EG, Bartel DP (2001) An abundant class of tiny RNAs with probable regulatory roles in Caenorhabditis elegans. Science 294:858–862
24. Lee RC, Ambros V (2001) An extensive class of small RNAs in Caenorhabditis elegans. Science 294:862–864
25. Bartel DP (2004) MicroRNAs: genomics, biogenesis, mechanism, and function. Cell 116:281–297
26. Kim VN, Nam JW (2006) Genomics of microRNA. Trends Genet 22(3):165–173
27. Hutvagner G, Zamore PD (2002) A microRNA in a multiple-turnover RNAi enzyme complex. Science 297:2056–2060
28. Wu W, Sun M, Zou GM, Chen J (2007) MicroRNA and cancer: current status and prospective. Int J Cancer 120(5):953–960
29. He L, Thomson JM, Hemann MT, Hernando-Monge E, Mu D, Goodson S, Powers S, Cordon-Cardo C, Lowe SW, Hannon GJ, Hammond SM (2005) A microRNA polycistron as a potential human oncogene. Nature 435:828–833
30. O'Donnell KA, Wentzel EA, Zeller KI, Dang CV, Mendell JT (2005) c-Myc-regulated microRNAs modulate E2F1 expression. Nature 435:839–843
31. Zhu S, Wu H, Wu F, Nie D, Sheng S, Mo YY (2008) MicroRNA-21 targets tumor suppressor genes in invasion and metastasis. Cell Res 18:350–359
32. Hua Z, Lv Q, Ye W, Wong CK, Cai G, Gu D, Ji Y, Zhao C, Wang J, Yang BB, Zhang Y (2006) MiRNA-directed regulation of VEGF and other angiogenic factors under hypoxia. PLoS One 1:e116
33. Yu F, Yao H, Zhu P, Zhang X, Pan Q, Gong C, Huang Y, Hu X, Su F, Lieberman J (2007) Song E: let-7 regulates self renewal and tumorigenicity of breast cancer cells. Cell 131:1109–1123
34. Cobb BS, Nesterova TB, Thompson E, Hertweck A, O'Connor E, Godwin J, Wilson CB, Brockdorff N, Fisher AG, Smale ST, Merkenschlager M (2005) T cell lineage choice and differentiation in the absence of the RNase III enzyme Dicer. J Exp Med 201:1367–1373
35. Okada H, Kohanbash G, Lotze MT (2010) MicroRNAs in immune regulation—opportunities for cancer immunotherapy. Int J Biochem Cell Biol 42:1256–1261
36. Rodriguez A, Vigorito E, Clare S, Warren MV, Couttet P, Soond DR, van Dongen S, Grocock RJ, Das PP, Miska EA et al (2007) Requirement of bic/microRNA-155 for normal immune function. Science 316:608–611
37. Paladini L, Fabris L, Bottai G, Raschioni C, Calin GA, Santarpia L (2016) Targeting microRNAs as key modulators of tumor immune response. J Exp Clin Cancer Res 35:103
38. Suzuki HI, Katsura A, Matsuyama H, Miyazono K (2015) MicroRNA regulons in tumor microenvironment. Oncogene 34:3085–3094
39. Graff JW, Dickson AM, Clay G, McCaffrey AP, Wilson ME (2012) Identifying functional microRNAs in macrophages with polarized phenotypes. J Biol Chem 287:21816–21825
40. Li L, Zhang J, Diao W, Wang D, Wei Y, Zhang CY, Zen K (2014) MicroRNA-155 and MicroRNA-21 promote the expansion of functional myeloid-derived suppressor cells. J Immunol 192:1034–1043
41. Gaziel-Sovran A, Segura MF, Di Micco R, Collins MK, Hanniford D, Vega-Saenz de Miera E, Rakus JF, Dankert JF, Shang S, Kerbel RS et al (2011) miR-30b/30d regulation of GalNAc

transferases enhances invasion and immunosuppression during metastasis. Cancer Cell 20:104–118

42. Liu X, Robinson SN, Setoyama T, Tung SS, D'Abundo L, Shah MY, Yang H, Yvon E, Shah N, Yang H et al (2014) FOXP3 is a direct target of miR15a/16 in umbilical cord blood regulatory T cells. Bone Marrow Transplant 49:793–799
43. Bezman NA, Chakraborty T, Bender T, Lanier LL (2011) miR-150 regulates the development of NK and iNKT cells. J Exp Med 208:2717–2731
44. Trotta R, Chen L, Ciarlariello D, Josyula S, Mao C, Costinean S, Yu L, Butchar JP, Tridandapani S, Croce CM, Caligiuri MA (2012) miR-155 regulates IFN-gamma production in natural killer cells. Blood 119:3478–3485
45. Matsuyama H, Suzuki HI, Nishimori H, Noguchi M, Yao T, Komatsu N, Mano H, Sugimoto K, Miyazono K (2011) miR-135b mediates NPM-ALK-driven oncogenicity and renders IL-17-producing immunophenotype to anaplastic large cell lymphoma. Blood 118:6881–6892
46. Smallwood DT, Apollonio B, Willimott S, Lezina L, Alharthi A, Ambrose AR, De Rossi G, Ramsay AG, Wagner SD (2016) Extracellular vesicles released by CD40/IL-4-stimulated CLL cells confer altered functional properties to CD4+ T cells. Blood 128:542–552
47. Xu S, Tao Z, Hai B, Liang H, Shi Y, Wang T, Song W, Chen Y, OuYang J, Chen J et al (2016) miR-424(322) reverses chemoresistance via T-cell immune response activation by blocking the PD-L1 immune checkpoint. Nat Commun 7:11406
48. Cho JS, Kook SH, Robinson AR, Niedernhofer LJ, Lee BC (2013) Cell autonomous and non-autonomous mechanisms drive hematopoietic stem/progenitor cell loss in the absence of DNA repair. Stem Cells 31:511–525
49. Sharma P, Allison JP (2015) The future of immune checkpoint therapy. Science 348:56–61
50. Cha E, Klinger M, Hou Y, Cummings C, Ribas A, Faham M, Fong L (2014) Improved survival with T cell clonotype stability after anti-CTLA-4 treatment in cancer patients. Sci Transl Med 6:238ra270
51. Rizvi NA, Hellmann MD, Snyder A, Kvistborg P, Makarov V, Havel JJ, Lee W, Yuan J, Wong P, Ho TS et al (2015) Cancer immunology. Mutational landscape determines sensitivity to PD-1 blockade in non-small cell lung cancer. Science 348:124–128
52. Zhang Y, Yang P, Sun T, Li D, Xu X, Rui Y, Li C, Chong M, Ibrahim T, Mercatali L et al (2013) miR-126 and miR-126* repress recruitment of mesenchymal stem cells and inflammatory monocytes to inhibit breast cancer metastasis. Nat Cell Biol 15:284–294
53. Chou J, Lin JH, Brenot A, Kim JW, Provot S, Werb Z (2013) GATA3 suppresses metastasis and modulates the tumour microenvironment by regulating microRNA-29b expression. Nat Cell Biol 15:201–213

Chapter 5

Apolipoprotein B mRNA Editing Enzyme, Catalytic Polypeptide-Like Gene Expression, RNA Editing, and MicroRNAs Regulation

Wei Cao and Wei Wu

Abstract

Apolipoprotein B mRNA editing enzyme, catalytic polypeptide-like (APOBEC) protein family is encoded by eleven genes located in human genome. APOBECs are a family of evolutionarily conserved cytidine deaminases in vertebrates, and particularly in mammals. APOBECs play key roles in innate immunity against viral infection and retrotransposons. Subtypes of APOBEC3 can cause specific mutations in RNA and DNA at distinct preferred nucleotide contexts in human cancer. The pervasive APOBEC3s activation in the host genome converts cytosine to uracile on single-stranded DNA, which has been suggested to depend on ATR/chk1 pathways. In this chapter, we review the expression profiling of APOBEC expression in normal and disease states, discuss how microRNAs interact with APOBEC gene family, and post-transcriptionally regulate APOBEC gene expression in the APOBECA-B fusion allele and APOBEC-mediated RNA editing. It is reasonable to speculate targeting specific microRNAs may reduce host genome mutagenesis via inactivation of APOBEC deaminases.

Key words MicroRNAs, APOBEC, Mutagenesis, Mutation signature, DND1, P-Bodies

1 Introduction

Apolipoprotein B mRNA editing enzyme, catalytic polypeptide-like (APOBEC) is a family of evolutionarily conserved cytidine deaminases [1]. There are 11 human genes encoding members of the APOBEC protein family which include: the activation-induced cytidine deaminase (*AICDA*) and *APOBEC1* on Chr 12p13.1, *APOBEC2* on Chr 6p21, seven *APOBEC3s* (*APOBEC3A, APOBEC3B, APOBEC3D/E, APOBEC3F, APOBEC3G, APOBEC3H*) on Chr 22q13.1, and *APOBEC4* on Chr 1q25.3 [2]. Except of APOBEC2 and APOBEC4, the other members of APOBEC proteins normally function in (1) innate immune response viral infection (e.g., HIV, HBV, HPV); (2) deamination of deoxycyditine (dC) to deoxyuridine (dU) in single-strand DNA; (3) generation of somatic hypermutation in the process of cancer development.

Wei Wu (ed.), *MicroRNA and Cancer: Methods and Protocols*, Methods in Molecular Biology, vol. 1699,
DOI 10.1007/978-1-4939-7435-1_5,

Recent studies support APOBEC3s activity is associated with tumorigenesis due to mutagenesis, in particular, APOBEC3B overexpressed in several human cancer types correlates with the presence of the APOBEC3B mutation signature [3, 4]. Further study demonstrated that oncogenes, loss of tumor suppressor genes, and drug-induced replication stresses activate transcription of APOBEC3B via an ATR/Chk1-dependent pathway in vitro. APOBEC3B activation can be attenuated through repression of oncogenic signaling pathways, small molecule inhibition of receptor tyrosine kinase signaling pathways, and alleviation of replication stress through nucleoside supplementation [5]. However, the regulation of *APOBEC* gene expression is largely unknown. In this chapter, we will discuss how microRNAs may be involved in controlling *APOBECs* gene expression.

1.1 MicroRNAs Biology

MicroRNAs are 20–22-nt regulatory RNAs that participate in the regulation of various biological functions in numerous eukaryotic lineages, including plants, insects, vertebrate, and mammals. 1881 precursors and 2588 mature miRNAs have been identified in humans and mapped to GRCh38 (http://www.mirbase.org/cgi-bin/browse.pl?org=has). ~60% of the genes in the human genome are predicted to be subject to miRNA regulation. The expression of many miRNAs is usually specific to a tissue or developmental stage, and the miRNA expression pattern is altered during the development of many diseases [6]. Mature miRNAs are generated from RNA polymerase II-transcribed primary miRNAs that are processed sequentially by the nucleases Drosha and Dicer. Although miRNA can guide mRNA cleavage, the basic function of miRNA is to mediate inhibition of protein translation through miRNA-induced silencing complexes (miRISCs), all four of the Ago proteins (Ago1–4) are found to present in miRISC. The guiding strand of miRNA in a miRISC interacts with a complementary sequence in the 3′-untranslated region (3′-UTR) of its target mRNA by partial sequence complementarities, resulting in translational inhibition [7]. A 7-nucleotide "seed" sequence (at positions 2–8 from the 5′-end) in miRNAs seems to be essential for this action.

The miRNA-mediated translational repression consistently correlates with an accumulation of miRNA-bound mRNAs at cytoplasmic foci known as processing bodies (P-bodies). Several lines of evidence have indicated that P-bodies are actively involved in miRNA-mediated mRNA repression [8]. The features of the P-bodies have: (1) the components of the P-body comprise GW182 and Rck/p54 associated directly with Ago-1; (2) P-body formation is a dynamic process that requires continuous accumulation of repressed mRNAs; (3) P-bodies serve not only as sites for RNA degradation, but also for storage of repressed mRNAs. These mRNAs may later return to polysomes to synthesize new proteins.

1.2 The Expression of APOBECs in Normal and Disease States

The expression of AID/APOBECs is tissue and cell type specific. AID was first discovered from a screen experiment between switch-induced and un-induced murine B lymphoma cells CH12F3-2 using a subtractive hybridization assay in 1999 and it is selectively expressed in activated B cells in germinal centers by immunization [9]. It is predominantly cytoplasmic. Helicobacter pylori infection in normal gastric epithelia can induce AID expression [10]. Overexpression of AID causes T cell lymphoma [11]. APOBEC1, the first APOBEC family member to be identified and characterized, is expressed in the human small intestine and in the liver in rodents, this protein is involved in the editing of the apolipoprotein B pre-mRNA [12, 13]. APOBEC1 presents in both nucleus and cytoplasm by virtue of an amino-terminal nuclear localization signal and a carboxy-terminal nuclear export signal. Overexpression of APOBEC1 causes hepatocellular carcinoma [14]. APOBEC2 expressed specifically in skeletal muscle and heart. Seven additional genes, or pseudogenes (designated APOBEC3A to 3G), were first identified as paralogs of APOBEC1 in 2002, and they are arrayed in tandem on chromosome 22 [15]. Jarmuz et al. [15] also found that APOBEC3 gene expression is tissue-specific. In normal tissues, APOBEC3B expression was demonstrated in peripheral blood leukocytes. APOBEC3G was demonstrated in spleen, testes, ovary, and peripheral blood leukocytes. APOBEC3A showed hybridization to peripheral leukocyte RNA. APOBEC3C was demonstrated to express in spleen, testes, peripheral blood leukocytes, heart, thymus, prostate, and ovary at moderate to high levels and at low levels in several other tissues. No site of expression was found for APOBEC3D, APOBEC3E, and APOBEC3F. In tumor cells, APOBEC3B was abundantly expressed in colorectal adenocarcinoma and chronic myelogenous leukemia cells and to a lesser extent in melanoma, lung carcinoma, Burkitt's lymphoma Raji, and HeLa cells. This is consistent with recent evidence of overexpression APOBEC3B in multiple cancers including breast cancer [3, 4]. APOBEC3G was expressed abundantly in colorectal adenocarcinoma and to a lower extent in Burkitt's lymphoma Raji cells, chronic myelogenous leukemia cells, and promyelocytic leukemia cells. APOBEC3C was expressed abundantly in colorectal adenocarcinoma and chronic myelogenous leukemia cells and to a lesser extent in melanoma, lung carcinoma, Burkitt's lymphoma Raji cells, lymphoblastic leukemia, HeLa cells, and promyelocytic leukemia cells. APOBEC3D is expressed at modest levels in colorectal adenocarcinoma cells and chronic myelogenous leukemia cells, and at low levels in lung carcinoma and HeLa cells [15]. APOBEC4 is expressed in testis [16].

1.3 APOBECs Interact with MicroRNAs

Little evidence shows how APOBECs genes are regulated. On the basis of these studies, it is reasonable to hypothesize that activation of APOBECs expression seems to be associated with viral infection or endogenous retrotransposons [17]. However, post-transcriptional regulation by microRNA machinery has been suggested from primate genome evolution, APOBECs, and RNA interactions.

The genetic evidence indicated that a deletion polymorphism produces a hybrid, APOBEC3A_B, in which the APOBEC3A coding sequencing is fused to the APOBEC3B 3′-UTR. The deletion is rare in Africans and Europeans (frequency of 0.9% and 6%), more common in East Asians and Amerindians (36.9% and 57.7%), and almost fixed in Oceanic populations (92.9%) [18]. The APOBEC3A_B carriers show more mutations of the putative APOBEC-dependent genome-wide signatures than cancers in non-carriers, conferring cancer susceptibility through increased activity of APOBEC-dependent mutational processes [19]. The APOBEC3A_B fusion product was expressed at much higher levels that a wild type of APOBEC3A product and had a potent hyper-editing activity on nuclear DNA [20]. The possible biological interpretation is that APOBEC3A 3′UTR is targeted by one or more microRNAs that repress APOBEC3A expression, and that this repression is relieved in the APOBEC3A_B allele, in which APOBEC3A is instead fused to the APOBEC3B 3′-UTR [21]. To explore this hypothesis, we predicted potential microRNA-binding sites in their 3′ UTR using miRWalk 2.0 algorithm. The length of APOBEC3A 3′-UTR (NM_001270406) is 674 bp with 174 microRNAs (2 out of 4 prediction methods), while the length of APOBEC3B 3′-UTR (NM_001270411) is 356 bp with 82 microRNAs. From the length of 3′UTR and microRNA-binding sites may suggest APOBEC3A_B allele is an active form.

APOBEC3G is found in P-bodies and stress granules. It is associated with a high molecular mass structure (>700 kDa) in replicating cells, and this interaction is RNase-sensitive. Further studies indicate that APOBEC3G interacts with many RNA-binding proteins, among which are several miRNA-related proteins, such as Ago1, Ago2, Mov10, and poly(A)-binding protein 1 (PABP1). These interactions are either partially or completely resistant to RNase A digestion. Therefore, APOBEC3G function seems to be related to P-body-related RNA processing and metabolism. As recent development has indicated that the function of P-body is closely related to miRNA activity, hence, APOBEC3G contacts the inhibition of protein synthesis by various microRNAs such as mir-10b, mir-16, mir-25, and let-7a [22]. In addition, APOBEC3G is able to counteract RNA-binding protein DEAD-END (DND1) repression and restore miRNA activity. APOBEC3G, by itself, does not affect the 3′-UTR of P27. APOBEC3G also blocks DND1 function to restore miR-372 and miR-206

inhibition through the 3′-UTRs of LATS2 and CX43, respectively [23]. More recent study showed APOBEC3G also interacts with lncRNA MALAT and microRNA2909 [24]. Taken together, microRNAs participate in APOBECs gene expression at posttranscriptional levels.

1.4 APOBEC-Mediated RNA Editing

RNA editing is a ubiquitous molecular process by which a nucleotide sequence is modified in the RNA transcript and results in an amino acid change in the given message from a specific gene. Mammalian RNA editing is genetically and biochemically classified into two groups: (1) insertion and /or deletions; (2) substitutions. The adenosine to inosine and cytosine to uracil (C to U) are the common two types of RNA editing in mammalian [25]. C to U apoB RNA deamination is exquisitely precise, targeting a single cytidine within a spliced ~14 kb nuclear apoB mRNA, creating a **U**AA termination codon in the edited transcript from a genomically templated **C**AA (glutamine) codon [12, 13, 25]. APOBEC1 not only edits target of ApoB RNA transcript partnering with ACF gene, but also edits non-canonic substrate, neurofibromatosis type 1 RNA [26]. Beyond its C to U deaminase activity on RNA substrates, Apobec-1 is an AU-rich RNA-binding protein with a consensus-binding site **UUUN[A/U]U** embedded in the 3′ untranslated region (3′UTR) of RNAs exhibiting rapid turnover, including c-myc, TNF-α, and IL-2 [27]. Genome-wide screen of Apobec-1-meidated C-to-U RNA editing in mouse model identified differentially targets in small intestine and liver, and most editing sites are in 3′ untranslating regions of gene [28]. This evidence is consistent with our hypothesis that APOBEC and microRNA reciprocally regulate the gene expression network. This kind of research is still in infant stage, we speculate that the gene expression diversity via RNA editing may help us to understand the mechanism of disease state.

2 Summary

APOBEC enzymes, which have evolved as key players in natural and adaptive immunity, have been proposed to contribute to cancer development and clonal evolution of cancer by inducing collateral genomic damage due to their DNA deaminating activity. APOBEC gene expression is activated by viral infection and controlled by microRNAs in some scenarios. Some APOBEC members contact microRNA-mediated repression of translation by interacting with Ago1, Ago2, and other proteins. APOBEC-mediated RNA editing increases the gene expression diversity and complexity in the mircroRNA regulatory networking. It is speculated that manipulating specific microRNAs may control APOBEC gene expression, subsequently, reduce the mutagenesis.

Acknowledgment

This work is supported by joint funding of natural science foundation of Henan province (grant #: 162300410279) and Henan science and technology research program (international collaborative project, 152102410088).

References

1. Refsland EW, Harris RS (2013) The APOBEC3 family of retroelement restriction factors. Curr Top Microbiol Immunol 371:1–27. Epub 2013/05/21
2. Harris RS, Liddament MT (2004) Retroviral restriction by APOBEC proteins. Nat Rev Immunol 4(11):868–877. Epub 2004/11/02
3. Burns MB, Temiz NA, Harris RS (2013) Evidence for APOBEC3B mutagenesis in multiple human cancers. Nat Genet 45(9):977–983. Epub 2013/07/16
4. Roberts SA, Lawrence MS, Klimczak LJ, Grimm SA, Fargo D, Stojanov P et al (2013) An APOBEC cytidine deaminase mutagenesis pattern is widespread in human cancers. Nat Genet 45(9):970–976. Epub 2013/07/16
5. Kanu N, Cerone MA, Goh G, Zalmas LP, Bartkova J, Dietzen M et al (2016) DNA replication stress mediates APOBEC3 family mutagenesis in breast cancer. Genome Biol 17 (1):185. Epub 2016/09/17
6. Wu W, Sun M, Zou GM, Chen J (2007) MicroRNA and cancer: current status and prospective. Int J Cancer 120(5):953–960
7. Sevignani C, Calin GA, Siracusa LD, Croce CM (2006) Mammalian microRNAs: a small world for fine-tuning gene expression. Mamm Genome 17(3):189–202
8. Liu J, Valencia-Sanchez MA, Hannon GJ, Parker R (2005) MicroRNA-dependent localization of targeted mRNAs to mammalian P-bodies. Nat Cell Biol 7(7):719–723. Epub 2005/06/07
9. Muramatsu M, Sankaranand VS, Anant S, Sugai M, Kinoshita K, Davidson NO et al (1999) Specific expression of activation-induced cytidine deaminase (AID), a novel member of the RNA-editing deaminase family in germinal center B cells. J Biol Chem 274 (26):18470–18476. Epub 1999/06/22
10. Matsumoto Y, Marusawa H, Kinoshita K, Endo Y, Kou T, Morisawa T et al (2007) Helicobacter pylori infection triggers aberrant expression of activation-induced cytidine deaminase in gastric epithelium. Nat Med 13 (4):470–476. Epub 2007/04/03
11. Robbiani DF, Nussenzweig MC (2013) Chromosome translocation, B cell lymphoma, and activation-induced cytidine deaminase. Annu Rev Pathol 8:79–103. Epub 2012/09/15
12. Navaratnam N, Morrison JR, Bhattacharya S, Patel D, Funahashi T, Giannoni F et al (1993) The p27 catalytic subunit of the apolipoprotein B mRNA editing enzyme is a cytidine deaminase. J Biol Chem 268(28):20709–20712. Epub 1993/10/05
13. Teng B, Burant CF, Davidson NO (1993) Molecular cloning of an apolipoprotein B messenger RNA editing protein. Science 260 (5115):1816–1819. Epub 1993/06/18
14. Yamanaka S, Balestra ME, Ferrell LD, Fan J, Arnold KS, Taylor S et al (1995) Apolipoprotein B mRNA-editing protein induces hepatocellular carcinoma and dysplasia in transgenic animals. Proc Natl Acad Sci U S A 92 (18):8483–8487. Epub 1995/08/29
15. Jarmuz A, Chester A, Bayliss J, Gisbourne J, Dunham I, Scott J et al (2002) An anthropoid-specific locus of orphan C to U RNA-editing enzymes on chromosome 22. Genomics 79 (3):285–296. Epub 2002/02/28
16. Rogozin IB, Basu MK, Jordan IK, Pavlov YI, Koonin EV (2005) APOBEC4, a new member of the AID/APOBEC family of polynucleotide (deoxy)cytidine deaminases predicted by computational analysis. Cell Cycle 4 (9):1281–1285. Epub 2005/08/06
17. Conticello SG (2008) The AID/APOBEC family of nucleic acid mutators. Genome Biol 9(6):229. Epub 2008/07/05
18. Kidd JM, Newman TL, Tuzun E, Kaul R, Eichler EE (2007) Population stratification of a common APOBEC gene deletion polymorphism. PLoS Genet 3(4):e63. Epub 2007/04/24
19. Nik-Zainal S, Wedge DC, Alexandrov LB, Petljak M, Butler AP, Bolli N et al (2014) Association of a germline copy number polymorphism of APOBEC3A and APOBEC3B with burden of putative APOBEC-dependent mutations in breast cancer. Nat Genet 46(5):487–491. Epub 2014/04/15

20. Caval V, Suspene R, Shapira M, Vartanian JP, Wain-Hobson S (2014) A prevalent cancer susceptibility APOBEC3A hybrid allele bearing APOBEC3B 3'UTR enhances chromosomal DNA damage. Nat Commun 5:5129. Epub 2014/10/10
21. Henderson S, Fenton T (2015) APOBEC3 genes: retroviral restriction factors to cancer drivers. Trends Mol Med 21(5):274–284. Epub 2015/03/31
22. Huang J, Liang Z, Yang B, Tian H, Ma J, Zhang H (2007) Derepression of microRNA-mediated protein translation inhibition by apolipoprotein B mRNA-editing enzyme catalytic polypeptide-like 3G (APOBEC3G) and its family members. J Biol Chem 282 (46):33632–33640. Epub 2007/09/13
23. Ali S, Karki N, Bhattacharya C, Zhu R, MacDuff DA, Stenglein MD et al (2013) APOBEC3 inhibits DEAD-END function to regulate microRNA activity. BMC Mol Biol 14:16. Epub 2013/07/31
24. Kaul D, Arora M, Garg A, Sharma S (2015) MALT1 induced immune response is governed by miR-2909 RNomics. Mol Immunol 64 (1):210–217. Epub 2014/12/17
25. Blanc V, Davidson NO (2003) C-to-U RNA editing: mechanisms leading to genetic diversity. J Biol Chem 278(3):1395–1398. Epub 2002/11/26
26. Mukhopadhyay D, Anant S, Lee RM, Kennedy S, Viskochil D, Davidson NO (2002) C–>U editing of neurofibromatosis 1 mRNA occurs in tumors that express both the type II transcript and apobec-1, the catalytic subunit of the apolipoprotein B mRNA-editing enzyme. Am J Hum Genet 70(1):38–50. Epub 2001/12/01
27. Anant S, Davidson NO (2000) An AU-rich sequence element (UUUN[A/U]U) downstream of the edited C in apolipoprotein B mRNA is a high-affinity binding site for Apobec-1: binding of Apobec-1 to this motif in the 3′ untranslated region of c-myc increases mRNA stability. Mol Cell Biol 20 (6):1982–1992. Epub 2000/02/25
28. Blanc V, Park E, Schaefer S, Miller M, Lin Y, Kennedy S et al (2014) Genome-wide identification and functional analysis of Apobec-1-mediated C-to-U RNA editing in mouse small intestine and liver. Genome Biol 15(6):R79. Epub 2014/06/21

Chapter 6

MicroRNAs Change the Landscape of Cancer Resistance

Jun Zhu, Wei Zhu, and Wei Wu

Abstract

One of the major challenges in the cancer treatment is the development of drug resistance. It represents a major obstacle to curing cancer with constrained efficacy of both conventional chemotherapy and targeted therapies, even recent immune checkpoint blockade therapy. Deciphering the mechanisms of resistance is critical to further understanding the multifactorial pathways involved, and developing more specific targeted treatments. To date, numerous studies have reported the potential role of microRNAs (miRNAs) in the resistance to various cancer treatments. MicroRNAs are a family of small noncoding RNAs that regulate gene expression by sequence-specific targeting of mRNAs causing translational repression or mRNA degradation. More than 1200 validated human miRNAs have been identified in human genome. While one miRNA can regulate hundreds of targets, a single target can also be affected by multiple miRNAs. Evidence suggests that dysregulation of specific miRNAs may be involved in the acquisition of resistance, thereby modulating the sensitivity of cancer cells to treatment. Therefore, manipulation of miRNAs may be an attractive strategy for more effective individualized therapies through reprograming resistant network in cancer cells.

Key words Cancer resistance, MicroRNAs, Drug persistent cells, Residual disease, Epigenome

1 Introduction

Cancer is a disorder of genome and epigenome alteration with characteristics of inherited heterogeneity, plasticity, and resistance [1, 2]. Evolutionally, cancer is a newly formed species, after cancer cells are borne from a part of the body, it deems to be an independent identity with its own operative system [3]. Cancer initiation, progression, and metastasis may be attributed to chromosomally mapped genomic locations of oncogenes and tumor suppressor genes, more complete details of the mutation processes give rise to the common genomic aberrations [4] and the unique genomic expression profiles in specific types of cancer [5, 6]. Advances in sequencing technology and dramatic decreases in its cost are providing us with the potential to accurately inspect the cancer genome at the level of single cells and the resolution of a single nucleotide [7]. From cancer functional genomics studies, 12 core

Wei Wu (ed.), *MicroRNA and Cancer: Methods and Protocols*, Methods in Molecular Biology, vol. 1699,
DOI 10.1007/978-1-4939-7435-1_6,

pathways were defined from so-called driver gene mutations [2]. Targeted molecular therapy began a new era to treat a subtype of cancer. Since last several years, immune checkpoint blockade therapy has received excellent objective responses and durable clinical outcome on melanoma [8], NSCNC, renal cell carcinoma [9], bladder cancer [10] with mono- or poly-agents. The common theme of cancer cell resistance (intrinsic or acquired) is an inevitable phenomenon regardless the modalities of treatment. The drug resistance is a major clinical problem resulting in therapeutic failure and uncontrolled disease progression. Even when patients initially respond well to cancer treatment, the residual disease can relapse or recur due to de novo mechanisms [11]. Resistance to anti-cancer drugs can be acquired by several mechanisms within neoplastic cells, including alteration of drug targets, expression of drug pumps, expression of detoxification mechanisms, reduced susceptibility to apoptosis, increased ability to repair DNA damage, and altered proliferation [12]. The changes in stroma and tumor microenvironment, and local immunity can also contribute to the development of resistance [13].

The cancer drug resistance can be categorized into two large groups: "kinetic resistance" and "genetic resistance." As the term indicates, kinetic resistance refers to the reduction in the effectiveness of the drug which is caused by the cell dividing cycle; genetic resistance develops as a consequence of genetic events such as mutations. There are also two hypotheses: random, stochastic origin [14] and drug-tolerant persister origin [15]. The stochasticity of drug resistance appears to be a spontaneous phenomenon caused by random genetic mutations or inherited epigenetic regulation; while determinism of drug resistance constitutes a subpopulation of tumor cells that emerge at relatively high frequency upon treatment of largely drug-sensitive cancer cell populations with various anticancer agents [15]. Most of these researches focus on 2% of protein coding genes, and neglect largely 98% of "dark matters" noncoding elements in the genome, which may contribute to the cancer drug resistance. In this chapter, we will discuss how small noncoding RNAs, microRNAs, are involving in the cancer drug resistance.

2 What Is MicroRNAs?

MicroRNAs are small noncoding RNAs 19–25 nucleotides in size involved in many biological processes such as survival, apoptosis, cell cycle, and gene regulation [16]. miRNAs was initially discovered in 1993 when studying developmental timing in *Caenorhabditis elegans* [17]. Mechanistically, miRNAs work by silencing gene expression and can act as both tumor suppressors and oncogenes in different types of cancers [18]. miRNAs regulate gene expression through modulation of multiple target mRNAs. Perfect

complementarity between the miRNA and the mRNA leads to mRNA degradation, whereas imperfect complementarity gives rise to the block of translation [19].

MicroRNA biogenesis occurs in various stages involving RNA polymerase II (Pol II) which transcribes the primary transcripts (pri-miRNA). These are cleaved by the RNAse III Drosha into precursor miRNAs (pre-miRNAs) [20]. The pre-miRNAs are then transported via Exportin-5 (Exp5) out of the nucleus and into the cytoplasm where they are further cleaved by Dicer, into a mature single-stranded miRNA. Once the mature miRNA is excised from the pre-miRNA hairpin it is then coupled onto RNA-induced silencing complex (RISC), which induces the target mRNA to either degrade or repress the translation of mRNA targets [16].

The discovery of small regulatory noncoding RNAs revolutionized our thinking on gene regulation. Indeed, major hallmarks of cancer, such as cell differentiation, cell proliferation, cell cycle, cell survival, and cell invasion, have been described as being regulated by miRs [18, 21]. A compelling body of evidence points to the direct involvement of miRNAs in resistance to cancer treatments. Below we will discuss miRs in cancer drug resistance.

3 MicroRNAs Regulate Drug Resistant Pathways

miRs influence molecular pathways that are involved in cancer drug resistance, such as drug metabolism, drug influx/efflux, DNA damage response, epithelial-to-mesenchymal transition [22], and cancer stem cells [23]. This has been observed in multiple cancer types [24]. Here, we only use lung cancer as an example. Despite the fact that acquired resistance may be the result of a secondary mutation in the EGFR gene, such as T790M or amplification of the MET proto-oncogene [25], there are other mechanisms that need to be explored. MicroRNAs (miRs) are a class of small noncoding RNAs that play pivotal roles in chemo-resistance.

Several studies showed that miR-221/222 and microRNA-30b/c are regulated by both epidermal growth factor (EGF) and MET receptors, whereas microRNA-103 and microRNA-203 are regulated by MET only. These microRNAs have a role in gefitinib-induced apoptosis by inhibition of target genes including BIM, APAF-1, PKC-ε, and SRC. Particularly, microRNA-221/222 and microRNA-30b/c, microRNA-214 induce resistance to gefitinib by targeting APAF-1 and BIM, PTEN and AKT pathways, while microRNA-103 and microRNA-203 function as tumor suppressor miRNAs in lung cancer, inducing sensitivity to tyrosine kinase inhibitors and MET inhibitor by targeting PKC-ε and SRC, respectively [26, 27]. Importantly, the use of a MET inhibitor plus gefitinib significantly sensitized gefitinib resistant cells to the drug

treatment. MicroRNA-221 and microRNA-222 have also been linked with resistance to TRAIL. microRNA-221/222, activated by MET though the c-Jun transcription factor, induced cell migration, invasion and TRAIL resistance in lung cancer by targeting PTEN and TIMP3 and activating the AKT pathway and metallopeptidases [28]. The miR-200c/LIN28B axis shows an important role in cells with acquired resistance to EGFR-TKI that harbor EMT features [22]. Thus, it is conceivable that the tweaking of these miRNAs with combination drug treatment could improve response in NSCLC.

It is also appreciated that genetically similar cells may behave differently in the face of identical selection pressures. Altered epigenetic states are thought to be a mechanism through which these observations can be explained. For example, minority drug-tolerant persister cells result in drug resistance dependent on the histone demethylase JARID1A, which can be both dynamic and transient [29]. In lung adenocarcinoma treated with TKI Erlotinib, relapse often occurs in patients due to a small fraction of non-dividing persisters. The drug-tolerance seems to originate, at least in the early stages, from altered chromatin configurations due to expression noise in chromatin modifiers. One study demonstrated the persisters in lung cancer cells line PC9, have an increased expression of a histone demethylase following the upstream activation of an IGF-1 receptor [29]. Improved tumor cell eradication was only possible by the use of a combinatorial treatment using an IGF-1 receptor inhibitor, in order to prevent altered chromatin states, followed by Erlotinib treatment. This again highlights the importance of understanding the molecular origins of phenotypic variability in isogenic populations while developing treatment strategies.

4 The Roles of MicroRNAs in Epigenome of Cancer Resistance

Genetic and epigenetic heterogeneity (the main form of non-genetic heterogeneity) are key elements in cancer progression and drug resistance, as they provide needed population diversity, complexity, and robustness. Despite drastically increased evidence of multiple levels of heterogeneity in cancer, the general approach has been to eliminate the "noise" of heterogeneity to establish genetic and epigenetic patterns. In particular, the appreciation of new types of epigenetic regulation like non-coding RNA, have led to the hope of solving the mystery of cancer that the current genetic theories seem to be unable to achieve [30].

Even as new drug resistance-related mutations are being identified in various cancers, the growing evidence indicated that non-mutational mechanisms such as epigenetic features may play a role in acquired resistance or reversible drug tolerance.

miR-371-3p can suppress drug tolerance in tumor cells from advanced cancer patients.

Using a library of miRNA mimics representing 879 human miRNA precursors, Sahu et al. did a drug response screen in a PC9 non-small cell lung cancer cell line exposed to the EGFR kinase inhibitor erlotinib. 885 miRNA inhibitors were also introduced into cells for knockdown study. The results showed more than half of the miRNA inhibitors led to higher-than-usual numbers of drug-tolerant cells, with just two anti-miRs decreasing the apparent drug tolerance. On the other hand, 39 of the miRNAs that did not have obvious effects on untreated cells seemed to dial down the number of drug-tolerant persister cells following erlotinib exposure. That effect was most pronounced for the pre-miR-371, which leads to both miR-371-3p and miR-371-5p, diminished expression in drug-tolerant persister cells [31]. The further functional studies found that miR-371-3p and miR-371-5p are regulators of the peroxiredoxin 6 gene PRDX6—a phospholipase signaling and oxidative stress-related gene with higher-than-usual expression in tumors from aggressive cancer with relatively poor outcomes. In addition, miRNA targets PRDX6, PLC-beta4, and STX12, these genes involved in phospholipase signaling.

In particular, enhanced expression of miR-371 seemed to dial down xenograft tumor growth, drug tolerance, and relapse in erlotinib-treated mice, while the expression of PRDX6 and other miR-371 targets were upregulated in other mouse tumors. Similarly, a search of data from the Cancer Genome Atlas suggested PRDX6 expression may also be ramped up in multiple human cancer types [31].

Therefore, combining current targeted therapies with inhibitors of [phospholipase signaling and reactive oxygen species] accumulation could provide a treatment strategy to delay some types of drug resistance in human cancer [31].

5 Reverse of Cancer Resistance State by Targeting MicroRNAs

Cancer resistance state may derive from drug-tolerant persister cells either stochastically or preexistly. It is the main cause of therapeutic failure. This state could be reversed via multiple modalities. Histon demethylase KDM5 inhibitor inhibits global levels of H3K4 trimethylation (H3K4me3) and decreases the number of drug-tolerant persisters in multiple cancer cell line models treated with standard chemotherapy or targeted agents, resulting in the ablation of a subpopulation of cancer cells that can serve as the founders for therapeutic relapse [32].

Autonomous (genetic, epigenetic, and proteomic) and non-cell autonomous (tumor microenvironment interaction) mechanisms of cancer resistance are very different. Over last 50 years,

researchers mainly focused on protein coding genes, pathways. Litter effects have been seen in treatment of cancer. We believe the noncoding RNAs are the hope of conquering cancer because microRNAs are the master of gene expression regulators. Many microRNAs could be served as therapeutic targets to enhance cancer cells sensitivity to treatment (chemotherapy or immunotherapy). One recent example is the findings of miR-371-3p as a suppressor of PRDX6 and suggests that co-targeting of peroxiredoxin 6 or modulating miR-371-3p expression together with targeted cancer therapies may delay or prevent acquired drug resistance [31]. The obstacles of microRNAs-based therapy are: (1) how to effectively deliver specific microRNAs to cancer cells; (2) off-target effects; (3) the control of dosage of microRNAs [33]. Nevertheless, few miRNAs have entered the preclinical and clinical stage and soon might be available in the market for use in humans.

References

1. Stratton MR, Campbell PJ, Futreal PA (2009) The cancer genome. Nature 458:719–724
2. Vogelstein B, Papadopoulos N, Velculescu VE, Zhou S, Diaz LA Jr, Kinzler KW (2013) Cancer genome landscapes. Science 339:1546–1558
3. Duesberg P, Mandrioli D, McCormack A, Nicholson JM (2011) Is carcinogenesis a form of speciation? Cell Cycle 10:2100–2114
4. Stephens PJ, Tarpey PS, Davies H, Van Loo P, Greenman C, Wedge DC, Nik-Zainal S, Martin S, Varela I, Bignell GR et al (2012) The landscape of cancer genes and mutational processes in breast cancer. Nature 486:400–404
5. Greenman C, Stephens P, Smith R, Dalgliesh GL, Hunter C, Bignell G, Davies H, Teague J, Butler A, Stevens C et al (2007) Patterns of somatic mutation in human cancer genomes. Nature 446:153–158
6. Wu W, Chan JA (2013) Understanding the role of long noncoding RNAs in the cancer genome. In: Wu W, Choudhry H (eds) Next generation sequencing in cancer research-decoding cancer genome, vol 1, 1st edn. Springer, New York, pp 199–215
7. Zhang X, Marjani SL, Hu Z, Weissman SM, Pan X, Wu S (2016) Single-cell sequencing for precise cancer research: progress and prospects. Cancer Res 76:1305–1312
8. Hodi FS, O'Day SJ, McDermott DF, Weber RW, Sosman JA, Haanen JB, Gonzalez R, Robert C, Schadendorf D, Hassel JC et al (2010) Improved survival with ipilimumab in patients with metastatic melanoma. N Engl J Med 363:711–723
9. Brahmer JR, Tykodi SS, Chow LQ, Hwu WJ, Topalian SL, Hwu P, Drake CG, Camacho LH, Kauh J, Odunsi K et al (2012) Safety and activity of anti-PD-L1 antibody in patients with advanced cancer. N Engl J Med 366:2455–2465
10. Powles T, Eder JP, Fine GD, Braiteh FS, Loriot Y, Cruz C, Bellmunt J, Burris HA, Petrylak DP, Teng SL et al (2014) MPDL3280A (anti-PD-L1) treatment leads to clinical activity in metastatic bladder cancer. Nature 515:558–562
11. Bivona TG, Doebele RC (2016) A framework for understanding and targeting residual disease in oncogene-driven solid cancers. Nat Med 22:472–478
12. Michelson S, Slate D (1989) Emergence of the drug-resistant phenotype in tumor subpopulations: a hybrid model. J Natl Cancer Inst 81:1392–1401
13. Majidinia M, Yousefi B (2017) Breast tumor stroma: a driving force in the development of resistance to therapies. Chem Biol Drug Des 89(3):309–318
14. Komarova N (2006) Stochastic modeling of drug resistance in cancer. J Theor Biol 239:351–366
15. Ramirez M, Rajaram S, Steininger RJ, Osipchuk D, Roth MA, Morinishi LS, Evans L, Ji W, Hsu CH, Thurley K et al (2016) Diverse drug-resistance mechanisms can emerge from drug-tolerant cancer persister cells. Nat Commun 7:10690
16. Bartel DP (2004) MicroRNAs: genomics, biogenesis, mechanism, and function. Cell 116:281–297

17. Lee RC, Ambros V (2001) An extensive class of small RNAs in Caenorhabditis elegans. Science 294:862–864
18. Wu W, Sun M, Zou GM, Chen J (2007) MicroRNA and cancer: current status and prospective. Int J Cancer 120(5):953–960
19. He L, Thomson JM, Hemann MT, Hernando-Monge E, Mu D, Goodson S, Powers S, Cordon-Cardo C, Lowe SW, Hannon GJ, Hammond SM (2005) A microRNA polycistron as a potential human oncogene. Nature 435:828–833
20. Lee RC, Feinbaum RL, Ambros V (1993) The C. elegans heterochronic gene lin-4 encodes small RNAs with antisense complementarity to lin-14. Cell 75:843–854
21. Wu W (2011) MicroRNA and cancer, Methods in molecular biology, vol 676. Springer, New York
22. Sato H, Shien K, Tomida S, Okayasu K, Suzawa K, Hashida S, Torigoe H, Watanabe M, Yamamoto H, Soh J et al (2017) Targeting the miR-200c/LIN28B axis in acquired EGFR-TKI resistance non-small cell lung cancer cells harboring EMT features. Sci Rep 7:40847
23. Zhang B, Pan X, Anderson TA (2006) MicroRNA: a new player in stem cells. J Cell Physiol 209:266–269
24. Wang V, Wu W (2009) MicroRNA-based therapeutics for cancer. BioDrugs 23:15–23
25. Liu TC, Jin X, Wang Y, Wang K (2017) Role of epidermal growth factor receptor in lung cancer and targeted therapies. Am J Cancer Res 7:187–202
26. Wang YS, Wang YH, Xia HP, Zhou SW, Schmid-Bindert G, Zhou CC (2012) MicroRNA-214 regulates the acquired resistance to gefitinib via the PTEN/AKT pathway in EGFR-mutant cell lines. Asian Pac J Cancer Prev 13:255–260
27. Garofalo M, Romano G, Di Leva G, Nuovo G, Jeon YJ, Ngankeu A, Sun J, Lovat F, Alder H, Condorelli G et al (2011) EGFR and MET receptor tyrosine kinase-altered microRNA expression induces tumorigenesis and gefitinib resistance in lung cancers. Nat Med 18:74–82
28. Garofalo M, Di Leva G, Romano G, Nuovo G, Suh SS, Ngankeu A, Taccioli C, Pichiorri F, Alder H, Secchiero P et al (2009) miR-221&222 regulate TRAIL resistance and enhance tumorigenicity through PTEN and TIMP3 downregulation. Cancer Cell 16:498–509
29. Sharma SV, Lee DY, Li B, Quinlan MP, Takahashi F, Maheswaran S, McDermott U, Azizian N, Zou L, Fischbach MA et al (2010) A chromatin-mediated reversible drug-tolerant state in cancer cell subpopulations. Cell 141:69–80
30. Heng HH, Bremer SW, Stevens JB, Ye KJ, Liu G, Ye CJ (2009) Genetic and epigenetic heterogeneity in cancer: a genome-centric perspective. J Cell Physiol 220:538–547
31. Sahu N, Stephan JP, Cruz DD, Merchant M, Haley B, Bourgon R, Classon M, Settleman J (2016) Functional screening implicates miR-371-3p and peroxiredoxin 6 in reversible tolerance to cancer drugs. Nat Commun 7:12351
32. Vinogradova M, Gehling VS, Gustafson A, Arora S, Tindell CA, Wilson C, Williamson KE, Guler GD, Gangurde P, Manieri W et al (2016) An inhibitor of KDM5 demethylases reduces survival of drug-tolerant cancer cells. Nat Chem Biol 12:531–538
33. Wu W (2011) Modulation of microRNAs for potential cancer therapeutics. In: Wu W (ed) MicroRNA and cancer, Methods in molecular biology, vol 676, pp 59–70

Chapter 7

MicroRNA, Noise, and Gene Expression Regulation

Wei Wu

Abstract

Gene regulatory network that determines the cellular functions exhibits stochastic fluctuations, or "noise," in different layers. Noise has begun to be appreciated for many previously unrecognized functions in important cellular activities. In fact, molecular noise is unavoidable in both microbial and eukaryotic cells, the feedback system is established evolutionally to reduce noise or optimize the noise for cellular homeostasis. The small noncoding RNAs, particularly, microNRAs, post-transcriptionally and negatively regulate gene expressions. MicroRNAs function as a novel layer to buffer noise level, and stabilize mRNA and protein level to maintain normal cellular function. Furthermore, the changing of microRNA expression levels may increase the stochastic fluctuation leading to abnormal cellular function, even diseases.

Key words MicroRNAs, Noise, Gene regulatory network, Stochastic fluctuation

1 Introduction

Stochasticity is a ubiquitous characteristic of life. Such apparent randomness, or "noise" can be observed in a wide range of organisms. Gene expression is the set of reactions that control the abundance of gene products, and influences the most aspects of cellular behavior. It is a fundamental stochastic process with randomness in transcription and translation leading to cell to cell variation in mRNA and protein levels [1]. Several potential sources of variation in gene expression have been discussed in refs. 2, 3, such as infrequent molecular events involving small numbers of molecules, cell cycle progression or cell division, subtle environmental differences, and random and directed genetic mutations. Noise, or variation, in the process of gene expression may contribute to this phenotypic variability. Both the magnitude and the frequency of the noise affect the consequence [4]. Small changes in protein abundance may have persisted long enough, whereas large fluctuations in abundance may not have any effect if they occur too frequently to affect cellular processes [2, 3]. Noise in gene expression and other cellular processes has been a major research focus for more than a decade. The

Wei Wu (ed.), *MicroRNA and Cancer: Methods and Protocols*, Methods in Molecular Biology, vol. 1699,
DOI 10.1007/978-1-4939-7435-1_7,

functional roles of noise in genetic circuits have been intensively reviewed recently by Eldar and Elowitz [5]. Noise apparently has an advantageous effect in prokaryotes (e.g., bacteria and phage lambda) and eukaryotes (yeast and mammalian). Noise allows simultaneous achievement of multiple steady-state phenotypes in a population, the transcriptome-wide noise controls lineage choice in mammalian progenitor cells [6, 7] and can be transmitted from one gene, in this case, a transcription factor, to a downstream target [2, 3]. On the other hand, noise is disadvantageous in most cellular processes, as precisely controlled levels of gene expression are presumably optimal. Therefore, noise in gene expression has been subjected to natural selection to reduce its deleterious effects [8]. Recently, small noncoding RNAs, as a noise controller, fine-tuned the gene expression network, have drawn compelling attention. In this chapter, I focus on the latest research on the noise that is controlled by microRNA in gene expression, and provide the insights into how the abnormal expression of microRNA affects the noise function in cancer cells.

2 Small Noncoding RNA, A New Regulator of the Gene Expression

Noise implies that protein and RNA numbers tend to be far from their mean values, and so cellular information processing must function through biochemical networks whose components potentially fluctuate significantly and unpredictably [9, 10]. The cells or organisms evolutionarily established the "intracellular buffering" system to maintain the homeostasis. The one we are familiar with is the signal transduction, genetic network architectures. The dimerization of transcription factors [11] has been found in noise reduction in genetic network as well. A small noncoding RNA (ncRNA) plays a very important role in the post-transcriptional regulation in various organisms. Some kinetic models of post-transcriptional regulation by ncRNA have been proposed; both theoretical analysis and quantitative experiments in prokaryotes and eukaryotes demonstrated that the intrinsic noise level is associated with ncRNA level and mRNA level. In complex gene expression regulatory networks, relative fluctuations in RNAs copy numbers could be measured with the Fano factor (a measure of the relative size of the internal fluctuation). To simplify the complexity of gene interaction, the one-to-one interaction (single ncRNA and single mRNA) model showed the bare poissonian limit in the regimen of both RNA silencing and surviving with the Langevin theory in E coli cells. However, one to two (single ncRNA and two target mRNAs) exhibited the strong anti-correlation in the regimen of crossover [12].

A delayed negative feedback regulation of gene expression has been modeled to show that the cyclic expression dynamics could be

observed when the normalized repression threshold, and the mRNA half-life are limited to a narrower range [13]. The authors further found that when the mRNA half-life decreases, the expression dynamics of the basal model shifts from stable to oscillations; and when the mRNA t1/2 decreases even further, the basal model returns to stable expression dynamics. After incorporating miRNAs into this system, because the miRNA increases the degradation rate of mRNA, then the effect of a miRNA on gene expression is initially destabilizing, and then stabilizes it. This is an interesting simulation study suggestive of the cut-off level of miRNA fine tuning the expression level.

3 Mathematical Modeling for MicroRNA Biogenesis

Wang et al. [14] established a mathematical modeling for the microRNA pathway with the ordinary differential equation. Following each step of the biogenesis of microRNA, the outcome of microRNA-mediated degradation of mRNA or protein synthesis inhibition, on the case of cleavage of mRNA by RISC, in light of the experimental observation, the formation of mRNA is ahead of the corresponding protein and peaks at about 5000 s time point in the model, then mRNA was found declining toward a steady state and its product following with a lagged miRNA expression is about 11 h time point. Furthermore, the increment of the miRNA concentration causes mRNA and protein concentration declines after a peak, followed by a late steady level. The mild attenuation of both mRNA and protein may reflect a miRNA regulates the mRNA translation in a very weak manner. In the case of inhibition of the translation by RISC, the mRNA and protein reach their steady states much more slowly than in case one, at about 50,000 and 60,000 s, respectively. And their concentrations (steady level) are about 0.8 nM and 8 nM, respectively.

4 Stochastic Simulation

Random fluctuation in genetic networks is unavoidable. As chemical reactions are probabilistic, and many genes, RNAs, and proteins are present at low amount per cell, such "noise" affects all life processes.

To elucidate the impact of miRNAs on mRNA destability or translation inhibition, the miR-1 and miR-155 was ectopically expressed in HeLa cells or miR-223 was knocked out in mouse neutrophiles, the ribosome profiling in these cells demonstrates that only a small fraction of repression observed in ribosome profiling (11–16%) was attributable to reduced translational

efficiency, at least 84% of the repression was attributable to decreased mRNA level [15].

In the defined topology, the relationship of miRNA and noise has been explored [16]. Gene regulatory networks involving positive and negative feedback have the potential to control the effects of noise via buffering its impact on gene expression. miRNAs play a role in feedback and feed forward network. As discussed in the chapter, the transcriptional feedback system is triggered by random fluctuations in gene expression, and the miRNA helps to reinforce selection of only one peak of senseless expression while filtering out others that might have been able to surpass the threshold in the absence of the miRNA. The miR-9a, as an example, contributes to the robustness of the noise-dependent switch.

5 The Noise, Randomness, and Cancer

The development of many cancers is believed due to the occurrence over a lifetime of random mutations in replicating stem cells [17]. In essence, total somatic mutations = (mutation rate) × (# cell divisions). It is also appreciated that genetically similar cells may behave differently in the face of identical selection pressures. A common mechanism for epigenomic disruption is stochasticity, whereby changes are introduced randomly that lead to gain or loss of DNA methylation at certain CpG dinucleotides, the preferred sites of DNA methylation in mammalian cells including cancer cells [18]. Arguably, this equation could be: total somatic mutations = (mutation rate + epigenetic changes) × (# cell divisions) [19].

Noise-driven heterogeneity in the rate of genetic-variant generation as a basis for evolvability, and noise-driven nongenetic heterogeneity among cancer cells could be a driving force in cancer evolution [20]. At the transcriptional level, increased expression noise in patients is correlated with low expression of p53 and immune activity in breast, liver, and lung cancers, which suggests the contributions of p53 signaling and host immune surveillance to gene expression noise in cancers; moreover, tumors in late stages increase expression noise, suggesting expression noise shifts the cell states [21].

Clusters of miRNA that co-targeted genes are important for the regulation of miRNA in disease such as chromosomal 19 microRNA cluster [22]. The aberrant expression of micoRNAs increases the noise of gene expression which accelerates cells from normal state to abnormal state [23]. The other side of the coin is the epigenetics affects miRNome as well as how epi-miRNAs can control epigenome [24]. Large-scale functional miRNA analysis in normal tissues and pathological counterparts revealed that complete miRNA network presents in normal tissues, while the miRNA

network is rewired or reprogrammed in cancer or lekeumia repecific manner [25]. It is conceivable that cancer is a noise-driven disease in the concept of physics. Reducing the noise with multi-dimensional interventions could reverse the cell state and control the cancer.

6 Summary

The intrinsic stochasticity of gene expression is usually mitigated in higher eukaryotes by post-transcriptional regulation channels that stabilize the gene products, most notably protein levels. The discovery of small noncoding RNAs (miRNAs) in specific motifs of the genetic regulatory network has led to identifying noise buffering as the possible key function they exert in gene regulation [26]. Noise has begun to be appreciated for many previously unrecognized functions in important cellular activities. Noise can change the cell state, drive cancer development, and create heterogeneity demonstrated by upfront single-cell RNAseq [27]. Controlling the noise in cancer with small molecules, immune intervention could reverse the cell state for therapeutic management.

References

1. Friedlander MR, Chen W, Adamidi C, Maaskola J, Einspanier R, Knespel S, Rajewsky N (2008) Discovering microRNAs from deep sequencing data using miRDeep. Nat Biotechnol 26:407–415
2. Raser JM, O'Shea EK (2004) Control of stochasticity in eukaryotic gene expression. Science 304:1811–1814
3. Raser JM, O'Shea EK (2005) Noise in gene expression: origins, consequences, and control. Science 309:2010–2013
4. Chalancon G, Ravarani CN, Balaji S, Martinez-Arias A, Aravind L, Jothi R, Babu MM (2012) Interplay between gene expression noise and regulatory network architecture. Trends Genet 28:221–232
5. Eldar A, Elowitz MB (2010) Functional roles for noise in genetic circuits. Nature 467:167–173
6. Chang HH, Oh PY, Ingber DE, Huang S (2006) Multistable and multistep dynamics in neutrophil differentiation. BMC Cell Biol 7:11
7. Chang HH, Hemberg M, Barahona M, Ingber DE, Huang S (2008) Transcriptome-wide noise controls lineage choice in mammalian progenitor cells. Nature 453:544–547
8. Fraser HB, Hirsh AE, Giaever G, Kumm J, Eisen MB (2004) Noise minimization in eukaryotic gene expression. PLoS Biol 2:e137
9. Swain PS, Elowitz MB, Siggia ED (2002) Intrinsic and extrinsic contributions to stochasticity in gene expression. Proc Natl Acad Sci U S A 99:12795–12800
10. Swain PS (2004) Efficient attenuation of stochasticity in gene expression through post-transcriptional control. J Mol Biol 344:965–976
11. Bundschuh R, Hayot F, Jayaprakash C (2003) The role of dimerization in noise reduction of simple genetic networks. J Theor Biol 220:261–269
12. Jia Y, Liu W, Li A, Yang L, Zhan X (2009) Intrinsic noise in post-transcriptional gene regulation by small non-coding RNA. Biophys Chem 143:60–69
13. Gironella M, Seux M, Xie MJ, Cano C, Tomasini R, Gommeaux J, Garcia S, Nowak J, Yeung ML, Jeang KT et al (2007) Tumor protein 53-induced nuclear protein 1 expression is repressed by miR-155, and its restoration inhibits pancreatic tumor development. Proc Natl Acad Sci U S A 104:16170–16175

14. Wang X, Li Y, Xu X, Wang YH (2010) Toward a system-level understanding of microRNA pathway via mathematical modeling. Biosystems 100:31–38
15. Guo H, Ingolia NT, Weissman JS, Bartel DP (2010) Mammalian microRNAs predominantly act to decrease target mRNA levels. Nature 466:835–840
16. Herranz H, Cohen SM (2010) MicroRNAs and gene regulatory networks: managing the impact of noise in biological systems. Genes Dev 24:1339–1344
17. Tomasetti C, Vogelstein B (2015) Cancer etiology. Variation in cancer risk among tissues can be explained by the number of stem cell divisions. Science 347:78–81
18. Swanton C, Beck S (2014) Epigenetic noise fuels cancer evolution. Cancer Cell 26:775–776
19. Wu S, Powers S, Zhu W, Hannun YA (2016) Substantial contribution of extrinsic risk factors to cancer development. Nature 529:43–47
20. Capp JP (2010) Noise-driven heterogeneity in the rate of genetic-variant generation as a basis for evolvability. Genetics 185:395–404
21. Han R, Huang G, Wang Y, Xu Y, Hu Y, Jiang W, Wang T, Xiao T, Zheng D (2016) Increased gene expression noise in human cancers is correlated with low p53 and immune activities as well as late stage cancer. Oncotarget 7:72011–72020
22. Wu W, Cao W, Chan JA (2013) Regulation of MicroRNAs for potential cancer therapeutics: the paradigm shift from pathways to perturbation of gene regulatory networks. In: Lopez-Camarillo C, Marchat LA (eds) MicroRNAs in cancer. CRC Press, Boca Raton, FL, pp 364–386
23. Grigolon S, Di Patti F, De Martino A, Marinari E (2016) Noise processing by microRNA-mediated circuits: the incoherent feed-forward loop, revisited. Heliyon 2:e00095
24. Iorio MV, Piovan C, Croce CM (1799) Interplay between microRNAs and the epigenetic machinery: an intricate network. Biochim Biophys Acta 2010:694–701
25. Volinia S, Galasso M, Costinean S, Tagliavini L, Gamberoni G, Drusco A, Marchesini J, Mascellani N, Sana ME, Abu Jarour R et al (2010) Reprogramming of miRNA networks in cancer and leukemia. Genome Res 20:589–599
26. Wilbert ML, Yeo GW (2011) Genome-wide approaches in the study of microRNA biology. Wiley Interdiscip Rev Syst Biol Med 3:491–512
27. Kim JK, Kolodziejczyk AA, Ilicic T, Teichmann SA, Marioni JC (2015) Characterizing noise structure in single-cell RNA-seq distinguishes genuine from technical stochastic allelic expression. Nat Commun 6:8687

Part II

Protocol Section

Chapter 8

Deep Sequencing Reveals a MicroRNA Expression Signature in Triple-Negative Breast Cancer

Yao-Yin Chang, Liang-Chuan Lai, Mong-Hsun Tsai, and Eric Y. Chuang

Abstract

Deep sequencing is an advanced technology in genomic biology to detect the precise order of nucleotides in a strand of DNA/RNA molecule. The analysis of deep sequencing data also requires sophisticated knowledge in both computational software and bioinformatics. In this chapter, the procedures of deep sequencing analysis of microRNA (miRNA) transcriptome in triple-negative breast cancer and adjacent normal tissue are described in detail. As miRNAs are critical regulators of gene expression and many of them were previously reported to be associated with the malignant progression of human cancer, the analytical method that accurately identifies deregulated miRNAs in a specific type of cancer is thus important for the understanding of its tumor behavior. We obtained raw sequence reads of miRNA expression from 24 - triple-negative breast cancers and 14 adjacent normal tissues using deep sequencing technology in this work. Expression data of miRNA reads were normalized with the quantile-quantile scaling method and were analyzed statistically. A miRNA expression signature composed of 25 differentially expressed miRNAs showed to be an effective classifier between triple-negative breast cancers and adjacent normal tissues in a hierarchical clustering analysis.

Key words Deep sequencing, Differentially expressed microRNA, MicroRNA expression signature, Triple-negative breast cancer, Sequencing data normalization

1 Introduction

MicroRNAs (miRNAs) are short, noncoding RNA molecules that are negative regulators of gene expression of their targeted messenger RNAs [1, 2]. Abundant evidences have shown the importance of miRNA regulations in various cellular functions, such as cellular development, differentiation, and growth control [3–6]. Over the past several years, it has also become clear that aberrant expression of miRNAs contributes to the tumorigenesis of many human malignancies [7–9]. While some miRNAs have shown to be associated with oncogenic or tumor-suppressing functions, amplification or overexpression of the oncogenic miRNAs or genetic losses of the tumor suppressor miRNAs have been found in many human cancers [9–12]. Excitingly, inhibition of oncogenic miRNAs in

Wei Wu (ed.), *MicroRNA and Cancer: Methods and Protocols*, Methods in Molecular Biology, vol. 1699,
DOI 10.1007/978-1-4939-7435-1_8,

solid tumors may become an evolving strategy for anticancer therapy [13]. It is thus very important to identify miRNAs that are deregulated among tumor specimens in a research of human cancer. In this chapter, the analytical procedures for an accurate identification of differentially expressed miRNAs between triple-negative breast cancers and adjacent normal tissues using deep sequencing technology are described. Triple-negative breast cancer is a type of breast cancer characterized by the lack of expression of the estrogen receptor (ER), the progesterone receptor (PR), and the human epidermal growth factor receptor 2 (HER2). Its tumor behavior is aggressive and currently there is no effective targeted medicine available for it. In this work, we describe how to analyze the expression levels of miRNA transcriptome in triple-negative breast cancer using deep sequencing technology. Deep sequencing is the process that determines the precise order of nucleotides in a strand of DNA/RNA molecule. The advent of deep sequencing technology has substantially improved the quality of scientific discovery in many fields of genomic research [14–17]. However, a deep sequencing experiment normally produces large quantity of digital data of nucleotide sequences. This large amount of raw information needs to be further processed with a series of bioinformatics methods so that its true biological value can be revealed. Here, we demonstrate how to obtain miRNA sequence reads from triple-negative breast cancer samples with deep sequencing experiments and miRNA alignment. The quantile-quantile scaling method was performed for the normalization of raw miRNA reads in each sample dataset. The miRNA expression data from triple-negative breast cancers and adjacent normal tissues were then statistically analyzed. A miRNA expression signature composed of 25 differentially expressed miRNAs was found to clearly distinguish triple-negative breast cancers from surrounding normal tissues in a hierarchical clustering analysis.

2 Materials

2.1 Breast Cancer Samples and Clinical Information

1. Triple-negative breast cancer samples and adjacent normal tissue samples. In this work, 24 triple-negative breast cancer samples and 14 adjacent normal tissue samples were collected at National Taiwan University Hospital (NTUH, Taipei, Taiwan) [18]. All triple-negative breast cancer samples were invasive ductal carcinomas and were negative in immunohistochemical analyses of ER, PR, and HER2. Written informed consents were obtained from all the breast cancer patients (*see* **Note 1**).
2. Clinical information of all the breast cancer patients in the study (Table 1). The clinical information includes age, stage,

Table 1
Clinical information on 24 triple-negative breast cancer patients

Sample ID	Age (years)	Stage	Grade[a]	Tumor size[b]	LYM[c]	Recurrence status[d]	Recurrence-free time (years)
452_T	54	I	2	1	0	0	6.6
477_T	27	I	3	1	0	0	6.5
593_T	55	I	3	1	0	0	5.9
602_T	44	I	3	1	0	0	5.9
621_T	62	I	2	1	0	0	5.8
894_T	54	I	2	1	0	0	4.6
922_T	63	I	3	1	0	0	4.5
417_T	33	IIA	3	2	0	0	6.8
507_T	54	IIA	3	1	1	0	6.4
545_T	55	IIA	3	2	0	0	6.2
557_T	60	IIA	3	2	0	0	6.1
574_T	57	IIA	2	2	0	0	6.0
582_T	83	IIA	3	2	0	1	3.5
619_T	37	IIA	3	2	0	1	1.8
673_T	61	IIA	2	2	0	1	0.7
887_T	49	IIA	3	2	0	0	4.6
917_T	51	IIA	3	2	0	0	4.5
918_T	38	IIA	3	2	0	0	4.5
941_T	52	IIA	3	1	1	0	4.4
677_T	65	IIB	3	2	1	0	5.5
881_T	58	IIB	3	2	1	0	4.7
893_T	55	IIB	3	2	1	1	1.5
291_T	85	IIIA	3	3	1	1	1.2
357_T	57	IIIC	3	2	1	0	7.1

[a]Grade: 1/2/3, low/intermediate/high
[b]Tumor size: 1/2/3, <2 cm/2 cm-5 cm/>5 cm
[c]LYM, lymph node metastasis: 0/1, negative/positive
[d]Recurrence: 0/1, negative/positive

grade, tumor size, lymph node metastasis, and recurrence status of the patients (*see* **Note 2**). All relevant clinical information of the patients who participate in human tissue experiments need to be properly documented.

2.2 Deep Sequencing Experiment

1. SOLiD™ 4 System (Applied Biosystems, Foster City, CA, USA).
2. SOLiD™ Total RNA-Seq Kit (Applied Biosystems).
3. SOLiD™ Library Micro Column Purification Kit (Applied Biosystems).
4. SOLiD™ EZ bead system (Applied Biosystems).
5. SOLiD™ slides, slide assembly carrier, and deposition chamber (Applied Biosystems).
6. Agilent 2100 Bioanalyzer (Agilent, Santa Clara, CA, USA).
7. DNA 1000 Kit (Agilent).

2.3 Computer Hardware, Software, and Human Genome Reference

1. Head node computer (2 + GHz CPU; 2 Gb RAM; 2 + Tb storage space).
2. Computing node computers (2 + GHz CPU; 2 Gb RAM; 500 + Gb storage space).
3. Redhat/CentOS 4+ Distros on 64-bit operating environment.
4. Supporting software: Java v1.6, Perl v5.8.5, Python v2.3+, JMS v5.3+, PBS/Torque v2.4.0+, Tomcat v6.0.18+.
5. SOLiD™ BioScope™ Software (Applied Biosystems).
6. Small RNA Analysis Tool (Applied Biosystems).
7. Human genome reference (RefSeq Hg19).
8. Human miRNA reference (miRBase v17+).
9. Microsoft Excel (Microsoft, Redmond, WA, USA).
10. Matlab vR2014a + (MathWorks, Natick, MA, USA).
11. Genesis v1.7.5+ (Thallinger Lab, Graz University of Technology, Graz, Austria).

3 Methods

3.1 Deep Sequencing Experiment

Deep sequencing experiments of 24 triple-negative breast cancer samples and 14 adjacent normal tissue samples were performed using the SOLiD™ 4 system. Raw miRNA expression reads were obtained from each sample after the deep sequencing experiment.

1. Extract total RNA from each of the triple-negative breast cancer samples and the adjacent normal tissue samples for the preparation of small RNA library.
2. Construct small RNA library from total RNA using the SOLiD™ Total RNA-Seq Kit following the manufacturer's instructions.
3. Purify the small RNA library using the SOLiD™ Library Micro Column Purification Kit. Assess the quality and size

distribution of the small RNA library using Agilent 2100 Bioanalyzer with the DNA 1000 Kit. The ratio of 120–130-bp DNA: 25–150-bp DNA needs to be greater than 50% in order to proceed with the templated bead preparation.

4. Prepare an emulsion of the library and amplify the library templated beads with the SOLiD™ EZ bead system.
5. Deposit the template beads onto a slide placed in the SOLiD™ deposition chamber.
6. Open the SOLiD™ deposition chamber, and then remove the slide carrier assembly. Place the slide carrier assembly onto the SOLiD™ 4 system.
7. Start the ligation sequencing procedure.

3.2 Sequence Alignment for miRNA Reads

The sequence reads collected from the SOLiD™ 4 sequencer were processed using the SOLiD™ BioScope™ Software.

1. Obtain the sequence files (csfasta files and quality files) from the SOLiD™ 4 system. Save all the files in a storage space connected to the computer clustering system. The computer clustering system comprises a head node computer and multiple computing node computers (*see* **Note 3**). A conceptual illustration of the computer clustering system built specifically for sequence alignment is shown in Fig. 1.
2. Filter out the sequence reads that contain ribosomal RNA, transfer RNA, and adaptor sequences using the SOLiD™ BioScope™ Software. The remaining reads are used in the miRNA sequence alignment.
3. Perform sequence alignment of the remaining reads to the human miRNA reference (miRBase v17.0) and the human genome reference (RefSeq Hg19) using the Small RNA Analysis Tool. Allow only one mismatch for the first sixteen bases of a

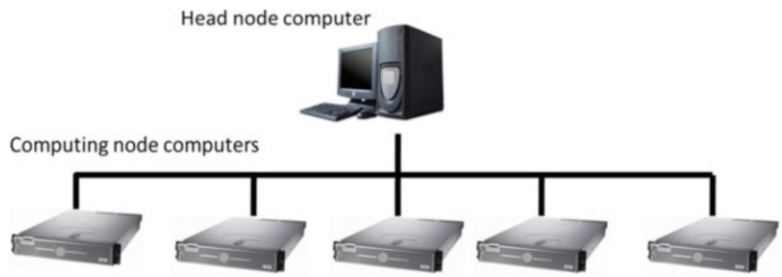

Fig. 1 A conceptual illustration of the computer clustering system built specifically for miRNA sequence alignment. A head node computer is connected with five computing node computers in this example. Users give commands of alignment jobs to the head node computer. The head node computer divides and forwards the sequencing jobs to these computing nodes, and then collects the final results

miRNA alignment. The maximum number of allowed mismatches for a miRNA read is set at four (*see* **Note 4**).

4. Disregard the miRNA reads that are mapped to multiple positions on the human genome to reduce ambiguous miRNA alignments (*see* **Note 5**), which is an option of selective filtering with the Small RNA Analysis Tool.
5. Compose a miRNA expression matrix (n-miRNAs vs. -m-samples) showing the number of reads of miRNAs obtained from each sample with Microsoft Excel (*see* **Note 6**).
6. Disregard the miRNAs with extremely low expression (mean expression <5 reads in all samples) in the miRNA expression matrix (*see* **Note 7**). In this work, 707 miRNAs were identified after this step.

3.3 Normalization of miRNA Reads

The quantile-quantile scaling method [19] was used for the normalization of miRNA expression reads in each sample dataset. The miRNA expression reads in each sample were converted to $\log_{10}$-scaled data for a pure scaling normalization.

1. Calculate the mean expression (reads) of each miRNA in all 38 samples. The mean-expression profile composed of 707 miRNAs is used as the quantile-quantile scaling reference.
2. Convert all the miRNA expression reads in the miRNA expression matrix to $\log_{10}$-scaled expression data using Microsoft Excel.
3. Generate a quantile-quantile plot with the $\log_{10}$-scaled expression data for each sample dataset (each sample vs. the mean-expression profile) using Matlab. In each quantile-quantile plot, draw a blue line to indicate the main diagonal (45-degree line), and draw a red line to indicate the best diagonal fit of the $\log_{10}$-scaled expression data of a particular sample dataset.
4. Calculate the shortest distance from the center of the red line (the best diagonal fit) to the main diagonal in each quantile-quantile plot. This value is the scaling factor for each sample dataset.
5. Vertically shift all the data points in each sample dataset using the scaling factor obtained from the previous step. This procedure linearly scales all the data points in a sample dataset with respect to the mean-expression profile in the logarithmic space.

3.4 Identification of Differentially Expressed miRNAs Between Triple-Negative Breast Cancers and Adjacent Normal Tissues

Differentially expressed miRNAs between triple-negative breast cancers ($N = 24$) and adjacent normal tissues ($N = 14$) were identified using two-tailed Student's t-test. The Holm step down procedure was performed for p-value adjustment to counteract multiple comparisons.

1. Open the miRNA expression matrix with Microsoft Excel. The normalized miRNA expression data are shown in $\log_{10}$-scale.
2. Calculate the p-value of each miRNA with the normalized miRNA expression data from triple-negative breast cancers ($N = 24$) and adjacent normal tissues ($N = 14$) using two-tailed Student's t-test (*see* **Note 8**).
3. Rank the miRNAs with their p-values. The miRNAs are ranked according to their p-values from low to high.
4. Convert the $\log_{10}$-scaled miRNA expression data into read counts.
5. Calculate the mean expression difference (reads) and fold change of each miRNA between triple-negative breast cancers ($N = 24$) and adjacent normal tissues ($N = 14$). Disregard the miRNAs if they do not meet the following criteria: mean expression difference > 100 reads and fold change >2 between the two groups.
6. Perform the Holm step down procedure to adjust the p-values. The procedure is described as follows.

   Adjusted $p_{(1)} = k + p_{(1)}$
   Adjusted $p_{(2)} = \max(\text{Adjusted } p_{(1)}, (k-1) + p_{(2)})$
   Adjusted $p_{(3)} = \max(\text{Adjusted } p_{(2)}, (k-2) + p_{(3)})$
   ...
   Adjusted $p_{(k-1)} = \max(\text{Adjusted } p_{(k-2)}, 2 + p_{(k-1)})$
   Adjusted $p_{(k)} = \max(\text{Adjusted } p_{(k-1)}, p_{(k)})$
   k is the number of microRNAs.
   $p_{(1)}$ to $p_{(k)}$ are sorted p-values from low to high.
7. Identify differentially expressed miRNAs (adjusted p-value <0.05) between triple-negative breast cancers and adjacent normal tissues (*see* **Note 9**). In this work, a list of 25 differentially expressed miRNAs representing the components of a miRNA expression signature was identified as shown in Table 2.

3.5 Hierarchical Clustering Analysis

Average-linkage hierarchical clustering analysis of 24 triple-negative breast cancers and 14 adjacent normal tissues was performed with the miRNA expression signature composed of 25 differentially expressed miRNAs identified in the previous section.

1. Open the Genesis software. Load the miRNA expression data file containing the normalized, $\log_{10}$-scaled miRNA expression data of 25 miRNAs from all 38 samples (*see* **Note 10**).

Table 2
The miRNA expression signature composed of 25 differentially expressed miRNAs between triple-negative breast cancers and adjacent normal tissues

			Triple-negative breast cancer			Adjacent normal tissue		
			Normalized	Range		Normalized	Range	
miRNA	Raw *p* Value	Adjusted *p* Value	Mean	Min	Max	Mean	Min	Max
hsa-miR-215	3.21E-08	4.66E-06	32	0	86	321	80	928
hsa-miR-497-5p	2.43E-06	3.49E-04	1980	354	6215	6520	2335	18,692
hsa-miR-204-5p	4.69E-06	6.71E-04	98	0	569	2518	37	14,352
hsa-miR-425-5p	5.98E-06	8.49E-04	23,266	7198	57,542	9180	4551	16,066
hsa-miR-96-5p	1.34E-05	1.89E-03	4568	898	12,421	1545	494	3892
hsa-miR-1301	1.72E-05	2.40E-03	592	0	4777	43	0	188
hsa-miR-335-3p	2.89E-05	4.02E-03	1173	118	4234	5591	440	11,145
hsa-miR-183-5p	5.13E-05	7.08E-03	6223	1305	24,697	1928	602	5753
hsa-miR-24-2-3p	6.04E-05	8.27E-03	6782	2062	17,902	3254	1553	5731
hsa-miR-130b-5p	7.64E-05	1.04E-02	3729	1413	10,634	1352	159	2856
hsa-miR-92a-3p	9.93E-05	1.34E-02	182	0	1151	0	0	0
hsa-miR-320a-3p	1.15E-04	1.54E-02	11,490	0	29,381	2273	0	26,275
hsa-miR-130b-3p	1.23E-04	1.64E-02	550	204	1683	246	110	579
hsa-miR-145-5p	1.47E-04	1.94E-02	256	9	603	877	202	2457
hsa-miR-126-3p	1.55E-04	2.03E-02	44,031	16,691	108,893	134,103	29,907	285,350
hsa-miR-139-5p	1.57E-04	2.04E-02	693	181	2537	6623	307	23,210
hsa-let-7a-3p	1.59E-04	2.05E-02	175	0	428	41	0	326

(continued)

Table 2
(continued)

miRNA	Raw *p* Value	Adjusted *p* Value	Triple-negative breast cancer			Adjacent normal tissue		
			Normalized Mean	Range Min	Range Max	Normalized Mean	Range Min	Range Max
hsa-miR-489-5p	1.59E-04	2.05E-02	8	0	63	118	0	483
hsa-miR-362-5p	1.69E-04	2.15E-02	2216	1186	5092	1006	297	2303
hsa-miR-429-5p	1.91E-04	2.40E-02	6416	1486	23,455	2082	406	8716
hsa-miR-19b-3p	2.43E-04	3.04E-02	569	0	3214	0	0	0
hsa-miR-362-3p	2.56E-04	3.17E-02	1043	565	2168	448	43	845
hsa-miR-320a-5p	2.72E-04	3.34E-02	1354	0	17,859	4369	0	15,247
hsa-miR-337-5p	3.44E-04	4.19E-02	386	9	961	1309	334	4086
hsa-miR-143-5p	3.91E-04	4.73E-02	43,060	3104	99,397	102,717	29,650	36,464

Normalized miRNA reads from each sample were obtained after quantile-quantile scaling. The raw p-value of each miRNA was calculated using the $\log_{10}$-scaled miRNA expression data after quantile-quantile scaling and was adjusted using the Holm step down procedure. Relative expression levels are shown

2. Start the hierarchical clustering calculation by selecting the menu item Clustering --> Calculate Hierarchical Clustering.
3. Select the option of average-linkage for the clustering algorithm. Specify that both genes and samples should be clustered.
4. Specify the maximum values (0 and 5) for saturated colors as shown in the hierarchical clustering plot. The maximum values represent the upper and lower bounds of the $\log_{10}$-scaled miRNA expression in the data file.
5. Change the color scheme of the expression image. Purple (color) indicates high expression and white (color) indicates low expression.
6. Specify the color of each tissue sample. Red (color) represents triple-negative breast cancer samples and green (color) represents adjacent normal tissue samples.
7. Save the hierarchical clustering plot as an image file. All triple-negative breast cancers and adjacent normal tissues are clearly divided into two clusters without any misclassification (Fig. 2).

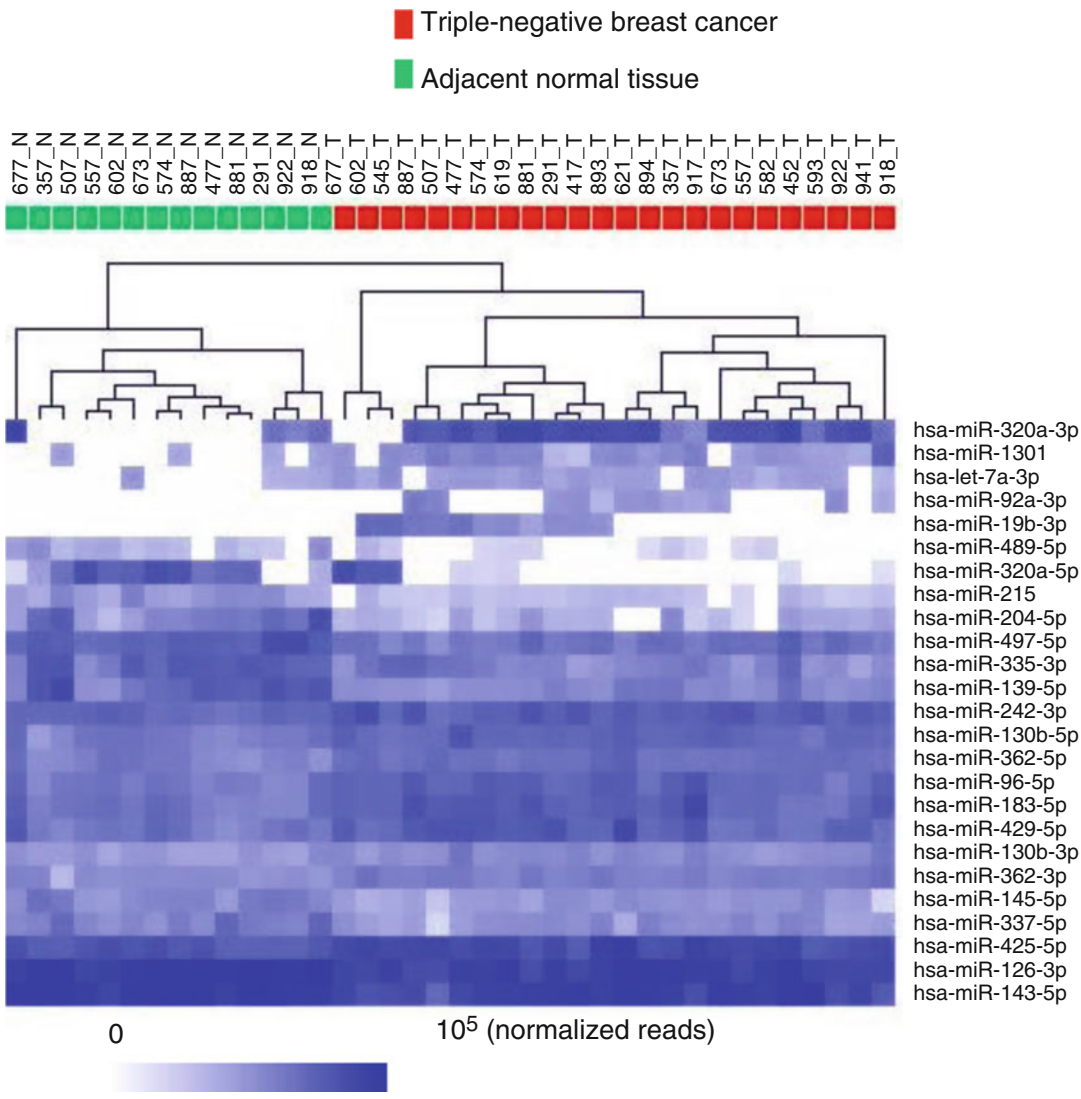

Fig. 2 Hierarchical clustering analysis of 24 triple-negative breast cancers (*red*) and 14 adjacent normal tissues (*green*) with the miRNA expression signature composed of 25 miRNAs. Each row represents the normalized miRNA expression data and each column represents a tissue sample. The dendrogram depicts similarities in the miRNA expression portraits among the samples. (Reproduced from [*Chang* et al., 2015] with permission from *Molecular Cancer*)

4 Notes

1. Use of human tissue in this research project was approved by the institutional review board. All the tissue samples were frozen at −80 °C in the storage system. Treatment of all the

breast cancer patients followed the National Comprehensive Cancer Network (http://www.nccn.org/) guidelines.

2. The AJCC/UICC TNM staging system was used for tumor classification. The recurrence data of breast cancer was not investigated in this example, but it is important clinical information for a retrospective analysis of recurrence-free survival of breast cancer patients.
3. Commands of sequence alignment are given directly to the head node computer. The head node computer automatically divides the alignment jobs and assigns them to its computing nodes that have sufficient computational resources to perform the jobs in the system.
4. The maximum number of allowed mismatches for a miRNA read is an important parameter in the setting of the Small RNA Analysis Tool. It will affect the final miRNA read counts after the alignment. If this number is set too high, more mismatches will be allowed in miRNA reads.
5. If a sequence read is mapped to multiple positions on the human genome, it is often difficult to determine the exact genomic location that this read was transcribed from. Thus ambiguous miRNA alignments were disregarded in this work in order to reduce the chances of false positive finding.
6. It is much easier to perform mathematical calculations of the miRNA expression reads with Microsoft Excel. A miRNA expression matrix (n-miRNAs vs. m-samples) is suggested to be constructed using Microsoft Excel at this step. miRNA IDs are shown on the first column of the matrix, and sample IDs are shown on the first row of the matrix. Each cell in the matrix contains the number of miRNA expression reads obtained from a particular tissue sample.
7. The miRNAs with extremely low reads in all samples were disregarded in this work as they were not significantly expressed in triple-negative breast cancer.
8. The Student's t-test was performed using Microsoft Excel command: TTEST(array1,array2,tails,type). array1: normalized miRNA expression data of a miRNA from triple-negative breast cancers; array2: normalized miRNA expression data of a miRNA from adjacent normal tissues; tails: 2; type: 3 - (two-sample unequal variance).
9. Understanding of the regulatory network of a miRNA and its associated biological function is an important research milestone following the deep sequencing data analysis of miRNA transcriptome. Experimentally validated target genes of the deregulated miRNAs identified in this work can be retrieved from TarBase [20] and miRecords [21] using the miRSystem

search engine [22]. Moreover, putative target candidates having complementary base-pairing matches in the 3′-UTR for the seed regions of these miRNAs also can be predicted using target prediction algorithms. The biological functions associated with the miRNA target genes can be investigated using the Ingenuity Pathway Analysis software (Ingenuity Systems, Redwood City, CA, USA).

10. The input file to the Genesis software is a tab-delimited text file. The miRNA expression data are shown in the form of a matrix (25-miRNAs vs. 38-samples). miRNA IDs are shown on the first column of the matrix, and sample IDs are shown on the first row of the matrix. The $\log_{10}$-scaled expression data of 25 miRNAs from 38 samples are presented in the body of the matrix.

Acknowledgment

This work was supported by the National Science Council (NSC97-2314-B-002-154-MY3), the Department of Health (DOH101-TDC-111-001), and the National Health Research Institutes (NHRI-EX105-10419BI) in Taiwan.

References

1. Ha M, Kim VN (2014) Regulation of microRNA biogenesis. Nat Rev Mol Cell Biol 15:509–524
2. Krol J, Loedige I, Filipowicz W (2010) The widespread regulation of microRNA biogenesis, function and decay. Nat Rev Genet 11:597–610
3. Ambros V (2004) The functions of animal microRNAs. Nature 431:350–355
4. Kloosterman WP, Plasterk RH (2006) The diverse functions of microRNAs in animal development and disease. Dev Cell 11:441–450
5. Gangaraju VK, Lin H (2009) MicroRNAs: key regulators of stem cells. Nat Rev Mol Cell Biol 10:116–125
6. Bentwich I (2005) A postulated role for microRNA in cellular differentiation. FASEB J 19:875–879
7. Croce CM (2009) Causes and consequences of microRNA dysregulation in cancer. Nat Rev Genet 10:704–714
8. Volinia S, Calin GA, Liu CG, Ambs S, Cimmino A, Petrocca F, Visone R, Iorio M, Roldo C, Ferracin M et al (2006) A microRNA expression signature of human solid tumors defines cancer gene targets. Proc Natl Acad Sci U S A 103:2257–2261
9. Shenouda SK, Alahari SK (2009) MicroRNA function in cancer: oncogene or a tumor suppressor? Cancer Metastasis Rev 28:369–378
10. Akao Y, Nakagawa Y, Hirata I, Iio A, Itoh T, Kojima K, Nakashima R, Kitade Y, Naoe T (2010) Role of anti-oncomirs miR-143 and -145 in human colorectal tumors. Cancer Gene Ther 17:398–408
11. Li D, Zhao Y, Liu C, Chen X, Qi Y, Jiang Y, Zou C, Zhang X, Liu S, Wang X et al (2011) Analysis of MiR-195 and MiR-497 expression, regulation and role in breast cancer. Clin Cancer Res 17:1722–1730
12. Guo ST, Jiang CC, Wang GP, Li YP, Wang CY, Guo XY, Yang RH, Feng Y, Wang FH, Tseng HY et al (2013) MicroRNA-497 targets insulin-like growth factor 1 receptor and has a tumour suppressive role in human colorectal cancer. Oncogene 32:1910–1920
13. Cheng CJ, Bahal R, Babar IA, Pincus Z, Barrera F, Liu C, Svoronos A, Braddock DT, Glazer PM, Engelman DM et al (2015) MicroRNA silencing for cancer therapy targeted to the tumour microenvironment. Nature 518:107–110

14. Mardis ER (2008) The impact of next-generation sequencing technology on genetics. Trends Genet 24:133–141
15. Morozova O, Marra MA (2008) Applications of next-generation sequencing technologies in functional genomics. Genomics 92:255–264
16. Davey JW, Hohenlohe PA, Etter PD, Boone JQ, Catchen JM, Blaxter ML (2011) Genome-wide genetic marker discovery and genotyping using next-generation sequencing. Nat Rev Genet 12:499–510
17. Teer JK (2014) An improved understanding of cancer genomics through massively parallel sequencing. Transl Cancer Res 3:243–259
18. Chang YY, Kuo WH, Hung JH, Lee CY, Lee YH, Chang YC, Lin WC, Shen CY, Huang CS, Hsieh FJ et al (2015) Deregulated microRNAs in triple-negative breast cancer revealed by deep sequencing. Mol Cancer 14:36
19. Schulte JH, Marschall T, Martin M, Rosenstiel P, Mestdagh P, Schlierf S, Thor T, Vandesompele J, Eggert A, Schreiber S et al (2010) Deep sequencing reveals differential expression of microRNAs in favorable versus unfavorable neuroblastoma. Nucleic Acids Res 38:5919–5928
20. Vergoulis T, Vlachos IS, Alexiou P, Georgakilas G, Maragkakis M, Reczko M, Gerangelos S, Koziris N, Dalamagas T, Hatzigeorgiou AG (2012) TarBase 6.0: capturing the exponential growth of miRNA targets with experimental support. Nucleic Acids Res 40:D222–D229
21. Xiao F, Zuo Z, Cai G, Kang S, Gao X (2009) Li T: miRecords: an integrated resource for microRNA-target interactions. Nucleic Acids Res 37:D105–D110
22. Lu TP, Lee CY, Tsai MH, Chiu YC, Hsiao CK, Lai LC, Chuang EY (2012) miRSystem: an integrated system for characterizing enriched functions and pathways of microRNA targets. PloS One 7:e42390

Chapter 9

Detection of Plasma MicroRNA Signature in Osteosarcoma Patients

Wendy Allen-Rhoades and Jason T. Yustein

Abstract

Circulating microRNAs are increasingly being used as noninvasive prognostic and predictive biomarkers for various types of cancer. We describe a method that uses real-time quantitative PCR (qPCR) for establishing a signature plasma microRNA profile that can distinguish patients with osteosarcoma from healthy control samples.

Key words Real-time quantitative PCR, MicroRNA, Plasma, Osteosarcoma, Biomarker

1 Introduction

Osteosarcoma is the primary bone tumor in children and young adults [1]. Currently, there are no reliable noninvasive biomarkers to detect and monitor for the presence of disease. MicroRNAs (miRNAs) can be detected in the plasma of all humans and there are specific patterns associated with disease and healthy states [2]. They are ideal candidates for biomarker development due to their stability in plasma and the unique expression patterns associated with diseases [2]. These plasma miRNAs can be detected with real-time quantitative PCR (qPCR) with relative ease and high sensitivity [3, 4]. Here, we describe miRNA expression profiling from whole blood or plasma utilizing qPCR technology in order to identify miRNAs that can be used as a biomarker for the presence of disease [5].

2 Materials

1. Blood or plasma samples from patients with osteosarcoma and healthy individuals.
2. K2 EDTA blood collection tubes.

Wei Wu (ed.), *MicroRNA and Cancer: Methods and Protocols*, Methods in Molecular Biology, vol. 1699,
DOI 10.1007/978-1-4939-7435-1_9,

3. Sterile centrifugal filter unit with pore size of 0.22 μm.
4. Vortex.
5. RNase-free tubes.
6. Chloroform.
7. Pipettes with sterile barrier tips (10 μl, 20 μl, 200 μl, and 1000 μl).
8. Ethanol: 100%.
9. Nuclease free water.
10. Thermal cycler.
11. Tabletop microcentrifuge with cooling, capable of 13,000 × *g* centrifugal force.
12. Swing bucket centrifuge for 96/384 well plates.
13. 96 or 384-well plate real-time qPCR cycler.
14. qPCR Software compatible with qPCR machine.
15. Qiagen miRNeasy kit.
16. Exiqon universal cDNA synthesis kit.
17. Exiqon spike-in kit (includes UniSp2, UniSp6, and MS2 carrier RNA).
18. Exiqon SYBR green master mix.
19. Exiqon microRNA qPCR panel (96-well optical plates or 384-well optical plates).

3 Methods

Carry out all the procedures at room temperature unless otherwise specified.

3.1 Blood and Plasma Preparation

1. Collect blood via venipuncture into a K2 EDTA tube (*see* **Note 1**). Cool centrifuge to 4 °C. Centrifuge blood at 1083 *g* × 30 min. Carefully remove the translucent plasma supernatant with a barrier tip pipette and avoid disturbing the buffy coat. Place plasma into an RNase-free microcentrifuge tube. Place the tube on ice if the sample will be used immediately, or store at −80 °C if the sample will be used at a later time.
2. Thaw frozen plasma samples by placing on ice. Pipette 250 μl of plasma into the top portion of a sterile 0.22 μm centrifugal filter unit. Centrifuge the sample at 12,000 × *g* for 4 min (*see* **Note 2**). Transfer 200 μl of filtered plasma to a new 1.5 ml microcentrifuge tube.

3.2 Prepare Spike-In Templates

3.2.1 RNA Spike-In

1. Use the Exiqon spike-in kit that contains UniSp2, UniSp4, and UniSp5. Spin down the vial before opening. Resuspend the spike-in mix by adding 80 µl of nuclease-free water to the vial. Leave for 20 min on ice to dissolve the RNA pellet. Vortex and spin down. Store in 10–20 µl aliquots at −20 °C to avoid excessive freeze-thaw cycles.

3.2.2 cDNA Synthesis Spike-In

1. Use the UniSp6 spike-in, which is found in the Exiqon universal cDNA synthesis kit. Spin down the vial before opening. Resuspend the UniSp6 spike-in by adding 80 µl of nuclease-free water to the vial. Leave for 20 min on ice to dissolve. Vortex and spin down. Store in aliquots at −20 °C.

3.3 RNA Extraction

1. Use Qiagen miRNeasy kit. Add 1000 µl of Qiazol lysis reagent to plasma and vortex. Immediately add 2 fmole of synthetic miRNA UniSp2 and 0.625 ng of MS2 carrier RNA (equals 1 µl of resuspended spike-in mixture) to sample and vortex (*see* **Note 3**). Incubate for 5 min. Add 200 µl of chloroform to the sample and vortex. Incubate for 2 min. Centrifuge the sample at 12,000 × *g* for 15 min at 4 °C. Warm centrifuge to room temperature (20–25 °C). Transfer the upper aqueous phase to a 2 ml tube. Add 900 µl of ethanol and mix by gently pipetting up and down. Transfer 750 µl to miRNeasy spin column. Spin for 30 seconds at 13,000 × *g* and discard flow-through. Remix the sample by pipetting and transfer the remaining sample to silica spin column in 750 µl aliquots until the entire sample is used. Add 700 µl of RWT buffer, spin for 1 min at 13,000 × *g* and discard flow-through. Add 500 µl of RPE buffer and spin for 1 min at 13,000 × *g*. Repeat this wash step for a total of three times and discard flow-through each time (*see* **Note 4**). Transfer miRNeasy column to a new, labeled collection tube and leave column open for 1 min. Carefully add 50 µl nuclease-free water to the center of the membrane. Incubate for 1 min. Spin for 2 min at 13,000 × *g*. Remove spin column, tightly close collection tubes, and store RNA at −80°C.

3.4 cDNA Synthesis

1. Use the Exiqon cDNA synthesis kit. Gently thaw reaction buffer and nuclease-free water and place on ice. Immediately prior to use, remove enzyme mix from the freezer. Mix all reagents by gently flicking the tubes and spin down prior to use. Set up the reverse transcription reaction in nuclease-free tubes in the following proportions (*see* **Note 5**): For a 20 µl reaction, add 4 µl of reaction buffer, 9 µl of nuclease-free water, 2 µl of enzyme mix, 1 µl of UniSp6 synthetic spike-in, and 4 µl of RNA (*see* **Note 6**). Mix the reaction by pipetting and spin down. Place the tube in a thermal cycler. Incubate for 60 min at 42 °C, heat inactivate the reverse transcriptase for 5 min at 95 °C. Immediately cool to 4 °C and store at −20 °C.

3.5 qPCR

1. (*see* **Note 7**) Remove the ready-to-use PCR plate from the freezer. Spin the plate at 2500 rpm × 1 min. For the 96-well optical plates, dilute the cDNA 20-fold in nuclease-free water and combine in an equal volume of 2× SYBR green master mix. Add 10 ul to each well. Seal the plate with optical sealing film, cover from light, and let it sit on ice for 5 min to completely dissolve the lyophilized primers that are pre-fabricated onto the plate. Centrifuge the plate in a swing bucket rotor at 370 *g* × 1 min. Place the plate in a qPCR cycler and run program with the following settings:

Process step	Settings, LC480 instrument	Settings, other instruments
Polymerase activation/ denaturation	95 °C, 10 min	95 °C, 10 min
Amplification	45 amplification cycles at 95 °C for 10 s, 60 °C for 1 min with a ramp-rate 1.6 °C/s	40 amplification cycles at 95 °C for 10 s, 60 °C for 1 min with a ramp-rate 1.6 °C/s (*see* **Note 8**)
Melt curve analysis	Yes	Yes

3.6 Data Analysis

1. Use provided software with qPCR instrument to export and analyze data (*see* **Note 9**).

4 Notes

1. Blood collection must be in tubes that do not contain heparin, as heparin is a strong inhibitor of qPCR reactions and will affect downstream analysis. Carefully collect blood on first attempt to avoid hemolysis.
2. Do not add the synthetic spike-in directly to the plasma sample, as components within the plasma will degrade the spike-in. Mix the lysis buffer and sample together, then add the synthetic spike-in.
3. The filter may clog if there is serum coagulate in the plasma sample. In this case, if visible, carefully remove the gel-like coagulate and discard. If nothing is visible, carefully pipette remaining plasma from the top of the filter unit into a new filter unit and centrifuge as above. Repeat as necessary until you have at least 200 μl of plasma to process.
4. On the third wash, spin the column for 2 min to completely remove any flow-through that may have gotten stuck between

the collection tube and the spin column. After this longer spin, be sure that the outside of the column is dry prior to transferring to a new collection tube. This will avoid contamination of the final eluate with ethanol.

5. For a profiling experiment, upscale the reaction as appropriate for the number of reactions that are in your desired panel. For example, if using the miRNome platform (752 miRNAs tested), the cDNA reaction must be scaled up to 72 μl of master mix (buffer, water, enzyme mix, spike-in) combined with 8 μl of RNA in order to have enough cDNA for downstream analysis with qPCR.
6. Carrier RNA is utilized to reduce the loss of small RNA molecules, but this application makes the quantification of isolated RNA inaccurate. Therefore, steady volume input is used for cDNA synthesis rather than RNA quantity. Likewise, it is impossible to assess the quality of the RNA isolated by standard methods.
7. There are several panels that Exiqon has available that work well for profiling of miRNAs in plasma. The entire miRNome panel interrogates 752 miRNAs and is only available for 384-well optical plates. Alternatively, there are more focused panels that can be run on 96-well optical plates. This protocol describes the use of the 96-well plates. Choose the panel that best suits your experimental needs and laboratory capability and adjust volumes accordingly. The settings and cycle times are identical regardless of plate size used.
8. The ramp-rate of 1.6 °C/s is equivalent to 100% under standard cycling conditions on the ABI instruments.
9. Do not use automatic baseline and threshold detection settings for ABI qPCR instruments; use manual settings.

Acknowledgments

This work was funded through the generous support of a St. Baldrick's Foundation Fellowship, the Amschwand Sarcoma Cancer Foundation's Dr. Stephan Fadem Fellowship, and a Conquer Cancer Foundation of ASCO Young Investigator Award, supported by WWWW Foundation (Quad W). Research is also supported by the Chair's Grant U10 CA98543 and Human Specimen Banking Grant U24 CA114766 of the Children's Oncology Group from the National Cancer Institute, National Institutes of Health, Bethesda, MD, USA. Additional support for research is provided by a grant from the WWWW (QuadW) Foundation, Inc. (www.QuadW.org) to the Children's Oncology Group. Any opinions, findings, and conclusions expressed in this material are those of

the authors and do not necessarily reflect those of the American Society of Clinical Oncology®, the Conquer Cancer Foundation, or the WWWW Foundation (Quad W).

References

1. Mirabello L, Troisi RJ, Savage SA (2009) Osteosarcoma incidence and survival rates from 1973 to 2004: data from the surveillance, epidemiology, and end results program. Cancer 115 (7):1531–1543
2. Calin GA, Croce CM (2006) MicroRNA signatures in human cancers. Nat Rev Cancer 6 (11):857–866
3. Cortez MA, Ivan C, Zhou P, Wu X, Ivan M, Calin GA (2010) microRNAs in cancer: from bench to bedside. Adv Cancer Res 108:113–157
4. Cortez MA, Bueso-Ramos C, Ferdin J, Lopez-Berestein G, Sood AK, Calin GA (2011 Aug) MicroRNAs in body fluids—the mix of hormones and biomarkers. Nat Rev Clin Oncol 8 (8):467–477
5. Allen-Rhoades W, Kurenbekova L, Satterfield L, Parikh N, Fuja D, Shuck RL, Rainusso N, Trucco M, Barkauskas DA, Jo E, Ahern C, Hilsenbeck S, Donehower LA, Yustein JT (2015) Cross-species identification of a plasma microRNA signature for detection, therapeutic monitoring, and prognosis in osteosarcoma. Cancer Med 4(7):977–988

Chapter 10

Identification of E6/E7-Dependent MicroRNAs in HPV-Positive Cancer Cells

Anja Honegger, Daniela Schilling, Holger Sültmann, Karin Hoppe-Seyler, and Felix Hoppe-Seyler

Abstract

Oncogenic types of human papillomaviruses (HPVs) are closely linked to the development of anogenital and head and neck cancers. The expression of the viral *E6* and *E7* genes is crucial for the transforming activities of HPVs. There is accumulating evidence that the HPV *E6/E7* oncogenes can profoundly affect the cellular microRNA (miRNA) composition. Since alterations of miRNA expression levels can contribute to cancer development and maintenance, it will be important to understand in depth the crosstalk between the HPV oncogenes and the cellular miRNA network. Here, we describe a method to identify E6/E7-dependent intracellular miRNAs by small RNA deep sequencing, upon silencing of endogenous *E6/E7* expression in HPV-positive cancer cells in vitro. In addition, we provide a protocol to identify E6/E7-dependent miRNA alterations in exosomes that are secreted by HPV-positive cancer cells in vitro.

Key words Human papillomavirus, Tumor virus, Cervical cancer, microRNA, Microvesicles, Exosomes

1 Introduction

Oncogenic types of human papillomaviruses (HPVs) are major human carcinogens. It is estimated that approximately 5% of the total human cancer incidence is closely linked to HPV infections [1]. Most HPV-associated cancers are located in the anogenital region and oropharynx. Best characterized is the causative role of HPVs for the development of cervical cancer, a disease that alone accounts for over 500.000 new cancer cases and over 250.000 cancer deaths per year worldwide [2].

Over 99% of cervical cancers contain the DNA of oncogenic HPV types, most often HPV16 and HPV18, which account for approximately 50% and 15% of cervical cancer cases, respectively. The oncogenicity of HPVs is closely linked to expression of the viral *E6* and *E7* oncogenes [3]. Their gene products inactivate critical tumor suppressor proteins. For example, E6 induces the proteolytic

Wei Wu (ed.), *MicroRNA and Cancer: Methods and Protocols*, Methods in Molecular Biology, vol. 1699,
DOI 10.1007/978-1-4939-7435-1_10,

degradation of p53 whereas E7 interferes with the function of the retinoblastoma protein, pRb [4].

The sustained expression of both E6 and E7 is considered to be essential for the maintenance of the malignant phenotype of HPV-positive cancer cells by inhibiting major tumor suppressive responses of the cell, such as induction of apoptosis and senescence [4, 5]. The exploration of the molecular mechanisms by which the *E6/E7* oncogenes maintain the malignant growth of HPV-positive cancers should thus not only be important for our understanding of viral transformation mechanisms but also could provide novel opportunities for therapeutic interference.

In recent years, microRNAs (miRNAs) have emerged as important new players in the carcinogenic process. Analyzing their functional contribution to cancer formation and maintenance is expected to yield new insights into the mechanisms of human carcinogenesis, to enable the development of novel therapeutic strategies and to provide novel diagnostic possibilities [6, 7].

Oncogenic HPVs probably do not express own miRNAs [8]. However, miRNA alterations have been found in cervical cancers, raising the question whether the viral E6/E7 oncogenes may contribute to the deregulation of the cellular miRNA network. Accordingly, many studies have analyzed possible effects of the *E6/E7* oncogenes on cellular miRNA expression levels. In these investigations, several different strategies have been employed, which in most cases involved the ectopic expression of the viral *E6/E7* oncogenes in various cell culture models, including primary human keratinocytes, HPV-negative cell lines, or organotypic raft cultures. Notably, a meta-analysis of over 250 papers identified by medline search for the keywords "miRNA/microRNA" and "HPV/cervical cancer" revealed only a very limited overlap of candidate miRNAs that may be involved in HPV-linked carcinogenesis [9]. It seems likely that these discrepant results are due to variations in the experimental setup, which could include the different nature of cellular models employed or the different intracellular amounts of E6 and E7 proteins resulting from ectopic expression.

In view of the latter considerations, the analysis of the interaction between the HPV oncogenes and the cellular miRNA network in HPV-positive cancer cell lines should have certain conceptional advantages. *First*, HPV-induced transformation of cervical epithelial cells to malignancy is a very rare process and requires the acquisition of additional cellular alterations, besides viral oncogene expression [3]. In contrast to primary keratinocytes, cell lines established from cervical cancers must have acquired these alterations during the carcinogenic process and thus allow miRNA analyses in the intracellular milieu of an HPV-transformed cell. *Second*, expression of the *E6/E7* oncogenes in cervical cancer cells often occurs from chromosomally integrated viral DNA sequences and is tightly controlled by cellular factors that regulate the HPV E6/E7

transcriptional promoter [10]. It remains unclear how this condition relates to the E6/E7 protein levels that are obtained upon ectopic *E6/E7* expression in heterologous cell models. Thus, it should be informative to investigate the E6/E7 dependence of cellular miRNAs upon modulating endogenous E6/E7 expression levels, in the cellular background of HPV-positive cancer cells (for further discussion of this issue, please refer to [9]).

Notably, miRNAs not only play an important role in the regulation of intracellular processes but may also be involved in cell to cell communication. Specifically, exosomes—which are small extravesicular particles mediating intercellular crosstalk [11]—have been found to contain miRNAs [12]. There is accumulating experimental evidence that these miRNAs can be transferred via exosomes from donor cells into recipient cells where they can affect expression of target genes [13]. The analysis of exosomal miRNAs that are secreted by cervical cancer cells therefore could provide insights into how the viral *E6/E7* genes affect intercellular communication. Moreover, the miRNA content of exosomes could be of diagnostic value, since these vesicles are secreted into various body fluids, including blood, sputum, and cervical secretions [14].

In the following, we describe methods (1) to potently block endogenous *E6/E7* expression in cervical cancer cells by RNA interference, (2) to isolate and analyze by small RNA deep sequencing E6/E7-dependent intracellular miRNAs, (3) to isolate and analyze by small RNA deep sequencing E6/E7-dependent miRNAs from exosome-enriched microvesicles that are secreted by cervical cancer cells, and (4) to verify deep sequencing results by qRT-PCR.

2 Materials

All non-standard materials and equipment are itemized in this section. In case a manufacturer's protocol is followed and the therein recommended materials are utilized, these are not further specified here.

2.1 Inhibition of Endogenous E6/E7 Expression in HPV-Positive Cancer Cells

2.1.1 Cell Culture and Transfections

1. HPV18-positive HeLa cancer cells (tumor bank of the German Cancer Research Center).
2. Cell culture medium: DMEM (Gibco, Life Technologies) containing 5% fetal bovine serum (Gibco, Life Technologies), 2 mM L-glutamine, 100 U/ml penicillin, 100 µg/ml streptomycin (Sigma-Aldrich).
3. Synthetic siRNAs (Silencer Select®, Ambion, Life Technologies). The respective target sequences in the HPV18 E6/E7 transcripts are as follows: HPV18 *E6/E7*-1 5′-CCACAACGUCACA CAAUGU-3′; HPV18 *E6/E7*-2 5′-CAGAGAAACACAA

GUAUAA-3′; HPV18 *E6/E7*-3 5′-UCCAGCAGCUGUUU-CUGAA-3′. Control siRNA "siContr-1" has the following sequence: sense strand: 5′-CAGUCGCGUUUGCGACUGGtt-3′; antisense strand: 5′-CCAGUCGCAAACGCGACUGtt-3′.

4. DharmaFECT I (Thermo Fisher Scientific).

2.1.2 Immunoblotting for the Verification of E6/E7 *Downregulation*

1. RIPA buffer (10 mM Tris (pH 7.5), 150 mM NaCl, 1 mM EDTA, 1% Nonidet P40, 0.5% Na-Deoxycholat, 0.1% SDS, supplemented with 25 μl/ml Pefabloc (Merck) and 10 μl/ml of Protease Inhibitor Cocktail (Sigma-Aldrich)).
2. Bio-Rad Protein Assay (Bio-Rad).
3. SDS sample buffer (for reducing conditions: 8% SDS, 250 mM Tris–HCl (pH 6.8), 20% β-mercaptoethanol, 40% glycerol, 0.008% bromphenol blue; for nonreducing conditions without β-mercaptoethanol).
4. NuPAGE Novex 4–12% Bis-Tris Mini Gels (Life Technologies).
5. Immobilon-P membrane (Millipore).
6. Trans-Blot Semi-Dry Transfer Cell) (Bio-Rad).
7. Skim milk powder (Saliter).
8. PBS (phosphate-buffered saline: 137 mM NaCl, 2.7 mM KCl, 4.3 mM Na_2HPO_4, 1.4 mM KH_2PO_4, pH 7.4).
9. PBS-T (PBS supplemented with 0.1% Tween-20).
10. ECL™ Prime Western Blotting Detection Reagent (GE Healthcare).
11. The following primary antibodies are used to monitor E6/E7 downregulation:
mouse anti-α-Tubulin (Merck), CP06, dilution 1:5000 (loading control); chicken anti-HPV18 E7 (E7C) [9]; mouse anti-HPV18 E6 (Arbor Vita Corporation Sunnyvale) AVC #399; mouse anti-p53 (BD Pharmingen), #554293, 1:500; mouse anti-pRb (Cell Signaling), #9309, 1:1000; rabbit anti-phospho (Ser807/811)-pRb (Cell Signaling), #9308, 1:1000; rabbit anti-CyclinA1 (Santa Cruz Biotechnology), 1:2000. The following HRP-conjugated secondary antibodies are applied: anti-mouse IgG (Promega), W4021, 1:5000; anti-chicken IgY (Promega), G1351, 1:2500; and anti-rabbit IgG (Promega), W4011, 1:3000.

2.2 Generation, Purification, and Characterization of Exosomes

2.2.1 Generation and Purification of Exosomes

1. Open-top ultracentrifugation tubes, polyclear (Seton Scientific).
2. Qubit Protein Assay (Life Technologies).
3. Optional: Whatman ZapCap-S Bottle-top Filter (200 nm pore size, Maine Manufacturing).

2.2.2 Characterization of Exosomes by Immunoblotting

Immunoblotting of exosomal samples is essentially performed with the materials described in Subheading 2.1.2 for cellular extracts.

1. The following primary antibodies are used as "exosomal markers" (*see* Subheading 3.2.2): mouse anti-β-Actin (Sigma-Aldrich), A2228, 1:10,000; mouse anti-Annexin 1 (BD Transduction), #610066, 1:10,000; mouse anti-CD63 (Santa Cruz Biotechnology), sc-5275, 1:400 under nonreducing conditions; mouse anti-CD9 (BD Pharmingen), #555370, 1:200 under nonreducing conditions; rat anti-Hsc70 (Stressgen), ADI-SPA-815, 1:1000.
2. The following primary antibodies are used as "negative markers for extracellular vesicles" (*see* Subheading 3.2.2): mouse anti-GRP78 (BD Transduction), #610979, 1:1000; mouse anti-EEA1 (BD Transduction Laboratories), #E41120, 1:2000.
3. The following HRP-conjugated secondary antibodies are applied: anti-mouse IgG (Promega), W4021, 1:5000; anti-rat IgG (Dianova), #112035003, 1:5000.

2.3 Small RNA Deep Sequencing and Data Analysis

2.3.1 Small RNA Extraction, Quantification, and Quality Determination

1. miRNeasy Mini Kit (Qiagen).
2. RNAse A (Roche).
3. Glycogen from *Mytilus edulis* (Sigma).
4. RNA 6000 Pico Kit (Agilent Technologies).
5. Small RNA Kit (Agilent Technologies).

2.3.2 Small RNA Deep Sequencing and Analysis

1. RNeasy MinElute Cleanup Kit (Qiagen).
2. NEBNext® Multiplex Small RNA Library Prep Set for Illumina (New England Biolabs (NEB): All materials not included in the set were purchased as recommended by the manufacturer.
3. NEBNext® Multiplex Oligos for Illumina®, Index Primers Set (NEB).
4. SuperScript® III Reverse Transcriptase (Life Technologies).
5. 6% TBE polyacrylamide gel (Life Technologies).
6. Filter tube (5 μm, IST Engineering).
7. High Sensitivity DNA Kit (Agilent Technologies).

2.3.3 miRNA qRT-PCR

1. miScript II Reverse Transcription Kit (Qiagen).
2. miScript SYBR Green PCR Kit (Qiagen).
3. Hs_RNU6-2_1 miScript Primer Assay (Qiagen): primer to detect RNU6-2 as endogenous normalization control (only cellular samples).
4. Individual miScript Primer Assays (Qiagen): depend on miRNAs of interest.

2.4 Equipment

1. Fusion SL Gel Detection System (Vilber Lourmat).
2. Sorvall WX Ultra80 ultracentrifuge) (Thermo Fisher Scientific).
3. SW28 rotor (Beckman Coulter).
4. NanoDrop® ND-1000 (NanoDrop Instruments).
5. Agilent 2100 Bioanalyzer (Agilent Technologies).
6. 7300 Real-Time PCR System Detector (Applied Biosystems).
7. HiSeq 2000 instrument (Illumina).

2.5 Software

1. BioID image analysis software (Vilber Lourmat).
2. 2100 Bioanalyzer Expert Software B.02.08. (Agilent).
3. miRDeep2 package ([15], Max Delbrück Center, Berlin, Germany).
4. miRBase v.18.0 (www.mirbase.org; [16–19]).
5. 7300 System SDS Software (Applied Biosystems).
6. Sigma Plot software (Systat Software Inc.).

3 Methods

3.1 Inhibition of Endogenous E6/E7 Expression in HPV-Positive Cancer Cells

3.1.1 Silencing of Endogenous E6/E7 Expression by RNA Interference (RNAi)

In order to investigate the influence of the HPV oncogenes on the intracellular miRNA composition of HPV-positive cancer cells and exosomes secreted thereof, endogenous HPV18 *E6/E7* expression in HeLa cervical carcinoma cells is blocked by RNAi. For this purpose, three different siRNAs, which each target all three HPV *E6/E7* transcript classes in HeLa cells [20], are employed. The three siRNAs are pooled at equimolar concentrations (referred to "si18E6/E7" in the text) to minimize potential off-target effects [21, 22]. "siContr-1," containing at least four mismatches to all known human genes, is used as control siRNA.

1. HPV18-positive HeLa cells are plated on 15 cm dishes to reach 80% confluence 72 h post transfection (*see* **Note 1**).
2. 24 h post plating, synthetic siRNAs are transfected with DharmaFECT I, according to the manufacturer's instructions, to reach a final siRNA concentration of 10 nM (*see* **Note 2**).

3. 48 h post plating, the cells are washed with DMEM and cultured for another 24 h in "vesicle-depleted medium" (*see* **Notes 3** and **4**).
4. 72 h post plating (48 h after transfection), the conditioned (exosome-containing) medium is harvested and proceeded as described in Subheading 3.2.1. The corresponding exosome-producing cells are harvested and pelleted by centrifugation at 800 × *g* for 3 min, resuspended and washed in 800 µl PBS, and re-pelleted.
5. Cell pellets are stored at −80 °C until further analysis.

3.1.2 *Immunoblotting for the Verification of* E6/E7 *Downregulation*

E6/E7 downregulation is monitored by detecting HPV18 E6 and E7 protein levels, 48 h after transfection with si18E6/E7 or siContr-1, respectively (*see* **Note 5**). Furthermore, functionality of the *E6/E7* knockdown can be checked by probing for the following proteins: p53 and p21 (*E6* silencing leads to increased p53 protein levels, due to the ability of E6 to induce the degradation of p53 [23] and consequently increased p21 protein levels, representing a downstream transcriptional target gene for p53 [24]), pRb (*E7* silencing is associated with an increase in total pRb protein levels, due to the ability of E7 to induce pRb degradation [25]), phosphorylated pRB and Cyclin A1 (*E7* silencing decreases the amounts of phosphorylated pRb and of Cyclin A1, indicating reactivation of the pRb cascade).

1. Cell pellets are lysed in RIPA buffer for 30 min on ice and proteins are collected in the supernatant upon centrifugation at 12,000 × *g* for 15 min at 4 °C.
2. Protein concentrations are determined using the Bio-Rad Protein Assay, employing bovine serum albumin as a standard.
3. For Western blot analysis, protein extracts are boiled in SDS sample buffer for 5 min at 95 °C and subsequently separated on NuPAGE Novex 4–12% Bis–Tris Mini Gels.
4. Proteins are electrotransferred onto an Immobilon-P membrane using the Trans-Blot Semi-Dry Transfer Cell.
5. Membranes are blocked with 5% skim milk powder in PBS-T for 1 h at room temperature.
6. Membranes are then probed with primary antibodies overnight at 4 °C in PBS-T, followed by incubation with the respective HRP-conjugated secondary antibody in PBS-T for 1 h at room temperature.
7. Proteins are visualized using the ECL™ Prime Western Blotting Detection Reagent. Images are acquired using the Fusion SL Gel Detection System, band densities are determined by BioID image analysis software.

3.2 Generation, Purification, and Characterization of Exosomes

To investigate the influence of viral *E6/E7* expression on the exosomal miRNA contents, exosomes secreted by HeLa cells are isolated from the cell culture medium by employing a protocol for exosome enrichment (*see* **Note 6**) involving sequential (ultra-) centrifugation steps [26], with minor modifications. A purification scheme is presented in Fig. 1.

3.2.1 Generation and Purification of Exosomes

1. For the generation of exosomes, cells are plated, transfected, and cultivated as described in Subheading 3.1.1.
2. 48 h post transfection, the conditioned medium is collected and cleared from intact cells and cellular debris by three rounds of centrifugation at 300 × *g*, 3000 × *g*, and 10,000 × *g* for 20 min. All the centrifugation steps are performed at 4 °C (*see* **Note 7**).
3. Subsequently, exosomes are pelleted from the resulting supernatant by ultracentrifugation at 100,000 × *g* for 70 min using a SW28 rotor, resuspended in 36 ml PBS to wash, and re-centrifuged at 100,000 × *g* for 70 min (*see* **Note 8**). All the centrifugation steps are performed at 4 °C.
4. The final pellet (enriched for exosomes) is resuspended in 100 μl PBS and an aliquot is analyzed by electron microscopy (for details *see* ref. 27).
5. For each exosome preparation, the total protein concentration is quantified using the Qubit Protein Assay. This allows a relative estimation of exosome yields for immunoblotting (assuming that the exosomal protein concentration relates to the amount of harvested exosomes).
6. Optional: additional filtration step (*see* **Note 9**).

3.2.2 Characterization of Exosomes by Immunoblotting

Initial characterization of exosome preparations is performed by immunoblotting. HeLa cell-derived exosome preparations stain positive for the exosomal markers HSC70, CD63, Annexin-1, β-Actin, and CD9 [9, 27], showing the typical exosomal enrichment for the tetraspanins CD63 and CD9 [26]. The absence of detectable signals for the endoplasmatic reticulum (ER) marker GRP78 and the early endosome marker EEA1 indicate only minor, or no, contamination with vesicles from other origins.

In principle, immunoblotting of exosomal samples is performed as described for cellular extracts in Subheading 3.1.2. However, exosome samples are directly boiled in SDS sample buffer (*see* **Note 10**) as described in Subheading 3.1.2, without prior protein extraction.

3.3 Small RNA Deep Sequencing and Data Analysis

In order to capture a broad spectrum of *E6/E7*-modulated miRNAs—unbiased by a pre-selection—analyses of total miRNA contents are accomplished by small RNA deep sequencing in a

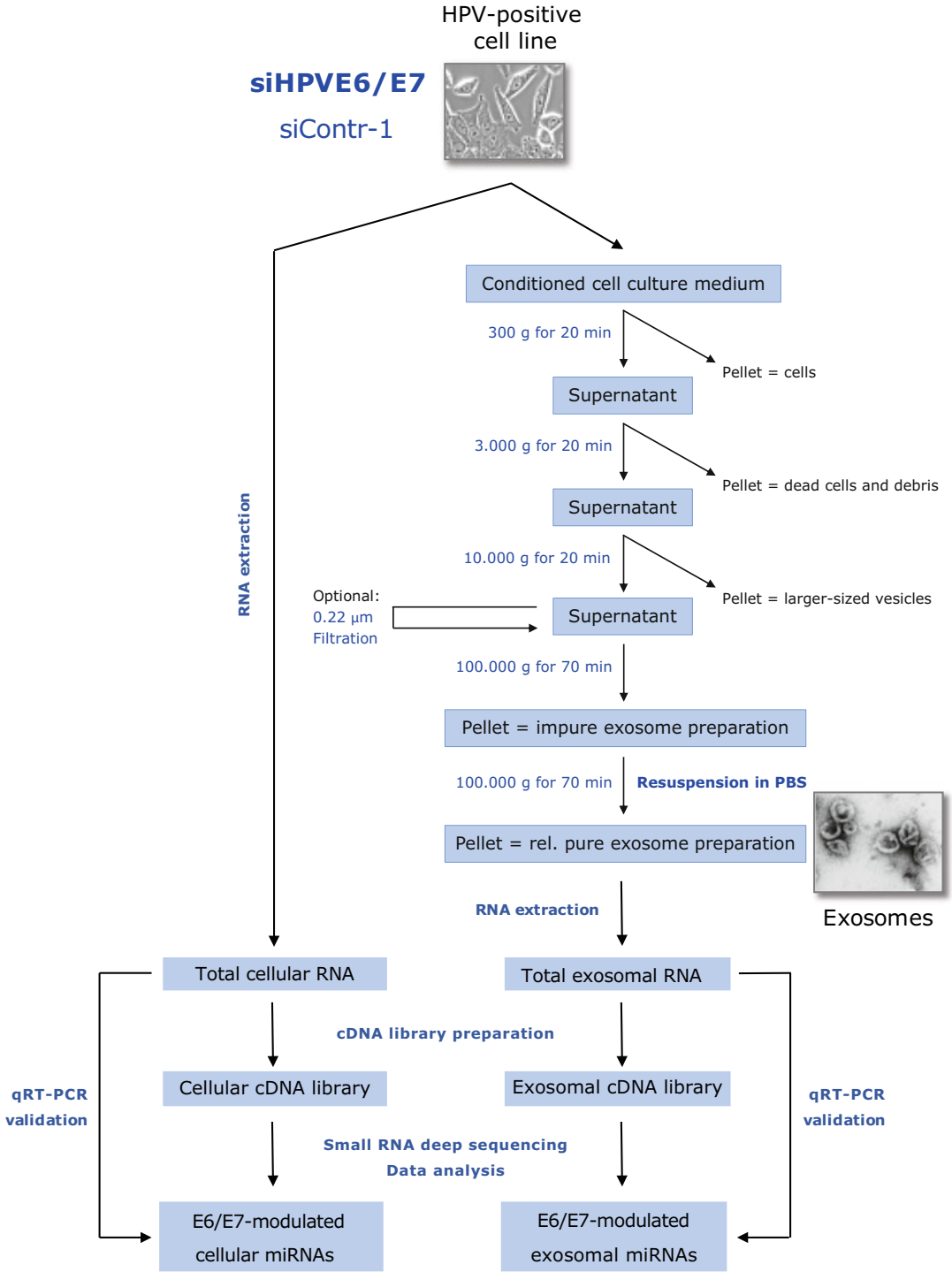

Fig. 1 Experimental strategy for the determination of HPV *E6/E7*-dependent cellular and exosomal miRNAs in cervical cancer cells

multiplex approach (*see* Subheading 3.3.2). Thus, RNA is extracted from HeLa cells in which endogenous *E6/E7* expression is silenced and from control-treated HeLa cells, as well from purified exosomes secreted thereof (*see* Subheading 3.3.1). After deep sequencing analyses, the regulation of the identified intracellular and exosomal *E6/E7*-modulated miRNAs is further validated by qRT-PCR (*see* Subheading 3.3.3).

3.3.1 Small RNA Extraction, Quantification, and Quality Determination

1. Total cellular RNA, including miRNA, is isolated with the miRNeasy Mini Kit following the manufacturer's protocol. All the optional washing steps are included and RNA is eluted in a final volume of 30 µl RNase-free water.

   Total exosomal RNA, containing the small RNA fraction, is extracted from one entire exosome preparation of 100 µl. The extraction of total exosomal RNA is performed using the protocol used for cells, but with the following slight modifications:

   (a) Exosome samples are pretreated with 100 ng/µl RNAse A for 30 min at 37 °C, immediately before extracting RNA.

   (b) Prior to the addition of chloroform and phase separation, 12 µg glycogen from *Mytilus edulis* are added to the sample.
2. RNA concentrations are measured with the NanoDrop® ND-1000 at 260 nm.
3. RNA quality is assessed with the Agilent 2100 Bioanalyzer using the RNA 6000 Pico Kit (total RNA) and the Small RNA Kit (small RNA). The 2100 Bioanalyzer Expert Software B.02.08. is applied to generate electropherograms (*see* **Note 11**).
4. RNA samples are stored at −80 °C until further analysis.

3.3.2 Small RNA Deep Sequencing and Analysis

Due to their low RNA yield, exosomal RNA samples (eluted in a final volume of 30 µl RNase-free water as described in Subheading 3.3.1) are further concentrated to a volume of 6 µl using the RNeasy MinElute Cleanup Kit. The entire volume of the 6 µl concentrated exosomal total RNA is used as input for the cDNA library preparations (*see* **Note 12**). For cells, 1 µg total RNA in a volume of 6 µl is applied.

Small RNA libraries are prepared using the NEBNext® Multiplex Small RNA Library Prep Set for Illumina with custom multiplex adaptors and primers (NEBNext® Multiplex Oligos for Illumina®, Index Primers Set 1). The manufacturer's guidelines are followed with a few modifications. In brief:

1. Multiplex 3′ Adaptor is ligated to the RNA at 25 °C for 1 h.
2. After hybridization of the Multiplex RT Primer, the Multiplex 5′ Adaptor is ligated to the RNA.

3. Afterward, reverse transcription is performed using the SuperScript® III Reverse Transcriptase.
4. The cDNA product is then amplified by PCR using an optimized cycling protocol: initial denaturation for 3 min at 94 °C, 13 cycles of denaturation for 80 s at 94 °C, annealing for 30 s at 62 °C, extension for 15 s at 70 °C, and final extension for 5 min at 70 °C.
5. Unique NEBNext® Index Primers are applied for each of the replicate samples per treatment (*see* **Note 13**).
6. Next, amplicons corresponding to adapter-ligated constructs from 21 to 30 nt RNA fragments are purified on a 6% TBE polyacrylamide gel and eluted at room temperature for 3 h.
7. The gel slurry is passed through a 5 μm filter tube and precipitated overnight at −80 °C.
8. The size, DNA concentration, and quality of each final small RNA library are determined twice using the High Sensitivity DNA Kit with the BioAnalyzer 2100. The concentration of each sample is then adjusted to 10 nM and equal volumes of barcode-labeled samples are pooled for multiplexed sequencing in one lane.
9. Sequencing (50 bp, single read) is performed on an Illumina HiSeq 2000 instrument.
10. For analyses, raw sequencing reads are pre-processed and mapped using the function mapper.pl of the miRDeep2 package as described [28]. Briefly, low-quality reads are filtered out, the adaptor sequence is clipped, and reads shorter than 18 nt are discarded. Accepted reads are mapped to known human miRNAs based on miRBase v.18.0 using the function quantifier.pl in miRDeep2. Since one mismatch is allowed during the mapping procedure, the raw read file of each miRNA that is further analyzed in detail is then manually checked to assure that the reads truly annotate to the respective miRNA. The obtained raw read counts of each sample are then normalized by dividing with the total number of reads mapping to known human microRNAs for each sample. Values are expressed as reads per million (RPM, *see* **Note 14**). Fold changes (FCs) are obtained by dividing the RPM of the si18E6/E7 treatment by the respective value of the siContr-1 treatment.

3.3.3 miRNA qRT-PCR

The *E6/E7*-mediated modulation of cellular and exosomal miRNAs is subsequently validated by qRT-PCR analyses (*see* **Note 15**). miRNA expression is detected using the miScript PCR System with miRNA specific primers according to the manufacturer's instructions.

1. For the detection of intracellular miRNA expression, 1 μg cellular RNA is converted to cDNA using the miScript II Reverse Transcription Kit in a reaction volume of 20 μl using 5× miScript HiFlex Buffer. Due to the low yield of exosomal RNA and consequently the lack of accurate RNA quantification, identical volumes of exosomal RNA (12 μl) are used for the cDNA synthesis to detect exosomal miRNA levels. An RT-control (addition of H_2O instead of reverse transcriptase) is prepared for each experiment.
2. qRT-PCR reactions are performed with the miScript SYBR Green PCR Kit on a 7300 Real-Time PCR System Detector using Qiagen's recommended cycling conditions. Two μl of a 1:100 dilution of the original cDNA are used for each reaction and samples are run in triplicate for each experiment. To monitor contamination of the reagents, a "no template control" (NTC) is included for each primer pair.
3. Data are analyzed using the comparative Ct ($2^{-\Delta\Delta Ct}$) method [29] with the small nuclear RNA *RNU6-2* as endogenous control for cellular samples and respective control-treated samples as reference (*see* **Note 16**). Normalization of exosomal samples is conducted against an average of the expression of miR-452-5p and miR-183-5p (*see* **Note 17**).
4. Statistical significance of the data is evaluated by the paired Student's t-test using the Sigma Plot software.

4 Notes

1. In order to obtain sufficient exosomes for subsequent deep sequencing analysis of their miRNA content, a large-scale experimental setup needs to be chosen. For each replicate and treatment condition, we plate HeLa cells into 20 cell culture dishes (15 cm diameter) to reach 80% confluency 72 h post plating (corresponding to roughly 1.5×10^6 plated cells per dish [9]). This requires large-scale pre-cultivation of the cells, days prior to the experiment. As a consequence, all the subsequent steps need to be scaled up, respectively.
2. Due to the large scale of the experiment (*see* **Note 1**), the transfection was optimized for a total transfection end-volume of 8 ml per 15 cm cell culture dish. This volume reduces the required amount of transfection medium to stay cost-effective (instead of using 20 ml medium for a 15 cm dish) and ensures just complete coverage of the cells with medium.
3. "Vesicle-depleted medium" is complete medium depleted of FBS-derived microvesicles by overnight centrifugation at 100,000 g and subsequent sterile filtration through a

0.22 μm filter. We recommend preparing enough "vesicle-depleted medium" containing 20% FBS in advance, storing it at −20 °C and diluting it with 0% FBS-containing culture medium to the ready-to-use 5% FBS-containing "vesicle-depleted medium," prior to usage (essentially, as described in [26]).

4. We usually generate and harvest just enough conditioned medium of one treatment/replicate to fill all six ultracentrifugation tubes (40 ml each) of one SW28 rotor (in the end corresponding to one exosome preparation). For this, each of the 20 cell culture dishes is covered with 12 ml "vesicle-depleted medium" to obtain a total of approximately 240 ml conditioned medium 24 h later.
5. Besides detecting HPV E6 and E7 protein levels by immunoblotting, efficient inhibition of *E6/E7* expression should furthermore be verified by detecting *E6/E7* mRNA levels by qRT-PCR (for details *see* [9]).
6. It should be noted that commonly used methods for exosome isolation, such as differential centrifugations with or without filtration steps (as used here), can only result in exosome-enriched microvesicle preparations, but not in preparations that are 100% pure for exosomes [11, 26]. For an extensive discussion of the strengths and limitations of sample collection methods and the analyses of microvesicles, please refer to a position paper of the International Society for Extracellular Vesicles [30].
7. The centrifugation steps of the conditioned medium at 300 × *g* and 3000 × *g* are performed in a standard refrigerated centrifuge using 50 ml tubes. The supernatant is poured into a fresh glass bottle after each centrifugation step. For the 10,000 × *g* ultracentrifugation step, the 40 ml-fitting ultracentrifugation tubes are filled with 38 ml precleared conditioned medium to avoid spilling.
8. To avoid loosening of the pellet comprised of cellular debris at the bottom of the ultracentrifugation tube, we recommend carefully collecting the supernatant into a fresh glass bottle after each ultracentrifugation step using a large glass pipette.
9. As a further control, it can be tested whether an additional filtration step would affect the miRNA results obtained from exosome preparations. During the qRT-PCR validation of our sequencing data, we thus included in our study [9] a filtration step for selected preparations. Specifically, the supernatant after the 10,000 × *g* centrifugation step (*see* Subheading 3.2.1) is pipetted into a Whatman ZapCap-S Bottle-top Filter (200 nm pore size) and filtered into a fresh glass bottle using a vacuum pump. Afterward, the filtered solutions proceed with

ultracentrifugation at 100,000 × *g* as described in Subheading 3.2.1. The three most up- and downregulated exosomal miRNAs upon intracellular *E6/E7*-repression based on the qRT-PCR validation were consistently re-detected and showed very similar quantitative changes in unfiltered and filtered extracts.

10. For the immunodetection of the tetraspanin proteins CD63 and CD9 a nonreducing SDS sample buffer (*see* Subheading 2.1.2) is required.
11. The total RNA profile shows distinct differences between cellular and exosomal RNA, with exosomes lacking discernible 18S and 28S rRNA peaks [12, 31]. Both cellular and exosomal RNA reveal a peak for transfer RNAs (tRNAs) and miRNAs in the small RNA profiles.
12. In our experiments [9], the resulting 6 μl concentrated exosomal total RNA used as input for the cDNA library preparations range between RNA quantities of 100 and 600 ng.
13. We multiplex all exosomal libraries to be sequenced together in one lane and all cellular libraries to be sequenced in a second lane, to avoid potential bias caused by different library complexities of exosomal and cellular samples [9].
14. It is assumed that miRNAs with a high intracellular abundance can lead to the repression of their target genes, whereas lowly concentrated miRNAs, identified in deep-sequencing studies with <100 RPM, are frequently not functional [32]. To identify miRNAs deregulated upon silencing of the viral oncogene expression, we set an arbitrary threshold of 1000 RPM for the individual miRNA in each sample, thereby focusing on the most frequently sequenced miRNAs.
15. We decided to regard a cellular or exosomal miRNA as *E6/E7*-dependent upon fulfilling both of the following criteria:
    (a) A more than 1.5-fold difference between si18E6/E7- and siContr-1-treated cells or exosomes secreted thereof, as identified by small RNA deep sequencing, and >1000 RPM in each sample.
    (b) A more than 1.5-fold difference between si18E6/E7- and siContr-1-treated cells, or exosomes secreted thereof, as verified by qRT-PCR.
16. In our hands, Ct-values for the endogenous control *RNU6-2* are consistent for si18E6/E7- or siContr-1-treated samples and across experimental conditions [9].
17. qRT-PCR normalization of exosomal samples is conducted against the geometric mean of the expression of miR-452-5p and miR-183-5p [9]. These two miRNAs were chosen as endogenous exosomal miRNAs for normalization since they were among the most frequently sequenced exosomal miRNAs

in HeLa cells (>1000 RPM in each sample) and showed virtually no regulation in exosomes upon silencing of HPV18 *E6/E7* versus control treatment based on the deep sequencing data (miR-452-5p: $FC_{mean} = 0.99$, miR-183-5p: $FC_{mean} = 1.04$). So far, there is no common RNA species available for normalization of exosomal miRNA levels. Therefore, reference miRNAs need to be chosen for each individual experimental setup.

Acknowledgments

The authors thank Julia Bulkescher, Claudia Lohrey, and Sandra Bastian for expert technical assistance, and Felicitas Bossler for helpful comments on the manuscript.
Conflict of interest: The authors declare no conflict of interest.

References

1. Schiller JT, Lowy DR (2012) Understanding and learning from the success of prophylactic human papillomavirus vaccines. Nat Rev Microbiol 10:681–692
2. American Cancer Society (2015) Global cancer facts and figures, 3rd edn. American Cancer Society, Atlanta
3. zur Hausen H (2002) Papillomaviruses and cancer: from basic studies to clinical application. Nat Rev Cancer 2:342–350
4. McLaughlin-Drubin ME, Münger K (2009) Oncogenic activities of human papillomaviruses. Virus Res 143:195–208
5. Hoppe-Seyler F, Hoppe-Seyler K (2011) Emerging topics in human tumor virology. Int J Cancer 129:1289–1299
6. Di Leva G, Garofalo M, Croce CM (2014) MicroRNAs in cancer. Annu Rev Pathol 9:287–314
7. Schwarzenbach H, Nishida N, Calin GA et al (2014) Clinical relevance of circulating cell-free microRNAs in cancer. Nat Rev Clin Oncol 11:145–156
8. Kincaid RP, Sullivan CS (2012) Virus-encoded microRNAs: an overview and a look to the future. PLoS Pathog 8:e1003018. doi:10.1371/journal.ppat.1003018
9. Honegger A, Schilling D, Bastian S et al (2015) Dependence of intracellular and exosomal microRNAs on viral E6/E7 oncogene expression in HPV-positive tumor cells. PLoS Pathog 11:e1004712. doi:10.1371/journal.ppat.1004712
10. Thierry F (2009) Transcriptional regulation of the papillomavirus oncogenes by cellular and viral transcription factors in cervical carcinoma. Virology 384:375–379
11. Colombo M, Raposo G, Théry C (2014) Biogenesis, secretion, and intercellular interactions of exosomes and other extracellular vesicles. Annu Rev Cell Dev Biol 30:255–289
12. Valadi H, Ekström K, Bossios A et al (2007) Exosome-mediated transfer of mRNAs and microRNAs is a novel mechanism of genetic exchange between cells. Nat Cell Biol 9:654–659
13. Zhang J, Li S, Li L et al (2015) Exosome and exosomal microRNA: trafficking, sorting, and function. Genomics Proteomics Bioinformatics 13:17–24
14. Properzi F, Logozzi M, Fais S (2013) Exosomes: the future of biomarkers in medicine. Biomark Med 7:769–778
15. Friedlander MR, Mackowiak SD, Li N et al (2012) miRDeep2 accurately identifies known and hundreds of novel microRNA genes in seven animal clades. Nucleic Acids Res 40:37–52
16. Griffiths-Jones S (2004) The microRNA registry. Nucleic Acids Res 32:D109–D111
17. Griffiths-Jones S, Grocock RJ, van Dongen S et al (2006) miRBase: microRNA sequences, targets and gene nomenclature. Nucleic Acids Res 34:D140–D144
18. Griffiths-Jones S, Saini HK, van Dongen S et al (2008) miRBase: tools for microRNA genomics. Nucleic Acids Res 36:D154–D158
19. Kozomara A, Griffiths-Jones S (2011) miRBase: integrating microRNA annotation and

deep-sequencing data. Nucleic Acids Res 39: D152–D157

20. Butz K, Ristriani T, Hengstermann A et al (2003) siRNA targeting of the viral E6 oncogene efficiently kills human papillomavirus-positive cancer cells. Oncogene 22:5938–5945
21. Parsons BD, Schindler A, Evans DH et al (2009) A direct phenotypic comparison of siRNA pools and multiple individual duplexes in a functional assay. PLoS One 4:e8471
22. Jackson AL, Linsley PS (2010) Recognizing and avoiding siRNA off-target effects for target identification and therapeutic application. Nat Rev Drug Discov 9:57–67
23. Scheffner M, Werness BA, Huibregtse JM et al (1990) The E6 oncoprotein encoded by human papillomavirus types 16 and 18 promotes the degradation of p53. Cell 63:1129–1136
24. el-Deiry WS, Tokino T, Velculescu VE et al (1993) WAF1, a potential mediator of p53 tumor suppression. Cell 75:817–825
25. McLaughlin-Drubin ME, Munger K (2009) The human papillomavirus E7 oncoprotein. Virology 384:335–344
26. Thery C, Amigorena S, Raposo G et al (2006) Isolation and characterization of exosomes from cell culture supernatants and biological fluids. Curr Protoc Cell Biol 3(11.) 1-3.22.29
27. Honegger A, Leitz J, Bulkescher J et al (2013) Silencing of human papillomavirus (HPV) E6/E7 oncogene expression affects both the contents and the amounts of extracellular microvesicles released from HPV-positive cancer cells. Int J Cancer 133:1631–1642
28. Weischenfeldt J, Simon R, Feuerbach L et al (2013) Integrative genomic analyses reveal an androgen-driven somatic alteration landscape in early-onset prostate cancer. Cancer Cell 23:159–170
29. Livak KJ, Schmittgen TD (2001) Analysis of relative gene expression data using real-time quantitative PCR and the 2(−Delta Delta C (T)) method. Methods 25:402–408
30. Witwer KW, Buzás EI, Bemis LT et al (2013) Standardization of sample collection, isolation and analysis methods in extracellular vesicle research. J Extracell Vesicles 2:20360. doi:10.3402/jev.v2i0.20360
31. Taylor DD, Gercel-Taylor C (2008) MicroRNA signatures of tumor-derived exosomes as diagnostic biomarkers of ovarian cancer. Gynecol Oncol 110:13–21
32. Mullokandov G, Baccarini A, Ruzo A et al (2012) High-throughput assessment of microRNA activity and function using microRNA sensor and decoy libraries. Nat Methods 9:840–846

Chapter 11

Combination of Anti-miRNAs Oligonucleotides with Low Amounts of Chemotherapeutic Agents for Pancreatic Cancer Therapy

Marta Passadouro and Henrique Faneca

Abstract

Pancreatic ductal adenocarcinoma (PDAC) is the most predominant type of pancreatic cancer and presents one of the highest mortality rates when compared with other carcinomas. The absence of efficient treatment options for PDAC prompted us to investigate whether microRNA inhibition, combined or not with chemotherapeutic agents, would constitute a promising therapeutic approach for this disease. In this chapter, we describe several methods and procedures that can be used to evaluate the potential of new therapeutic strategies involving oligonucleotides against overexpressed microRNAs, in PDAC, either alone or in combination with low amounts of chemotherapeutic drugs.

Key words Cationic liposomes, Lipoplexes, Anti-miRNAs oligonucleotides, Chemotherapy, Combined antitumor strategies, Pancreatic cancer therapy

1 Introduction

Pancreatic ductal adenocarcinoma (PDAC) is a highly aggressive and mortal cancer, representing about 95% of pancreatic cancer cases [1]. Despite its moderate incidence when compared with other carcinomas, PDAC has one of the highest mortality rates, with an overall median survival of 2–8 months and a five-year survival rate of only 1–4% [2, 3]. Usually, the treatment of pancreatic cancer involves highly invasive surgery and/or chemotherapy, clinical results being largely unsatisfactory, including side effects often devastating to patients. Therefore, the development of new and efficient antitumor strategies is urgently required [4].

In this regard, gene therapy constitutes a promising strategy, due to the discovery of new molecular targets associated with this disease, which provided the opportunity to generate novel therapeutic approaches. The data published in the last years have shown that microRNAs (miRNAs) are key regulators in cancer, being

Wei Wu (ed.), *MicroRNA and Cancer: Methods and Protocols*, Methods in Molecular Biology, vol. 1699,
DOI 10.1007/978-1-4939-7435-1_11,

involved in a variety of biological processes relevant for tumor development, such as proliferation, angiogenesis, and metastization, consequently constituting promising targets for antitumor therapies [5]. Several studies have indicated that the overexpression of some miRNAs, as it is the case of miR-21, miR-221, miR-222, and miR-10b, is strongly associated with cancer, including PDAC, due to the ability of these miRNAs to regulate the function of several important genes, such as tumor suppressor genes [6–10].

Therefore, we developed a new therapeutic strategy, mediated by a lipid-based nanosystem, involving anti-microRNAs oligonucleotides (AMOs) against overexpressed miRNAs in PDAC, being observed a significant antitumor activity [10]. Moreover, we demonstrated that combination of this antitumor gene therapy strategy, involving AMOs, with low amounts of chemotherapeutic agents resulted in a synergistic and significant antitumor effect in PDAC cell lines [10]. The potential of these new therapeutic approaches was evaluated from several points of view, from intracellular distribution of nanosystems to antitumor activity in PDAC cells.

Studies on the intracellular distribution allow understanding the mechanisms by which the nanosystems mediate the delivery of genetic material into target cells. The biological activity studies permit evaluating the AMOs delivery efficacy of the developed nanosystems, through the quantification of both the miRNAs and the mRNA levels of their targets. The fluorescence in situ hybridization experiments allow visualizing the degree of miRNA inhibition induced by the developed delivery approach. The cell viability assays permit evaluating the effect of the therapeutic strategies involving AMOs and their combination with low amounts of chemotherapeutic drugs [10].

2 Materials

2.1 Cationic Liposomes

1. 1-palmitoyl-2-oleoyl-sn-glycero-3-ethylphosphocholine (EPOPC) (Avanti Polar Lipids, Alabaster, AL) and Cholesterol (Chol) are dissolved at 100 mg/ml and 50 mg/ml, respectively, in chloroform (Sigma, St. Louis, MO) and stored at −20 °C.
2. Carboxyfluorescein-dioleoylphosphatidylethanolamine (carboxyfluorescein-PE) (Avanti Polar Lipids) is dissolved at 2 mg/ml in chloroform, protected from the light and stored at −20 °C.
3. Lipid film hydration is performed with deionized water (*see* **Note 1**).

4. Lipid films are obtained in a Heidolph VV 2000 rotatory evaporator (Heidolph Instruments GmbH & Co, Schwabach, Germany).
5. Liposome sonication is performed in a Sonorex RK100H sonicator (Bandelin Electronic, Berlin, Germany).
6. Mini-extruder from Avanti Polar Lipids.
7. Polycarbonate membranes of 50 nm pore-diameter from Whatman (Maidstone, UK).
8. Filters of 0.22 μm pore-diameter from Schleicher & Schuell (Dassel, Germany).

2.1.1 Lipid Concentration

1. Inorganic phosphate (KH_2PO_4) standard solution is prepared at 0.65 mM in a 50 mM hydrochloric acid solution and stored at 4 °C.
2. Acidic hydrolysis: Perchloric acid at 70–72%.
3. Ammonium molybdate solution is prepared at 0.22% (w/v) in a 2% (v/v) sulfuric acid solution and stored at room temperature (*see* **Note 2**).
4. Fiske and Subbarow reagent: 15% (w/v) $NaHSO_3$, 0.5% (w/v) Na_2SO_3, 0.25% (w/v) 1-amino-2-hydroxy-4-naphthalenesulfonic acid. Protect from light and store at 4 °C (*see* **Note 3**).

2.2 Cationic Liposome/AMOs Lipoplexes

1. HEPES-buffered saline (HBS): 100 mM NaCl, 20 mM HEPES (Sigma, St. Louis, MO), pH 7.4. Store at 4 °C.
2. AMOs: miRCURY LNA Inhibitor (Exiqon, Vedbaek, Denmark) solutions are prepared in Nuclease-free water (Exiqon, Vedbaek, Denmark) at 10 μM and stored at −20 °C. The miRCURY LNA Inhibitor sequences used are:
   - miRCURY LNA Inhibitor for hsa-miR-21: CAACATCAGTCTGATAAGCT.
   - miRCURY LNA Inhibitor for hsa-miR-221: AATCTACATTGTATGCCA.
   - miRCURY LNA Inhibitor for hsa-miR-222: AGGATCTACACTGGCTACTGA.
   - Negative Control A: GTGTAACACGTCTATACGCCCA.
3. Human serum albumin (HSA) (Sigma, St. Louis, MO) solution is prepared in HBS at 640 μg/ml and stored at 4 °C.

2.3 Cell Culture

1. Dulbecco's modified Eagle's medium-high glucose (DMEM-HG) (Gibco/BRL, Bethesda, MD) supplemented with 10% heat-inactivated fetal bovine serum (FBS) (Gibco/BRL, Bethesda, MD), penicillin (100 U/ml), and streptomycin (100 μg/ml) (Sigma). Store at 4 °C and warm to working temperature of 37 °C.

2. Solution of trypsin (0.25%) and ethylenediamine tetraacetic acid (EDTA) (1 mM) from Sigma. Store at 4 °C and warm for working temperature of 37 °C.
3. Cells are cultured in 75 cm^2 flasks (Corning Costar Corporation, Cambridge, MA, USA).
4. Phosphate-buffered saline (PBS): Prepare 10× stock solutions with 1.37 M NaCl, 27 mM KCl, 100 mM Na_2HPO_4, 18 mM KH_2PO_4 (adjust to pH 7.4 with HCl) and autoclave before storage at room temperature. Prepare working solution by dilution of one part with nine parts water.

2.4 Intracellular Distribution of Lipoplexes

1. H766T cells are seeded in 12-well culture plates (Corning Costar Corporation), previously covered with sterile coverslips.
2. Transfection medium: Dulbecco's modified Eagle's medium high glucose (DMEM-HG) (Gibco/BRL) without serum and antibiotics. Store at 4 °C and warm to a working temperature of 37 °C.
3. Staining of acidic compartments: LysoTracker Red DND-99 (Molecular Probes, Eugene, OR), stored at −20 °C, is freshly prepared at 200 nM in DMEM-HG medium and warmed to a working temperature of 37 °C.
4. Wash buffer: PBS at room temperature.
5. Cell fixation buffer: 4% (w/v) paraformaldehyde in PBS, store at 4 °C.
6. Nuclear stain: Prepare a 1 mg/ml Hoechst 33342 (Molecular Probes) solution in PBS and store at 4 °C. Prepare a working solution at 1 μg/ml by dilution in PBS.
7. Mounting medium: Mowiol (Merck Millipore, Darmstadt, Germany) stored at room temperature.
8. Images are taken with a LSM-510 META confocal microscope (Carl Zeiss Inc., Jena, Germany), under the 40× oil immersion objective.

2.5 Biological Activity

2.5.1 Hybridization In Situ

1. H766T cells are seeded onto multi-chambered coverglass slides from Lab-Tek (Rochester, NY, USA) appropriated for confocal microscopy.
2. Transfection medium: Dulbecco's modified Eagle's medium high glucose (DMEM-HG) (Gibco/BRL) without serum and antibiotics. Store at 4 °C and warm to a working temperature of 37 °C.
3. Probes (for miR-21 and a scrambled probe) labeled with Digoxigenin (DIG) (Exiqon, Vedbaek, Denmark), prepared in RNase-free water [treat water with 0.1% Diethylpyrocarbonate (DEPC)] stored at −20 °C and protected from light.

4. Detection of DIG-labeled probe: Fab fragments from polyclonal Anti-DIG antibodies conjugated to horseradish peroxidase (Roche, Basel, Switzerland). Store at −20 °C.
5. Tyramide Signal Amplification (TSA) System: TSA is a modified substrate for horse-radish peroxidase (HRP). TSA plus Cy3 System allows the fluorescent detection. Reagents and solutions needed for the amplification system: 1× PBS; 1× TBS (50 mM Tris–HCl, pH 7.6; 150 mM NaCl); TBS with 0.1% (v/v) Tween 20 (TBS-T); 4% (w/v) paraformaldehyde in PBS (for tissue fixation); 70% Ethanol (for cell permeabilization); 1 μg/ml Hoechst 33342 (nucleus staining); MOWIOL (mounting medium) and RNase-free water (*see* **Note 4**).
6. Acetylation solution: 0.1 M Triethanolamine; 0.5% (v/v) Acetic anhydride; RNAse-free water (*see* **Note 5**).
7. Hybridization Buffer: 50% (v/v) Formamide; 25% (v/v) SSC 20× (0.75 M NaCl, 0.075 M sodium citrate); 2× Denhardt's Solution (mixture of blocking agents, containing: 1% (v/v) Ficoll (type 400), 1% (v/v) polyvinylpyrrolidone, and 1% (v/v) bovine serum albumin) (*see* **Note 6**); 1% (v/v) Blocking reagent (*see* **Note 6**); 0.1% (v/v) CHAPS detergent; 250 μg/ml yeast tRNA; 500 μg/ml salmon sperm DNA; 0.5% (v/v) Tween 20 (*see* **Note 6**).
8. Washing solution 1: 50% (v/v) Formamide; 5% (v/v) SSC 20× (0.75 M NaCl, 0.075 M sodium citrate); 0.1% (v/v) Tween 20 **(***see* **Note 7)**.
9. Washing solution 2: 1% (v/v) SSC 20× (0.75 M NaCl, 0.075 M sodium citrate) **(***see* **Note 8)**.
10. Peroxidase Inactivation solution: 3% hydrogen peroxide in TBS-T.
11. Blocking solution: 10% (v/v) Heat-inactivated goat serum; 0.5% (v/v) Blocking agent; TBS-T **(***see* **Note 8)**.
12. Images are taken with a LSM-510 META confocal microscope (Carl Zeiss Inc., Jena, Germany), under the 40× oil immersion objective.

2.5.2 MicroRNA and mRNA Quantification Levels

1. H766T cells are seeded in 12-well culture plates (Corning Costar Corporation) (*see* **Note 9**).
2. Transfection medium: Dulbecco's modified Eagle's medium high glucose (DMEM-HG) (Gibco/BRL) without serum and antibiotics. Store at 4 °C and warm to a working temperature of 37 °C.

RNA Extraction

3. RNA extraction is performed using miRCURY™ RNA Isolation kit—Cell & Plant from (Exiqon, Vedbaek, Denmark). The kit is supplied with the following: lysis solution; RNase-free water; wash solution (complement by adding 50 ml of 99%

ethanol to wash solution); elution buffer; and mini spin columns 50 collection tubes 100 elution tubes (1.7 ml). As supplementary solutions for RNA extraction, PBS (RNase-free), 99% ethanol, and β-mercaptoethanol are also used at room temperature (*see* **Note 10**).

4. An RNase-free environment is created using RNAseZip (Sigma-Aldrich, Munich, German), as a decontamination solution, to clean the RNA extraction working zone.
5. RNA is quantified using a Nanodrop UV-Vis spectrophotometer (Thermo Fisher Scientific, Wilmington, USA).

MicroRNA cDNA Synthesis

1. For microRNA analysis, cDNA synthesis step is performed using Universal cDNA synthesis kit (Exiqon, Vedbaek, Denmark), containing reaction buffer (5× concentrated), enzyme mix (10× concentrated) and nuclease-free water. Store at −20 °C and keep on ice while using.
2. cDNA synthesis is performed and monitored using a Veriti 96-Well Thermal Cycler from Applied BioSystems (Life Technologies, Carlsbad, CA, USA).

mRNA cDNA Synthesis

1. For mRNA analysis, the cDNA synthesis step is performed using One Strand cDNA Synthesis kit (BioRad, Hercules, CA, USA), containing iScript reaction mix (5× concentrated), iScript reverse transcriptase, nuclease-free water. Store at −20 °C and keep on ice while using.
2. cDNA synthesis is performed and monitored using a Veriti 96-Well Thermal Cycler from Applied BioSystems (Life Technologies, Carlsbad, CA, USA).

RT-qPCR for MicroRNA Quantification Levels

1. MiRCURY LNA Universal RT microRNA PCR kit (Exiqon, Vedbaek, Denmark), containing ExiLENT SYBR Green master mix (2× concentrated) and Nuclease-free water.
2. The following MicroRNA LNA™ PCR primer set (Exiqon, Vedbaek, Denmark), targeting the sequence of hsa-miR-21 (UAGCUUAUCAGACUGAUGUUGA), hsa-miR-221 (ACCUGGCAUACAAUGUAGAUUU), and hsa-miR-222 (CUCAGUAGCCAGUGUAGAUCCU) is used. U6snRNA (hsa) PCR primer set is used to quantify the hsa-U6snRNA as a reference gene (primer sequence not disclosed).
3. The RT-qPCR reactions are performed and monitored using a real-time instrument ABI Prism 7300 qPCR System from Applied BioSystems (Life Technologies, Carlsbad, CA, USA).

RT-qPCR for mRNA Quantification Levels

1. A SsoAdvanced SYBR Green Supermix from BioRad (Hercules, CA, USA) is used to perform RT-qPRC reactions. Store at −20 °C and thaw during 20 min on ice before using.

2. Specific primer set from Qiagen (Hilden, Germany) is used for $P27^{Kip1}$/CDKN1B (ref: QT00998445); PTEN (ref: QT02423400) and HPRT1 (ref: QT00059066) and RPL13 (ref: QT00067963) genes (sequence not disclosed). Store at −20 °C and thaw during 20 min on ice before using.
3. The RT-qPCR reactions are performed and monitored using a real-time instrument ABI Prism 7300 qPCR System from Applied BioSystems (Life Technologies, Carlsbad, CA, USA).

2.6 Viability Assay (Alamar Blue)

1. H766T cells are seeded in 48-well culture plates (Corning Costar Corporation).
2. Transfection medium: Dulbecco's modified Eagle's medium high glucose (DMEM-HG) (Gibco/BRL) without serum and antibiotics. Store at 4 °C and warm to 37° prior to use.
3. Alamar Blue dye: 10% (v/v) Alamar Blue in DMEM-HG (prepared from a 0.1 mg/ml stock solution of Alamar Blue, stored at −20 °C). The solution is prepared immediately before use.
4. Chemotherapeutic drugs are used at the following concentration: 1 μM of docetaxel, 5 μM of gemcitabine, and 15 μM of sunitinib. Docetaxel and gemcitabine were purchased from Sigma-Aldrich (Munich, Germany) and stock solutions were prepared in DMSO (Sigma-Aldrich, Munich, Germany) and in distilled water, respectively, and subsequently stored at −20 °C and room temperature, respectively. Sunitinib malate (Sutent®) was kindly offered by Pfizer (Basel, Switzerland) and the stock solutions were prepared in DMSO from Sigma-Aldrich (Munich, Germany) and stored at −20 °C.
5. Absorbance is measured in a SPECTRAmax PLUS384 spectrophotometer (Molecular Devices, Union City, CA).

3 Methods

3.1 Cationic Liposomes

1. Small unilamellar cationic liposomes (SUV) used are prepared by extrusion of multilamellar liposomes (MLV) composed of 1:1 (mol ratio) mixtures of 1-palmitoyl-2-oleoyl-sn-glycero-3-ethylphosphocholine (EPOPC) and cholesterol (Chol) [11, 12].
2. For intracellular distribution studies, EPOPC:Chol (1:1) liposomes are labeled with 0.1 mole % carboxyfluorescein-dioleoylphosphatidylethanolamine (carboxyfluorescein-PE) (*see* **Note 11**).
3. The necessary volumes of the stock lipids, dissolved in chloroform at the referred concentration (Subheading 2.1.), are

mixed at the desired molar ratio in glass tubes previously washed with chloroform. The glass tubes containing the lipid mixtures are placed in the rotatory evaporator (220 rpm) and allowed to dry under vacuum (−0.8 bar) for 1 h at 37 °C.

4. The dried lipid films are hydrated with 1 ml of water (to a final lipid concentration of 6 mM) with constant vortexing to promote the formation of MLV.
5. The resulting MLV are sonicated for 3 min and extruded 21 times through two stacked polycarbonate filters of 50 nm pore-diameter, using the referred mini-extruder (Subheading 2.1.) to obtain a homogeneous suspension of SUV. The SUV are then diluted three times with water and filter-sterilized utilizing 0.22 μm pore-diameter filters. The suspension is stored at 4 °C until use.

3.1.1 Lipid Concentration

1. Cationic liposome concentration is determined by the quantification of the phospholipid content (EPOPC) through colorimetric analysis [13, 14] (*see* **Note 12**).
2. Standards (0; 32.5; 65; 130; 260 nmoles of inorganic phosphate) and samples (volume corresponding to approximately 100 nmoles of phosphate from EPOPC) are placed in glass tubes previously washed with chloroform. The standards and samples are then submitted to acidic hydrolysis with 0.5 ml of perchloric acid at 70–72% for 2 h at 180 °C, to promote the conversion of organic phosphate into inorganic phosphate (*see* **Note 13**).
3. After hydrolysis, the tubes containing the standards and samples are allowed to cool to room temperature and then 7.5 ml of ammonium molybdate, which converts the inorganic phosphate into phosphomolybdic acid, are added to each tube. After the addition of 0.3 ml of Fiske and Subbarow reagent to each tube containing the standards and samples, the phosphomolybdic acid is reduced to molybdate blue upon incubation in a water boiling bath during 15 min.
4. The standards and samples are allowed to cool to room temperature and the absorbance is read at 830 nm. The determination of the phosphate concentration of the liposomal samples is based on the standard curve obtained for the absorbance.

3.2 Cationic Liposome/AMOs Lipoplexes

1. Cationic liposome/AMOs complexes are prepared in HBS using liposomal suspensions of known concentrations and solutions of AMOS and HSA, both prepared in HBS at 80 nM and 640 μg/ml, respectively. All the solutions are previously filtered under aseptic conditions [10, 12].
2. Complexes are prepared in sterile polypropylene tubes in order to avoid interactions between AMOs and the tube walls. The

concentration of AMOs is maintained constant (80 nM) independently of the total volume of the complexes, since the physico-chemical characteristics of the complexes could change with its concentration. Complexes are prepared by using 50 μl of HBS, a variable small volume of AMOs solution (80 nM) and the necessary volume of liposomes, which is dependent on the liposome concentration, followed by the addition of 50 μl of HSA solution, in order to obtain 32 μg of HSA/μg of oligonucleotides.

3. Lipoplexes are prepared by sequentially mixing the established HBS volume with the necessary volume of liposomes and HSA, being liposomes incubated with the protein for 15 min to allow the establishment of interaction between these two components, followed by slow addition of the AMOS solution to the suspension. After that, the final mixture is gently shaked and incubated for further 15 min at room temperature to allow the formation of the complexes through the establishment of electrostatic interactions. Lipoplexes are used immediately after preparation [11, 12].

3.3 Cells

1. Hs766T cells (pancreatic adenocarcinoma cell line derived from a lymph node metastasis) are grown in 75 cm^2 flasks and maintained at 37 °C, under 5% CO_2, in DMEM-HG supplemented with 10% (v/v) heat-inactivated FBS, penicillin (100 U/ml) and streptomycin (100 μg/ml) (*see* **Note 14**).
2. When the cells reach 80–90% of confluence, the culture medium is removed and the cells are washed with 3 ml of the trypsin solution (*see* **Note 15**). After this washing step, the cells are detached upon incubation at 37 °C, for 2–3 min, with 3 ml of fresh trypsin solution (*see* **Note 16**). The cells are then resuspended in 10 ml of DMEM-HG medium and counted in a hemocytometer to determine the cell suspension density.
3. The cell suspension is diluted with DMEM-HG medium to obtain a final density of 50×10^3 cells/ml and the cells are plated in multiwell plates, the number of wells per plate depending on the wanted study. For intracellular distribution and in situ hybridization studies, the cells are plated 24 h before the experiments in 12-multiwell plates, at 120×10^3 cells/well, and multi-chambered coverglass slides, at 20×10^3 cells/well, respectively, in order to obtain a cell confluence of 60–70% at the beginning of the experiments. The multiwells are then placed in the incubator at 37 °C, under 5% CO_2. All the steps involved in cell preparation are performed under sterile conditions in a bioguard hood.

3.4 Intracellular Distribution of Lipoplexes

1. Twenty-four hours before transfection, 120×10^3 Hs766T cells in 2.4 ml of DMEM-HG culture medium are added to each well of a 12-multiwell plate, previously covered with coverslips [10].
2. At the time of transfection, the culture medium is removed and the cells are incubated for 30 min with 0.5 ml/well of 200 nM LysoTracker Red DND-99 (prepared in the DMEM-HG medium), which labels acidic compartments of live cells. The cells are then washed once with DMEM-HG medium without serum and antibiotics and subsequently covered with 0.5 ml of the same medium prior to the addition of lipoplexes [11, 15].
3. To observe the intracellular distribution of the complexes, EPOPC:Chol liposomes labeled with 0.1% carboxyfluorescein-PE and associated with HSA are complexed with the AMOs at the (4/1) (+/−) charge ratio. The resulting lipoplexes are incubated with the cells for 2 h at 37 °C.
4. After 2 h of incubation with the complexes containing 80 nM of AMOs, the cells are washed twice with PBS and the nuclei are labeled through cell incubation with 0.5 ml/well of the fluorescent DNA-binding dye Hoechst 33342 (1 μg/ml), for 5 min at room temperature.
5. The cells are then washed once with PBS and immediately mounted in the Mowiol mounting medium, and observed under a confocal microscope, using a 40× oil objective. Excitation at 577 nm induces LysoTracker Red fluorescence (red emission), excitation at 497 nm induces carboxyfluorescein fluorescence (green emission), and excitation at 350 nm induces Hoechst 33342 fluorescence (blue emission). An example of the obtained results is shown in Fig. 1.

3.5 Biological Activity

1. Twenty-four hours before transfection, 20×10^3, 40×10^3, and 120×10^3 Hs766T cells in the DMEM-HG culture medium are added to each well of a multi-chambered coverglass slide (appropriate for confocal microscopy), 48-multiwell plate, and 12-multiwell plate, respectively. At the time of transfection, the culture medium is removed, and the cells are washed once with the DMEM-HG medium without serum and antibiotics, and then covered with 0.5 ml of the same medium.
2. EPOPC:Chol (1:1) liposomes with HSA are complexed with AMOs, at the 4/1 (+/−) cationic lipid/AMOs charge ratio.
3. The resulting lipoplexes containing 80 nM of AMOs are incubated with the cells, for 4 h at 37 °C. Then the transfection medium is replaced with DMEM-HG and the cells are further incubated for 48 h.
4. The cells are washed with PBS and immediately submitted to RNA extraction or stored at 20 °C until use.

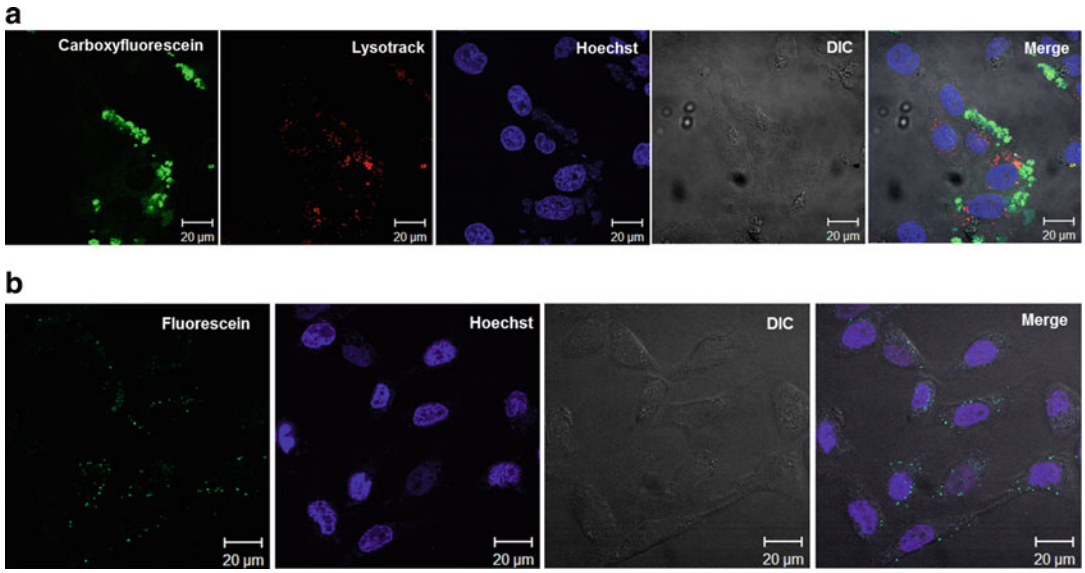

Fig. 1 Internalization of HSA-EPOPC:Chol/AMOs (+/−)(4/1) lipoplexes in Hs766T pancreatic adenocarcinoma cells. (**a**) Cells were transfected with lipoplexes prepared from carboxyfluorescein-labeled EPOPC:Chol liposomes and stained with LysoTracker red (200 nM), for acidic compartment labeling, and Hoechst 33342 (1 μg/ml), for nucleus labeling. (**b**) Cells were transfected with lipoplexes containing fluorescein-labeled oligonucleotides and stained with Hoechst (1 μg/ml), for nucleus labeling. Confocal microscopy images were obtained with 40× magnification. DIC means differential interference confocal microscopy. Bars correspond to 20 μm

3.5.1 Fluorescence In Situ Hybridization

1. Transfection is performed with lipoplexes containing anti-miR-21 or scrambled (control) oligonucleotides, as described in Subheading 3.4.
2. Forty-eight hours after transfection, the cells are washed with PBS. In situ hybridization protocol begins with the cells being fixed with 4% paraformaldehyde for 30 min at room temperature and then permeabilized at 4 °C with 70% ethanol for 4 h [10, 16] (*see* **Notes 17** and **18).**
3. The cells are incubated with a fresh acetylation solution for 30 min at room temperature and then rinsed twice with TBS.
4. Pre-hybridization is performed for 2 h at 52 °C, in the absence of LNA probe, in the hybridization buffer.
5. The hybridization step is carried out overnight, at the same temperature, using the digoxigenin-labeled (DIG-labeled) probe for miR-21 and a scrambled probe, in a humid atmosphere (*see* **Note 19**).
6. After incubation, three stringency washes are performed also at 52 °C to completely remove the non-hybridized probe. First, the cells are washed twice with washing solution 1, for 30 min each at hybridization temperature, and then the cells are

washed once with washing solution 2, for 20 min at hybridization temperature.

7. An additional washing step is performed once with TBS-T, for 15 min at room temperature with slight agitation.
8. Endogenous peroxidase activity is inactivated by incubation in a peroxidase inactivation solution for 30 min, followed by three washes with TBS-T at room temperature with slight agitation.
9. The slides are then placed in a blocking solution for 1 h at room temperature, with moderate agitation.
10. The cells are incubated for 1 h at room temperature with an anti-DIG antibody conjugated with the horseradish peroxidase. The cells are washed twice with TBS-T, 5 min each wash, at room temperature, with slight agitation.
11. To amplify the antibody signal, slides are further incubated with a TSA plus Cy3 solution for 10 min, in the dark, at room temperature with slight agitation. The cells are then washed twice with TBS, 5 min each washing, at room temperature with slight agitation.
12. The cells are finally stained with the fluorescent DNA-binding dye Hoechst 33342 (1 μg/ml) for 5 min in the dark, washed with cold PBS, and mounted in Mowiol.
13. Confocal images are acquired in a point scanning confocal microscope, using a 40× oil objective. Excitation at 497 nm induces fluorescein fluorescence (green emission) and excitation at 350 nm induces Hoechst 33342 fluorescence (blue emission). An example of the obtained results is shown in Fig. 2.

3.5.2 MicroRNA and mRNA Quantification Levels

RNA Extraction

1. Forty-eight hours after transfection, H766T cells are washed with PBS, lysed by adding 350 μl of lysis buffer to each well and by performing scratch, and homogenized through up and down movements with the support of a pipette [10].
2. The total RNA is transferred to a 1.5 ml sterile polypropylene tube and 200 μl of 99% ethanol are added to each tube and mixed by vortexing the tube for 10 s (*see* **Note 20**).
3. A column, for each experimental condition, is assembled into a collection tube and 600 μl of lysate with ethanol is loaded into the column, adsorbed to a silica matrix, and posteriorly subjected to centrifugation at 14,000 × *g* for 1 min. Flow-through is discarded and the column reassembled into the collection tube.
4. The previous step is repeated until the whole lysate was passed through the column.

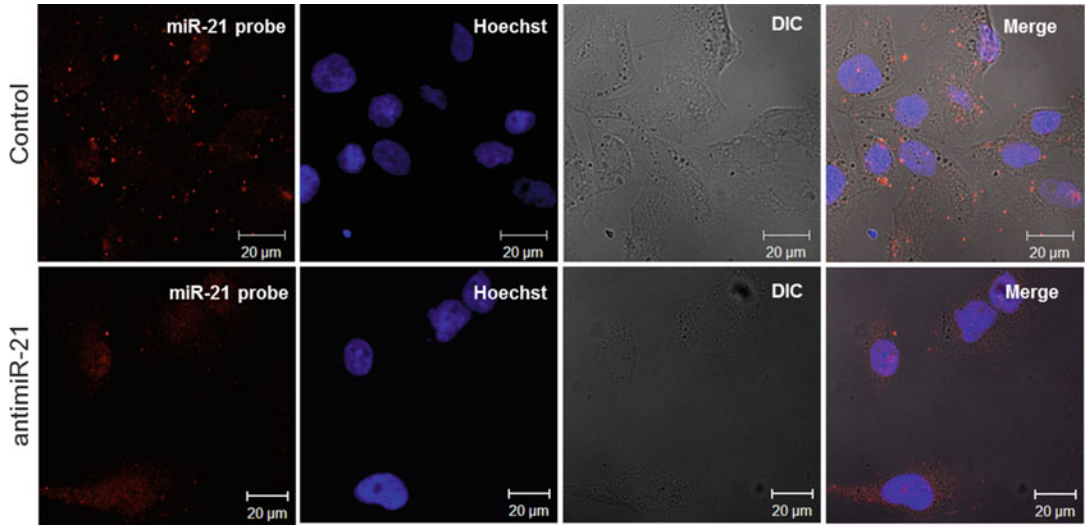

Fig. 2 MicroRNA modulation in Hs766T cells. Confocal analysis of *FISH* staining in Hs766T cells transfected with lipoplexes containing 80 nM of AMOs against miR-21 (antimiR-21) or 80 nM of scrambled oligonucleotides (control). After 48 h, the cells were subjected to miR-21 labeling with 5′-DIG (digoxigenin) LNA probes (*red dots*), as described in Methods. Nuclear staining was accomplished using Hoescht 33342 (1 μg/ml). Confocal microscopy images were obtained with 40× magnification. DIC means differential interference confocal microscopy. Bars correspond to 20 μm

5. The washing step is performed by adding 400 μl of wash solution to the column, followed by a centrifugation at 14,000 × *g* for 1 min. This procedure is performed two more times. Flow-through is discarded and column reassembled.
6. In order to thoroughly dry the resin, the column is submitted to an additional centrifugation step at 14,000 × *g* for 2 min.
7. The column is then transferred into a fresh 1.7 ml tube and 50 μl of elution buffer is added to each column (*see* **Note 21**). Centrifugation is performed at 14,000 × *g* for 1 min (*see* **Note 22**).
8. RNA sample is stored at −20 °C if used on the next following days, or at −80 ° C for long-term storage.

MicroRNA cDNA Synthesis

1. RNA samples and cDNA synthesis reagents are thaw on ice for 20 min. All the reagents are gently mixed and spun-down prior to use [10].
2. For microRNA first strand synthesis, 25 ng of template RNA is used, up to a volume of 6 μl, providing a template for all microRNA real-time assays. RNA samples handling and mix preparation are performed on ice the whole time (*see* **Note 23**).
3. For each first strand synthesis mix, 4 μl of reaction buffer is added to RNA template solution and gently mixed, followed by the addition of 2 μl of enzyme mix to each tube (*see* **Note 24**).

4. First Strand synthesis is performed during 60 min incubation at 42 °C, followed by a heat-inactivation step of the reverse transcriptase for 5 min at 95 °C. Tubes are then immediately cooled to 4 °C, cDNA is diluted 1:60 with RNase-free water, and stored at 4 °C, if used in a short period time, or stored at −20 °C until use.

mRNA cDNA Synthesis

1. RNA samples and cDNA synthesis reagents are thaw on ice for 20 min. All reagents are mixed gently and spun-down prior to use [10].
2. For mRNA first strand synthesis, 0.5 μg of template RNA is used, up to a volume of 15 μl, providing a template for all mRNA real-time assays. RNA samples handling and mix preparation are performed on ice the whole time (*see* **Note 23**).
3. For each first strand synthesis mix, 4 μl of reaction buffer is added to RNA template solution and gently mixed, followed by an addition of 1 μl of enzyme mix to each tube.
4. The mix is incubated for 5 min at 25 °C, 30 min at 42 °C, followed by a heat-inactivation step of the reverse transcriptase for 5 min at 85 °C. Finally, cDNA is diluted 1:5 with RNase-free water and stored at 4 °C, if used in a brief period time, or stored at −20 °C until use.

RT-qPCR for MicroRNA Quantification Levels

1. All the reagents are thaw on ice, for 20 min, gently mixed, and spun-down prior to use [10].
2. Specifically for miR-221, miR-222, miR-21, miR-10b, and the reference RNA (U6snRNA), a miRCURY LNA Universal RT reaction mix, consisting of 5 μl of ExiLENT SYBR Green master mix, 1 μl of primer set and 4 μl of cDNA template, are prepared. Each reaction is performed in duplicate (*see* **Note 25**).
3. The PCR conditions consist in 10 min at 95 °C, for polymerase activation, and 40 cycles of amplification with 10 s at 95 °C and 1 min at 60 °C, ramp-rate 1.6 °C/s.
4. A melting curve protocol is started immediately after amplification and consists of 1 min heating at 55° followed by 80 steps of 10 s, with a 2 °C increase at each step.
5. The threshold values for threshold cycle determination (Ct) are generated automatically by the SDS Optical System software.
6. Relative miRNA levels are determined following the ΔΔCt method in comparison with control cells.

RT-qPCR for mRNA Quantification Levels

1. All the reagents are thaw on ice, for 20 min, mixed gently and spin-down prior to use [10].

2. For $p27^{kip1}$ mRNA, PTEN mRNA as target genes and HPRT and/or RPL13 mRNA as reference genes, the resulting cDNA is subjected to real-time qRT-PCR using the specific primer set.
3. A master mix, consisting of 0.5 μl of Fw primer and 0.5 μl Rev. primer and 5 μl of SsoAdvance SYBR Green supermix is prepared.
4. Each reaction is performed in duplicate, by adding 6 μl of master mix to 4.5 μl of template *c*DNA.
5. The reaction conditions consist of enzyme activation at 95 °C for 10 min, followed by 40 cycles at 95 °C for 15 s (denaturation), 30 s at 55 °C (annealing), and 35 s at 72 °C (elongation).
6. A melting curve protocol is started immediately after amplification and consists of 1 min heating at 55° followed by 80 steps of 10 s, with a 2 °C increase at each step.
7. The threshold values for threshold cycle determination (Ct) are generated automatically by the SDS Optical System software.
8. Relative mRNA levels are determined following the ΔΔCt method in comparison with control cells.

3.6 Cell Viability Assays

1. Twenty-four hours before transfection, 40×10^3 Hs766T cells in DMEM-HG culture medium are added to each well of a 48-multiwell plate.
2. Twenty-four hours after transfection (according to Subheading 3.4), chemotherapeutic drugs are diluted in the medium and added to each well (*see* **Note 26**) and incubated for 20 h at 37 °C in a 5% CO2 humidified atmosphere.
3. Cell viability and proliferation are evaluated by a modified Alamar Blue assay, under different experimental conditions. For this purpose 300 μl of DMEM-HG medium containing 10% (v/v) Alamar Blue are added to each well and the cells are incubated at 37 °C for 1 h in a 5% CO2 humidified atmosphere [10, 15].
4. One-hundred fifty microliters of supernatant are collected from each well, and carefully transferred to 96-well plates in order to avoid air bubble formation.
5. Absorbance is measured at 570 and 600 nm and cell viability (as a percentage of untreated control cells) is calculated according to eq. $(A570–A600)$ of treated cells $\times 100/(A570–A600)$ of control cells. An example of the obtained results is shown in Fig. 3.

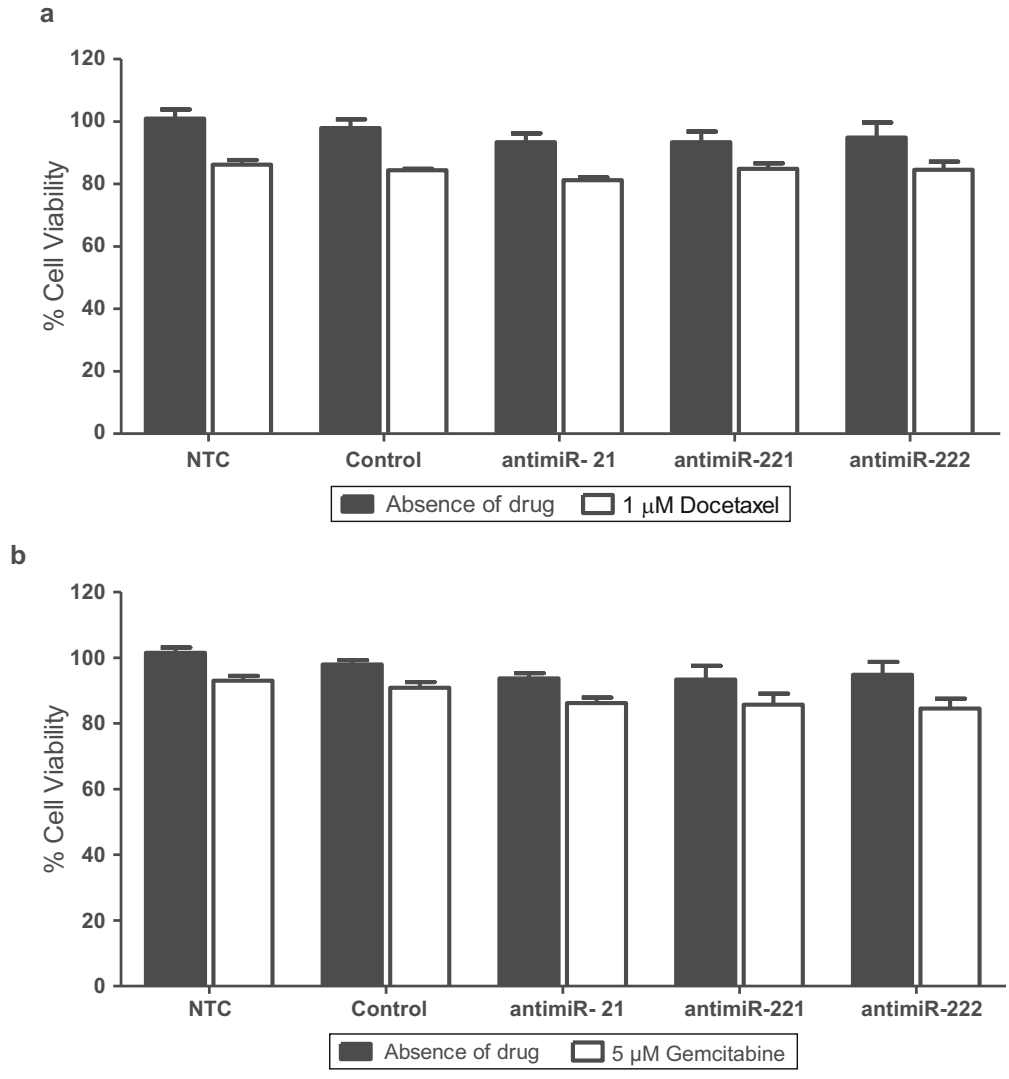

Fig. 3 Cell viability after treatment with anti-miR oligonucleotides and chemotherapeutic drugs. Hs766T cells were transfected with lipoplexes containing 80 nM of antimiR-21, antimiR-221, antimiR-222, or scrambled (control) oligonucleotides. After 24 h, the cells were incubated in the absence or presence of 1 μM of docetaxel (**a**), 5 μM of gemcitabine (**b**) or 15 μM of sunitinib (**c**), for 24 h. Cell viability was measured by the Alamar Blue assay as described in Material and Methods. Data are expressed as the percentage of nontreated control (NTC) cells and correspond to mean ± S.D. obtained from triplicates of three independent experiments. $^{*}p < 0.05$, $^{***}p < 0.001$ correspond to values that differ significantly from those obtained in the control condition

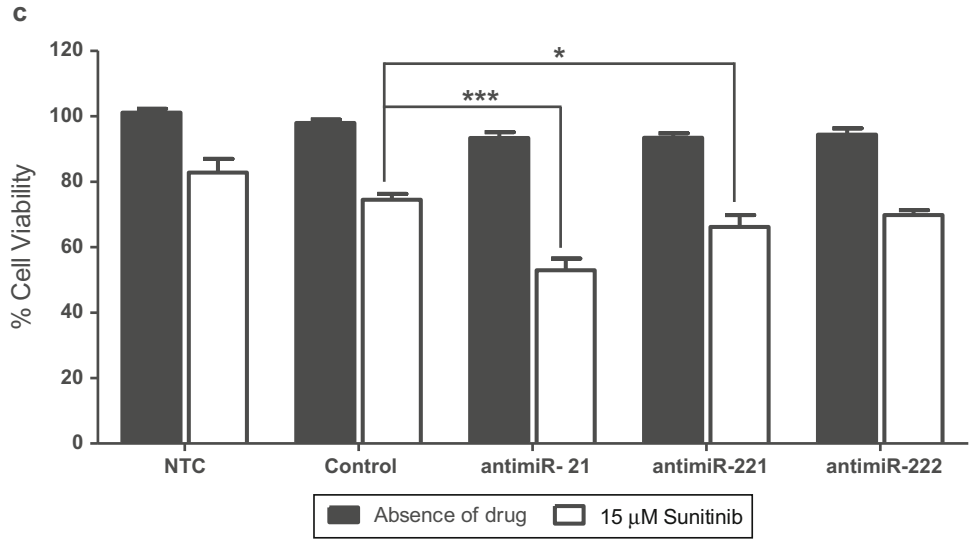

Fig. 3 (continued)

4 Notes

1. All the solutions should be prepared in water with a resistivity of 18.2 MΩ-cm and total organic content of less than five parts per billion.
2. Since the use of the sulfuric acid solution results in an exothermic reaction this solution should be prepared on ice.
3. The preparation of the Fiske and Subbarow reagent requires continuous stirring of the solution for 4 h. The solution is then allowed to stand overnight and is subsequently filtered.
4. Prepare all the solutions with RNase-free water by treating water with 0.1% DEPC. TBS and HEPES solutions cannot be treated with 0.1% DEPC, because it reacts with amine groups making DEPC unavailable to inactivate RNases. This effect is overcome by 1% DEPC. Autoclave in the end to remove any traces of DEPC.
5. This solution should be prepared freshly (immediately before use). All the components are very toxic. Use in hotte.
6. This solution should be prepared the day before the beginning of the experiment and stored at −20 °C. The composition of the hybridization buffer may vary, according to the effectiveness of the hybridization process.
7. This solution should be prepared the day before the beginning of the experiment and stored at 4 °C.

8. This solution should be prepared the day before the beginning of the experiment and stored at 4 °C.
9. The maximum recommended input of cells for RNA extraction, with the indicated extraction kit, is 3×10^6 cells.
10. Lysis Buffer was prepared using 10 μl of β-mercaptoethanol per 1 ml of Lysis Solution, in order to inactivate the high RNase content existing in pancreatic tumor cells.
11. Percentage of carboxyfluorescein-PE higher than 0.1 mol% leads to an overload of fluorescence inside the cells, which decreases the quality of the confocal microscopy images.
12. The amount of phospholipids is evaluated by colorimetric analysis of the molybdate blue resulting from the conversion of inorganic phosphate into phosphomolybdic acid. After being reduced, phosphomolybdic acid acquires a blue coloration (molybdate blue), whose intensity is proportional to the amount of inorganic phosphate produced from the acidic hydrolysis of the phospholipids [13, 14].
13. The time of acidic hydrolysis can be reduced to 1 h by increasing the temperature to 250 °C or above. An alternative procedure involving sulfuric acid digestion is described in [17].
14. Hs766T cells grow as a monolayer and should be detached by treatment with a trypsin solution (0.25%) before reaching 100% confluence in order to be maintained in the exponential growth phase.
15. The washing procedure facilitates the complete removal of the culture medium (which inhibits trypsin action due to the presence of the serum), including Ca^{2+} and Mg^{2+}, which are necessary to the cell attachment.
16. During cell detachment, vigorous shaking of the cells should be avoided in order to prevent the formation of cell clusters, which can complicate the determination of cell density.
17. The cells can be left in PBS at 4 ° C for a few days, until proceeding with the protocol.
18. In this step, the original protocol (70% ethanol overnight) was modified in accordance with what was described in Subheading 3.5.1..
19. Do not exceed more than 16 h of incubation as it may cause unspecific labeling. Incubate for longer than 16 h only when the detection is weak. To accomplish a humid atmosphere, use a recipient full of water and keep it inside the incubator.
20. With medium-high RNA content samples, it should be visible a small white tangle.

21. Add the elution buffer carefully, without touch with the pipette into the resin. Make sure the elution buffer covers all the resin surface.
22. Decrease the volume of elution buffer if low RNA content is expected.
23. When RNA samples are highly concentrated, dilution in RNase-free water is advised.
24. When a large number of cDNA syntheses are performed, a master mix containing the whole volume of reaction buffer and enzyme mix is prepared, and posteriorly distributed in equal volumes per each tube.
25. When a larger number of conditions are being tested, a master mix is prepared and carefully distributed for each of 96-well plates, where the template cDNA has previously been added. The 96-well plate is sublimated to spin-down prior to being inserted in the thermocycler to avoid bubbles.
26. All drug stocks are kept on ice, except for gemcitabine that is kept at room temperature, and protected from light during these experiments.

References

1. Saif MW (2011) Pancreatic neoplasm in 2011 : an update. J Pancreas 12:316–321
2. Hidalgo M, Von Hoff DD (2012) Translational therapeutic opportunities in ductal adenocarcinoma of the pancreas. Clin Cancer Res 18:4249–4256
3. Siegel R, Naishadham D, Jemal A (2012) Cancer statistics, 2012. CA Cancer J Clin 62:10–29
4. Marco MDI, Cicilia RDI, Macchini M et al (2010) Metastatic pancreatic cancer : is gemcitabine still the best standard treatment ? (Review). Oncol Rep 23:1183–1192
5. Mardin WA, Mees ST (2009) MicroRNAs: novel diagnostic and therapeutic tools for pancreatic ductal adenocarcinoma? Ann Surg Oncol 16:3183–3189
6. Zhang Y, Li M, Wang H et al (2009) Profiling of 95 microRNAs in pancreatic cancer cell lines and surgical specimens by real-time PCR analysis. World J Surg 33:698–709
7. Szafranska E, Davison TS, John J et al (2007) MicroRNA expression alterations are linked to tumorigenesis and non-neoplastic processes in pancreatic ductal adenocarcinoma. Oncogene 26:4442–4452
8. Volinia S, Calin G, Liu CG et al (2006) A microRNA expression signature of human solid tumors defines cancer gene targets. Proc Natl Acad Sci U S A 103:2257–2261
9. Bloomston M, Frankel WL, Petrocca F et al (2007) MicroRNA expression patterns to differentiate pancreatic adenocarcinoma from normal pancreas and chronic pancreatitis. JAMA 297:1901–1908
10. Passadouro M, Pedroso de Lima MC, Faneca H (2014) MicroRNA modulation combined with sunitinib as a novel therapeutic strategy for pancreatic cancer. Int J Nanomedicine 9:3203–3217
11. Faneca H, Düzgünes N, Pedroso de Lima MC (2010) Fluorescence methods for evaluating lipoplex-mediated gene delivery. In: Weissig V (ed) Methods in molecular biology: liposomes, vol 606. Humana Press Inc., New Jersey, pp 425–437
12. Faneca H, Simões S, Pedroso de Lima MC (2004) Association of albumin or protamine to lipoplexes: enhancement of transfection and resistance to serum. J Gene Med 6:681–692

13. Fiske CH, Subbarow Y (1925) The colorimetric determination of phosphorus. J Biol Chem 66:375–400
14. Bartlett GR (1959) Phosphorus assay in column chromatography. J Biol Chem 234:466–468
15. Faneca H, Faustino A, Pedroso de Lima MC (2008) Synergistic antitumoral effect of non-viral HSV-Tk/GCV gene therapy and vinblastine in mammary adenocarcinoma cells. J Control Release 126:175–184
16. Lu J, Tsourkas A (2011) Quantification of miRNA abundance in single cells using locked nucleic acid-FISH and enzyme-labeled fluorescence. Methods Mol Biol 680:77–88
17. Düzgüneş N (2003) Preparation and quantitation of small unilamellar liposomes and large unilamellar reverse-phase evaporation liposomes. Methods Enzymol 367:23–27

Chapter 12

Evaluation of MicroRNA Delivery In Vivo

Rikki A.M. Brown, Kirsty L. Richardson, Felicity C. Kalinowski, Michael R. Epis, Jessica L. Horsham, Tasnuva D. Kabir, Marisa H. De Pinho, Dianne J. Beveridge, Lisa M. Stuart, Larissa C. Wintle, and Peter J. Leedman

Abstract

MicroRNAs (miRNAs) are a family of short noncoding RNA molecules that fine-tune expression of mRNAs. Often their altered expression is associated with a number of diseases, including cancer. Given that miRNAs target multiple genes and "difficult to drug" oncogenes, they present attractive candidates to manipulate as an anti-cancer strategy. MicroRNA-7 (miR-7) is a tumor suppressor miRNA that has been shown to target oncogenes overexpressed in cancers, such as the epidermal growth factor receptor (EGFR) and the nuclear factor-κ B subunit, RelA. Here, we describe methods for evaluating systemic delivery of miR-7 using a lipid nanoparticle formulation in an animal model. The microRNA is delivered three times, over 1 week and tissues collected 24 h after the last injection. RNA and protein are extracted from snap frozen tissues and processed to detect miRNA distribution and subsequent assessment of downstream targets and signaling mediators, respectively. Importantly, variability in efficiency of miRNA delivery will be observed between organs of the same animal and also between animals. Additionally, delivering the microRNA to organs other than the liver, particularly the brain, remains challenging. Furthermore, large variation in miRNA targets is seen both within tissues and across tissues depending on the lysis buffer used for protein extraction. Therefore, analyzing protein expression is dependent upon the method used for isolation and requires optimization for each individual application. Together, these methods will provide a foundation for those planning on assessing the efficacy of delivery of a miRNA in vivo.

Key words MicroRNA, miR-7, Systemic microRNA delivery, EGFR, RelA, Akt signaling, RNA isolation, Protein extraction, Mouse tissues

1 Introduction

MicroRNAs (miRNAs) are short, noncoding RNA molecules (~22 nucleotides) that fine-tune the expression of messenger RNAs (mRNAs). They function through imperfect pairing to the 3-′-untranslated region (3′-UTR) of specific target mRNAs, repressing their translation or inducing degradation [1]. miRNAs have crucial roles in many processes in normal biology and development, and altered expression of miRNAs is associated with numerous

Wei Wu (ed.), *MicroRNA and Cancer: Methods and Protocols*, Methods in Molecular Biology, vol. 1699,
DOI 10.1007/978-1-4939-7435-1_12,

diseases, including cancers [2]. In cancer, the low abundance of tumor suppressor miRNAs permits elevation of oncogenes and conversely, high expression of oncogenic miRNAs downregulates tumor suppressor genes, thereby facilitating uncontrolled growth, metastasis, and resistance to therapies [3]. Thus, they present ideal pharmacological targets to exploit as an anti-cancer strategy.

The epidermal growth factor receptor (EGFR) is overexpressed in a number of cancers including primary liver (hepatocellular carcinoma, HCC) and head and neck cancer [4, 5]. The EGFR activates downstream signaling primarily through the phosphatidylinositol 3-kinase (PI3K)-Akt pathway, which promotes proliferation and metastasis of cancer cells [6]. The nuclear factor-kappa B (NF-κB) signaling pathway is also hyperactive in cancers, such as HCC and melanoma, whereby it induces tumor growth, metastasis, and resistance to therapies [7, 8]. Constitutive activation of Akt can upregulate NF-κB and promote tumor progression, thus implicating these pathways as important therapeutic targets [9]. MicroRNA-7 (miR-7) is a tumor suppressor miRNA, its expression being significantly decreased in several tumors, including HCC, head and neck cancer, glioma, and colorectal carcinoma [10, 11]. miR-7 inhibits expression of numerous oncogenes, including EGFR and the NF-κB subunit RelA [10, 11]. Accumulating evidence has shown that through regulation of these pathways, miR-7 is able to inhibit proliferation and metastasis, and sensitize drug-resistant cells to other therapies such as the EGFR inhibitor, erlotinib [12, 13]. Therefore, miR-7 is an attractive candidate for future clinical development and in particular for miRNA replacement therapy.

Delivery of a miRNA for clinical benefit however is not without its challenges. Current approaches have been described in a number of reviews, including that by Krützfeldt [14]. The most advanced approach for systemic delivery is via lipid nanoparticles as a carrier system, a number of which are currently underway in Phase I–III human clinical trials in the treatment of solid cancers [15]. However, delivery to organs other than the liver is challenging and toxicity of the carrier remains a concern [15]. Therefore, preclinical assessment of miRNA replacement using animal models is required to evaluate the efficiency of delivery to liver and other organs, while elucidating the potential safety. Here, we describe a method for evaluating the efficiency of systemic delivery of a miRNA, miR-7 using a lipid formulation in vivo. The miRNA is complexed with a lipid nanoparticle, which when injected intravenously will circulate in the bloodstream, reach its target organ, passively fuse with the cell membrane, and deliver its pay-load. To determine miRNA distribution following delivery, several tissues are collected during necropsy, rapidly frozen and disrupted via homogenization with appropriate lysis buffers for RNA and protein isolation. TaqMan miRNA probes specific for the miRNA of interest and internal

controls are used to determine the fold change of the miRNA in the organs of choice, following miRNA administration. Expression of target mRNAs is determined by reverse transcription-quantitative polymerase chain reaction (RT-qPCR) and reduced expression serves in validating functional consequences of miRNA delivery into tissues. Given that miRNAs do not always degrade transcripts, but rather repress their translation, a decrease in target mRNA transcripts may not always be evident. Importantly, confirming the downstream consequence on the corresponding target protein expression will indicate successful delivery and imply therapeutic potential (through downregulation of oncogenic signaling). Together these techniques allow effective evaluation of the efficiency of systemic delivery of miRNAs in vivo.

2 Materials

2.1 In Vivo Study

1. Ambion Pre-miR miRNA precursor molecules: miR-7-5p (miR-7, Thermo Fisher Scientific, Waltham, MA, USA, #AM17100, PM10047) and miRNA negative control #1 (miR-NC; Thermo Fisher Scientific, #AM17110). Resuspended to 50 μM stocks with RNase-free water and stored at −20 °C.
2. Invivofectamine 3.0 Reagent (Thermo Fisher Scientific).
3. RNase-free water (Thermo Fisher Scientific).
4. Phosphate-buffered saline (PBS) pH 7.4.
5. Insulin syringe 0.5–1.0 cc.
6. Needles 26–29 gauge.
7. 5–8 week old male or female C57BL/6 mice.
8. Custom-made mouse restraining device (*see* Fig. 1c).
9. Small animal heat lamp or heat source approved for small animal use. Avoid heat sources that may cause thermal injuries to the mice.

2.2 Preparation of Animal Tissue and Lysis

1. Animal dissection kit.
2. Container with 100% ethanol and dry ice for flash freezing tissue.
3. 1.5 mL collection tubes with screw cap (Sarstedt, Nümbrecht, Germany).
4. 2 mL Tough tubes for homogenization (Qiagen, Hilden, Germany).
5. Stainless-steel beds 5 mm (Qiagen). Treat beads with RNase away (Thermo Fisher Scientific) for 1 h, and then rinse with

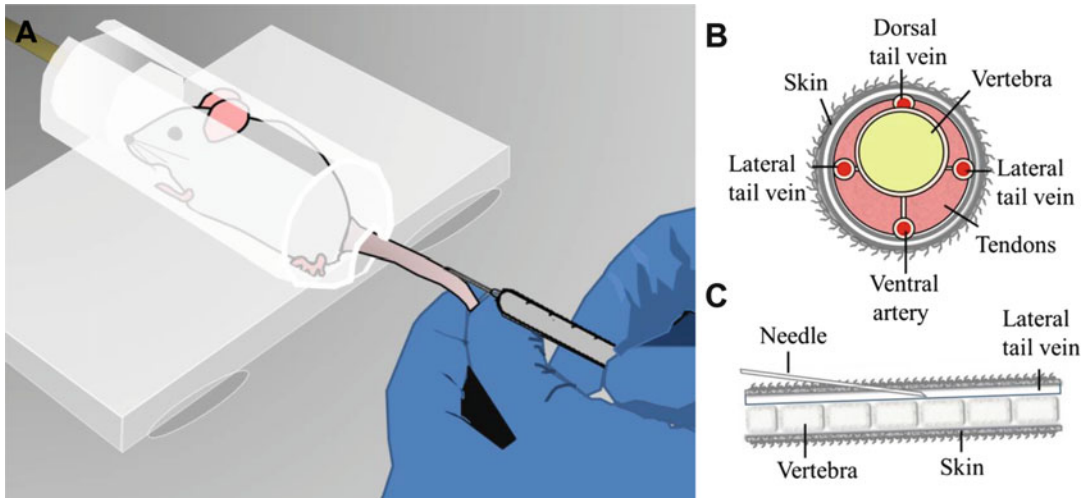

Fig. 1 Demonstration of mouse restraint, location of blood vessels, and positioning of needle for tail vein injection of compound (**a**) mouse restrainer and tail vein injection technique, (**b**) axial section of mouse tail anatomy, and (**c**) sagittal cross section of mouse tail with needle in position

water treated with 0.1% (v/v) diethylpyrocarbonate (DEPC, Sigma-Aldrich, St. Louis, MO, USA).

6. Scalpel, petri dish, and esky with dry ice for cutting tissues.
7. TissueLyser II (Qiagen) or another instrument capable of homogenizing tissues.

2.3 Preparation of RNA, Reverse Transcription, and RT-qPCR

1. mirVana™ miRNA Isolation Kit, with phenol (Thermo Fisher Scientific).
2. 100% ethanol (200 proof).
3. Qubit RNA HS kit (Thermo Fisher Scientific).
4. QuantiTect Reverse Transcription kit (Qiagen).
5. QuantiTect Primer Assays (Qiagen): Mm_EGFR_1_SG (#QT00101584), Mm_HPRT_1_SG (#QT00166768) and Mm_B2M_2_SG (#QT01149547).
6. Sensimix SYBR Hi-ROX Kit (Bioline, London, UK).
7. Ultrapure DNase/RNase-free water (Thermo Fisher Scientific).
8. Nanodrop spectrophotometer (Thermo Fisher Scientific).
9. Qubit 3.0 Fluorometer (Thermo Fisher Scientific).
10. PCR Thermo cycler.
11. Rotorgene 6000 (Qiagen) or another instrument capable of performing RT-qPCR.

2.4 Taqman miRNA Assay

1. TaqMan MicroRNA Reverse Transcription Kit (Thermo Fisher Scientific).
2. TaqMan MicroRNA Assays (Thermo Fisher Scientific): dme--miR-7 (#000268) and snoRNA202 Control (#4427975).
3. TaqMan Fast Universal PCR Master Mix (2×), no AmpErase, no UNG (Thermo Fisher Scientific).
4. Clear Adhesive Films (Thermo Fisher Scientific).
5. Ultrapure DNase/RNase-free water (Thermo Fisher Scientific).
6. PCR Thermo cycler.
7. Rotorgene 6000 (Qiagen) or another instrument capable of performing RT-qPCR.

2.5 Preparation of Protein Extracts for SDS-PAGE and Immunoblotting

1. Radioimmunoprecipitation assay buffer (RIPA): 5 M NaCl, 0.5% deoxycholate (w/v), 1% Nonidet P-40 (NP-40; v/v), 10% sodium dodecyl sulfate (SDS; w/v), 1 M Tris, pH 8.0. Store at 4 °C.
2. Laemmli buffer: 62.5 mM Tris–HCl, pH 6.8, 25% glycerol (v/v), 2% SDS (w/v), 0.01% bromophenol blue (w/v). Store at room temperature.
3. Urea buffer: 4% SDS (w/v), 125 mM Tris, 8 M Urea, 40% glycerol (v/v). Store at room temperature.
4. Cytoplasmic extraction buffer (CEB): 10 mM HEPES pH 7.5, 3 μM $MgCl_2$, 40 mM KCl, 5% glycerol (v/v), 0.2% NP-40 (v/v). Store at 4 °C.
5. Reverse Phase Protein Array (RPPA) buffer: 1% Triton X-100 (v/v), 50 mM HEPES, pH 7.4, 150 mM NaCl, 1.5 mM $MgCl_2$, 1 mM EGTA, 100 mM NaF, 10 mM Na pyrophosphate, 1 mM Na_3V_{O4}, 10% glycerol (v/v). It must be prepared fresh.
6. Tissue protein extraction reagent (T-Per; Thermo Fisher Scientific). Store at room temperature.
7. To each protein lysis buffer add one Complete Mini EDTA-free Protease Inhibitor Cocktail tablet (Roche, Indianapolis, IN) and two PhosSTOP Phosphatase Inhibitor Cocktail tablets (Roche) per 10 mL of buffer prior to use to inhibit protease and phosphatase activity in homogenates.
8. DC protein assay kit II (Bio-Rad, Hercules, CA, USA) for the determination of total protein concentrations from tissue homogenates.
9. Microtiter plate and spectrophotometer capable of reading absorbance at 750 nm.

2.6 SDS-Polyacrylamide Gel Electrophoresis (SDS-PAGE)

1. NuPAGE Novex 4–12% Bis-Tris Precast Gels (Thermo Fisher Scientific). Store at 4 °C.
2. NuPAGE MOPS SDS Running Buffer (20×; Thermo Fisher Scientific). Dilute to 1× with deionized water. Store at room temperature.
3. NuPAGE LDS Sample Buffer (4×; Thermo Fisher Scientific), NuPAGE Sample Reducing Agent (10×; Thermo Fisher Scientific) and NuPAGE Antioxidant (Thermo Fisher Scientific). Store LDS Sample Buffer at room temperature and other reagents at 4 °C.
4. Precision Plus Protein Kaleidoscope Prestained SDS-PAGE protein markers (Bio-Rad). Store at −20 °C.
5. XCell SureLock Mini-Cell SDS-PAGE Gel Electrophoresis System (Thermo Fisher Scientific).

2.7 Immunoblotting for Active and Total EGFR, Akt and RelA, and α-Tubulin (or Other Housekeeping Genes)

1. Transfer buffer: 25 mM Tris, 190 mM glycine, 10% methanol (v/v). Store at 4 °C.
2. Polyvinylidene difluoride (PVDF) membrane for common immunoblotting applications (EMD Millipore, Billerica, MA, USA).
3. Precut filter paper (90 mm × 70 mm) (Bio-Rad).
4. Tris-buffered saline with Tween (TBS-T): 20 mM Tris–HCl pH 7.4, 150 mM NaCl, 0.1% Tween 20 (v/v). Store at room temperature.
5. Blocking buffer: 5% nonfat dried milk (w/v; supermarket sourced) in TBS-T. Store at 4 °C.
6. Primary antibodies: anti-phospho-EGFR (Tyr-1173, Cell Signaling Technology, Danvers, MA, USA, #4407), anti-EGFR (Abcam, Cambridge, UK, #ab52894), anti-Akt (Cell Signaling Technology, #9272), anti-phospho-Akt (Ser-473; Cell Signaling Technology, #4060), anti-phospho-RelA (Ser-536, Cell Signaling Technology, #3033), anti-RelA (Cell Signaling Technology, #8242), anti-α-tubulin (Abcam, #ab4074). Dilute primary antibodies 1:1000 (v/v) in 1% (w/v) nonfat dried milk in TBS-T prior to use. Some antibodies may be stored at −20 °C and reused.
7. Secondary antibodies: Amersham ECL Rabbit or Mouse IgG, HRP-linked whole Ab (GE Healthcare, Little Chalfont, UK). Dilute antibodies to 1:10,000 (v/v) in 1% (w/v) nonfat dried milk in TBS-T prior to use. The appropriate secondary antibodies are used according to the species in which the primary antibody to be detected was raised.
8. Luminata Crescendo Western HRP substrate (EMD Millipore) and ECL-Hyperfilm (GE Healthcare).

9. Western blot stripping buffer: 25 mM glycine-HCl pH 2.0, 1% SDS (w/v). Store at room temperature.

3 Methods

Therapeutic application of microRNAs can involve either local or systemic delivery strategies. Local delivery involves direct injection into the tissue of interest, while systemic delivery requires administration of the miRNA to multiple targeted organs via circulation. Local delivery can involve injection of naked RNA molecules; however, systemic delivery generally requires a carrier to withstand degradation by the circulating exonucleases and to evade immune cells and clearance by the kidneys. Current carrier modalities include lipid moieties, non-lipid nanoparticles, polymers, peptides, and other conjugates. Here, we describe how to evaluate the systemic delivery of miR-7, using a lipid formulation as a carrier. All animal experimentation and protocols must be approved by an Institutional Animal Ethics Committee and must conform to governmental regulations regarding the acquisition, transport, housing, care, and disposal of laboratory animals prior to starting experiments.

3.1 Preparation of miRNA for In Vivo Delivery

1. Centrifuge synthetic precursor miRNA molecules briefly to ensure all lyophilized precursor miRNA molecules are collected at the bottom of the tube. Resuspend precursor miRNA molecules to a concentration of 10 mg/mL using RNase-free water. Vortex to mix and centrifuge the tube briefly to ensure all solution is collected at the bottom of the tube.
2. Prepare a sample that is equivalent to 1 mg/kg miRNA in a 20 g mouse with a 100 μL injection volume. When preparing a master mix of miRNA complex for injection, include enough for one extra injection to account for pipetting error or difficulties when performing the tail vein injection technique. Prepare separate master mixes for the miRNA of interest and the negative control miRNA.
3. Using the 10 mg/mL miRNA precursor stock prepare 4.17 μL of precursor miRNA molecule solution at a concentration of 4.8 mg/mL in RNase-free water (*see* table below) to a 1.5 mL tube. Thaw complexation buffer (supplied with the Invivofectamine 3.0 Reagent kit) and add 4.17 μL to the miRNA precursor to give a 1:1 ratio of precursor miRNA molecule and complexation buffer solution.
4. Bring Invivofectamine 3.0 solution to room temperature and add an equal volume to the precursor miRNA molecule and complexation buffer solution (8.34 μL) (1:1 ratio). Centrifuge

the tube briefly to ensure all solution is collected at the bottom of the tube.

5. Incubate the mixture for 30 min at 50 °C.
6. Dilute the mixture sixfold by adding 83.32 μL PBS pH 7.4. Pipette up and down to mix well. This forms the 100 μL for injection and is equivalent to 1 mg/kg miRNA in a 20 g mouse. The complex can be stored at 4 °C for up to 1 week.
7. Weigh the mouse to be injected. Use this weight to calculate the exact volume to inject into the tail vein to give 1 mg/kg miRNA. For example, if the mouse weighs 18 g the injection volume will be 90 μL for that mouse.
8. Proceed with tail vein injection of the complex.

Reagent	**1×**
Precursor miRNA (4.8 mg/mL)	4.17 μL
Complexation buffer	4.17 μL
Invivofectamine 3.0	8.34 μL
PBS	83.32 μL
Total volume	**100 μL**

3.2 In Vivo miRNA Delivery

1. The lateral veins of the tail are the most frequently used veins for intravenous injection (*see* Fig. 1). Warm the mouse for 5–15 min in the cage using a small animal heat lamp or by placing the mouse in an approved warming container (*see* **Note 1**). This enables the veins to be seen when the tip of the tail is lifted and rotated slightly in either direction.
2. The mouse should be secured in a suitable restrainer (*see* Fig. 1a). The injection site can be prepared by swabbing the area with a suitable disinfectant such as 70% ethanol (*see* **Note 1**) to clean the surface.
3. Draw the solution into the syringe and dispel any bubbles by manually flicking the side of the syringe with your finger and moving the plunger to a point until a miniscule of droplet becomes visible at the tip of the needle. Make sure the bevel is up and the syringe positioned so that the volume marks can be clearly seen when injecting.
4. Extend the tail with one hand to produce a flat and more visible working area; the tail should be under tension. With the other hand, insert the needle at a minimal angle, feeding the needle into the vein approximately 5 mm (*see* Fig. 1b, c) and slowly inject the solution (*see* **Notes 2** and **3**).

5. Dispose of all used sharps into a biological hazard sharps container. Monitor the animal following injection for signs of immobility or respiratory compromise (if symptoms are visible euthanasia is required or consult with a certified veterinarian if available).
6. Injections are to be performed three times for 1 week (total of three injections).
7. At the endpoint of experiment (24 h after last injection), the mice should then be humanely euthanized with an approved method in your Animal Ethics Application.

3.3 Preparation of Tissue(s) and Homogenization with Qiagen TissueLyser II

1. To evaluate miRNA delivery and regulation of its target gene expression both RNA and protein samples must be collected. For RNA a method must be selected to extract both total and short RNAs. For the assessment of relative protein expression the localization of the protein of interest must be taken into account and the most appropriate lysis buffer for the tissue (s) selected. Therefore, it is best to compare lysis buffers and optimize conditions for your particular application. Figure 3a shows examples comparing several different lysis buffers in different tissues using the methods described herein. From these results T-Per Tissue Lysis Reagent was found to be optimal (highest detection across cell compartments and most consistent across tissues) and was used to analyze protein target gene expression in tissues following systemic delivery of miR-7 as demonstrated in Fig. 3b.
2. To collect the tissues secure the carcass on a clean dissection board and use dissecting scissors to expose the tissues of interest. In the example data (*see* Figs. 2 and 3) provided liver and lung samples were collected first, followed by tongue and brain. Take care during lung and brain collection as the tissues are delicate and easily damaged (*see* **Notes 4** and **5**).
3. Immediately following dissection transfer tissue to a collection tube. Drop the tube into a container containing 100% ethanol with dry ice to rapidly freeze tissues. Samples may be stored at −80 °C for short-term and Liquid N2 for long-term.
4. Prior to starting disruption and homogenization place the TissueLyser Adaptor(s) at −20 °C for 30 min. Store tissue on dry ice during the preparation to prevent thawing. Place a petri dish on dry ice and coax the tissue out of the tube. Cut the organ with the scalpel with a gentle rocking motion, weigh out appropriate amount of tissue and add to a 2 mL tough tube (*see* **Note 6**).
5. Add an appropriate amount of lysis buffer. In the example data provided 100 μL of lysis buffer from a mirVana miRNA isolation kit was added to approximately 10 mg of tissue for RNA

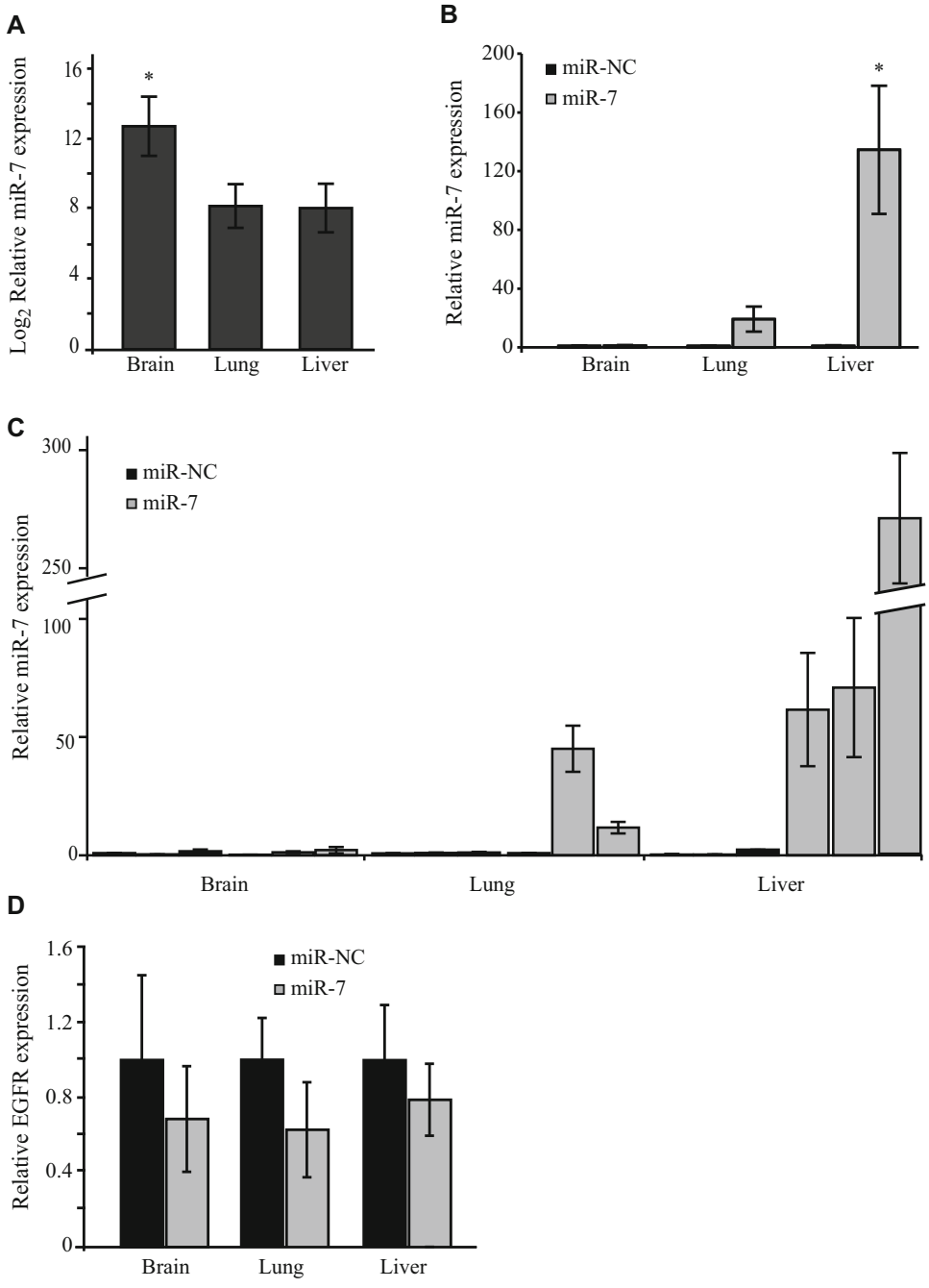

Fig. 2 Endogenous miR-7 expression is highest in brain, but following systemic administration is primarily upregulated in liver tissue and slightly in lung. (**a**) Endogenous miR-7 expression in murine tissues. Brain, lung, and liver tissue samples were collected from C57BL/6 ($n = 3$) mice, RNA was extracted from tissues using the mirVana miRNA isolation kit and TaqMan MicroRNA Assays were used to detect miR-7 via RT-qPCR. miR-7 expression was normalized using Sno202 as a reference gene. Values indicate the average normalized miR-7 expression in different tissues on a Log2 scale with 95% confidence interval error bars. *$p < 0.05$. (**b**) miR-7 expression in murine tissues following systemic miRNA administration. C57BL/6 mice (n = 3 per group) were

extraction. For protein lysis 350 μL of various lysis buffers were added to 5–15 mg of tissue (*see* **Note 7**). Store samples on wet ice.

6. Add a stainless-steel bead with forceps in each tube.
7. Place the tubes in the TissueLyser Adaptor, balancing the tubes and assemble the apparatus according to the manufacturer's instructions (Qiagen).
8. Set the oscillation frequency to 30 Hz and homogenize the tissues in 1 min intervals, resting the samples on ice in between rounds of homogenization. Soft tissues that homogenize easily may require only 1 min in total (e.g., brain), while fibrous tissues (e.g., tongue) require more time. Therefore, the time should be optimized for the tissue of interest. Disruption for 6×1 min at 20–30 Hz is usually sufficient to release RNA. The position of the tubes in the Adaptor should be rotated and cooled on ice in between cycles for uniform disruption (*see* **Note 8**).
9. Store the samples at −80 °C for a single freeze/thaw cycle to ensure best recovery. After thawing, transfer the homogenate to a microcentrifuge tube and discard the tough tube and bead (do not reuse beads). Clear the homogenate of debris by centrifuging at maximum speed ($10{,}000 \times g$) for 5 min at 4 °C and transfer the supernatant to a new tube (*see* **Note 9**). Continue with RNA extraction or protein analysis.

3.4 Total RNA Extraction Including Small RNAs from Tissue Homogenate

1. Although some RNA extraction kits allow enrichment for small RNAs, total RNA extraction procedures must be followed to isolate both coding and noncoding long (>200 base pairs) and short RNAs (<200 base pairs) to assess miRNA distribution and its target gene regulation.
2. To perform RNA extraction, add 1/10 volume of miRNA Homogenate Additive to the tissue homogenate (for example for 100 μL of homogenate add 10 μL Homogenate Additive), and mix well by vortexing briefly. Leave the mixture on ice for 10 min.

Fig. 2 (continued) treated systemically with miR-NC or miR-7 and brain, liver, and lungs collected to compare miR-7 delivery into these tissues. RNA was extracted and RT-qPCR was performed as described previously. Values indicate average normalized miR-7 expression relative to miR-NC-treated mice across the different tissues. Error bars are 95% confidence intervals. **p*-value <0.05 comparing miR-NC and miR-7 expression in liver by Student's *t*-test. (**c**) miR-7 expression in murine tissues of individual animals following systemic miRNA administration. Values represent normalized miR-7 expression relative to miR-NC treated mice from individual mice, highlighting variability across animals. Error bars are 95% confidence intervals. (**d**) Relative EGFR expression within selected organs. Mice were treated systemically with miR-NC or miR-7 and assessed for effects on EGFR within the brain, liver, and lungs of mice. EGFR expression was normalized to HPRT-1 and B2M reference genes and found to be nonsignificant between treatments ($p > 0.05$; CI = 0.95)

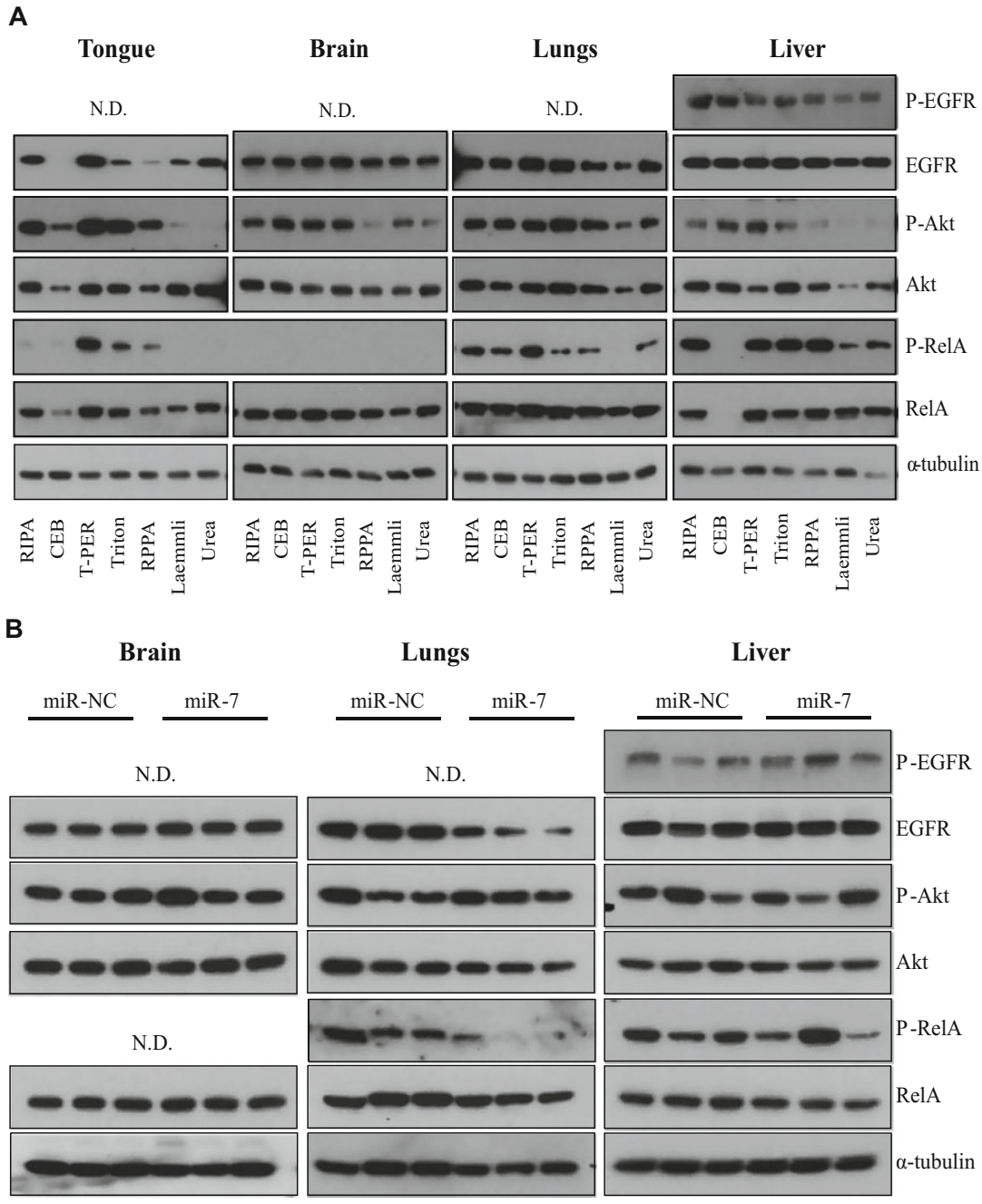

Fig. 3 Extraction of proteins from tissues requires optimization for individual application and can be used to evaluate regulation of target protein expression following systemic miRNA delivery. (**a**) Evaluation of different lysis buffers for protein detection in murine tissues. Tongue, brain, liver, and lung samples were collected from C57BL/6 mice ($n = 1$) weighed and distributed into different protein lysis buffers for homogenization. Homogenates were run on denaturing gels, transferred to PVDF and processed for immunoblotting analysis of EGFR, Akt, RelA, and their active phosphorylated forms, denoted "P-". α-tubulin was used as a loading control. (**b**) Relative expression of miR-7 target proteins following systemic delivery of miRNA in murine

3. Add a 1:1 volume of Acid-Phenol:Chloroform that is equal to the initial lysate volume before. For example, if the original lysate volume was 100 μL, add 100 μL Acid-Phenol: Chloroform. Vortex briefly.
4. Centrifuge for 5 min at 10,000 × *g* at room temperature to separate the aqueous and organic phases. After centrifugation, the interphase should be compact; if it is not, repeat the centrifugation.
5. Carefully remove the aqueous (upper) phase without disturbing the lower phase, and transfer it to a fresh RNase-free tube. Note the volume removed.
6. Add 1.25 volumes of room temperature 100% ethanol to the aqueous phase (e.g., if 100 μL was recovered in **step 4**, add 125 μL ethanol).
7. For each sample, place a filter cartridge into one of the collection tubes supplied.
8. Pipette the lysate/ethanol mixture (from the previous step) onto the filter cartridge (up to 700 μL at a time, reuse the filter cartridge if larger lysate volumes are recovered).
9. Centrifuge for ~15 s at 10,000 × *g* to pass the mixture through the filter.
10. Discard the flow-through, and repeat until all of the lysate/ethanol mixture is through the filter. Reuse the collection tube for the wash steps.
11. Apply 700 μL miRNA Wash Solution 1 (working solution mixed with ethanol) to the filter cartridge and centrifuge for ~15 s at 10,000 × *g*. Discard the flow-through from the collection tube, and replace the filter cartridge into the same collection tube.
12. Apply 500 μL Wash Solution 2/3 (working solution mixed with ethanol) and repeat the centrifugation as in the previous step. Repeat washing a second time with the Wash Solution 2/3.
13. After discarding the flow-through from the last wash, replace the Filter Cartridge in the same collection tube and spin the assembly for 1 min to remove any residual fluid (ethanol) from the filter.

Fig. 3 (continued) tissues (C57BL/6 mice $n = 3$). Following miR-7 administration brain, lung and liver samples were processed in T-Per lysis reagent and immunoblotting performed to detect the miR-7 protein targets listed previously and α-tubulin as a loading control. Variation is observed across animals within the same treatment group and with the exception of P-RelA and EGFR decreasing in lung, no obvious trend in protein expression is observed comparing treatment groups. N.D., not detected

14. Transfer the filter cartridge into a fresh collection tube (provided with the kit). Apply 100 μL of preheated (95 °C) Elution Solution or nuclease-free water to the center of the filter, and close the cap. Spin for ~20–30 s at maximum speed to recover the RNA.
15. Collect the eluate (which contains the RNA) and store it at −80 °C for later use.
16. To determine the purity of the RNA samples use a Nanodrop spectrophotometer following the manufacturer's instructions (*see* **Note 10**).
17. To quantitate the RNA samples using the Qubit system set up 2 Assay tubes for the standards and 1 tube for each RNA sample. Prepare the Working Solution by diluting the Qubit RNA Reagent 1:200 in RNA Buffer supplied (200 μL of Working Solution is required for each standard and sample). Prepare the standards with 190 μL of Working Solution and 10 μL of Standard from the tubes supplied. For RNA samples 1–20 μL may be added to Assay tubes and made up to a 200 μL total volume with Working Solution. Vortex briefly and incubate at room temperature for 2 min. Select RNA Assay on the Qubit 2.0 Fluorometer to calibrate with the standards, enter the sample volume added to assay tubes, and quantitate the samples.

3.5 Taqman miRNA PCR for miR-7

1. Allow all kit components to thaw on ice, mix by vortexing, centrifuge and store on ice during the preparation of the samples.
2. In a microcentrifuge tube, prepare separate master mixes for miR-7 and snoRNA202 by scaling the volumes listed in the table below to the desired number of RT reactions, including enough for duplicate reactions (technical replicates) for each RNA sample and to account for pipetting error. Mix gently and centrifuge to bring solution to the bottom of the tube, and then store on ice.

Reagent	**1×**
100 mM dNTPs (with dTTP)	0.15 μL
MultiScribe reverse transcriptase, 50 U/μL	1.00 μL
Reverse transcription buffer (10×)	1.50 μL
RNase inhibitor, 20 U/μL	0.19 μL
RT primer (5×)	3.00 μL
Nuclease-free water	4.16 μL
Total volume	**10.00 μL**

3. Dilute RNA samples to 2 ng/μL with nuclease-free water. Dispense 10 μL of RT master mix into each RT reaction tube or plate well. Add 5 μL (i.e., 10 ng) of RNA sample in duplicate (technical replicates) into the corresponding RT reaction tube or plate well for each assay set.
4. Seal the tubes, mix gently, and centrifuge to bring the solution to the bottom of the tube. Load the reaction tubes or plate into the thermal cycler and start the reaction with the parameters in the table below.

Step	HOLD	HOLD	HOLD	HOLD
Time	30 min	30 min	5 min	∞
Temperature	16 °C	42 °C	85 °C	4 °C

5. In a microcentrifuge tube, prepare the PCR master mixes by scaling the volumes listed in the table to the desired number of PCR reactions. Include extra reactions in your calculation for no template controls and to allow for pipetting error. Mix gently and centrifuge to bring solution to the bottom of the tube. Store on ice.

Reagent	**1×**
TaqMan miRNA assay probe (20×)	1.0 μL
TaqMan universal PCR master mix II (2×), no UNG	10 μL
Nuclease-free water	4.0 μL
Total volume	**15 μL**

6. Dilute RT samples (from **step 4**) to 50 μL.
7. Dispense 15 μL of PCR master mix into each PCR reaction tube or well, including extras for no template control.
8. Add 5 μL of RT product into the corresponding PCR reaction well for each assay set (single PCR reactions as RTs were performed in duplicate). Load the reaction plate or tubes into the real-time quantitative PCR machine and run with the following parameters with detection set to the Green channel and acquiring at the end of the extension step.

	Enzyme activation	PCR (40 cycles)	
Step	HOLD	Denature	Anneal/extend
Time	10 min	15 s	60 s
Temp	95 °C	95 °C	60 °C

9. The general process for analyzing the data from gene expression assays involves viewing the amplification plots and setting

the baseline and threshold values to acquire comparative computed cycle of threshold (CT) values.

10. Statistical analysis of data should be performed in Microsoft Excel or other statistical software. Analysis may be performed using the $2^{-\Delta\Delta CT}$ method derived by Livak and Schmittgen [16] as outlined in the table below. Alternatively, software such as GenEx is a helpful tool for qPCR analysis as pre-processing allows the data to be corrected for PCR efficiency. The example data has been analyzed with basal miR-7 expression in mouse tissues (Fig. 2a) and following systemic delivery of miR-7 via tail vein injection using GenEx software (Fig. 2b, c).

	$CT_{(GE)}$	$CT_{(HK)}$	ΔCT	$\Delta\Delta CT$	$2^{-\Delta\Delta CT}$	$2^{-\Delta\Delta CT}$ control	Comparative expression
Control group (miR-NC)	Raw values	Raw values	$\Delta CT_{miR\text{-}NC} = CT_{(GE)} - CT_{(HK)}$	$\Delta CT_{miR\text{-}NC} - \Delta CT_{miR\text{-}NC}$	2^ (−ΔΔCT)	Average replicates	$2^{-\Delta\Delta CT}{}_{miR\text{-}NC} / 2^{-\Delta\Delta CT}{}_{miR\text{-}NC}$
Experimental group (miR-X)	Raw values	Raw values	$\Delta CT_{miR\text{-}X} = CT_{(GE)} - CT_{(HK)}$	$\Delta CT_{miR\text{-}X} - \Delta CT_{miR\text{-}NC}$	2^ (−ΔΔCT)	–	$2^{-\Delta\Delta CT}{}_{miR\text{-}X} / 2^{-\Delta\Delta CT}{}_{miR\text{-}NC}$

GE: Gene of interest; HK: Housekeeping control.

3.6 Reverse Transcription and Real-Time qPCR for Target Gene Expression

1. Thaw the RNA template on ice and all QuantiTect RT kit components at room temperature. Mix and spin tubes to bring the solution to the bottom of the tube.
2. Prepare the genomic DNA elimination reaction on ice according to the table below, preparing duplicate reactions (technical replicates) for each RNA sample. Mix and store on ice.

Reagent	**1×**
gDNA wipeout buffer (7×)	2 µL
Template RNA	Up to 1 µg*
Nuclease-free water	Variable
Total volume	**14 µL**

*In the example in Fig. 2c a total of 250 ng of RNA was reverse transcribed.

3. Place tubes or plates into a thermo cycler and incubate for 2 min at 42 °C. Then place immediately on ice.
4. Prepare the reverse-transcription master mix on ice according to the table below. Include enough master mix to perform duplicate reactions for each RNA sample and to account for pipetting error. Mix and then store on ice.

Reagent	1×
Quantiscript reverse transcriptase	1 μL
Quantiscript RT buffer (5×)	4 μL
RT primer mix	1 μL
Total volume	**6 μL**

5. Distribute 6 μL of reverse transcription master mix to each RNA sample such that the total volume is 20 μL. Mix and store on ice.
6. Place the tubes or plate into the thermo cycler and incubate for 15 min at 42 °C, followed by 3 min incubation at 95 °C to inactivate the Reverse Transcriptase. Store cDNA on ice during the preparation of the PCR reaction or at −20 °C for long-term storage.
7. For RT-qPCR set up a master mix reaction according to the table below. Include enough reactions to include several standards, no template controls and extra to account for pipetting error. Make serial dilutions of one cDNA template to calculate PCR efficiency. For example, dilute at least one sample 1:10, 1:100, and 1:1000 in duplicate.

Reagent	1×
SensiMix SYBR Hi-ROX (2×)	10 μL
Quantitect primer assay (10×)	0.9 μL
Nuclease-free water	7.1 μL
Total volume	**18 μL**

8. Dispense 18 μL of PCR master mix into each PCR reaction tube or well, including extras for standards and no template control.
9. Add 2 μL of cDNA template or standard into the corresponding PCR reaction well for each assay set (single PCR reactions as RTs were performed in duplicate). Load the reaction plate or tubes into the real-time quantitative PCR machine and run with the following parameters with the detection channel set to Green and acquiring at the end of the extension step.

	Enzyme activation	PCR (40 cycles)		
Step	HOLD	Denature	Anneal/extend	Melt curve
Time	10 min	10 s	30 s	
Temp	95 °C	95 °C	60 °C	57–95 °C in 0.1 °C increments

10. Obtain the CT values and analyze as described for the Taqman assay (Subheading 3.4, **step 10**; *see* **Notes 11** and **12**). Figure 2d shows example data analyzing EGFR expression in tissues following systemic miR-7 delivery. HPRT-1 and B2M were the most appropriate housekeeping controls according to geNORM (GenEx software, Exiqon, Ver 4.4.2.308) and were used to normalize EGFR expression.

3.7 Protein Estimation Using DC Protein Kit II

1. Add 20 μL of Reagent S to each mL of Reagent A that will be needed for the run. If precipitate forms, warm the solution and vortex.
2. Prepare serial dilutions of a protein standard (BSA) in each of the lysis buffers from 0–1.5 mg/mL.
3. Pipet 5 μL of standards or protein samples (generated in Subheading 3.3, **step 9**) into a sterile microtiter plate. Samples may need to be diluted to fall within standard curve, e.g., 1:5 dilution. Remember to take this dilution factor into account when calculating concentration.
4. Add 25 μL of Reagent A + S mixture into each well.
5. Add 200 μL Reagent B into each well. Gently agitate the plate to mix the reagents. Dispel any bubbles with a clean tip.
6. Allow 15 min for color development before reading plate but reactions will be stable for up to 1 h. Read absorbance at 750 nm using a spectrophotometer.
7. Use the absorbance values from the standards to generate a standard curve and use the equation $y = mx + b$ to solve for the protein concentration, taking the initial dilution factor into account. For example, if the samples were diluted 1:5 multiply the concentration calculated from the equation by 5 to determine the original sample concentration.

3.8 SDS-PAGE and Electrotransfer to PVDF Membrane

1. SDS-PAGE and immunoblotting is used for the analysis of relative levels of specific proteins in the tissue homogenates (prepared in Subheading 3.3). For the detection of proteins of interest, protein samples are loaded on a gel and a current run through which separates cellular proteins based on their

molecular weight on a polyacrylamide gel under denaturing conditions, and then transferred onto a PVDF membrane for immunoblot analysis.

2. Sample preparation: in a 1.5 mL tube, place an appropriate volume of tissue homogenate corresponding to 15 μg of protein (quantitated in Subheading 3.7, **step 7** above). To each of these tubes, add 2 μL of 10× reducing agent, 5 μL of 4× LDS sample buffer and distilled water to a final volume of 20 μL.
3. Centrifuge sample tubes briefly to ensure all components are collected at the base of the tube, and incubate at 70 °C for 10 min to denature proteins. After heating, mix samples and centrifuge briefly and cool on ice.
4. Prepare the apparatus for SDS-PAGE: assemble the XCell SureLock Mini-Cell SDS-PAGE Gel Electrophoresis tank according to the manufacturer's instructions. After removing well combs and sticker lining, rinse gels with distilled water and secure into place in the electrophoresis tank. Rinse the wells with 1× NuPAGE MOPS SDS Running Buffer.
5. Fill the inner chamber of the tank (chamber between the gels) with 1× NuPAGE MOPS SDS Running Buffer (~200 mL), supplemented with 500 μL of NuPAGE Antioxidant, until the buffer level covers the wells. Fill the outer chamber with 300 mL of the same running buffer without NuPAGE Antioxidant.
6. Load the protein samples into the wells of the gel. In a separate well on each gel, load a suitable volume of molecular weight (MW) prestained markers (e.g., Bio-Rad Precision Plus Protein Kaleidoscope).
7. Run gels at 150 V and 4 °C until the dye front has almost reached the base of the tank, or until the MW region where the proteins of interest lie is well separated. During this time, prepare the transfer buffer and prechill at 4 °C.

3.9 Immunoblotting for Protein Expression

1. This protocol is derived from the method of Towbin and coworkers [17]. Transfer: following SDS-PAGE, disassemble the gel apparatus and casting plates, and transfer gels into the cold transfer buffer.
2. Assemble the Bio-Rad transfer cassettes by placing, in order, on the "black" side of the cassette, a transfer sponge, a piece of precut filter paper, the polyacrylamide gel, a piece of PVDF Western Blotting Membrane that has been prewet with 100% Methanol, a piece of precut filter paper and a transfer sponge. Pre-soak all items with transfer buffer. Ensure that all surfaces are in contact and all air bubbles are eliminated (a 15 mL centrifuge tube or equivalent may be used to smooth out the bubbles). Close the cassette and place into the Bio-Rad transfer

tank (containing a magnetic stirrer bar) such that the PVDF membrane is between the gel and the anode. Fill the tank with 1 L of transfer buffer.

3. Perform the transfer overnight at 25 V (constant voltage) at 4 °C, with gentle stirring.
4. After transfer, the protein-bound PVDF membranes may either be stored in PBS at 4 °C for later use, or transferred directly into blocking buffer for immunoblotting.
5. Blocking: cover the PVDF membranes with an adequate volume of blocking buffer and gently rock at RT for 1 h.
6. Using the MW markers as a guide, the PVDF membranes may be trimmed and divided into smaller blots, in order to immunoblot for the desired proteins. Place the diluted primary antibodies in the trays containing the appropriate blots (based on the predicted MW for each protein of interest), and incubate for 1 h at room temperature, with gentle rocking.
7. Remove the primary antibodies (can be stored for later use at −20 °C) and wash the blots for 3 × 10 min in blocking buffer.
8. Incubate blots with the diluted secondary antibodies for 1 h at room temperature, with gentle rocking.
9. Discard the diluted secondary antibody solutions and wash the blots for 3 × 10 min in TBS-T.
10. Drain off excess solution and on a glass plate, add Luminata Crescendo Western HRP Reagent dropwise to the blots and incubate for 5 min (*see* **Note 13**). Drain off excess reagent and place blots between plastic sheets in a cassette and expose to Hyperfilm in a dark room for 1 s to 20 min as required. Process the film in a developer following the manufacturer's directions.
11. To strip the membrane wash for 30 min in Western blot Stripping Buffer with gentle rocking at room temperature (*see* **Note 14**). Rinse in PBS for 10 min. Expose blots to Hyperfilm to establish if stripping was successful. Repeat glycine/SDS wash and PBS rinse if necessary. To reprobe the blots, add diluted primary antibody and proceed as described above (no need to reblock with Blocking Buffer).
12. Examples of the signals for EGFR, phospho-EGFR, Akt, phospho-Akt, RelA, phospho-RelA, and α-Tubulin (loading control) are shown in Fig. 3. Several buffers have been compared to determine the preferred lysis method across different tissues (*see* Fig. 3a). The example proteins described herein are not only direct or indirect targets of miR-7, but also represent proteins of different cellular localization (EGFR is membrane bound; Akt, phospho-Akt and RelA are cytoplasmic; and phospho-RelA can be found in the nucleus). T-Per Tissue

Lysis Reagent was then selected as the optimal buffer and used to compare protein expression in tissues from mice treated with systemic miR-7 or miR-NC (*see* Fig. 3b).

4 Notes

1. Ensure the lamp is not so close as to burn the skin of the mouse (ears are especially susceptible to burns from heat lamps), and avoid prolonged exposure times, which will lead to dehydration and sudden death. If the vein remains difficult to view after pre-warming the animal, application of 70% ethanol can further assist in visualization.
2. Accurate placement is confirmed when the blood vessel is visually flushed during compound administration and no resistance felt while pushing on the syringe plunger.
3. The formation of a bolus (tissue will appear white and bulge) at the site of injection indicates improper needle placement. A second attempt should be performed by removing the needle and re-inserting into the same vessel closer to the base of the tail or on the opposite lateral tail vein.
4. For the collection of lungs, cut the rib cage to expose the thoracic cavity. Make two lateral incisions up each side of the ribcage and diaphragm, followed by an incision transversely across the top of the sternum. Cut away neck muscles and bone overlaying the trachea. Then, cut the trachea and gently lift the trachea upward using forceps while snipping away connective tissue with scissors to completely remove the lungs. Rinse lungs in PBS prior to snap freezing to remove any blood [18].
5. For the collection of the brain, use scissors and forceps to remove the skin and muscle overlying the skull. Make a lateral incision at the base of the skull, severing the spinal cord. Using small scissors, insert the bottom blade into the foramen magnum, the opening where the skull opens into the spinal canal, and keeping the scissor tips pointed upward, begin cutting directly up and through the midline of the skull. Use forceps to peel back both halves of the skull exposing the brain. Use curved forceps to slide along the outer edge of the brain and underneath starting at the frontal lobes to disconnect any connective tissue or nerves and gently lift the brain out with a scooping motion with the curved forceps [18].
6. Once the tissue has been removed from the −80 °C freezer, it is important to process it immediately without thawing. This is necessary because as cells thaw, ice crystals rupture both interior and exterior cellular compartments, releasing RNases.

7. The success of homogenization is dependent on the size and composition of beads, the ratio of buffer to samples, amount of starting material, and the parameters used for speed and duration during disruption. The protocol described herein is an example only and should be optimized for individual application.
8. When using a TissueLyser Adapter Set, samples nearer to the TissueLyser move more slowly than samples further away from the TissueLyser. To ensure uniform disruption and homogenization at least two shaking steps should be carried out. After the first shaking step, the TissueLyser Adapter Set should be disassembled and the rack of tubes should be rotated so that the tubes that were nearest to the TissueLyser are now outermost. Cool the tubes for 5 min on ice in between cycles to prevent sample degradation. The TissueLyser Adapter Set should then be reassembled before continuing with the next shaking step.
9. Some fibrous tissues may be difficult to disrupt completely; however, small amounts of debris should have no effect on subsequent RNA purification. Clearing the lysate helps to remove this material prior to RNA and protein extraction.
10. The 260/280 and 260/230 ratios of absorbance values are used to assess the purity of RNA. A 260/280 ratio of ~2.0 is generally accepted as "pure" for RNA. If the ratio is much lower it may indicate the presence of protein, phenol, or other contaminants that absorb at or near 260 or 280 nm. The 260/230 values are commonly in the range of 2.0–2.2 for "pure" nucleic acid. If the ratio is much lower, it may indicate the presence of EDTA, carbohydrates, phenol, or other contaminants that absorb at 260 or 230 nm.
11. The PCR efficiency should be approximately 100%, particularly when using validated primers such as the Quantitect Primer Assays. If the efficiency is below 90%, it may indicate that the extension time is too short or primer concentration is too low. If the efficiency is greater than 110%, it may indicate degradation of template, presence of PCR inhibitors, nonspecific amplicons, and/or primer-dimers. Melt curve analysis and 4% agarose gel electrophoresis will help to determine the issue. For example, pure homogeneous PCR products produce a single, sharply defined melting curve with a narrow peak. In contrast, primer-dimers melt at relatively low temperatures and have broader peaks. Consult user manual for recommendations for separate trouble shooting issues.
12. To normalize RT-qPCR values between samples use endogenous reference genes as internal controls. The housekeeping genes used herein are examples only and should be optimized

for individual application. Ideal reference genes would be expressed in all cells, have constant copy number in all cells and medium copy number for more accuracy (or similar copy number to gene of interest) and should not change with experimental treatment. Review the literature and technical information in your field to determine which genes other researchers commonly use, test several genes or use a panel such as the RT2 profiler arrays (Qiagen) and then use software such as geNorm and NormFinder to determine the optimal reference gene or combination of genes to achieve the least intra-and inter sample variation for data normalization.

13. For proteins with low expression or suboptimal primary antibodies the luminescent signal can be boosted with the aid of an enhancing kit such as the Luminata Forte HRP Western Substrate (EMD Millipore), as was the case for the detection of phospho-EGFR in liver and phospho-RelA in lung samples in Fig. 3.
14. PVDF membranes may be stripped, but nitrocellulose generally does not strip well. Membranes must be kept wet for stripping to be effective.

5 Discussion

From the examples provided herein, systemic delivery of miR-7 using Invivofectamine 3.0 Reagent as a carrier in normal mice (not bearing tumors) is delivered primarily to liver, consistent with the literature and has little effect on other organs examined. Delivery of miR-7 (and other miRNAs) to non-hepatic tissue using this reagent may require local administration with an established method of delivery. The methods described can also be applied to evaluate local miRNA administration.

Our studies with different lysis buffers demonstrate how variable the assessment of protein levels can be, for some proteins detection of it being wholly dependent on the nature of the lysis buffer. For example, phospho-Akt displayed marked variability using different lysis buffers. Similarly, EGFR levels varied in some tissues with the lysis buffer (tongue) and not in others (liver and brain). With several injections (total of three) of miR-7 most targets did not demonstrate an effect, although in the lung, EGFR and phospho-RelA were downregulated at the protein level, consistent with each acting as a biomarker of miR-7 effect in vivo. It should be noted, however, that in this case small animal numbers were used and the study was not statistically powered to detect significant differences from a therapeutic aspect. Nevertheless, the data pre-

sented herein, where we have identified some of the key pitfalls, will provide a foundation for those planning on assessing the efficacy of delivery of their miRNA in vivo.

Acknowledgments

This work was supported by the National Health and Medical Research Council of Australia and the Cancer Council of Western Australia.

References

1. Lin H, Hannon GJ (2004) MicroRNAs: small RNAs with a big role in gene regulation. Nat Rev Genet 5(7):522–531
2. Kloosterman WP, Plasterk RHA (2006) The diverse functions of microRNAs in animal development and disease. Dev Cell 11 (4):441–450
3. Zhang B, Pan X, Cobb GP, Anderson TA (2007) microRNAs as oncogenes and tumor suppressors. Developmental biol 302(1):1–12
4. Yamaguchi K, Carr BI, Nalesnik MA (1995) Concomitant expression of TGFα and EGF-R in human hepatoma. J Surg Oncol 58 (4):240–245
5. Ang KK, Berkey BA, Tu X, Zhang HZ, Katz R, Hammond EH, Fu KK, Milas L (2002) Impact of epidermal growth factor receptor expression on survival and pattern of relapse in patients with advanced head and neck carcinoma. Cancer Res 62(24):7350–7356
6. Normanno N, De Luca A, Bianco C, Strizzi L, Mancino M, Maiello MR, Carotenuto A, De Feo G, Caponigro F, Salomon DS (2006) Epidermal growth factor receptor (EGFR) signaling in cancer. Gene 366(1):2–16
7. Tai DI, Tsai SL, Chang YH, Huang SN, Chen TC, Chang KS, Liaw YF (2000) Constitutive activation of nuclear factor κB in hepatocellular carcinoma. Cancer 89(11):2274–2281
8. Ueda Y, Richmond A (2006) NF-κB activation in melanoma. Pigment Cell Res 19 (2):112–124
9. Dhawan P, Singh AB, Ellis DL, Richmond A (2002) Constitutive activation of Akt/protein kinase B in melanoma leads to up-regulation of nuclear factor-κB and tumor progression. Cancer Res 62(24):7335–7342
10. Kalinowski FC, Brown RA, Ganda C, Giles KM, Epis MR, Horsham J, Leedman PJ (2014) microRNA-7: a tumor suppressor miRNA with therapeutic potential. Int J Biol Chem 54:312–317
11. Horsham JL, Kalinowski FC, Epis MR, Ganda C, Brown RA, Leedman PJ (2015) Clinical potential of microRNA-7 in cancer. J Clin Med 4(9):1668–1687
12. Kalinowski FC, Giles KM, Candy PA, Ali A, Ganda C, Epis MR, Webster RJ, Leedman PJ (2012) Regulation of epidermal growth factor receptor signaling and erlotinib sensitivity in head and neck cancer cells by miR-7. PLoS One 7(10):e47067
13. Giles KM, Brown RA, Ganda C, Podgorny MJ, Candy PA, Wintle LC, Richardson KL, Kalinowski FC, Stuart LM, Epis MR, Haass NK, Herlyn M, Leedman PJ (2016) microRNA-7-5p inhibits melanoma cell proliferation and metastasis by suppressing RelA/NF-κB. Oncotarget 7(22):31663–31680
14. Krützfeldt J (2016) Strategies to use microRNAs as therapeutic targets. Best Pract Res Clin Endocrinol Metab 30(5):551–561
15. Robb T, Reid G, Blenkiron C (2017) Exploiting microRNAs as cancer therapeutics. Target Oncol:1–16
16. Livak KJ, Schmittgen TD (2001) Analysis of relative gene expression data using real-time quantitative PCR and the 2− ΔΔCT method. Methods 25(4):402–408
17. Towbin H, Staehelin T, Gordon J (1979) Electrophoretic transfer of proteins from polyacrylamide gels to nitrocellulose sheets: procedure and some applications. Proc Natl Acad Sci U S A 76:4350–4254
18. Parkinson CM, O'Brien A, Albers TM, Simon MA, Clifford CB, Pritchett-Corning KR (2011) Diagnostic necropsy and selected tissue and sample collection in rats and mice. JoVE 54:2966. doi:10.3791/2966

Chapter 13

Angiogenesis Analysis by In Vitro Coculture Assays in Transwell Chambers in Ovarian Cancer

Ali Flores-Pérez, Dolores Gallardo Rincón, Erika Ruiz-García, Raquel Echavarria, Laurence A. Marchat, Elizbeth Álvarez-Sánchez, and César López-Camarillo

Abstract

Angiogenesis is an important biological process in tumor growth and metastasis of tumor cells, and it has been associated with poor clinical outcomes in ovarian cancer. In vitro assays are useful tools for understanding the complex mechanisms of angiogenesis under a variety of conditions. Capillary-like formation and transwell migration assays are two of the most common techniques used in angiogenesis research. Here, we show an easy coculture model to study the role of microRNAs on angiogenesis that combines tube formation and cell migration assays. Recently, we reported that miR-204 is repressed in breast cancer and restoration in cancer cell lines results in angiogenesis inhibition. Here, we restored the expression of miR-204 by transfection of precursor molecule in the tumorigenic SKOV3 ovarian cancer cell line, and analyzed the effects in cell migration, invasion, and tube formation of endothelial cells using matrigel-coated transwell chambers.

Key words Angiogenesis, Co-culture assay, Transwell chambers, HUVEC, SKOV3 ovarian cancer

1 Introduction

Ovarian cancer represents the seventh most common cause of death from gynecologic malignancies in the world and the majority of patients are diagnosed in advanced stages. The American Cancer Society has estimated that in 2016 around 22,280 women will be diagnosed with ovarian cancer and 14,240 women will die by the illness in the United States. Hereditary ovarian cancers are characterized by BRCA1 and BRCA2 gene mutations and represent close to 5% of all ovarian cancer cases. The current standard of care for newly diagnosed ovarian cancer is a combination of radical surgery and platinum-based chemotherapy. Unfortunately, recurrence and resistance to therapy and metastatic disease are still a big problem in ovarian cancer treatment, and there is an urgent need to develop novel treatment options. Since angiogenesis plays an important role

Wei Wu (ed.), *MicroRNA and Cancer: Methods and Protocols*, Methods in Molecular Biology, vol. 1699,
DOI 10.1007/978-1-4939-7435-1_13,

in ovarian cancer progression, angiogenesis inhibitors represent a promising therapeutic strategy for this disease [1–3].

Angiogenesis is a complex mechanism of vascular remodeling which involves formation of new blood vessels from pre-existing ones. This biological process requires proper activation of proliferation, extracellular matrix remodeling, migration, and invasion as well as differentiation pathways in endothelial cells [4–6]. Although angiogenesis normally occurs during embryonic development and wound healing, it is also required for tumor growth and cancer metastasis [7–9], and is considered the most devastating hallmark of cancer.

MicroRNAs (miRNAs) are small noncoding RNAs with negative regulatory activity in the cell. Notably, miRNAs expression is often dysregulated in cancer. Recent studies have associated miRNAs with angiogenesis, suggesting that these small RNAs could be potential targets for the development of anti-angiogenic therapies. For example, inhibition of the miR-23-24 cluster repressed blood vessel sprouting in vitro [10], whereas miR-126, miR-378, miR-296, and miR-17/92 expression exhibited pro-angiogenic properties in endothelial cells [11].

One of the main methodologic problems in angiogenesis research is the selection of appropriate assays that effectively evaluate the impact of a treatment or biological mechanism on the vasculature. Many variables such as the delivery method of pro- and anti-angiogenic factors, gene silencing/gene expression techniques, and even the cell type are important for successful experiments. Current methodologies being used to study angiogenesis in vitro include tube formation assays and transwell migration assays. In tube formation assays endothelial cells are cultured on the top of matrigel or a basement membrane-like matrix coat (BME), and the formation of tubular structures is analyzed. In transwell migration assays the endothelial cells are seeded into polycarbonate membrane transwell inserts with a pore size of 8-μm, and maintained in a non-supplemented medium. The migration of these cells through the membrane, induced by a chemoattractant added to the lower chamber, is then quantified. On the other hand, angiogenesis coculture assays analyze the influence of one specific cell type on endothelial tube formation [12–15]. Here, we combined SKOV3 ovarian cancer cells with human umbilical vein endothelial cells (HUVECs) in a coculture assay to analyze the effect of miR-204 on two key steps of angiogenesis: “initiation” (induction of migration and invasion) and “resolution” (tube formation assay).

2 Materials

Ultrapure water, prepared by purifying deionized water to attain a sensitivity of 18 M Ω cm at 25 °C, was used to prepare all solutions.

2.1 Cell Cultures and Buffer Solutions

1. Cell lines: ovarian cancer cell line SKOV3 (ATCC), human umbilical vein endothelial cells (HUVEC, ATCC).
2. Culture media: Dulbecco's Modified Eagle Medium (DMEM) supplemented with 10% fetal bovine serum (FBS), penicillin (10,000 U/ml), and streptomycin (10,000 μg/ml). Medium 200 supplemented with 10 ml of Large Vessel Endothelial Supplement (LVES 50×). Optimem serum-reduced media.
3. Phosphate-buffered saline (PBS 10×) 137 mM NaCl, 1.47 mM KH_2PO_4, 6.47 mM $NaH_2PO_4.12H_2O$, 2.68 mM KCl, dissolve to 1× and adjust to pH 7.0, autoclaved.
4. PBS 1×−6 μM EDTA, pH 7.0 autoclaved.
5. Transfectant reagent (Siport amine).
6. 50 μM pre-miR-204 (ThermoFisher).
7. 50 μM scramble miRNA (Precursor negative control #1, ThermoFisher).
8. 24-well Transwell chambers, 8 μm pore size polycarbonate membrane (Corning).
9. Basement membrane matrix or Matrigel 1× (Becton and Dickinson).
10. Pro-angiogenic factors VEGF/FGF.

3 Methods

3.1 Initiation of Cell Cultures

1. Use DMEM supplemented medium to grown SKOV3 cells and M200 supplemented medium to HUVEC cells.
2. Warm supplemented medium at 37 °C.
3. Add 15 ml of supplemented medium to each properly labeled T-75 culture flask. In the case of starting cultures from frozen cells continue to **step 5**, otherwise go to **step 9**.
4. Rapidly, thaw a frozen vial of HUVEC or SKOV3 cells in a 37 °C water bath.
5. Transfer the cryotube into a biosafety hood. Disinfect the outside of the cryotube with 70% ethanol.
6. Recover the cell suspension and place in a 15 ml tube and centrifuge for 3 min at 300 × *g*.

7. Discard the freezing medium and resuspend with warm supplemented medium (SKOV3/DMEM, HUVEC/M200 medium).
8. Seed 2.5×10^5 viable cells in T-75 (prepared with medium) culture flasks.
9. Incubate the cultures at 37 °C and 5% CO_2.
10. Change culture medium 24–36 h after seeding and every other day thereafter, until the culture is at 80% confluency (4–6 days).

3.2 Transfection of SKOV3 Cancer Cells

1. 24 h before transfection trypsinize the SKOV3 ovarian cancer cells using your routine procedure. Inactivate trypsin by resuspending the cells in a supplemented medium.
2. Seed 2.5×10^5 cells per well in 6-well plates in 2.5 ml of supplemented medium to achieve ~80% confluency after 24 h.
3. Incubate cells overnight using normal cell culture conditions.
4. Dilute 5 μl of transfection reagent Siport amine in 100 μl opti-MEM in a 1.5 ml microtube and incubate for 10 min to room temperature.
5. In other 1.5 ml microtube dilute 7.5 μl of pre-miR-204 or Scramble miRNA (10 μM) in 100 μl of opti-MEM. Incubate at room temperature for 10 min.
6. After incubation, mix diluted Siport and diluted pre-miR-204 or Scramble miRNA, mix by pipetting up and down, spin and incubate at room temperature for 10 min to allow transfection complexes to form.
7. Rinse the cells with PBS pH 7.0 two times and dispense the nucleic acid/siPORT complexes onto the cells. Gently tilt the plate back and forth to evenly distribute the complexes.
8. Add the supplemented medium to achieve a final volume of 2.5 ml. Incubate the transfected cells under normal cell culture conditions for 24–48 h.

3.3 Preparation of Transwell Chambers Coated with Matrigel

1. 24 h before assay thaw BME at 4 °C, overnight.
2. Incubate pipet tips, Transwell chambers, and PBS-pH 7.0 at 4 °C, overnight.
3. Dilute BME to 0.5× with cool BME dilution buffer or PBS pH 7.0 (*see* **Note 1**).
4. Coat Transwell inserts with 100 μl of 0.5× diluted BME and lower chamber (receiver) with 300 μl of 0.5× diluted BME.
5. Incubate overnight at 37 °C and 5% CO_2.

3.4 Seed SKOV3 Ovarian Cancer Cells

1. 24–48 h after transfection, rinse SKOV3 cells two times with PBS-pH 7.0 and add 64 μl of trypsin 0.25% and 1.5 ml PBS–EDTA per well. Then incubate cells for 5 min at 37 °C.

Centrifuge cell suspension at 300 × *g* for 3 min, discard the supernatant, and resuspend the pellet in 1 ml of medium without supplements.

2. Seed 1.0×10^5 transfected cells (pre-miR-204 or Scramble miRNA) into the BME-coated lower Transwell chamber and add 400 μl of medium without supplements.
3. Incubate cells for 24 h at 37 °C and 5% CO_2.

3.5 Angiogenesis Tube Formation Assay

1. 24 h after seeding transfected cancer cells in BME-coated lower chamber, harvest HUVECs with trypsin/PBS-EDTA (as described above).
2. Seed HUVECs at a density of 1.0×10^4 cells, resuspended in 100 μl of medium without supplement, in Transwell insert over SCOV3 transfected cells.
3. Positive control—Add 10 μl of angiogenic factors VEGF (18 ng/ml) and FGF1 (60 ng/ml) dissolved in 1 ml of supplemented medium on BME-coated lower chamber without SKOV3 cells with HUVECs seeded in transwell insert (upper chamber).
4. Negative control 1—BME-coated lower chamber with 400 μl of medium without supplements and HUVECs seeded in transwell insert (upper chamber).
5. Negative control 2—SKOV3 cells seeded in BME-coated lower chamber maintained in 1 ml of supplemented medium with VEGF (18 ng/ml) and FGF (60 ng/ml). No HUVECs are seeded in transwell insert (upper chamber) (*see* **Note 2**).
6. Well-developed HUVEC tube networks usually form 12–24 h after the cells are seeded into the BME-coated transwell inserts. Inspect tube formation and define visual patterns by photographing the cells under an inverted light microscope, 20×–100× magnification (*see* **Note 3**).
7. Assign a numerical value to each pattern. This way a numerical value is associated with a degree of angiogenesis progression.

3.6 Results

As the role of miR-204 in angiogenesis in ovarian cancer is unknown, here we investigated its contribution in this cellular process by using a new implemented method to quantify angiogenesis in vitro. We carried out tube formation assays using HUVEC cells, which is one of the simple but well-established in vitro angiogenesis assays based on the ability of endothelial cells to form three-dimensional capillary-like tubular structures.

In Fig. 1 we showed the schematic representation of a typical transwell chamber. Cocultures of HUVEC with SKOV3 ovarian cancer cells under different conditions were performed. As expected, HUVEC cells alone did not form tubule-like structures

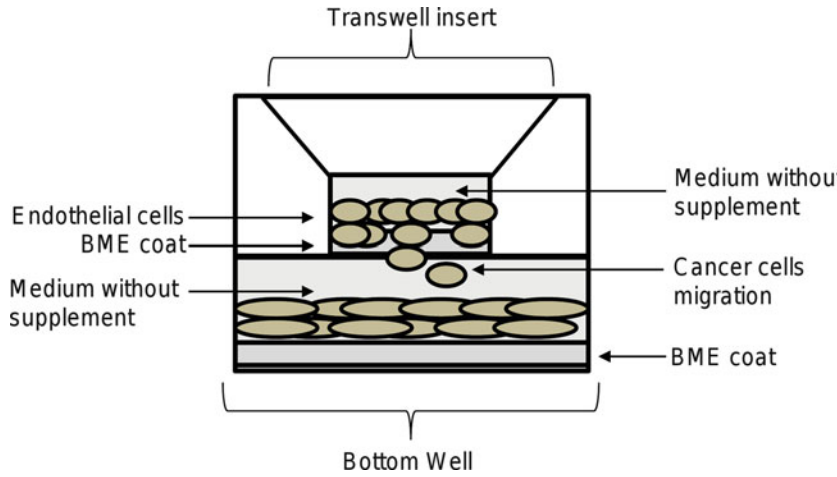

Fig. 1 Schematic representation of transwell chambers

(Fig. 2a). In contrast, a strong angiogenic effect was observed in HUVEC cells treated with recombinant VEGFA used as positive control (Fig. 2b). Typical HUVEC tubular networks on the matrigel were observed at 24 h. Co-incubation of HUVEC with SKOV3 cells transfected with scramble control also resulted in an angiogenic behavior as the number of endothelial cells branch points and capillary tubes were increased in comparison with monoculture controls (Fig. 2d). In contrast, SKOV3 cells treated with VGFA did not show capillary-like formation (Fig. 2c). Interestingly, coculture of HUVEC with SKOV3 cells transfected with miR-204 resulted in a marked inhibition of endothelial cell tubules and branch point formation, and the tubular networks were disrupted at 24 h (Fig. 2e). Taken altogether these data indicate that miR-204 inhibits the angiogenesis induced by ovarian cancer cells in vitro. In addition, these data highlight the feasibility of carried out angiogenesis assays in vitro with minimal requirements.

4 Notes

1. The concentration of BME needed for each assay depends on the cell type. We recommend testing various BME concentrations (0.1× to 1×) to find the optimal concentration for a particular cell type.
2. It is advised to use a noninvasive cell line as a negative control.
3. It is recommended to monitor tube formation using an inverted microscope at 6, 12, 24, and 48 h after plating HUVECs into the BME-coated Transwell insert.

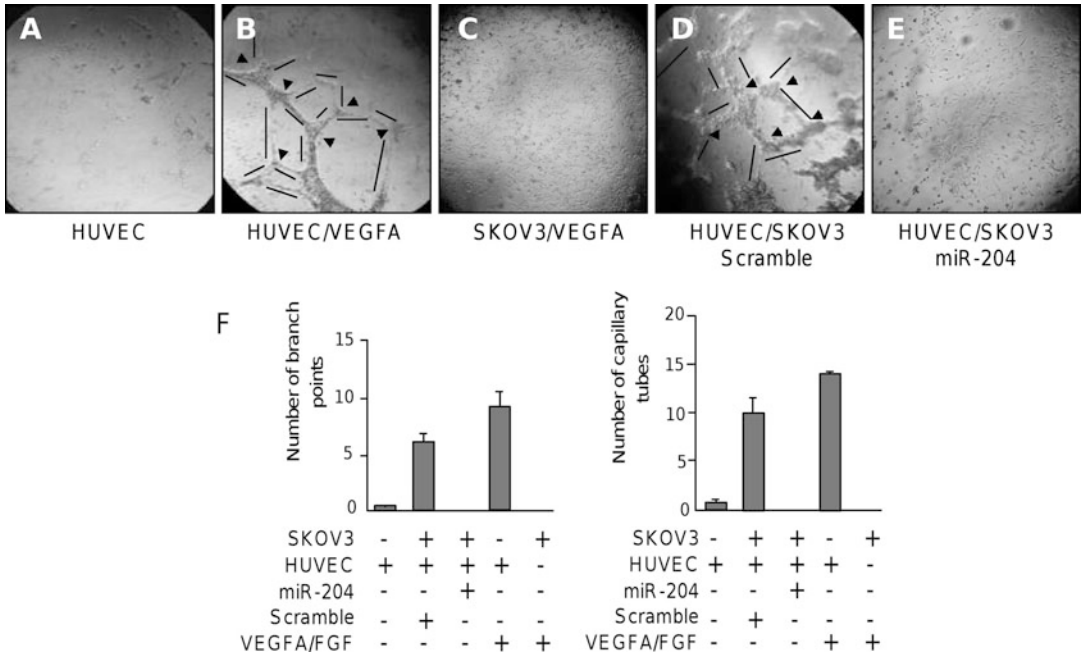

Fig. 2 Angiogenesis in vitro assay. (**a**) Monoculture of HUVECs. Cells were seeded in the upper chamber (*insert*) and medium without supplements was added to both, upper and lower, chambers. (**b**) Monoculture of HUVECs. Cells were seeded in the upper chamber and maintained in the medium without supplements. Complete medium with pro-angiogenic factors VEGF (18 ng/ml) and FGF1 (60 ng/ml) was added to the lower chamber. (**c**) Monoculture of SKOV3 cells. Cells were seeded in the lower chamber and maintained in complete medium with pro-angiogenic factors VEGF (18 ng/ml) and FGF1 (60 ng/ml). (**d**) Coculture of HUVEC/SKOV3 cells. SKOV3 cells transfected with Scrambled miRNA were seeded in the lower chamber and maintained in medium without supplements. 24 h later, HUVECs were seeded in the upper chamber and maintained in the medium without supplements. (**e**) Coculture of HUVEC/SKOV3 cells. SKOV3 cells transfected with pre-miR-204 were seeded in the lower chamber and maintained in the medium without supplements. 24 h later, HUVECs were seeded in the upper chamber and maintained in the medium without supplements. (**f**) Quantification of branch points and capillary tube formation. Data were obtained by two different observers. Results shown are the mean of three independent experiments ± S.D. *Arrowheads* indicate branch points. *Arrows* denote capillary-like tubes structures

References

1. Ferlay J, Soerjomataram I, Dikshit R, Eser S, Mathers C, Rebelo M et al (2014) Cancer incidence and mortality worldwide: sources, methods and major patterns in GLOBOCAN 2012. Int J Cancer. doi:10.1002/ijc.29210. PMID:25220842. Published online 9 October 2014
2. Susana B, Stanley B (2013) New strategies in the treatment of ovarian cancer: current clinical perspectives and future potential. Clin Cancer Res 19:961–968
3. Jackson AL, Eisenhauer EL, Herzog TJ (2015) Emerging therapies: angiogenesis inhibitors for ovarian cancer. Expert Opin Emerg Drugs 20(2):331–346
4. Tuija M, Alitalo K (1995) Endothelial receptor tyrosine kinases involved in angiogenesis. J Cell Biol 129:895–898
5. Wolf-Dietrich C, Fernandez A, Joussen A, Eike-Gert A, Flynn E, Lo KM, Gillies S, Javaherian K, Folkman J, Shing Y (2001) Effect of antiangiogenic therapy on slowly growing, poorly vascularized tumors in mice. J Natl Cancer Inst 93:382–387
6. Kilarski W, Petersson L, Fuchs PF, Zielinski MS, Gerwins P (2012) An in vivo

neovascularization assay for screening regulators of angiogenesis and assessing their effects on pre-existing vessels. Angiogenesis 15:643–655

7. Holash J, Wiegand SJ, Yancopoulos GD (1999) New model of tumor angiogenesis: dynamic balance between vessel regression and growth mediated by angiopoietins and VEGF. Oncogene 18:5356–5362
8. Nishida N, Hirohisa Y, Nishida T, Kamura T, Kojiro M (2006) Angiogenesis in cáncer. Vasc Health Risk Manag 2:213–219
9. Muthukkaruppan VR, Kubai L, Auerbach R (1982) Tumor-induced neovascularization in the mouse eye. J Natl Cancer Inst 69:699–708
10. Zhoua Q, Gallaghera R, Ufret-Vincentya R, Lia X, Olsonb E, Wanga S (2011) Regulation of angiogenesis and choroidal neovascularization by members of microRNA-23∼27∼24 clusters. PNAS 108:8287–8292
11. Wang S, Olson EN (2009) AngiomiRs-key regulators of angiogenesis. Curr Opin Genet Dev 19:205–211
12. Shaik S, Nucera C, Inuzuka H, Gao D, Garnaas M, Frechette G et al (2012) SCFa-TRCP suppresses angiogenesis and thyroid cancer cell migration by promoting ubiquitination and destruction of VEGF receptor 2. J Exp Med 209:1289–1307
13. Chen Y, Wei T, Yan L, Lawrence F, Qian H, Burkholder P et al (2008) Developing and applying a gene functional association network for anti-angiogenic kinase inhibitor activity assessment in an angiogenesis co-culture model. BMC Genomics 9:264–273
14. Carolyn A, Staton MWR, Nicola J, Brown A (2009) Critical analysis of current in vitro and in vivo angiogenesis assays. Int J Exp Path 90:195–221
15. Martin J, Siemerink IK, Ilse MC, Vogels AW, Griffioen JF, Noorden V, Schlingemann R (2012) CD34 marks angiogenic tip cells in human vascular endothelial cell cultures. Angiogenesis 15:151–163

Chapter 14

Application of Individual qPCR Performance Parameters for Quality Control of Circulating MicroRNA Data

Anna Brunet-Vega, María Elisa Quílez, María José Ramírez-Lázaro, and Sergio Lario

Abstract

Although circulating miRNAs are promising candidates for biomarkers, several challenges must be overcome before miRNAs can be used for diagnosis and monitoring. One is quality control for the RNA extraction and quantification process. RNA quality control techniques are unsuitable as circulating miRNAs are in the fM range. Additionally, biofluids may contain inhibitors of the reverse transcriptase and polymerase enzymes, which may survive RNA purification. Herein, we describe the protocol we have used to check the robustness of miRNA purification and measurement by the addition of spike-ins and by evaluating the quality of the qPCR data, respectively.

Key words Circulating miRNA, Quantitative PCR, Quality control, PCR efficiency

1 Introduction

Circulating miRNA expression used as a biomarker for cancer and non-cancer diseases has shown significant discrepancies between studies [1]. Although some of the factors contributing to these inconsistencies have been identified [2], no robust protocol for circulating miRNA quantification has been reported. In this article, we describe the methods we have used to check the robustness of miRNA measurements by the addition of spike-ins and by evaluating the quality of qPCR [3, 4].

The use of spike-ins is critical to control technical factors that affect final miRNA levels. Caution should be taken with the use of spike-ins because they might not reflect biological differences. Therefore, spike-ins helps identify outlier samples as a quality control for the quantification process, but should not be used for normalization [4].

Regarding the quality of miRNA measurement we have evaluated the individual qPCR reactions in terms of PCR efficiency

Wei Wu (ed.), *MicroRNA and Cancer: Methods and Protocols*, Methods in Molecular Biology, vol. 1699,
DOI 10.1007/978-1-4939-7435-1_14,

because efficiency data are critical in gene quantification procedures [5]. Although the standard curve method is the most common method used for calculating PCR efficiency, it has been shown that the mean of the individual PCR efficiencies is a better estimate of amplicon efficiency [6]. One approach for the estimation of individual PCR efficiency is by applying linear regression in the log-linear region (window-of-linearity) of the PCR amplification [6]. Another point to consider is that *Cq* values are in a logarithmic scale that underestimates variability in PCR replicas [7]. This can be overcome by determining the starting concentration per sample (N_0) using *Cq* values corrected by amplicon efficiency. The use of N_0 has advantages such as the estimation of the real quantification variability and the possibility of applying correction factors. Individual and mean PCR efficiencies per amplicon, *Cq*, and N_0 values can be easily obtained using LinRegPCR software [6] from raw data exported in Real-time PCR Data Markup (RDLM) language [8] from qPCR software. Several PCR platforms and software are compliant with RDML (for a complete list visit http://www.rdml.org/). As an example, we show the analysis of three spike-ins and three circulating plasma miRNAs extracted using two alternate commercially available kits. We used a phenol-chloroform-based extraction method from Qiagen and another kit without the use of toxic phenol or chloroform from Exiqon, based on spin column chromatography.

2 Materials

2.1 Equipment

- Thermocycler. Analytic-Jena, Jena, Germany.
- QuantStudio 7 Flex Real-Time PCR System (Applied Biosystems, Foster City, CA, USA).
- A set of low range pipets are needed. These are dedicated pipets used only for RNA isolation, cDNA synthesis, and qPCR applications.
- Common laboratory equipment: vortex mixer, centrifuges, and minifuges.

2.2 Biofluid miRNA Isolation Kits

- RNA Spike-in kit, Exiqon A/S (cat#203203, Vedbaek, Denmark) (*see* **Note 1**).
- miRCURY™ RNA Isolation Kits – Biofluids (cat#300113, Exiqon A/S, Vedbaek, Denmark).
- miRNeasy Serum/Plasma Kit (cat#217184, Qiagen, Toronto, Canada).

Table 1
Individual miRNA assays used in this study

Synthetic Spike-in	Primer set reference	Use
UniSp4	203953	RNA isolation evaluation
UniSp5	203955	RNA isolation evaluation
Cel-miR-39-3p	203952	cDNA synthesis evaluation
hsa-miR-451	204734	Hemolysis monitoring
hsa-miR-23a	204772	Circulating miRNA
hsa-miR-103	204063	Circulating miRNA
hsa-miR-191	204306	Circulating miRNA

2.3 First-Strand cDNA Synthesis and Quantitative Real-Time PCR (qRT-PCR) Reagents

- miRCURY LNA Universal RT microRNA PCR System (Exiqon A/S, Vedbaek, Denmark).
- Exiqon individual miRNA primer sets. See Table 1.

2.4 Software

- QuantStudio 6 and 7 Flex Real-Time PCR System Software, Version 1.0.
- RDML Ninja [9]. RDML Editor, RDML 1.2 compliant. http://sourceforge.net/projects/qpcr-ninja/
- LinRegPCR [6].http://www.hartfaalcentrum.nl/index.php?main=files&fileName=LinRegPCR.zip&description=LinRegPCR:%20analysis%20of%20qPCR%20data&sub=LinRegPCR#history.

2.5 Reagents

- Nuclease-free water.
- Absolute etanol, molecular grade.
- Isopropanol, molecular grade.
- Chloroform, molecular grade

2.6 Plastic

- DNA LoBind Tubes, (Eppendorf, Hamburg, Germany).

3 Methods

Please refer to a general guide for working with RNA [10].

3.1 Plasma Collection and Storage

1. Drawn whole blood (at least 5 ml) into Vacutainer tubes containing EDTA as an anticoagulant.
2. Mix by inverting 8–10 times (*see* **Note 2**).

3. Centrifuge 3500 × *g* for 10 min, 4°C.
4. Remove 300 µl aliquots of plasma into fresh tubes without disturbing the cell pellet.
5. Store aliquots at −80 °C.

3.2 Preparation of the Spike-Ins (UniSp4, UniSp5, and Cel-miR-39-3p) for RNA Isolation and cDNA Synthesis Steps

1. Spin down vials before opening.
2. Add 80 µl nuclease-free water (*see* **Note 3**).
3. Leave for 20 min on ice to dissolve RNA.
4. Mix by vortexing, spin and place on ice.
5. Store spike-ins in single-use aliquots at −20 °C to avoid freeze-thaw cycles.

3.3 Extraction Method 1: Phenol-Chloroform-Based Protocol (miRNeasy Serum/Plasma kit)

1. To 200 µl of sample, add 1 ml of QIAzol Lysis Reagent.
2. Mix by vortexing.
3. Incubate for 5 min at room temperature.
4. Add 1 µl RNA Spike-in mixture containing UniSp4 and UniSp5 spike-ins (*see* Subheading 3.2 and **Note 3**).
5. Add 200 µl chloroform. Shake vigorously for 15 s.
6. Incubate at room temperature for 2–3 min.
7. Centrifuge for 15 min at 12,000 × *g*, 4 °C.
8. Carefully transfer the upper aqueous layer to a fresh tube (*see* **Note 4**).
9. Add 1.5 volumes of absolute ethanol to precipitate the RNA. Mix by pipetting.
10. Carefully apply 700 µl of the mixture to a RNeasy MinElute spin column in a 2 ml collection tube.
11. Centrifuge at ≥8000 × *g* for 15 s, room temperature.
12. Discard the flow-through.
13. Repeat steps 10–12 to load the remainder of the sample.
14. Wash the spin column by adding 700 µl of RWT buffer.
15. Centrifuge at ≥8000 × *g* for 15 s, room temperature. Discard the flow-through.
16. Wash the spin column by adding 500 µl of RPE buffer.
17. Centrifuge at ≥8000 × *g* for 15 s, room temperature. Discard the flow-through.
18. Wash the spin column by adding 500 µl of 80% ethanol.
19. Centrifuge at ≥8000 × *g* for 15 s, room temperature. Discard the flow-through.
20. Place the spin column in a new collection tube.

21. Centrifuge the columns with the lids open at max speed for 5 min at room temperature. Discard the collecting tube (*see* **Note 5**).
22. Place the spin column in a fresh 1.5 ml collection tube.
23. Add 14 μl RNase-free water directly onto the center of the spin-column membrane (*see* **Note 6**). Close the lid gently and incubate for 1 min (*see* **Note 7**).
24. Centrifuge at max speed for 1 min at room temperature to elute the RNA.
25. Immediately store RNA on ice or at −80 °C (*see* **Note 8**).

3.4 Extraction Method 2: Non Phenol-Chloroform Based Protocol (miRCURY™ RNA Isolation Kit)

1. To 200 μl of sample, add 60 μl of Lysis solution BF. Mix by vortexing.
2. Incubate for 3 min at room temperature.
3. Add 1 μl RNA Spike-in mixture (*see* Subheading 3.2 and **Note 3**).
4. Add 20 μl of Protein Precipitation Solution BF. Mix by vortexing for 5 s.
5. Incubate for 1 min at room temperature.
6. Centrifuge for 3 min at 11,000 × *g*, room temperature.
7. Transfer the supernatant into a new 2.0 ml tube.
8. Add 270 μl Isopropanol. Vortex for 5 s.
9. Carefully apply the mixture to a microRNA Mini spin-column BF in a 2 ml collection tube.
10. Incubate for 2 min at room temperature.
11. Centrifuge for 30 s at 11,000 × *g*, room temperature. Discard the flow-through.
12. Wash the spin column by adding 100 μl of Wash Solution 1 BF.
13. Centrifuge for 30 s at 11,000 × *g*, room temperature. Discard the flow-through.
14. Wash the spin column by adding 700 μl of Wash Solution 2 BF.
15. Centrifuge for 30 s at 11,000 × *g*, room temperature. Discard the flow-through.
16. Wash the spin column by adding 250 μl of Wash Solution 2 BF.
17. Centrifuge for 2 min at 11,000 × *g*, room temperature (*see* **Note 4**). Discard the flow-through.
18. Place the spin column in a fresh 1.5 ml collection tube.
19. Add 50 μl RNase-free water directly onto the center of the spin-column membrane (*see* **Note 5**). Close the lid gently and incubate for 1 min.

20. Centrifuge for 1 min at 11,000 × *g*, at room temperature to elute the RNA (*see* **Note 7**).
21. Immediately store RNA on ice or at −80 °C (*see* **Note 8**).

3.5 First-Strand cDNA Synthesis

For the cDNA synthesis we use the miRCURY LNA Universal RT microRNA PCR System (Exiqon) (*see* **Note 9**).

1. Thaw RNA on ice for 15–20 min.
2. On ice prepare a master mix containing 2 μl of 5× Reaction buffer, 4.5 μl nuclease-free water, 1 μl Enzyme mix, 0.5 μl cel-miR-39 RNA spike-in (*see* **Note 10**).
3. On ice, dispense 8 μl cDNA master mix in 0.2 ml strip tubes.
4. Add 2 μl of extracted circulating RNA. Mix by gentle vortexing, spin and place on ice.
5. Place the tubes in a pre-warmed thermal cycler programmed as follows:

   60 min at 42 °C – 5 min at 95 °C – 2 min at 4 °C - hold at 4 °C
6. Remove the reactions from the thermal cycler. If you continue to the next step keep the reactions on ice. If you do not continue, store the first-strand reactions at −20 °C. If necessary, aliquot in Lobind tubes (*see* **Note 11**).

3.6 Quantitative Real-Time PCR

1. If cDNA was stored frozen, thaw on ice for 15–20 min.
2. Dilute the cDNA 1:50 in molecular biology grade water (*see* **Note 12**). Also dilute the genomic and amplicon controls included in the first-strand cDNA synthesis step.
3. On ice prepare a master mix for each miRNA to be amplified according to the protocol specified in the miRCURY LNA Universal RT microRNA PCR System: 5 μl of SYBER Green PCR Master mix and 1 μl PCR primer mix (*see* **Note 13**).
4. Dispense 6 μl PCR Master Mix into each well of a 384-well plate (*see* **Note 14**).
5. Pipet 4 μl of diluted cDNA into the corresponding wells. Mix by pipetting several times (*see* **Note 15**).
6. Seal the plate following the addition of sample to each reaction mix.
7. Spin for 30 s at 1600 × *g*.
8. Place the plate in the real-time PCR instrument. Cycling parameters are (*see* **Note 16**):
   95 °C for 10 min—40× [95 °C for 10 s - 60 °C for 60 s]—followed by melting curve analysis.

3.7 QuantStudio Real-Time PCR Data Analysis and Export in RDML Format

1. Launch the QuantStudio 6 and 7 Flex Real-Time PCR System Software and open the .eds file corresponding to your experiment.
2. If still not done, assign plate wells to targets, samples, controls, and biological replicate groups analyzed. Target assignment is recommended for subsequent analysis with LinRegPCR software.
3. Analyze the run using the QuantStudio software. Check the possible warnings given by the software. It is also very important to verify the specificity of amplification by melting curve analysis. Check the presence of abnormal melting plots.
4. From the ***Experiment Menu***, click ***Export***. Select the RDML Format. Enter a file name and location for saving the RDML file. Click ***Start Export***.

3.8 Conversion of RDML File Version 1.0 to Version 1.2 with RDML-Ninja

1. The QuantStudio 6 and 7 Flex Real-Time PCR System Software exports RDML files in RDML version 1.0. For easy import to LinRegPCR the RDML file has to be converted to RDML version 1.2. To do this launch RDML-Ninja and open the exported RDML file of your experiment. Conversion is done in two steps.
2. Select the tab ***RDML*** and ***Migrate version 1.0→1.1***. Click ***Ok*** when prompted.
3. Select the tab ***RDML*** and ***Migrate version 1.1→1.2***. Click ***Ok***.
4. Rename and save the converted file.

3.9 LinRegPCR Software Analysis

1. Launch LinRegPCR. Select ***File*** and ***Read from RDML***. Select the converted RDML file of your experiment.
2. Click the button of the corresponding ***Monitoring Chemistry***. In our case is ***DNA-binding dye***.
3. In ***Amplification of*** click on ***ss-DNA*** and in ***Data are baseline corrected*** select ***No*** (*see* **Note 17**).
4. Figure 1a shows the LinRegPCR main window after import (*see* **Note 18**).
5. In user settings tab, click on ***Exclude samples without amplification*** and ***Exclude samples outside 5% of group median***.
6. In user settings tab, click on ***Strictly continuous Log-linear phase*** button (*see* **Note 19**).
7. Click ***Determine Baselines***. Figure 1b shows the LinRegPCR main window after analysis.
8. Click on ***Display on survey graphs*** to see the amplification analysis grouped by amplicon (Fig. 1c.)
9. Export analysis to an Excel file. Select ***File*** and ***Save to Excel***.

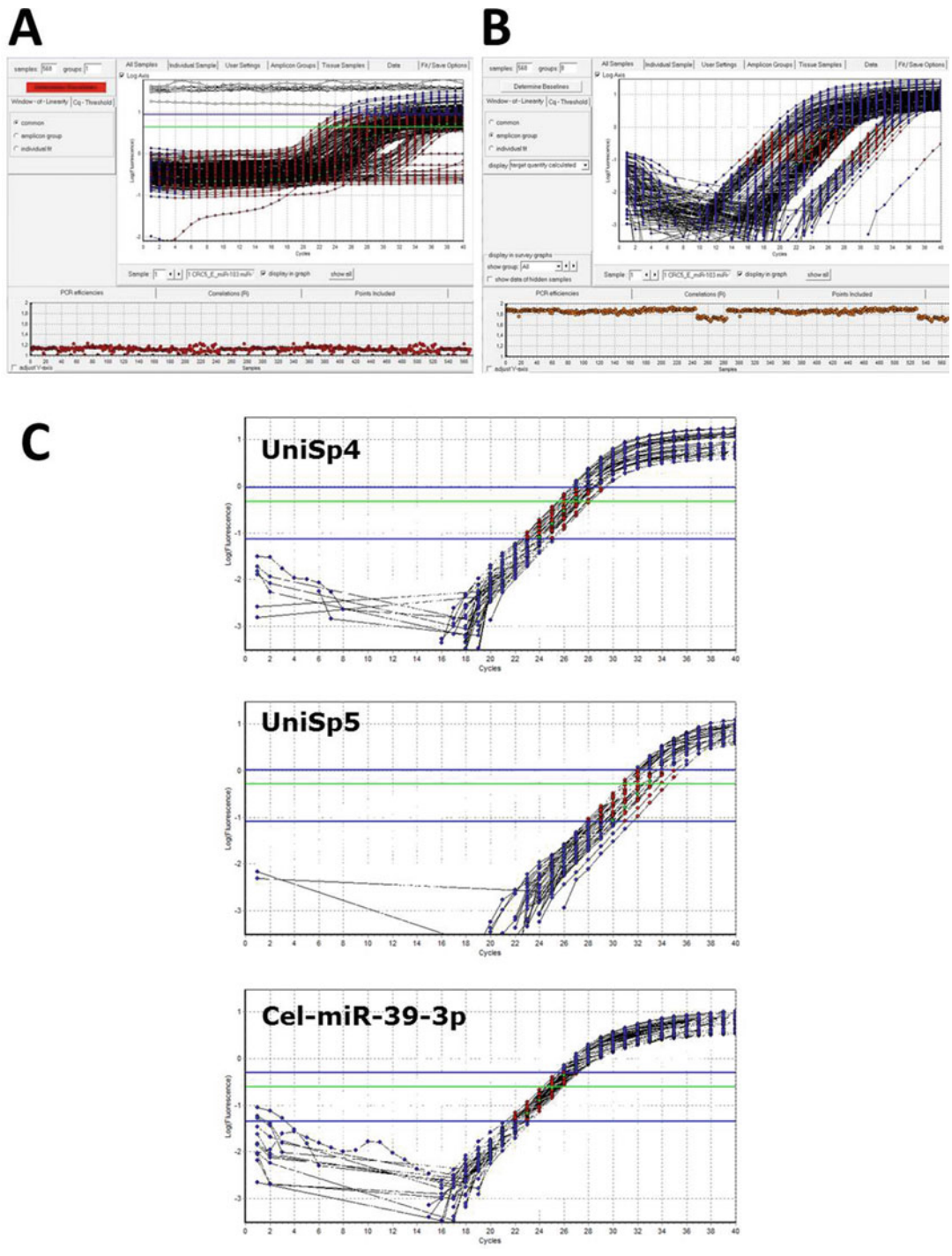

Fig. 1 Screenshot of the LinRegPCR program analysis window before (**a**) and after baseline analysis (**b**). The amplification analysis grouped by the amplicon for UniSp4, Unisp5, and cel-mir-39-3p spike-ins is shown in (**c**). *Outer vertical lines* represent the limits of the window of linearity, and the central line represents the threshold (*Nq*)

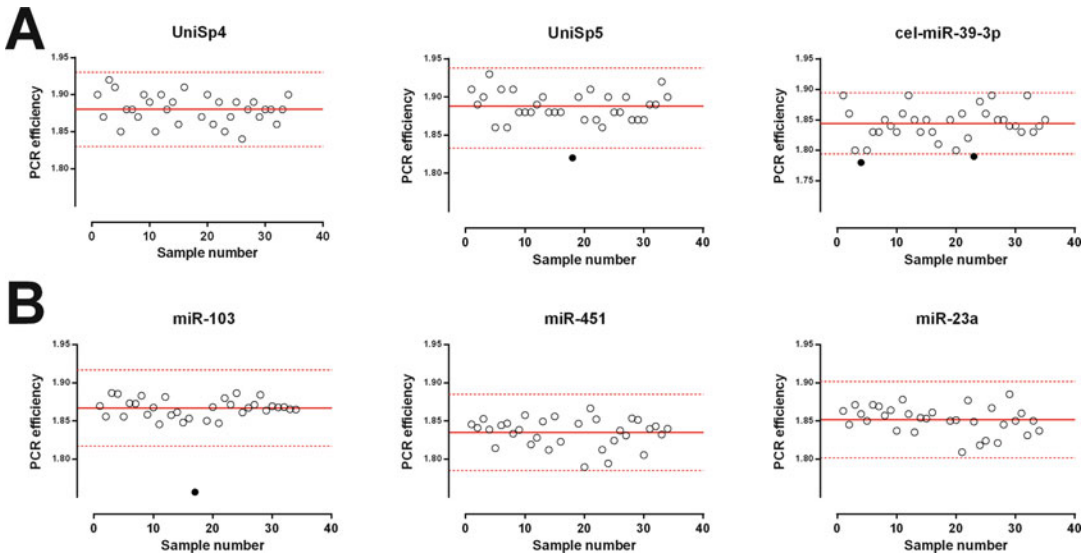

Fig. 2 Median (*solid lines*) and ±0.05 (*dotted lines*) of PCR efficiency values of the spike-ins (Panel (**a**), UniSp4, UniSp5, and cel-miR-39) and circulating miRNAs (Panel (**b**), miR-23a, miR-103, miR-451) as determined by the window-of-linearity method. The *open circles* (○) represent valid individual efficiency values and *closed circles* (●) represent samples outside the median ± 0.05. *Cq* or N_0 of these samples have to be interpreted with caution

3.10 Excel File Analysis

1. The Excel worksheet shows the following data: ***Name***, ***indiv_PCR_eff***, ***Amplicon***, ***Tissue***, ***threshold***, ***mean_PCR_eff***, ***Cq***, ***N0***, ***Sample_Use***, and ***Quality_checks*** (*see* **Note 20**).
2. The ***Quality_checks*** column shows one or more of the following values: 0, passed all checks; 1, no amplification; 2, baseline error; 3, no plateau; 4, noisy sample; 5, PCR efficiency outside 5%; 6, excluded from mean Eff; 7, excluded by user; 8, included by user; 9, manual baseline.
3. Samples or replicates with ***No_plateau***, ***Baseline_error;*** or ***noisy_sample*** label should be excluded for subsequent analysis.
4. Check the ***PCR_efficiency_outside_5%*** label. Samples or replicates marked with this label should be interpreted with caution (*see* **Note 21 and** Fig. 2).
5. Check the ***mean_PCR_eff*** column. ***mean_PCR_eff*** is the mean of the individual PCR efficiencies for each ***Amplicon***. We consider that the ***mean_PCR_eff*** should be greater than 1.75 (*see* **Note 22**).
6. Check ***Cq*** and ***N0***. ***N0*** is the starting concentration per sample (N_0) corrected by the PCR efficiency. It is calculated using the formula

$$N_0 = N_q / E^{Cq}$$

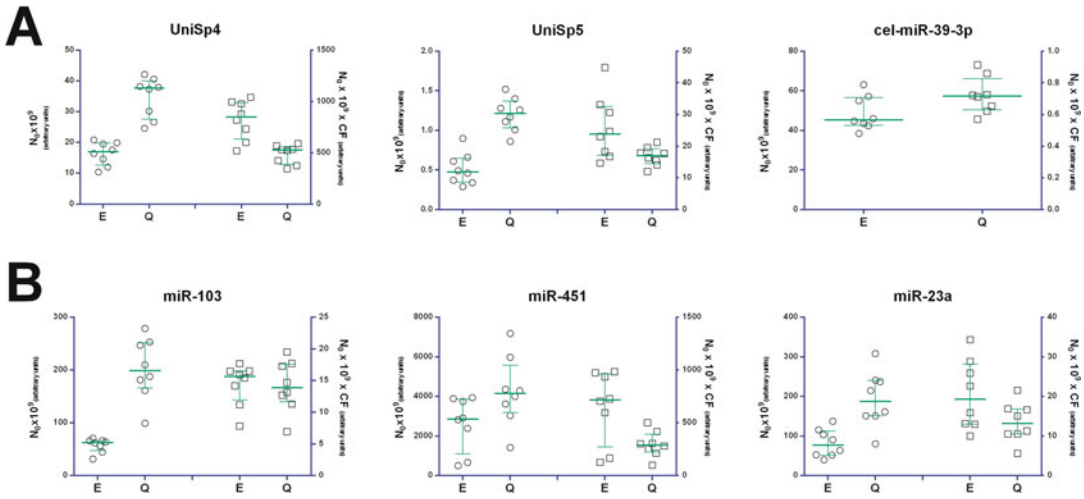

Fig. 3 Comparison of two extraction methods (E,Q) by the quantification of spike-ins and circulating miRNAs by means of qPCR and N_0 calculations. Panels show N_0 and N_0xCF. Unlike *Cqs*, N_0xCF allows the direct comparison of isolation methods. Panel (**a**) shows N_0 and N_0xCF for the spike-ins added during RNA isolation (UniSp4, UniSp5) and retrotranscription (cel-miR-39). N_0 and N_0xCF of naturally circulating plasma miRNAs are in panel (**b**) (miR-23a, miR-103, miR-451). The *open circles* represent N_0values (○, *left axis*) and *open squares* represent corrected N_0 (□, *right axis*). *CF* correction factor

where N_q is the fluorescence threshold set to determine *Cq*. N_0 is expressed in arbitrary fluorescence units. *Cq* values are in a logarithmic scale, which means that with 100% amplification efficiency, the amount of PCR produced doubles with every cycle. The coefficients of variation of replicates in qPCR are usually calculated from *Cq* values, but the logarithmic expression of *Cq* values often leads to underestimation of the real variability [7]. To correct this effect, we use the linearized N_0 for calculating variability (*see* **Note 23**). N_0 is also useful when comparing extraction methods with different input and elution requirements. N_0 can be adjusted by a correction factor to allow direct method comparison (Fig. 3).

4 Notes

1. Alternatively, spike-ins can be ordered from commercial vendors such as IDT or Eurofins MWG operon with HPLC purification or from Qiagen (miRNeasy Serum/Plasma Spike-In Control, cel-miR-39 miRNA mimic, cat#219610).
2. This is a very important step to ensure adequate anticoagulation of the specimen.
3. After resuspension, the concentration of the spike-ins UniSp4, and UniSp5 is 0.02 fmole/μl and 0.0002 fmole/μl, respectively. The final concentration of cel-miR-39-3p is

0.002 fmole/μl. In our lab we do not amplify UniSp2, the most concentrated spike-in (2 fmole/μl), because its expression is really above the expression level of biological miRNAs in plasma.

4. Avoid transferring any interphase or the organic (lower) phase as it would contaminate the sample with DNA or phenol, respectively.
5. The spin column has to be completely dry before eluting the RNA tube. Residual ethanol may interfere with downstream reactions.
6. QIAGEN recommends not use less than 10 μl.
7. The incubation time for 1 min at room temperature before elution is not in the original protocol.
8. We transfer and aliquot the purified RNA into 0.5 ml low-binding tubes.
9. Several systems exist for the measurement of miRNA by qPCR: TaqMan® MicroRNA Assays (ThermoFisher), miScript Primer Assay (Qiagen), MystiCq sytem (Sigma), qScript™ microRNA Quantification System (Quanta Biosciences), Mir-X miRNA system (Clontech), among others. We chose Exiqon because in a comparative study that analyzed 196 miRNAs in 12 platforms it was one of the best performing systems [11].
10. To rule out genomic and amplicon contamination, we include a control without Enzyme Mix (genomic) and a control without cDNA template (amplicon).
11. Exiqon recommends store at 4 °C if the cDNA is used within the following 4 days. In our laboratory, the first-strand cDNA synthesis and the qPCR amplification are performed in the same day.
12. Use the largest volume possible when making the dilution. In our laboratory the 1:50 dilution is performed by adding 2 μl of cDNA to 98 μl of water. Use a 0.1–2.5 μl range pipette for pipetting the cDNA.
13. Please refer to the miRCURY LNA Universal RT microRNA PCR System user guide, some components of the PCR Master mix may change depending on the real-time PCR instrument used.
14. In our lab we carefully design the PCR plates in miRNA quantification experiments. The objective is to minimize the number of PCR plates in order to reduce the quantification errors introduced by inter-plate comparisons.
15. We run the PCR experiments in triplicate. We use filter barrier pipette tips to avoid aerosol contamination. Because we are

working with multichannel pipette and with small volumes, we recommend changing the tips for each sample.

16. Please refer to the miRCURY LNA Universal RT microRNA PCR System user guide, real-time PCR instruments from different vendors may need different amplification ramp rates and cycle numbers.
17. The RDML file contains the raw fluorescence data.
18. Note that the number of samples in LinRegPCR main window doubles the number of samples analyzed. We don't know the source of this duplication.
19. These are the default settings. Analysis can be relaxed by checking other options. Please refer to the LinRegPCR manual for additional information.
20. *Cq* is the quantification Cycle. *Cq* is the standard name for *Ct* or *Cp* [12].
21. After 26 cycles of amplification a difference of 5% in PCR efficiency between two PCR reactions can result in a twofold difference of final product concentration [5, 13]. This is especially relevant for miRNAs, since miRNA fluctuations seem to be smaller (3–5 fold-change) than observed for mRNAs [14]. This is critical for circulating miRNAs, whose *Cq* values are between 25 and 30 for moderately expressed miRNAs and >30 for low abundant miRNAs.
22. For applications with high initial number of template molecules a high PCR efficiency might not be so critical. For circulating miRNAs high PCR efficiency is crucial since they are often detected at $Cq > 25$. The PCR efficiency of >1.75 (>75%) is the cutoff we use in our laboratory as the minimum PCR efficiency to consider a miRNA assay as valid.
23. N_0 is a very small number (10^{-6} to 10^{-10}). We usually multiply N_0 by 10^9 for the easy interpretation of the data.

Acknowledgments

This study was supported by grant 1007/C/2013 from the Marató de TV3 (http://www.tv3.cat/marato/en/#), by grant PI12/01802 from Proyectos de Investigación en Salud, Instituto de Salud Carlos III (http://www.eng.isciii.es/ISCIII/es/general/index.shtml), and by grant CIR2011040 from the Fundació Parc Taulí (CIR2011040, http://www.tauli.cat/tauli/en/Fpt/fpt.htm). CIBERehd is funded by the Instituto de Salud Carlos III.

References

1. Jarry J, Schadendorf D, Greenwood C, Spatz A, van Kempen LC (2014) The validity of circulating microRNAs in oncology: five years of challenges and contradictions. Mol Oncol 8:819–829
2. Tiberio P, Callari M, Angeloni V, Daidone MG, Appierto V (2015) Challenges in using circulating miRNAs as cancer biomarkers. Biomed Res Int 2015:731479
3. Brunet-Vega A, Pericay C, Quilez ME, Ramirez-Lazaro MJ, Calvet X et al (2015) Data on individual PCR efficiency values as quality control for circulating miRNAs. Data Brief 5:321–326
4. Brunet-Vega A, Pericay C, Quilez ME, Ramirez-Lazaro MJ, Calvet X et al (2015) Variability in microRNA recovery from plasma: comparison of five commercial kits. Anal Biochem 488:28–35
5. Pfaffl M (2004) In: Bustin SA (ed) Quantification strategies in real-time PCR. In A–Z of Quantitative PCR. International University Line, La Jolla, pp 89–113
6. Ruijter JM, Ramakers C, Hoogaars WM, Karlen Y, Bakker O et al (2009) Amplification efficiency: linking baseline and bias in the analysis of quantitative PCR data. Nucleic Acids Res 37:e45
7. Livak KJ, Schmittgen TD (2001) Analysis of relative gene expression data using real-time quantitative PCR and the 2(−Delta Delta C (T)) method. Methods 25:402–408
8. Lefever S, Hellemans J, Pattyn F, Przybylski DR, Taylor C et al (2009) RDML: structured language and reporting guidelines for real-time quantitative PCR data. Nucleic Acids Res 37:2065–2069
9. Ruijter JM, Lefever S, Anckaert J, Hellemans J, Pfaffl MW et al (2015) RDML-ninja and RDMLdb for standardized exchange of qPCR data. BMC Bioinformatics 16:197
10. Nielsen H (2011) Working with RNA. Methods Mol Biol 703:15–28
11. Mestdagh P, Hartmann N, Baeriswyl L, Andreasen D, Bernard N et al (2014) Evaluation of quantitative miRNA expression platforms in the microRNA quality control (miRQC) study. Nat Methods 11:809–815
12. Johnson G, Nour AA, Nolan T, Huggett J, Bustin S (2014) Minimum information necessary for quantitative real-time PCR experiments. Methods Mol Biol 1160:5–17
13. Freeman WM, Walker SJ, Vrana KE (1999) Quantitative RT-PCR: pitfalls and potential. BioTechniques 26(112–122):124–115
14. Heegaard NHH, Carlsen AL; Skovgaard, K; Heegaard, PMH. (2015) Circulating extracellular microRNA in systemic autoimmunity. In: Igaz P eds. Circulating microRNAs in disease diagnostics and their potential biological relevance. Springer Basel

Chapter 15

Construction of Multi-Potent MicroRNA Sponge and Its Functional Evaluation

Suhwan Chang

Abstract

MicroRNA is a small, endogenous RNA that inhibits specific gene expression by interacting mostly on the UTR region of target mRNA. Among various methods to inhibit the microRNA, microRNA sponge is a construct designed to inhibit specific microRNA by providing excess amount of target mRNA. Here, we describe a method to generate multi-potent miRNA sponge which can inhibit multiple microRNAs simultaneously. In addition, two methods to examine the functionality of miRNA sponge will be introduced. This tool can be used to stably inhibit multiple microRNAs either in cell or in vivo, expanding the scope of functional analysis of specific microRNAs.

Key words MicroRNA, Sponge, UTR, Multi-potent, Target mRNA

1 Introduction

MicroRNA is a small (19 ~ 23 nt) endogenous RNA that was first discovered in nematode (*C. elegans*) on 1993. Like other protein coding mRNAs, the microRNA is generated by RNA polymerase II [1]. However, many microRNAs are located in the intronic or exonic region of a gene, so its expression is dependent on the host gene promoter [2]. Once it is transcribed, it generates a stem-loop structure that is recognized by Drosha complex in nucleus [3]. The complex cleaves the root of the stem-loop that generates 65-70 nt size of precursor form of microRNA. The precursor microRNA is then transported into cytoplasm where it is recognized by Dicer complex [4]. This complex cleaves the precursor microRNA again, to generate 19–23 nt double-stranded RNA (mature microRNA). Finally, a complex called RISC (RNA-Induced Silencing Complex) takes one (usually upper) strand of the mature microRNA into the complex and scans its target mRNA [5]. Once 7 ~ 8 nt of the 5′ end (seed sequence) of microRNA matches with a target mRNA, there will either degradation of

Wei Wu (ed.), *MicroRNA and Cancer: Methods and Protocols*, Methods in Molecular Biology, vol. 1699,
DOI 10.1007/978-1-4939-7435-1_15,

mRNA or translational inhibition take place that results in the inhibition of target-gene expression [6].

There are more than 1000 kinds of microRNA reported in humans [7, 8]. To inhibit this microRNA, an antisense oligonucleotide called antagomiR has been designed and widely used [9]. Due to its specificity and ease of overexpression by transfection, the antagomiR is thought as a good tool for the microRNA inhibition. However, the expression is transient and often goes beyond physiological level [10, 11]. To overcome these limitations, a construct called microRNA sponge was invented [12]. The construct consists of an expression cassette of inert gene (such as GFP or luciferase) and tandem repeat of binding sites of a specific microRNA on the 3′UTR region of the cassette. Basically, the principle of the microRNA sponge is to functionally inhibit specific microRNA, by providing excess amount of artificial substrate (mRNA) to absorb most of the available endogenous microRNA [12]. As the sponge is an expression construct essentially, it can be used to stably inhibit microRNAs in cell (*see* **Note 1**) or even in vivo [13]. Also, if we introduce multiple microRNA-binding sites, it is possible to inhibit multiple microRNAs simultaneously. With these ideas, we designed and tested multi-potent microRNA for cancer research [14] and the detailed procedure will be described here.

2 Materials

2.1 Generation of MicroRNA Sponge

As a backbone for the microRNA sponge, any expression vector can be used. There are several points to be considered such as:

(a) The promoter of the sponge expression: It can be CMV or Actin promoter to accomplish universal and overexpression. Alternatively, a tissue specific promoter (e.g., Nestin, MMTV, Pdx.) or inducible (Tet-on/off) promoter can be used as well.

(b) Substrate gene: Nontoxic and inert (means minimally affect any cell signaling) genes can be used. Here, the RFP and luciferase gene will be described as examples.

(c) Number of microRNAs to inhibit simultaneously: Theoretically, there is no limitation on the number of target microRNA. Depending on the purpose, we think 3 ~ 4 microRNA inhibition is feasible to analyze.

(d) Sequence of the microRNA binding site (MBS): For the prefect matching, a complementary sequence of mature form of microRNA can be used. For imperfect matching (means there are bulges outside of seed sequence), 3 ~ 4 variations can be introduced to the perfect matching sequence [15].

All solutions need to be made with laboratory grade, ultra-pure water (DDW or TDW).

1. Sponge DNA backbone vector (pMiReport and mRFP).
2. Restriction enzyme (SanDI, Hind III and SpeI).
3. Calf Intestinal Alkaline phosphatase.
4. T4 DNA ligase.
5. Competent cell.
6. LB media (liquid).
7. LB plate (+ amplcillin).
8. Shaking incubator (37 °C).
9. Plate incubator (37 °C).
10. Heat block.
11. Plasmid miniprep/Gel extraction kit.
12. PCR machine (general materials for colony PCR).

2.2 Functional Validation of MicroRNA Sponge by Luciferase Assay

1. Cell line (293 T or other Cancer cell line).
2. Cell culture media (DMEM-10% FBS supplemented with antibiotics).
3. 24-well plate.
4. MicroRNA specific reporter vector.
5. SV40-Renilla luciferase control vector.
6. Target microRNA mimic.
7. Transfection agent (Lipofectamine 2000/oligofectamine).
8. Opti-MEM media.
9. Dual luciferase assay kit.
10. Luminometer.
11. PBS.
12. Non-transparent 96-well plate.

2.3 Functional Evaluation of MicroRNA Sponge by Real-Time PCR of MicroRNAs

1. Cell line (293 T or other Cancer cell line).
2. Cell culture media (DMEM-10% FBS supplemented with antibiotics).
3. PBS.
4. Trizol (or any commercial RNA prep Kit).
5. DEPC-treated water.
6. miScript RT kit (Qiagen, Cat No./ID: 218,161).
7. PCR machine.
8. RNase inhibitor.
9. miScript real-time PCR kit (Qiagen, Cat No./ID: 218,073).
10. Real time PCR system.

3 Methods

3.1 Construction of MicroRNA Sponge (Luciferase-Based)

1. We used pMIR-Report vector (Life Technologies) as a backbone. First, a linker consisting of Eco0109I and SanDI (for directional multimerization) was generated (Table 1 for linker sequence).
2. Cut the pMIR-Report vector with SpeI/Hind III followed by CIAP treatment and gel purification by Qiagen Gel extraction kit (Qiagen. Cat.no. 28706).
3. Anneal the linker oligo in annealing buffer (10 mM Tris, pH 7.5–8.0, 50 mM NaCl, 1 mM EDTA) as follows:
   (a) Mix equal 10 μl of 100 μM of both complementary oligos in a 1.5 ml microcentrifuge tube.
   (b) Place the tube in a heat block at 90–95 °C for 5 min.
   (c) Remove the heat block from the heater unit and allow to cool to room temperature (takes 1 ~ 2 h, depending on the block size).
   (d) Store on ice or at 4 °C until ready to use.
4. Ligate the annealed oligo with pMIR-Report vector (Hind II/SpeI cut) at 16 °C, 4 h to overnight
   (molar ratio of vector:insert = 1: 10).

Table 1
Linker sequence

Primer name	Sequences
1-Perfect_miR155_21_221222-SP_S	5′-GTC CCACCCCTA TCA CGA TTA GCA TTA AAATTT CAACAT CAGTCT GAT AAG CTA AAT TACCCA GAGCAA TGT AGC TGG-3′
2-Perfect_miR155_21_221222-SP_AS-1	5′-GAC CCA GCT ACA TTG CTC TGG GTA ATT TAGCTT ATC AGA CTG ATG TTG AAA TTT TAA TGCTAA TCG TGA TAG GGG TGG-3′
3-Bulge_miR155_21_221222-SP_S (*see* **Note 3**)	5′-GTC CCA TTT TGT TTT AGC ATT AAA ATT TCAACA TCA GGACATAAG CTA AAT TAC CCA GCCTATGTA GCT GG-3′
4-Bulge_miR155_21_221222-SP_AS-1	5′-GAC CCA GCT ACA TAGGCT GGG TAA TTT AGCTTA TGT CCT GAT GTT GAA ATT TTA ATG CTAAAA CAA AAT GG-3′
5-Linker_SpeI_EcoO109I_SanDI_EcoO109I_HindIII_S	5′-CTA GTA GGGCCC GGG TCCCAG GGC CCA-3′
3-Linker_SpeI_EcoO109I_SanDIEcoO109IHindIII_AS-1	5′-AGC TTG GGC CCT GGG ACC CGG GCC CTA-3′

5. Transform the ligate into the competent cells and plate onto LB-Ampicillin agar plate.
6. Identify the linker inserted clone by colony PCR. The insert size is estimated by colony PCR primers annealed to right up/downstream of the SpeI/HindIII sites of the vector.
7. Prepare the linker inserted pMIR-Report vector by plasmid miniprep kit.
8. Verify the linker sequence by sequencing (*see* **Note 2**) and cut the vector with SanDI, followed by CIAP treatment and gel purification.
9. As a model system, we aimed to inhibit 4 microRNAs, namely miR-155, miR-21, miR-221/222 [14]. The primer sequences for linker are listed in the Table 1. In addition, an oligonucleotide pair harboring miRNA binding sites (MBS) of miR-155, miR21, and miR-221/222 with spacers (AATT) was designed and the SanDI linker was added at the each end (Table 1 for sequences).
10. This monomer unit was phosphorylated by PNK and ligated to the pMIR-Report/SanDI linker vector by SanDI site. This ligation generated monomerized as well as multimerized sponge vectors.
11. To generate multimerized sponge vector, increase the molar ratio of vector: insert up to 1:100.The insert size was initially estimated by colony PCR with two primers annealed to right up/downstream of the SpeI/HindIII sites of the vector.
12. Seed the colony-PCR positive clones and prepare plasmid DNA. The cloned sponge vector is sequenced to verify the correct MBS multimerization.

3.2 Functional Evaluation of the MicroRNA Sponge by Luciferase Assay

This protocol is to measure the activity of microRNA sponge in the presence of microRNA mimic. Compare to the control, the mimic-transfected samples will show reduced level of luciferase activity. This is a mark that luciferase sponge (*see* **Note 4**) can absorb transfected microRNA.

1. Seed 3×10^4 cells in each well of a 24-well plate, 18–24 h prior to transfection.
2. Dilute 100 ng of sponge with 5–10 nM of microRNA mimic in 25 μl of Opti-MEM per well.
3. Dilute 0.5 μl of lipofectamine (or other liposomal transfection reagents) into 25 μl of Opti-MEM per well.
4. Mix the samples of 3 and 4 and incubate for 20 min.
5. Change the media of the 24 well into 200 μl of Opti-MEM per well.
6. Add the DNA-liposome mixture in 4. Into each well.

7. Incubate for 24–48 h.
8. Wash the cells with PBS and add 200 μl of 1× passive lysis buffer (Promega).
9. Shake at RT for 20 min and take 10 μl of lysates into a non-transparent 96-well plate.
10. Measure the luciferase activity in Luminometer (e.g., Glomax from Promega) using dual luciferase assay reagents (Promega, E1960).

3.3 Functional Evaluation of the MicroRNA Sponge, by Real-Time PCR Measurement of the Target MicroRNAs.

In addition to the luciferase assay, this protocol describes how to measure the level of endogenous, target microRNA in the presence of microRNA sponge. Notably, it is not clear if the mRNA-bound microRNA is degraded or recycled [16]. However, we observed the expression of microRNA sponge results in reduced level of the target microRNA [14], suggesting degradation is a major fate. Based on this, we describe here how to measure the target microRNA level in the expression of microRNA sponge (*see* **Note 5**)

1. Seed 4×10^5 of cells on 60 mm dish 18–24 h prior to transfection.
2. Transfect 500 ng of microRNA sponge into the cell (described in Subheading 3.2).
3. After 48 h, wash the cells with PBS and lyse with 1 ml Trizol reagent.
4. Prepare total RNA by following the Trizole RNA purification protocol. Alternatively, a spin column for microRNA purification can be used.
5. Measure the amount and quality of the total microRNA.
6. Take 1 μg of the total RNA for the reverse transcription.
7. Reverse transcription (by miScript RT kit (Qiagen)).
   (a) Prepare total RNA and thaw RT buffer, dNTP and DEPC-treated water.
   (b) Set up a RT reaction as follows:

Reverse transcription reaction components	
Component volume/reaction	
5× miScriptHiSpec buffer or	
5× miScriptHiFlex buffer*	4 μl
10× miScriptNucleics mix 2 μl	2 μl
RNase-free water	Variable
miScript reverse transcriptase mix	2 μl
Template RNA	1 μg
Total volume 20 μl (*see* **Note 6**)	

8. Incubate for 60 min at 37 °C.
9. Incubate for 5 min at 95 °C to inactivate miScript Reverse Transcriptase Mix.
10. Add 90 μl of distilled water to dilute RT product.
11. Prepare 2× SYBR Green PCR mix and Universal primer (Qiagen).
12. Set up a real-time PCR reaction as follows (*see* **Note 7**):

	Volume/reaction	Volume/reaction(S)
Component	(384-well)	(96-well)
2× QuantiTect	5 μl	12.5 μl [6]
SYBR green PCR		
Master mix		
10× miScript	1 μl	2.5 μl
Universal primer		
10× miScript	1 μl	2.5 μl
Primer assay		
RNase-free water	Variable	Variable
Template cDNA	≤1 μl	≤2.5 μl
Total volume	10 μl	25 μl [16]

S: small scale (scaled-down) in 96 well

13. Using a real-time PCR machine, run the PCR reaction with the following cycles:

Step	Time	Temperature additional comments
PCR	15 min	95 °C HotStarTaq DNA polymerase is activated by this heating step
Initial activation step		
3-step cycling:*†‡		
Denaturation	15 s	94 °C
Annealing	30 s	55 °C
Extension	30 s	70 °C perform fluorescence data collection
Cycle number	40 cycles	

4 Notes

1. The sponge vector can be stably expressed like other expression plasmids. In our case, we have successfully developed a stable cell line with a RFP-based inducible sponge [14].
2. In the multimerization step of the MBS (microRNA Binding Site), there can be recombination among the monomer MBS that generate partial deletion or inversion. Therefore, it is necessary to verify the correct cloning by sequencing.
3. In our model experiment, we found the "bulged" sponge has little less activity than perfect sponge, for the microRNA inhibition, but it showed does dependent capacity [14]. We think this is closer to the physiological substrate but this idea needs more data to be proved.
4. Instead of luciferase, GFP (or RFP) construct can be used as a sponge vector. In this case, the expression of sponge can be monitored by fluorescence microscopy.
5. Another way to functionally analyze the microRNA sponge is to check the level of target proteins. Due to its nature of microRNA-target interaction, there are multiple target proteins that can be increased by the sponge expression. Therefore, it might be helpful to select candidates to examine by taking information from database such as MiRTarBase (http://mirtarbase.mbc.nctu.edu.tw/).
6. The RT reaction can be scale down to total 20 or 10 μl if there are not many microRNA samples to be analyzed.
7. In addition to microRNAs, the RT product can be used to measure any other cellular genes to examine correlation between microRNA and target mRNA expression.

Acknowledgments

This research was supported by the Korea Health Technology R&D Project through the Korea Health Industry Development Institute (KHIDI) (grant number: HI13C1538), funded by the Ministry of Health &Welfare, Republic of Korea.

References

1. Lee RC, Feinbaum RL, Ambros V (1993) The C. Elegans heterochronic gene lin-4 encodes small RNAs with antisense complementarity to lin-14. Cell 75:843–854
2. Kim VN (2005) MicroRNA biogenesis: coordinated cropping and dicing. Nat Rev Mol Cell Biol 6:376–385
3. Krol J, Krzyzosiak WJ (2004) Structural aspects of microRNA biogenesis. IUBMB Life 56:95–100
4. Lee Y, Ahn C, Han J, Choi H, Kim J, Yim J, Lee J, Provost P, Radmark O, Kim S, Kim VN (2003) The nuclear RNase III Drosha initiates microRNA processing. Nature 425:415–419

5. Chendrimada TP, Gregory RI, Kumaraswamy E, Norman J, Cooch N, Nishikura K, Shiekhattar R (2005) TRBP recruits the dicer complex to Ago2 for microRNA processing and gene silencing. Nature 436:740–744
6. Tijsterman M, Plasterk RH (2004) Dicers at RISC; the mechanism of RNAi. Cell 117:1–3
7. Gregory RI, Chendrimada TP, Cooch N, Shiekhattar R (2005) Human RISC couples microRNA biogenesis and posttranscriptional gene silencing. Cell 123:631–640
8. Hertel J, Langenberger D, Stadler PF (2014) Computational prediction of microRNA genes. Methods Mol Biol 1097:437–456
9. Schmitz U, Wolkenhauer O (2013) Web resources for microRNA research. Adv Exp Med Biol 774:225–250
10. Scherr M, Venturini L, Battmer K, Schaller-Schoenitz M, Schaefer D, Dallmann I, Ganser A, Eder M (2007) Lentivirus-mediated antagomir expression for specific inhibition of miRNA function. Nucleic Acids Res 35:e149
11. Chiba Y, Misawa M (2010) MicroRNAs and their therapeutic potential for human diseases: MiR-133a and bronchial smooth muscle hyperresponsiveness in asthma. J Pharmacol Sci 114:264–268
12. Catalucci D, Latronico MV, Condorelli G (2008) MicroRNAs control gene expression: importance for cardiac development and pathophysiology. Ann N Y Acad Sci 1123:20–29
13. Ebert MS, Neilson JR, Sharp PA (2007) MicroRNA sponges: competitive inhibitors of small RNAs in mammalian cells. Nat Methods 4:721–726
14. Ebert MS, Sharp PA (2010) MicroRNA sponges: progress and possibilities. RNA 16:2043–2050
15. Jung J, Yeom C, Choi YS, Kim S, Lee E, Park MJ, Kang SW, Kim SB, Chang S (2015) Simultaneous inhibition of multiple oncogenic miRNAs by a multi-potent microRNA sponge. Oncotarget 6:20370–20387
16. Kluiver J, Slezak-Prochazka I, Smigielska-Czepiel K, Halsema N, Kroesen BJ, van den Berg A (2012) Generation of miRNA sponge constructs. Methods 58:113–117
17. Baccarini A, Chauhan H, Gardner TJ, Jayaprakash AD, Sachidanandam R, Brown BD (2011) Kinetic analysis reveals the fate of a microRNA following target regulation in mammalian cells. Curr Biol 21:369–376

Chapter 16

MicroRNA Sequencing Data Analysis Toolkits

Wei Wu

Abstract

MicroRNA (miRNA) is a non-protein-coding small RNA molecule that negatively regulates gene expression by degradation of mRNA or suppression of mRNA translation. MiRNAs play important roles in biological processes such as cellular development, differentiation, proliferation, apoptosis and stem cell self-renewal and cancer development. The expression profile of microRNAs is tissue-, cell-type specific. PCR- and microarray-based arrays are the commonly used for differential expression of microRNAs between different diseased conditions. With the next-generation sequencing or massively parallel DNA sequencing technology advanced and the cost is plummeting, microRNAseq approach is widely used for the genome-wide discovery of known and unknown miRNA expression. However, the analysis of microRNAseq is computational expensive, here I provide guidelines and available tools for microRNAseq analysis.

Key words microRNA, microRNAseq, Massively parallel DNA sequencing, Bioinformatics, Data analysis

1 Introduction

MicroRNA (miRNA) is a non-protein-coding small RNA molecule that negatively regulates gene expression by the degradation of mRNA or suppression of mRNA translation [1]. MiRNAs play important roles in biological processes such as cellular development, differentiation, proliferation, apoptosis, and stem cell self-renewal [2, 3]. Studies show that deregulation of miRNA expressions is contributing to tumorigenicity, invasion, and metastasis [4, 5]. Changed miRNA expression patterns can be employed for cancer diagnostic and prognostic biomarkers [6–8]. More than 30% of protein-coding genes are predicted to be conserved targets of microRNAs [9]. A single microRNA can regulate many hundreds of genes, subsequently disrupting entire gene networks [1]. Therefore, defining microRNA profiling between different states, such as "cancer cells" versus "normal cells" helps to understand the biology of diseases. Indeed, specific microRNA expression signatures have been implicated in the tumorigenesis [4]. There are several assays such as microarray-based and PCR-based

Wei Wu (ed.), *MicroRNA and Cancer: Methods and Protocols*, Methods in Molecular Biology, vol. 1699,
DOI 10.1007/978-1-4939-7435-1_16,

Table 1
Available tools for miRNA-Seq analysis (*see* Notes 1 and 2)

	platform	Sample size	Web links
mirTools	Web-server	One sample at one	http://centre.bioinformatics.zj.cn/mirtools/
miRanalyzer	Web-server	Pair-wise	http://bioinfo5.ugr.es/miRanalyzer/miRanalyzer.php
miRNAkey	Java interface	Pair-wise	http://ibis.tau.ac.il/miRNAkey/
miRDeep	Java interface	One sample at one	http://www.australianprostatecentre.org/research/software/mirdeep-star
wapRNA	Web-server	One sample at one	http://waprna.big.ac.cn/
omiRas	Web-server	2 or more samples	http://tools.genxpro.net/omiras/
CAP-miRSeq	Command-based	20 samples or more at once	http://bioinformaticstools.mayo.edu/research/cap-mirseq/

assays that are widely used for profiling microNRA expression in diseased tissues versus non-diseased tissues. However, these technologies are hindered by several limitations: (1) low sensitivity for low expressed miRNAs; (2) large technical variations; (3) lack of ability to detect novel miRNAs and structural sequence changes. In contrast, massively parallel sequencing technology for miRNA expression profiling (miRNA-Seq) can overcome these limitations and has become increasingly popular in biomedical research. Although significant computational resources and bioinformatics expertise are needed to analyze miRNA-seq data, many analytical tools have been developed over the past few years to assist researchers to obtain the biological results (*see* Table 1). This chapter will present you the principles and components of pipeline for miRNA-seq data analysis (Fig. 1).

2 Materials

1. Computer requirement: window, mac, or linux system. A free tool VirtualBox can be installed following instruction (https://www.virtualbox.org/wiki/End-user_documentation) for command line program. In general, you will need a computer with at least 8 GB RAM and 500GB disk space and 8 cores.
2. Software:
   (a) Reference genome (https://support.illumina.com/sequencing/sequencing_software/igenome.html).
   (b) miRBase known miRNA references including hairpin precursor miRNA sequences in FASTA format, mature

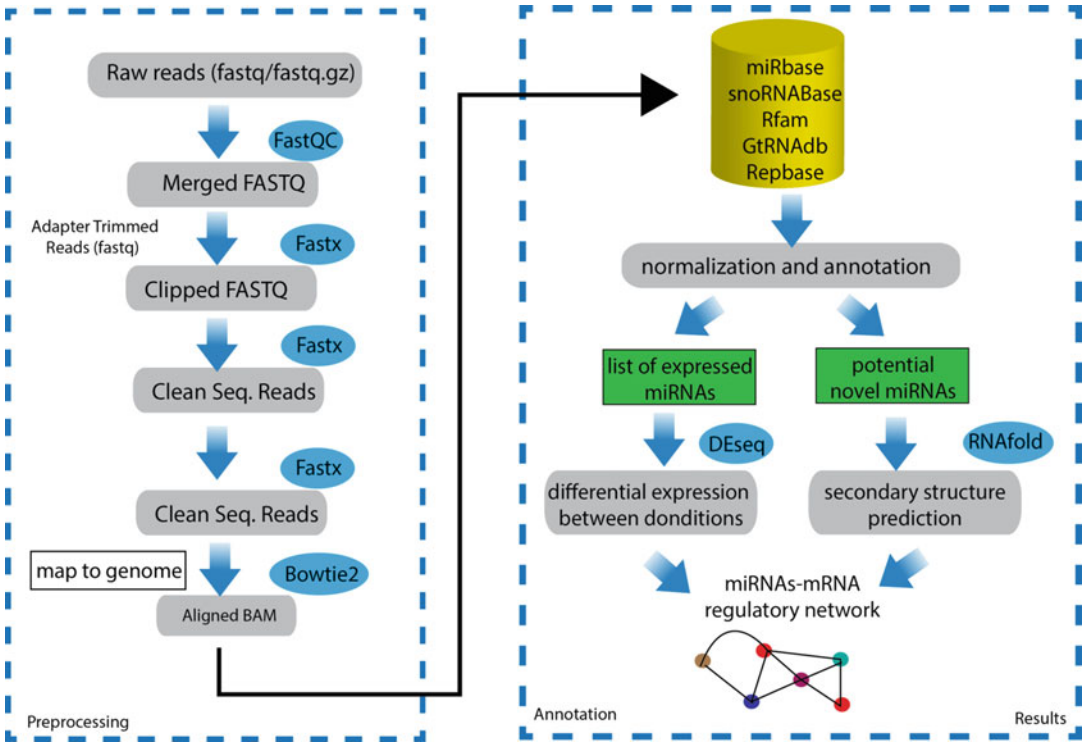

Fig. 1 The diagram depicts the workflow of microRNAseq analysis

miRNA sequences in FASTA format and miRNA GFF3 file.

(c) Gencode annotation GTF file.

(d) Aligners: most common short read aligners including Bowite, Bowtie2, BWA, STAR, and Subread (*see* **Note 3**).

(e) Specific algorithms for microRNA analysis such as CAP-miRSeq.

3 Methods

There are main three sequencing platforms: illumina Hiseq systems, Life Technologies SOLiD sequencing, and Roche 454 sequencing. Each platform has its own specific library preparation kits, sequencing protocols, and data processing pipelines. The comprehensive description of these methods is referred to companies' websites. Here, the principles including small RNA library preparation and data analysis are described.

3.1 Small RNA Preparation

The samples could be derived from different sources such as from cell lines, tissues, even body fluids. The total RNA is extracted and isolated using a commercial product such as Trizol (Invitrogen)

reagent. 50 ~ 100 μg total RNA is usually required for gel purification and size selection, followed by adding adaptors at 3′ and 5′, reverse transcription and PCR amplification and sequencing.

3.2 Data Analysis

After the sequencing has finished, the sequencing machines will generate raw sequencing data with all As, Cs. Gs, and Ts in fastq or fastq.gz format. These raw data need to be preprocessed:

1. Reads are first carried out quality check, and low quality bases are trimmed from the 3′ end. The tool "cutadapt" could be used for adapter sequence trim, and reads less than 15 bases after trimming are discarded. The read length distribution is expected to be at 22–23 bases for a good miRNA-seq library preparation.
2. Remove contaminations like mRNA, tRNA, snoRNA and so on; select reads length between 18 and 26 bp;
3. Map to mature miRNA downloaded from miRBasev20 using various aligners, usually Bowtie2. There is additional mapping with miRDeep2 mapper or others for de novo miRNA prediction for the genomic regions not defined by miRBase annotation.
4. Detect the differential expression between two samples using DESeq or DEseq2 (*see* **Note 4**).

4 Notes

1. The web-based tools are easy to use but lack of flexibility and reliability, and not suited for high-throughput data analysis. In generally, they do not detect single nucleotide variants or mutations on the coding region of microRNAs.
2. The algorithms in Table 1 are the commonly used tools by the time of publication, users may find newly developed algorithms over time.
3. There are multiple aligners including BWA, Bowtie, Bowtie 2, Novoalign and STAR. Users may choose the one to meet your needs.
4. For differential expression of miRNAs between various conditions, users may also choose Edge R software.

References

1. Wilbert ML, Yeo GW (2011) Genome-wide approaches in the study of microRNA biology. Wiley Interdiscip Rev Syst Biol Med 3:491–512
2. Wu W, Sun M, Zou GM, Chen J (2006) MicroRNA and cancer: current status and prospective. Int J Cancer 120(5):953–960
3. Watanabe Y, Kanai A (2011) Systems biology reveals MicroRNA-mediated gene regulation. Front Genet 2:29
4. Zhu S, Wu H, Wu F, Nie D, Sheng S, Mo YY (2008) MicroRNA-21 targets tumor suppressor

genes in invasion and metastasis. Cell Res 18:350–359

5. Wu W (2011) MicroRNA and cancer. Methods Mol Biol 676:59–70
6. Zhang L, Huang J, Yang N, Greshock J, Megraw MS, Giannakakis A, Liang S, Naylor TL, Barchetti A, Ward MR et al (2006) microRNAs exhibit high frequency genomic alterations in human cancer. Proc Natl Acad Sci U S A 103:9136–9141
7. Yu SL, Chen HY, Chang GC, Chen CY, Chen HW, Singh S, Cheng CL, Yu CJ, Lee YC, Chen HS et al (2008) MicroRNA signature predicts survival and relapse in lung cancer. Cancer Cell 13:48–57
8. Zhao JJ, Lin J, Lwin T, Yang H, Guo J, Kong W, Dessureault S, Moscinski LC, Rezania D, Dalton WS et al (2010) microRNA expression profile and identification of miR-29 as a prognostic marker and pathogenetic factor by targeting CDK6 in mantle cell lymphoma. Blood 115:2630–2639
9. Wu W, Cao W, Chan JA (2013) Regulation of MicroRNAs for potential cancer therapeutics: the paradigm shift from pathways to perturbation of gene regulatory networks. In: Lopez-Camarillo C, Marchat LA (eds) MicroRNAs in cancer. CRC Press, Boca Raton, FL, pp 364–386

INDEX

A

Acute myeloid leukemias 27
ADAR1 25
A549 human non-small cell lung cancer cells 16
Akt 15, 33, 86, 156, 160
Akt signaling 15, 33
Algorithm 78, 107, 213
Angiogenesis 29, 33, 34, 46, 69, 136, 179–185
Antagomir 36, 48, 202
Antibody
  anti-AKT 160
  anti-EGFR 160
  anti-HER2 100
  anti-phospho-AKT 160
  anti-phospho-HER2 ..... 26, 33
  anti-β-actin 123
Anti-microRNAs oligonucleotides (AMOs) 135–143, 145–149, 151, 152
Anti-miRNA antisense 36, 202
APOBEC 75–79
Apoptosis 4, 11, 12, 14, 23, 27, 29–32, 34, 46, 47, 51, 69, 70, 84, 85, 120, 211
AR 56, 60
ARHGAP9 54
ATM 9–12, 14–16
ATR 10–12, 14–16, 76
ATP8A2-ψ 51–52

B

B cell chronic lymphocytic leukaemia (B-CLL) 10
Bcl-2 29
BCR-ABL 11
BIM 85
Biogenesis 12, 14, 24, 28, 31, 47–49, 69, 70, 85, 93
Bioinformatics 17, 46–49, 51, 100, 212
Biomarker 16, 17, 35, 45, 47, 48, 50–52, 113, 187, 211
Bladder cancer 12, 84
BMI1 32
BRCA1 ..... 11, 15, 16, 56, 179
BRCA2 ..... 11, 179
Breast cancer 12, 13, 24, 26, 27, 50, 77

C

Cancer 3, 24, 45, 67, 76, 83, 92, 99, 117, 135, 156, 179, 187, 202
Cancer cell reprogramming 67, 69–71, 95
Cancer stem cells (CSC) 69, 85
Caspase 3 30
Cationic liposome 136, 137, 141, 142
Cell culture 120, 121, 126, 130, 137, 181, 182, 203
Cell viability 136, 149
CellMiner 46, 52
Cervical adenocarcinoma 18
Cervical cancer 18, 119–121
Cervical squamous cell carcinoma 18
CDK2 ..... 12, 16
CDK4 16
CDK6 16
Chemotherapy 4–6, 8, 9, 11, 32, 71, 87, 135, 179
CHK1 ..... 11, 12, 16, 76
Circulating miRNA 35, 36, 187, 189, 195, 198
C-myc 14, 34, 50
Co-culture Assays 179–184
Coding gene 24, 46, 49, 69, 84, 88, 211
Colorectal cancer 13, 53
Combined antitumor strategies 70, 135
Computational approaches 46, 47
CTLA-4 ..... 68, 71, 72
Cycle threshold 92, 148
Cyclin D 16, 30

D

Data analysis 116, 123, 124, 126–130, 193, 211–214
Data normalization 99, 177
Deep sequencing 17, 29, 99, 100, 102–105, 107, 121, 123, 124, 126–130, 132
Di George syndrome Critical Region 8 (DGCR8) 12, 15, 24
DIANA 46
Dicer 12, 15, 24, 47, 50, 70, 76, 85, 201
Differentially expressed microRNA 50, 100, 105

Wei Wu (ed.), *MicroRNA and Cancer: Methods and Protocols*, Methods in Molecular Biology, vol. 1699,
DOI 10.1007/978-1-4939-7435-1, © Springer Science+Business Media, LLC 2018

Differentiation 23, 29, 31, 32, 47, 69–71, 85, 99, 180, 211
Dimethyl sulfoxide (DMSO) 141
DNA damage response (DDR) ... 4–8, 11, 12, 14–18, 85
DNA methylation 94
DNA methyltransferase inhibitor 6
DNA-PK 9, 12
Double-strand breaks (DSB) 5, 8–11, 16
Drosha 15, 24, 76, 85, 201
Drug Cocktail 122, 159
Dulbecco's Modified Eagle Medium (DMEM) 121, 125, 137–139, 143, 149, 181, 203

E

E-cadherin 26, 32, 34
EcoRI 204
Epidermal growth factor receptor (EGFR) 15, 85, 87, 156, 158
Epigenetic 5, 7, 8, 37, 84, 86, 87, 94
Epigenome 83, 86, 94
ER-alpha 28, 32, 34
ERBB2 56
ESR2 56
Etoposide 16
Exosome 121, 123, 125–127, 130, 132
Exportin-5 (XPO5) 15, 47, 85
Expression data 100, 104
Expression profiling 14, 113, 212

F

FAP-1 32–33
FHOD1 32
FlexmiR 30
Fluorescence-labeled beads 136
FOXO3a 31
FOXP3 70

G

Gene expression 26, 31, 45, 69, 75–79, 84, 88, 91–95, 99, 170–172, 180, 202, 211
Gene prediction 8, 16, 26, 69, 211, 214
Gene regulatory network 18, 26, 30, 69, 84, 94
Genomic instability 4, 16
Glioblastoma 12, 24, 27, 28, 50

H

Hairpin 26, 47, 85, 212
HeLa cell line 77, 93, 121, 124, 126
HemoCytometric chamber 143
Hierarchical clustering 100, 105
High-throughput 17, 46, 48
HMGA2 ..... 31, 32, 37, 50
HMCN1 57
HOXA3 61
HOXD10 ..... 27, 28
H-ras 32
Human epidermal growth factor receptor 2 (HER2) 26, 33, 100
Human microRNA prediction 129
Human papillomaviruses (HPVs) 75, 119, 121–127, 129–133
Human umbilical vein endothelial cells (HUVECs) 180, 181, 183, 185
Hybridization 17, 47, 77, 127, 136, 138, 145

I

IL-2 79
IL-6 71
IL-8 ..... 33, 71
IL-17 71
IL-17A 71
IL-17F 71
Immune cells 67, 70, 71, 161
Immunoblotting 122, 123, 125, 126, 131, 159, 160
Immunotherapy 68, 71
IMP-1 50
Indoleamine 2,3-dioxygenase (IDO) 72
In situ hybridization (ISH) 136, 143, 145
Invasive ductal carcinoma (IDC) 32, 100
Isopropanol 189, 191

J

Java 102, 212
JAM-A 34
JARID1A 86
Jun 14, 86
Junk DNA 45, 48

K

Keratinocyte serum-free medium (KSFM) 120
KRAS 37, 51, 55, 62
Knockdown 29, 31, 50, 52, 87

L

Label-free detection 152
Let-7 ..... 31, 32, 50, 51, 69
Let-7a 31, 37, 55, 59, 78, 106
Let-7b 31, 37
Let-7c 31
Let-7d 31
Let-7e 31, 58, 61
Let-7f 31
Let-7g 31

Let-7i 31, 57
Lin-4 69
LIN28A 31
LIN28B 31, 86
Lipofectamine 2000 203
Lipoplexes 138
Locked nuclear acid (LNA) 137, 140, 145, 148, 189, 192
Luciferase reporter gene assay 202, 204–206

M

Massively parallel DNA sequencing 212
Mature microRNA 201
MCF-7 ..... 28, 29, 51
MetaCore pathway 84
Metastasis 24, 27–30, 32–34, 36, 46, 69, 83, 101, 143, 156, 180, 211
MGMT 6, 7, 53
Microarray 17, 34, 46, 47, 52, 211
Microprocessor 15
Microprocessor SVM 15
MicroRNA Expression Signature 99, 100, 102–105, 107, 211
MicroRNA mimics 203
MicroRNA precursor cloning 12, 15, 161, 212
MicroRNAseq 211, 213
Microsatellite instability (MSI) 9
Microvesicles 121, 130
miR-1 93
miR-10 ..... 27, 28, 36
miR-10a 27, 28, 62
miR-10b 27, 28, 35, 36, 53, 62, 78, 136, 148
miR-17-92 29–30
miR-15a/16 14
miR-17 60
miR-18 29
miR-19 ..... 29, 51
miR-20a 18, 30, 53
miR-24 ..... 15, 51
miR-26a 16
miR-27a 16, 55, 57, 59
miR-29 ..... 14, 54
miR-30d 53, 70
miR-34C 16, 54, 70
miR-92 29
miR-98 31
miR-107 ..... 14, 54, 57, 60
miR-222 ..... 51, 56, 58, 63, 70, 136, 137, 140, 148, 150, 151
miR-135b 53, 63, 71
miR-138 ..... 15, 53
miR-143 ..... 37, 51, 107, 108
miR-146 ..... 16, 58, 59, 61, 62, 70
miR-155 ..... 24, 30, 31, 35, 51, 58, 59, 63, 70, 93, 205
miR-181a 16, 53, 54, 57–59, 70
miR-185 16
miR-192 ..... 14, 54, 59, 63
miR-194 ..... 14, 54, 63
miR-200 32–33
miR-200c 32, 51, 53, 54, 56, 58, 62, 86
miR-203 ..... 18, 53, 54, 56, 58
miR-204 ..... 55, 57, 60, 61, 106, 108, 180–185
miR-205 33–34
miR-206 78
miR-214 ..... 16, 70
miR-215 ..... 14, 54, 58, 59, 63, 106, 108
miR-218 18
miR-221 ..... 18, 51, 56–58, 63, 85, 136, 137, 140, 148, 150, 151, 205
miR-223 ..... 16, 38, 93
miR-296 ..... 63, 180
miR-339 70
miR-371-3p 87–88
miR-371-5p 55, 57, 63, 87
miR-372 78–79
miR-378 ..... 53, 58, 180
miR-424 ..... 16, 62, 71
miR-506 16
miR-545 ..... 16, 55, 57, 63
miR-605 14
miR-21 inhibitor 15, 18, 28, 35, 50, 51, 70, 136, 140, 205
miRBase 69, 102, 103, 124, 129, 212, 214
miRDeep 124, 212, 214
miRNA
  miR-7 ..... 156, 157
  miR-18a 16
  miR-21 ..... 15, 18, 24, 28, 205
  miR-29b 72
  miR-34 ..... 14, 16, 70
  miR-101 16
  miR-145 ..... 14, 34, 37
  miR-155 ..... 24, 30, 31, 70, 93, 205
  miR-125a 58
  miR-126 ..... 72, 180
  miR-143 37
miRNA delivery 157, 162
miRNA library 87, 102, 123, 129, 213
miRNA-Masking antisense oligonucleotides 36
miRNA mimic therapy 38, 48, 87, 196, 203
miRNA modulation 18
miRNA:: mRNA interaction 69
miRNA network 94, 120
miRNA replacement therapy 48, 156
miRNA sponge 37

miRNA targets 87
miRNome 69, 94, 117
mirPS 69
MLH1 ..... 9, 53, 62
MMR 9
Mouse tissues 155, 170
Multiple-AMO 137
Multiple-target AMO technology 85, 161
Multi-potent 201–208
Mutagenesis 76
Mutation signature 76
Myeloid-derived suppressor cells (MDSCs) 70

N

Nanoparticles 156, 161
Noise 86, 91–95
Non-homologous end-joining (NHEJ) 5, 6, 9–11, 16
Northern blot 17, 34, 47
NOTCH2 ..... 34, 59
NR6A1 31
Nucleotide excision repair (NER) 5–7, 11
Nup153

O

O^6-methylguanine DNA methyltransferase 6, 7, 53
Oncogene 11, 12, 24, 27, 29–31, 34, 36, 37, 46–49, 53, 76, 83, 119, 120, 132, 156
Oncogene-induced senescence (OIS) 12
Oncogenies 46
Oncomir 27, 28, 48, 50, 69
Open reading frame (ORF) 25
Optimem 181
Osteosarcoma 12, 113–117

P

p53 ..... 12, 14, 94, 120, 122, 125
Pancreatic cancer therapy 135–143, 145–149, 151, 152
PAPD5 15
PARP1 ..... 8, 59
PARP2 8
Pasha 24
Pathway 4–13, 15, 16, 23, 29, 30, 33, 34, 38, 46, 47, 52, 71, 72, 76, 83–88, 93, 110, 156, 180
P-bodies 76, 78
PCR efficiency 187, 195, 198
PD-1 ..... 68, 71, 72
PDCD4 ..... 29, 50
PD-L1 ..... 68, 71, 72
Phosphatase and tensin homolog (PTEN) 29, 50, 86, 141, 149
Phosphatidylinositol 3-kinase (PI3K) 156
PI3K 10, 14, 15, 33, 156
PI3K-related protein kinase (PIKK) 10
Plasma 16–18, 35, 36, 113–117, 188–190, 196, 197
Plasmid 203, 205
Polo-like kinase 1 (Plk1) 12, 13, 16
Polyacrylamide gel electrophoresis 160
Poly (ADP-ribose) polymerase 1, 8
Polycistronic transcription unit 29
Polymerase-β (Pol β) 9
Polymerase chain reaction (PCR) 48, 116, 129
Polymorphisms 78
PPM1F 32
PRDX6 ..... 87, 88
Precursor microRNA 201
Predicted 76
Pre-miRNA 12, 15, 24, 47, 85, 87
Pre-RISC 13
Primary miRNA (pri-miRNA) 12, 15, 24, 47, 85
Probe 125, 138, 145, 156
Processing 4, 8, 11, 14, 31, 76, 78, 92, 213
Prostate cancer 12
Protein extraction 125, 126, 159
Pseudogenes 45–48, 50–53

Q

Qiagen 114, 115, 123, 124, 130, 141, 157–159, 163, 165, 177, 188, 196, 197, 203, 204, 207
Quantitative PCR (qPCR) 47, 113, 114, 116, 117, 140, 141, 148, 157, 158, 170–172, 187–193, 196–198
Quality Control 187–193, 196–198
Quantification 17, 47, 48, 117, 123, 128, 130, 136, 139, 140, 142, 146, 148, 185, 187, 188, 196–198
Quantile 100, 104, 107

R

RAD51 11
RASSF1 ..... 53, 58
RB1 57
RBSP3 16
Real-time PCR 124, 130, 188, 189, 192, 193, 203, 206, 207
Real-time quantitative PCR 169, 171
Reference miRNAs (Ref-miRs) 133
RelA 156, 160
Residual disease 84
Resistance 3–5, 7, 9, 17, 19, 24, 28, 31, 32, 83–88, 156, 175, 179

Reverse transcriptase 48, 123, 140, 148, 167
Reverse transcription 115, 124, 129, 130, 158, 159, 170–172, 206
RNAbinding domains (RBDs) 31, 58
RNA editing 75–79
RNA interference (RNAi) 121
RNA isolation 139, 188, 190, 191
RNA-induced silencing complex (RISC) 12, 69, 93, 201
RNase III endonuclease 25
RNase inhibitor 167, 203
ROS 6, 7, 9
RPL 141, 149
RNA polymerase II 24, 25, 47, 49, 76, 85, 201
RNA binding protein 24, 78, 79
RUNX1 59

S

SAM 6
SDS-polyacrylamide gel electrophoresis (SDS-PAGE) 160–159
Seed sequence 76, 201, 202
Senescence 4, 11, 12, 16, 120
Sequencing data normalization 214
Single-strand breaks (SSB) 5, 6, 8
SIP1 32
SKOV3 ovarian cancer 180, 182
SMAD4 63
SMAD protein 63
Small interfering RNA (siRNAs) 4, 121, 124
SOCS1 30
Sponge 201–208
Sprouty2 (SPRY2) 29
SSC profiler 139
Stem cells 34, 47, 51, 68, 69, 85, 94, 211
STX12 87
Stochastic fluctuation 91
Suz12 32–33
Systemic microRNA delivery 155

T

Taq DNA polymerase 207
TaqMan® 156, 197
Tamoxifen 28
Target mRNA 12, 26, 76, 84, 85, 92, 155, 201, 208
TargetScan 46
Tat-interacting protein 28
Temozolomide (TMZ) 6
Terminal oligoPyrimidine (TOP) 28
TGF-β 30, 32, 33
TIMP3 86
T-lymphoma 28
TOPO topoisomerase 6
TRAIL 86
Transfection 26, 121, 124–126, 130, 138, 139, 141, 143, 145, 146, 149, 182, 203, 205, 206
Transwell chambers 179–184
TRIM25 31
Triple negative breast cancer (TNBC) 29, 99, 100, 102–105, 107
Tropomyosin 1 (TPM1) 29, 50
Trypsin 138, 143, 182, 183
TSmiRs 69
Tumor 18, 24, 26–29, 31, 33–38, 46, 48, 49, 67, 69–71, 86, 87, 99, 101, 109, 113, 120, 121, 180
Tumor environment 68
Tumorigenesis 30, 36, 47, 49, 76, 211
Tumor-suppressor miRNAs 31, 36, 50, 99, 156
Tumor virus 119
TUT4 31
Twist 28

U

Ultraviolet (UV) 4, 7, 14, 15
UniSp4 ..... 115, 189, 190, 194–196
UniSp5 ..... 115, 189, 190, 195, 196
Universal PCR Master Mix 159
Universal primer 207
Untranslated region (UTR) 25, 155
Upregulation 5, 13, 29, 34, 36, 50, 51, 70
Upstream 11, 16, 86
Uracil N-glycosylase (UNG) 159
Urea 159

V

Variable 143, 170, 177, 180, 206, 207
Variance 109
Variation 9, 52, 72, 91, 120, 167, 177, 196, 202, 212
Vector 36, 202–205
  Renilla luciferase 203
Viability assay 136, 141, 149–151
Viral infection 67, 75, 78, 79
Virus
  adenovirus 34
  lentivirus 37
VEGF 24, 33, 55, 57, 181, 183–185

W

W4011 122
W4021 ..... 122, 123
Web-server 212
Website 213
Web-tool 52
WEE1 ..... 12, 16

Western blot 122, 125, 161
Wip1 13
Workflow 213

X

Xeroderma pigmentosum (XP) 7
XPO5 15
XRCC1 8
XRCC4 9
XRCC5 9
XRCC6 9

Y

Yeast 92, 139

Z

ZC3H8 60
ZEB2 32–34
ZNF589 60
ZP4 62